UNIVERSITÀ DEGLI STUDI DI MILANO

FACOLTÀ DI DI SCIENZE MATEMATICHE, FISICHE E NATURALI

DIPARTIMENTO DI CHIMICA INORGANICA METALLORGANICA E ANALITICA

"Lamberto Malatesta"

CORSO DI DOTTORATO DI RICERCA IN

CHIMICA INDUSTRIALE CICLO XXIII

TESI DI DOTTORATO DI RICERCA

NEW ORGANOMETALLIC COMPLEXES WITH LUMINESCENT AND NON LINEAR OPTICAL PROPERTIES

CHIM 03

ROSSI ESTER
Matr: R07827

Tutor :
Chiar.mo Prof. RENATO UGO

Co-Tutor :
dott.ssa CLAUDIA DRAGONETTI

Coordinatore :
Chiar.ma Prof.ssa DOMINIQUE MARIE ROBERTO

ANNO ACCADEMICO 2009/2010

INDEX

RESULTS AND DISCUSSION:

INTRODUCTION AND SCOPE

Organometallic chromophores with both luminescent and second-order non linear optical (NLO) properties are of growing interest as new molecular multifunctional materials, since they offer additional flexibility, when compared to organic chromophores, by introducing NLO-active electronic charge-transfer transitions between the metal and the ligand, tunable by virtue of the nature, oxidation state and coordination sphere of the metal centre.[1-3] Moreover, owing to their remarkable luminescent properties, organometallic complexes of transition-metals have recently received considerable attention as phosphorescent emitters for *Organic Light Emitting Diodes* (OLEDs).[4] In particular, various platinum(II) complexes with a cyclometallated 1,3-di(2-pyridyl)benzene ligand seem very promising in this respect because of their intense luminescence.[5]

Besides, in the last decades organometallic and coordination complexes have emerged as interesting molecular chromophores for second-order non linear optical (NLO) applications, because they may offer a great diversity of tunable electronic properties by virtue of the metal centre.[6] For example, coordination of various organic push-pull NLO-phores acting as ligands such as stilbazoles bearing a NR_2 donor group produces a significant increase of their quadratic hyperpolarizability due to a red-shift of the intraligand charge-transfer transition, major origin of their second order NLO response.[6] In particular, the product $\mu\beta$ (μ = dipole moment, β = quadratic hyperpolarizability) of *cis*-[$Ir(CO)_2Cl$(4,4'-*trans*-$NC_5H_4CH{=}CHC_6H_4NMe_2$)], measured in solution by the Electric-Field Induced Second Harmonic (EFISH) generation technique, is 3 times higher than that of the free stilbazole ligand[7] and comparable to that of an important NLO-phore such as Disperse Red One, an NLO chromophore currently used in electro-optics polymers.[8]

The porpose of my Ph.D. work has been the synthesis of novel Pt(II) planar complexes for application in light emitting devices as well as the study of the effect of the coordination to a metal centre on second order NLO properties of new highly π-delocalised ligands and octupolar structures. Thus, this thesis is organised in three main sections:

1. Luminescent properties of cyclometallated Pt(II) complexes;
2. Second order NLO properties of different organometallic chrmophores;
3. Experimental section

Section 1 begins with a short introduction on the basic concept of luminescence, focusing in particular on Pt(II) organometallic semiconductor for display and lighting applications. Then the synthesis and photophysical characterisation of new cyclometallated Pt(II) complexes with a substituted 1,3-di(2-pyridyl)benzene ligand is presented. These compounds were prepared to get a better understanding of the effect on luminescence properties – *e.g.*

emission wavelength and efficiency - of different substituents on both terdentate and ancyllary ligand (*e.g.* including the introduction of strong-field co-ligands as σ-phenyl acetylides). On account of their remarkable brightness, some of these complexes have been applied to the manifacturing of OLEDs, exploiting excimer emission. The different performances between vacuum-deposited and solution-processed devices are also discussed.

After a brief introduction on non linear optics, Section 2 provides an investigation on the NLO response of new push-pull anellated hemicyanine ligands and their related *cis*-[Ir(CO)$_2$ClL] complexes. NLO properties were determined by the Electric Field Induced Second Harmonic generation technique, working with a non-resonant incident wavelength of 1.907 μm.

In this section are also presented the preliminary results for the second-order NLO response of both known[5] and new members of the platinum(II) complexes family described in Section 1. This study was conductued by both EFISH and *Hyper Light Scattering* (HLS) techniques.

Section 2 concludes by examining the $\beta_{HLS,1.907}$ values of a tripodal octupolar ligand that has been easily coordinated to organometallic fragments (*i.e.* Zn complexes of a commercial porphyrin or phtalocyanine, respectively).

In the last section, details are given on the synthesis and characterization of all of the complexes.

This Ph.D. thesis leds to the discovery of new organometallic complexes and coordination compounds appealing as building blocks for molecular materials with both non linear and luminescence properties.

References

[1] Maury, O.; Le Bozec, H. *Acc. Chem. Res.* **2005**, *38*, 691.

[2] Humphrey, M.G.; Samoc, M. *Advances in Organometallic Chemistry* **2008**, *55*, 61.

[3] Di Bella, S.; Dragonetti, C.; Pizzotti, M.; Roberto, D.; Tessore, F.; Ugo, R. in *Topics in Organometallic Chemistry 28. Molecular Organometallic Materials for Optics*, Le Bozec, H. and Guerchais V. (eds.), Springer Verlag Berlin Heidelberg **2010**, pp 1-55.

[4] Evans, R.C.; Douglas, P.; Winscom, C.J. *Coord. Chem. Rev.* **2006**, *250*, 2093.

[5] Murphy, L.; Williams, J.A.G. in *Topics in Organometallic Chemistry 28. Molecular Organometallic Materials for Optics*, Le Bozec, H. and Guerchais V. (eds.), Springer Verlag Berlin Heidelberg **2010**, pp 75-111.

[6] for example see (a) E. Cariati, M. Pizzotti, D. Roberto, F. Tessore and R. Ugo, *Coordination Chemistry Reviews,* **2006**, *250*, 1210. (b) B. J. Coe, *Acc. Chem. Res.,* **2006**, *39*, 383.

[7] Roberto, D.; Ugo, R.; Bruni, S.; Cariati, E.; Cariati, F.; Fantucci, P.C.; Invernizzi, I.; Quici, S.; Ledoux, I.; Zyss, J. *Organometallics,* **2000**, *19*, 1775.

[8] Singer, K. D.; Sohn, E.; King, L.A.; Gordon, H. M.; Katz H. E. and Dirk, P. W. *J. Opt. Soc. Am*. *B* **1989**, *6*,1339.

SUMMARY

Organic light-emitting diodes (OLEDs) are emerging as leading technology for the new generation of full-color displays and solid-state lighting.[1,2] In these electroluminescent devices the radiative deactivation of electronically excited states is formed by recombination of charge carriers, *i.e.* electrons and holes, injected from the electrodes. Since this recombination is statistically controlled, the luminous efficiency of OLEDs may potentially be improved by up to a factor of four when phosphorescent emitters are used. It appears then that complexes of third row transition metal ions are particularly appropriate for this purpose[3,4] since the high spin-orbit coupling constant associated with them efficiently promotes triplet radiative decay. In this respect platinum(II) derivatives have attracted considerable attention for decades, mainly due to their unique luminescent properties and molecular aggregations.[3,5-7] Nevertheless untill the late '80s no square planar platinum(II) compound was known to significantly emit in solution under ambient conditions, even though several were emissive in the solid state or at low temperature.[8-10] Since that time many improvement have been made for rational design of highly efficient luminescent platinum(II) phosphors.[3,11,12] In particular, complexes of N^C^N-coordinating ligands, where N^C^N refers to a ligand that binds the metal through two nitrogen atoms and a central metal-carbon bond, seem very promising in this respect as shown by their impressively high quantum yield values[3].

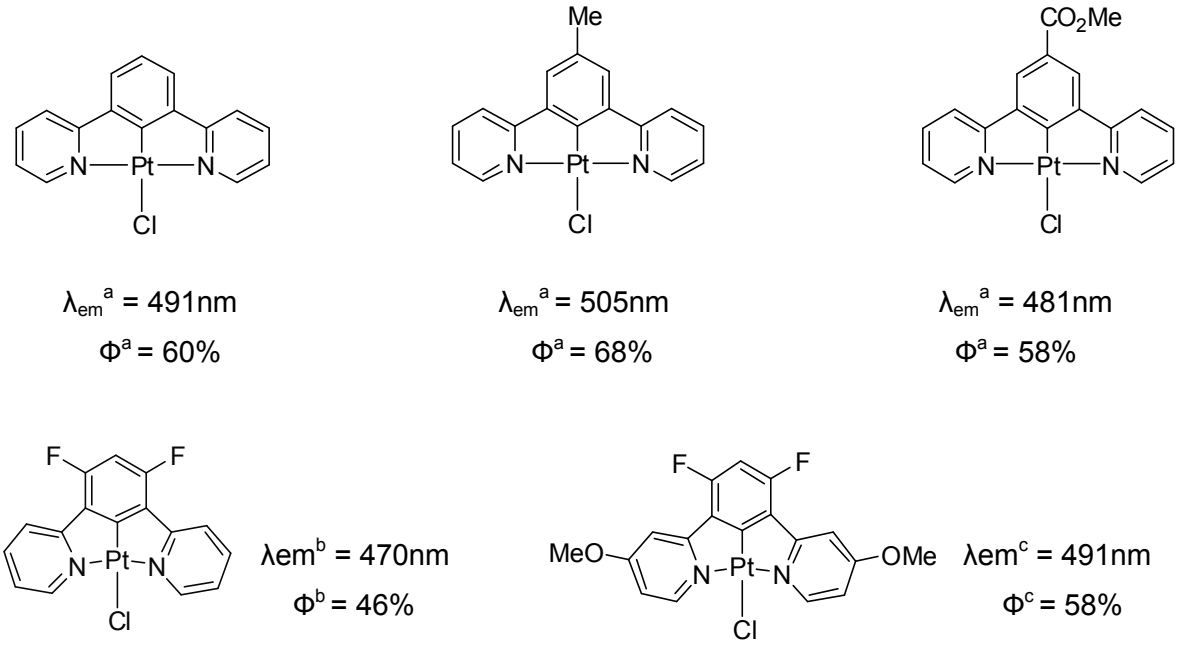

Figure 1: Schematic structure of cyclometallated Pt(II) complexes based on substituted 1,3-di(2-pyridyl)benzene ligand. λ_{em} is the wavelenght of the first emission maximum and Φ is emission quantum yield in solution. [a] data from literature[13]; [b] data from literature [14]; [c] data from literature[15].

Furthermore in systems based on substituted 1,3-*di*(2-pyridyl)benzene ligands such as the ones presented in Figure 1, the selection of substituents on both central and lateral rings offers a good versatile method for colour tuning.[13, 14]

These observations prompted us to develop new Pt(II) systems, [PtL^{n}Y], also based on substituted 1,3-di(2-pyridyl)benzene, L^n, with various Y ancillary ligands, [Y= chloride, acetilyde, thiocyanate, phenylthiazole thiol or tetrazole thiol], in order to explore their emission properties.

By preparing complex **[PtL^{3}Cl]** we first studied the effect of a fluorine atom in 4 position on the central phenyl ring, which has never been investigated before (Fig.2).

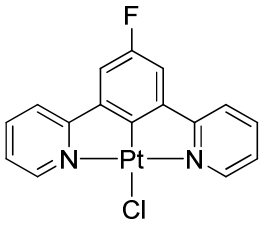

[PtL^{3}Cl]

Figure 2: Schematic structure of 4-F substituted 1,3-di(2-pyridyl)benzene Pt(II) chloride complex.

Then, in analogy with cyclometallated phenylpyridine iridium complexes, we synthesized a new ligand, which bears CF_3 substituent on the pyridyl rings, and its related Pt complex **[PtL^{4}Cl]** (Fig.3). In fact in the case of Ir(III) complexes, it has been reported that the presence of CF_3 substituent on the cyclometallated phenylpyridines leads to a striking improvement in luminescence efficiency (from 14% for the unsubsituted phenylpyridines to 68% for the CF_3 substituted)[16] and therefore we wondered if CF_3 could have a similar effect on our platinum systems.

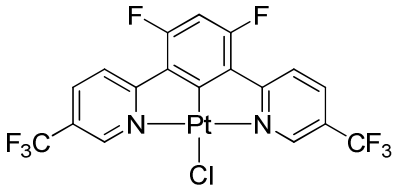

[PtL^{4}Cl]

Figure 3: Schematic structure of 4-F substituted 1,3-di(2-pyridyl)benzene Pt(II) chloride complex.

As far as ancillary ligands are concerned we explored the effect of coordination to platinum through sulphur since, surprisingly, it had not been previously investigated. To this aim we started studying the effect of the substitution of Cl by sulphur donor ligands (*i.e.* thiocyanate, phenylthiazole thiol, tetrazole thiol, Fig.4) in parent platinum chloride complex of 1,3-di(2-pyridyl)toluene, **[PtL^{1}Cl]** (Fig.5), which was reported as the brightest amongst compounds of this class (Φ_{lum} =68%[3]).

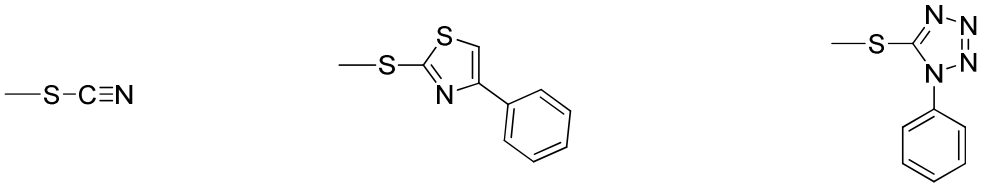

Figure 4: Schematic structure of sulphur donor ligands.

To improve the solubility of the complexes, we also consider the 4-mesitylated ligand, whose platinum(II) chloro complex, **[PtL^{2}Cl]** (Fig.5), was also reported as highly luminescent (Φ_{lum} =62%[17]).

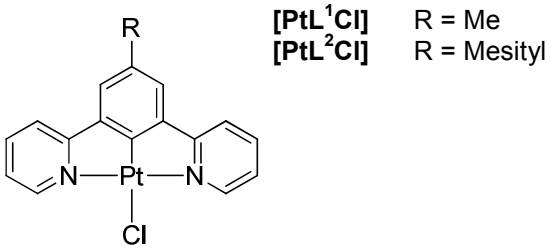

Figure 5: Schematic structure of Pt(II) chloride complexes: [PtL^{1}Cl], [PtL^{2}Cl]

This bulky aryl substituent leads to a decrease in π-stacking fenomena and therefore reduces self-quenching of complexes. This effect is an attractive feature for practical applications: for example in OLED technology, where local concentrations may be quite high, self-quenching is a wasteful energy sink that decreases the device efficiency.

However, despite the many attempts, only the derivatives obtained by reaction of **[PtL^{1}Cl]** and **[PtL^{2}Cl]** with sodium thiocyanate resulted to be stable (Fig. 6). Their infrared spectra showed the presence of a strong sharp peak at 2096 cm^{-1} typical of ν(SCΞN) of isothiocyanate ligands. Therefore, unexpectedly on the basis of its soft character, the Pt atom bounds the SCN$^-$ ion through the N atom, in our systems. This coordination was confirmed by X-ray crystallography.

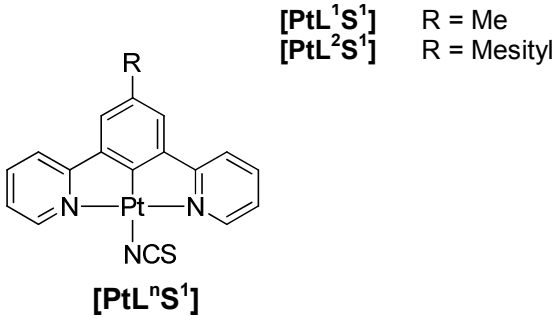

Figure 6: Schematic structure of the two isothiocyanate derivatives, [PtL^{1}S^1] and [PtL^{2}S^1]

Meanwhile, searching for other ancillary ligands that could promote luminescence we investigated substituted acetylides. In fact, it is known that the strong ligand field associated with alkyne raises the energy of d–d states making them thermally inaccessible, therefore withdrawing their deactivating effect.[12,18-20] As expected, the complexes obtained are in most of the cases quite strongly emissive in fluid solution at room temperature (Φ_{lum} ranges from 20 - 77%). In particular this strategy proved to be very successful in the case of the (3,5-difluorophenyl)ethynyl complex, **[PtL^{1}A^1]** (Fig.7)**,** which is exceptionally bright (Φ_{lum}= 77% at room temperature in deoxygenated dichloromethane). This result encouraged us to prepare the more soluble mesityl derivative, **[PtL^{2}A^1],** which again leads to an improved emission efficiency with respect to the parent platinum chloride (Φ_{lum} =66% vs Φ_{lum}=62% [17] at room temperature in deoxygenated dichloromethane).

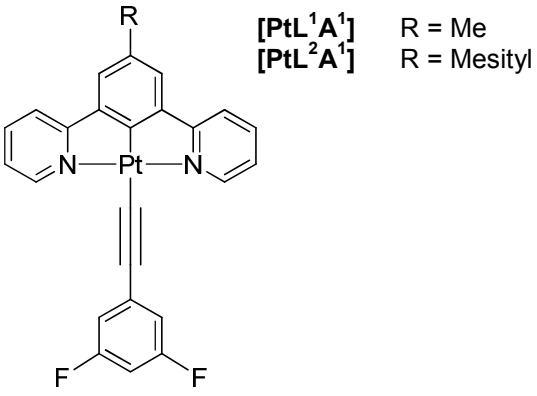

Figure 7: Schematic structure of the two most luminescent acetylide derivatives,**[PtL^{1}A^1]** and **[PtL^{2}A^1]**

Although among acetylides, the compounds with **L^4** bearing CF_3 on the lateral pyridyl rings exhibit not very remarkable quantum yields, their luminescence is essentially unique with respect to oxygen quenching. In fact, it is known that the typically long-lived triplet excited state lifetime of platinum complexes enables efficient quenching reactions by surrounding

triplet molecules as dioxygen.[21] We found that derivatives of **[PtL^{4}Cl]** are less quenched by dissolved oxygen as shown by their bimolecular rate constants for this process, Kq_{O2}, which are an order of magnitude lower than those reported, for different cyclometallated platinum systems (Kq_{O2} calculated by Stern-Volmer equation: 10^8 $M^{-1}s^{-1}$ versus 10^9 $M^{-1}s^{-1}$).[17, 22] This property is more immediately evident by comparing a degassed sample of **[PtL^{4}Cl],** for example, with an air saturated solution in dichlorometane: the luminescence quantum yield decreases only by a factor of three from 53% to 16%, while in the other cases it diminishes ten-twenty times. This appealing characteristic could be an advantage in the preparation of devices.

The apparently controversial effect on emission of a fluorine in 4-position on the central phenyl ring, **[PtL^{3}Cl]**, can be rationalised in terms of electron density distribution caused by the balancement of two opposite electronic contributions of this element. In fact despite being strongly electronegative, and therefore inductively electron-withdrawing, fluorine is also a mesomerically electron releasing group. The result is an emission at wavelenght similar to that of a weak electron-donor such as methyl, **[PtL^{1}Cl]** (**[PtL^{3}Cl]** λ_{em}= 504, 542 nm Vs **[PtL^{1}Cl]** λ_{em}= 505, 539 nm).[17]

The coordinative unsaturation of square-planar platinum(II) complexes gives rise to ground- and excited-state interactions that are not possible in octahedral and tetrahedral metal complexes. Such axial interactions are also responsible for self-quenching and cross-quenching, including excimer and exciplex formation.[7, 23, 24] The strong inclination to self aggregation of this class of complexes is proved by the high self-quenching constant values obtained (of the order of magnitude of 10^9). This renders the most emissive complexes of interest for use in optoelectronics. For example, **[PtL^{4}Cl]** has been used as single dopant in prototype devices with reasonable efficiency. In these displays colour variation was realised by mixing of molecular exciton and excimer phosphorescent emissions from the phosphor, a technique which has been previously used with similar system in order to obtain white light by means of a single dopant.[15]

Also complexes **[PtL^{1}Cl]**, **[PtL^{3}Cl]** and **[PtL^{1}S^1]** have been used for the manufacturing of *white organic light-emitting diodes* (WOLEDs), where a double layer system was deposited by spin coating. This new approach leads to lower efficiencies, (external quantum efficiency for **[PtL^{1}Cl]** Φ_{EL}=0.23%), than those reported for thermal-evaporation depositions (Φ_{EL} =8.5% for **[PtL^{1}Cl]**).[25] However, the spin coating techique has the appealing advantage of being cheaper and simpler.

The second topic of my Ph.D. research work has been the study of the second order *Non Linear Optical* (NLO) response of push-pull ANellated hemicyaNINE (*ANNINE*) ligands

(**L^n** = **L^3** and **L^4,** Fig.8), and their related **[IrL^n]** complexes. These new NLO-phores are of particular interest because of their photostability in contrast to corresponding non-anellated chromophores. In fact styryl-type molecules are subjected to *cis-trans* photoisomerism around the C=C double bond and photorotamerism of the aromatic rings, thus reducing the chromophore NLO activity.[30] Moreover, the isolated double bond may be easily oxidized, thus interrupting the π-conjugation between the donor and the acceptor groups. These problems have been overcome by including the double bond in a rigid polyaromatic system, which, together with stability, ensures highly electronic delocalization.

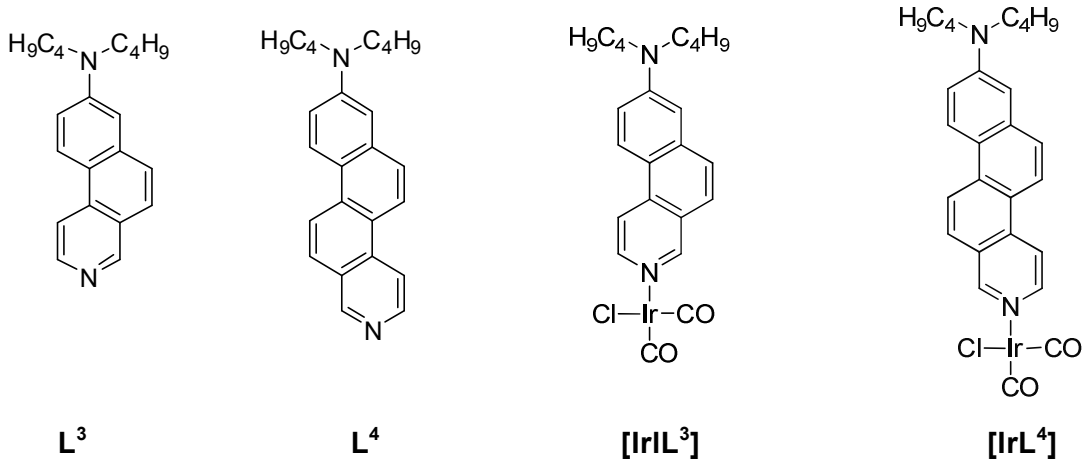

Figure 8: Schematic structure of annine ligands and their related iridium complexes.

These new NLO-phores are of particular interest because of their photostability in contrast to corresponding non-anellated chromophores. In fact styryl-type molecules are subjected to *cis-trans* photoisomerism around the C=C double bond and photorotamerism of the aromatic rings, thus reducing the chromophore NLO activity.[30] Moreover, the isolated double bond may be easily oxidized, thus interrupting the π-conjugation between the donor and the acceptor groups. These problems have been overcome by including the double bond in a rigid polyaromatic system, which, together with stability, ensures highly electronic delocalization.

The experimental absorption data are reported in Tab. 1, along with the $\mu\beta_{1.907}$ values measured with the *Electric Field Induced Second Harmonic generation* (EFISH) technique.[31] Unexpectedly coordination of **L^1** to the "Ir(CO)$_2$Cl" moiety leads to a decrease in β value which even becomes negative when **L^2** is coordinated (Tab. 1) indicating that μ of the excited state is lower than μ of the ground state. This fact can be reasonably attributed to the sum of two opposite contribution: ILCT transition ($\beta > 0$) and

MLCT transition ($\beta < 0$). This behaviour is in contrast with that observed upon coordination of the correspondent not anellated compound, *N*-methyl-*N*-hexadecylaminostilbazole, to the same Ir(I) moiety where $\mu\beta_{1.907}$ is enhanced but remains positive, being dominated by an ILCT transition.[33] The increasing NLO response when an ANNINE substituted with a withdrawing group –CN is coordinated to the Ir fragment would be in agreement with the importance of the MLCT. Remarkably, an increase of the β-conjugation of the free ligand leads to a huge positive effect on the second order NLO response with an enhancement factor of 4.4 on going from **L^3** to **L^4** reaching a $\mu\beta_{1.907}$ value much higher than that of the related stilbazole ($\mu\beta_{1.907}$ = 60 x 10^{-30} esu).[33]

Table 1: Absorption data , EFISH $\mu\beta_{1.907}$ and μ values of **L^1, L^2** and related compounds.

COMPOUND	λ_{MAX} [a] [nm] (ε [M^{-1} cm^{-1}])	$\mu\beta_{1.907}$ [a,b] [10^{-48}esu]	μ [c] (μ_{theor}) [D]	$\beta_{1.907}$ [10^{-30}esu]
L^3	278 (28626), 347 (14397)	430	3.5 (7.6)	123[d] (56)[e]
***cis*-[IrL^3]**	279 (35420), 390 (25670)	620	(16.2)	(38)[e]
L^4	305 (41462), 361 (17179)	1800	4.2 (8.0)	429[d](224)[e]
***cis*-[IrL^4]**	272(34541), 421 (12737)	-2310	(16.9)	(-137)[e]

[a]In $CHCl_3$ at 10^{-4}M with an incident radiation of 1.907μm. [b]The error on EFISH measurements is ± 10%. [c]Experimental μ obtained in $CHCl_3$ by the Guggenheim method;[31,32] the error is ± 1 D. [d]Obtained by using experimental μ. [e]Obtained by using theoretical μ.

Our third target has been the synthesis and characterisation of octupolar chromophores with potential NLO properties which can be easily coordinated to an organometallic fragment such as a Zn-porphyrin or Zn-Phtalocyanine. We investigated the second order NLO properties of both free and coordinated octupolar core, as well as free Zn-porphyrin and Zn-phtalocyanine, by Harmonic Light Scattering (HLS) technique. The β_{HLS} values obtained are quite high (free octupolar core $\beta_{HLS,1.907}$ = 667 x 10^{-30} esu at a concentration of 10^{-3} M), suggesting the great potentiality of this class of chromophores. From data also emerges that, unfortunately, the coordination of the organometallic fragments to our octupolar core, **O^{1}Zn^1** (Fig. 9) and **O^{1}Zn^2** (Fig. 10) did not lead to a substantial change in $\beta_{HLS,1.907}$ value. However, this study allows to put in evidence the remarkably high $\beta_{HLS,1.907}$ value displayed by the Zn-porphyrine itself ($\beta_{HLS,1.907}$ = 1003 x 10^{-30}) which, interestingly, is significantly higher than that of other more structurelly sofisticated Zn-porphyrines (for comparison see ref. [34]).

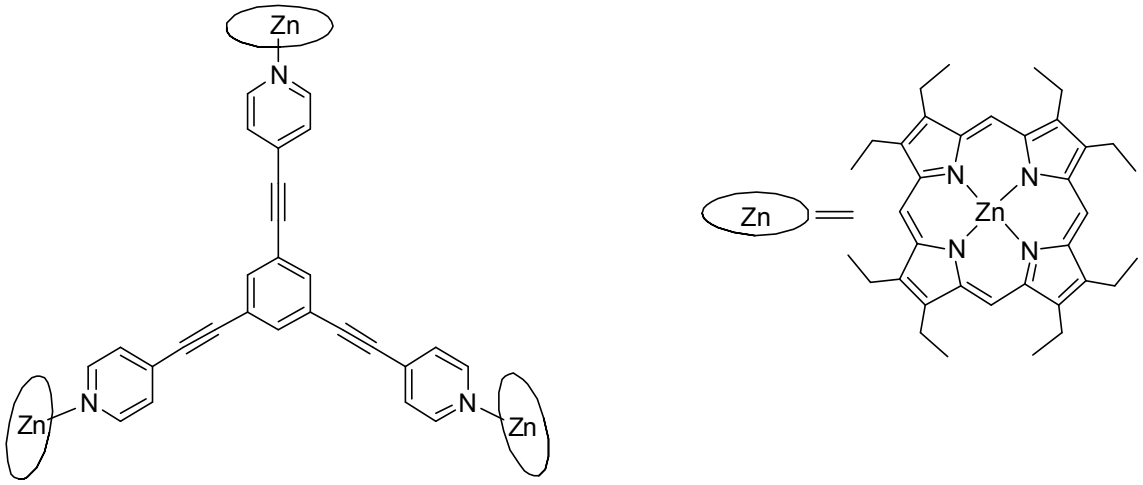

O^1Zn^1

Figure 9: Schematic structure of the coordination compound an octupolar core with a Zn-porphyrin, **O^1Zn^1**.

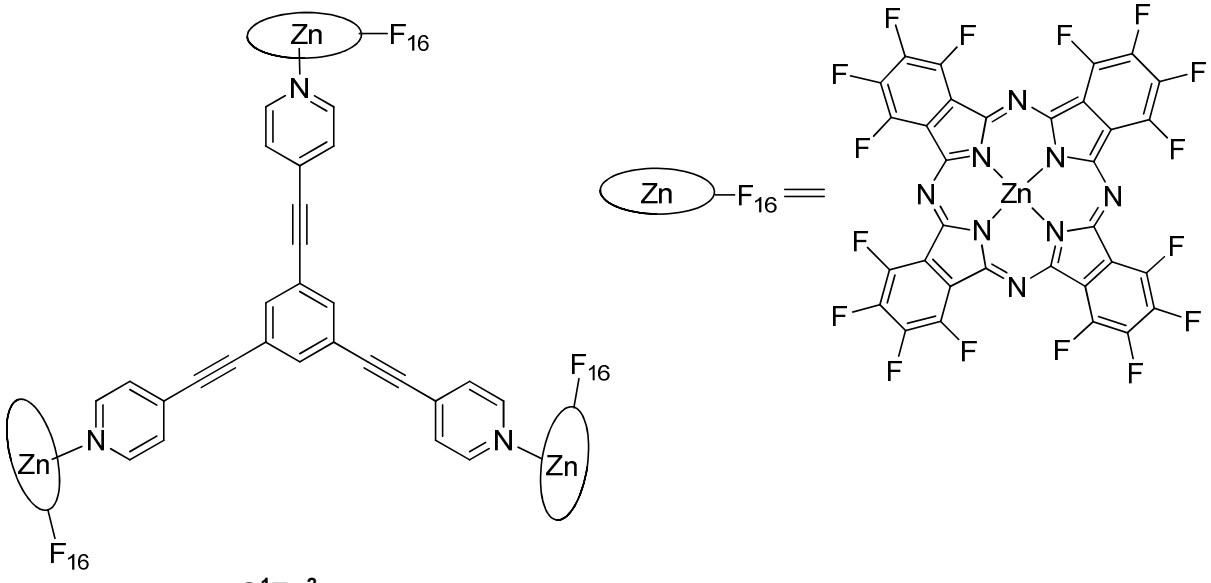

O^1Zn^2

Figure 10: Schematic structure of the coordination compound of octupolar core with a Zn Phtalocyanine, **O^1Zn^2**.

References

[1] Jüstel, T.; Nikol, H.; Ronda, C. *Angew. Chem. Int. Ed*, **1998,** *37*, 3084.

[2] D'Andrade, B.W.; Forrest, S.R. *Adv. Mater.,* **2004,** *16,* 1585.

[3] *Evans*, *R.C. ;* Douglas, P.; Winscom, C. J. *Coord. Chem. Rev.,* **2006,** *250,* 2093.

[4] Baldo, M. A.; O'Brien, D. F.; You, Y.; Shoustikov, A.; Sibley, S.; Thompson, M. E.; Forrest, S. R. *Nature,* **1998**, *395*, 151.

[5] Sandrini, D.; Maestri, M.; Balzani, V.; Chassot, L.; von Zelewsky, A. *J. Am. Chem. Soc.,* **1987,** *109,* 1120.

[6] Kavitha, J.; Chang, S.-Y.; Chi, Y.; Yu, J.-K.; Hu, Y.-H.; Chou, P.-T.; Peng, S.-M.; Lee, G.-H.; Tao, Y.-T.; Chien, C.-H.; Carty, A.J. *Adv. Funct. Mater.,* **2005,** *15,* 223.

[7] Williams, J. A. G.; Beeby, A.; Davies, S.; Weinstein, J.A.; Wilson, C.; *Inorg.Chem*., **2003,** *42*, 8609.

[8] Barigelletti, F.; Sandrini, D.; Maestri, M.; Balzani, V.; von Zelewsky, A.; Chassot, L.; Jolliet, P.; Maeder, U. *Inorg. Chem.,* **1988,** *27*, 3644.

[9] Houlding, V.H; Miskowski, M. *Inorg. Chem.,* **1989***, 28* 1529.

[10] Ballardini, R.; Varani, G.; Indelli, M.T.; Scandola, F. *Inorg. Chem*., **1986**, *25*, 3858.

[11] Murphy, L.; Williams, J. A. G. *Topics in organometallic chemistry*, **2010**, *28* 75.

[12] Williams, J. A. G.; Develay, S.; Rochester, D. L.; Murphy, L. *Coord. Chem. Rev.*, **2008**, *252*, 2596.

[13] Rochester, D. L.; Develay, S.; Záliš, S.; Williams, J. A. G. *Chem. Soc. Rev.*, **2009**, *38*, 1783.

[14] Cocchi, M.; Kalinowski, J.; Fattori, V.; Williams, J. A. G.; Murphys, L. *Appl. Phys. Lett.* **2009**, *94*, 073309.

[15] Cocchi, M.; Kalinowski, J.; Murphys, L.; Williams, J. A. G.; Fattori, V. *Organic Electronics* **2010**, *11*, 388.

[16] Lowry, M. S.; Goldsmith, J. I.; Slinker, J. D.; Rohl, R.; Pascal, R. A.; Malliaras, G. G.; Bernhard, S. *Chem. Mater*., **2005**, *17*, 5712

[17] Farley, S. J.; Rochester, D. L.; Thompson, A. L.; Howard, J. A. K.; Williams, J. A. G. *Inorg. Chem,.* **2005**, *44*, 9690.

[18] Crites, D.K.; Cunningham, C.t.; Mc Millin, D.R. *Inorganica Chimica Acta* **1998**, *273*, 346.

[19] Yam, V. W.-W.; Tang, R. P.-L.; Wong, K. M.-C.; Cheung, K.-K.; *Organometallics* **2001**, *20*, 4476.

[20] Lu,W.; Mi, B.-X.; Chan, M. C. W.; Hui, Z.; Che, C.-M.; Zhu, N.; Lee, S.-T. *J. Am. Chem. Soc*., **2004**, *126*, 4958.

[21] Djurovich, P. I.; Murphy, D.; Thompson, M.E.; Hernandez, B.; Gao, R.; Hunt, P.L.; Selke, M. *Dalton Trans*., **2007**, 3763.

[22] Santoro, A.; Whitwood, A.C.; Williams, J. A. G.; Kozhevnikov, V. N.; Bruce, D. W. Chem Mater, **2009**, *21*, 3871.

[23] Ma, B.; Djurovich, P. I.; Thompson, M. E. *Coord. Chem. Rev*. **2005**, *249,* 1501.

[24] Pettijohn, C.N.; Jochnowitz, E. B.; Chuong, B.; Nagle, J. K.; Vogler, A. *Coord. Chem. Rev.* **1998,** *171,* 85.

[25] Cocchi, M.; Virgili, D.; Fattori, V.; Williams, J. A. G.; Kalinowski, J.; *Appl. Phys. Lett.,* **2007**, *90*, 023506.

[26] Grove, L. J.; Rennekamp, J. M.; Jude, H.; Connick, B. *J. AM. Chem. Soc*., **2004**, *126*, 1594.

[27] Sagara, Y.; Kato, T. *Nature Chemistry,* **2009**,*1*, 605.

[28] Bailey, R. C.; Hupp, J. T. *J. AM. Chem. Soc*., **2002**, *124*, 6767.

[29] Ni, J.; Wu, Y.-H.; Li, B.; Zhang, L. Y.; Chen, Z.-N. *Inorg. Chem*., **2009**, *48*, 10202.

[30] Sekkat, Z.; Knoll, W. in *Photoreactive Organic Thin Films*, ed. Accademic Press: San Diego, California.

[31] Ledoux, I., Zyss, J. *Chem. Phys.,* **1982**, *73*, 203.

[32] Guggenheim, E. A. *Trans. Faraday Soc.,* **1949**, *45*, 714.

[32] Thompson, H. B. *J. Chem. Educ*., **1966**, *43***,** 66.

[33] Locatelli, D.; Quici, S.; Righetto,S.; Roberto,D.; Tessore, F.; Ashwell, G.J.; Amiri, M. *Prog. in Solid State Chem.,* **2005**, *33*, 223.

[34] (*a*) Sen, A.; Ray, P. C.; Das, P. K.; Krishnan, V. *J. Phys. Chem*. **1996**, *100*, 19611; (*b*) Kim, K.S.; Vance, F.W.; Hupp, J.T.; Le Cours, S.M.; Therien, M. J. *J. Am. Chem. Soc.* **1998,** *120,* 2606; (*c*) Zhang, T.-G.; Zhao, Y.; Asselberghs,I.; Persoons, A.; Clays,K.; Therien, M. J. *J. Am. Chem. Soc*. **2005**, *127*, 9710.

LUMINESCENT PLATINUM COMPOUNDS

INTRODUCTION

1. Basic Principles of Luminescence

Luminescence is the photophysical phenomenon related to the emission of light from a substance originated by the decay of an electronically excited specie. Depending on the nature of excitation different kind of luminescence are distinguished. For example, photoluminescence occurrs on account of absorption of high-energy light (photons), whereas electroluminescence is due to electrical excitation. Once a molecule is excited, the energy absorbed can be released through different processes - *i.e.* emission of light or other deactivation pathways - which may compete if they take place on a comparable time-scale. The key radiative and non-radiative processes involved are typically represented by Jablonski diagram as illustrated in Fig. 1. There are only two pathways for the emissive decay of excited-state electrons and these are fluorescence and phosphorescence. The former is the result of a spin-allowed electronic transition ($\Delta S=0$), for example from the first excited state of an aromatic molecule to the ground state, $S_0 \rightarrow S_1$; whereas the latter is the forbidden relaxation of an excited state with spin symmetry different from the ground state ($\Delta S \neq 0$), typically from the first triplet excited state to the singlet ground state, $T_1 \rightarrow S_0$. At room temperature phosphorescence is rarely observed in organic molecules solutions. In fact, in these conditions the phosphorescent process is so slow - lifetimes are of the order of 1s - that faster processes of non-radiative decay of triplet state normally predominates. Only by cooling the sample down to low temperatures and rigidifying it to inhibit such processes, the phosphorescent light is observable.

In the case of photoluminescence the proportion of triplet and singlet formed depends upon the relative magnitude of raditive rate constant of singlet state, k_r^S, and rate constant for a non-radiatively relaxation patways from $S_1 \rightarrow T_1$ called interystem crossing, k_{ISC}. Irrespectively of the triplet yield, once formed, the radiative rate constant of the triplet state, k_r^T, is normally low. If a heavy atom – such as a third transition metal ion – is brought close to the π-system of the molecule, in such a way that there is significant mixing of the orbitals, then k_r^T can be greatly increased due to the large spin-orbit coupling associated with heavy atom. Radiative emission can now compete with deactivating processes allowing phosphorescence to be observed at room temperature.

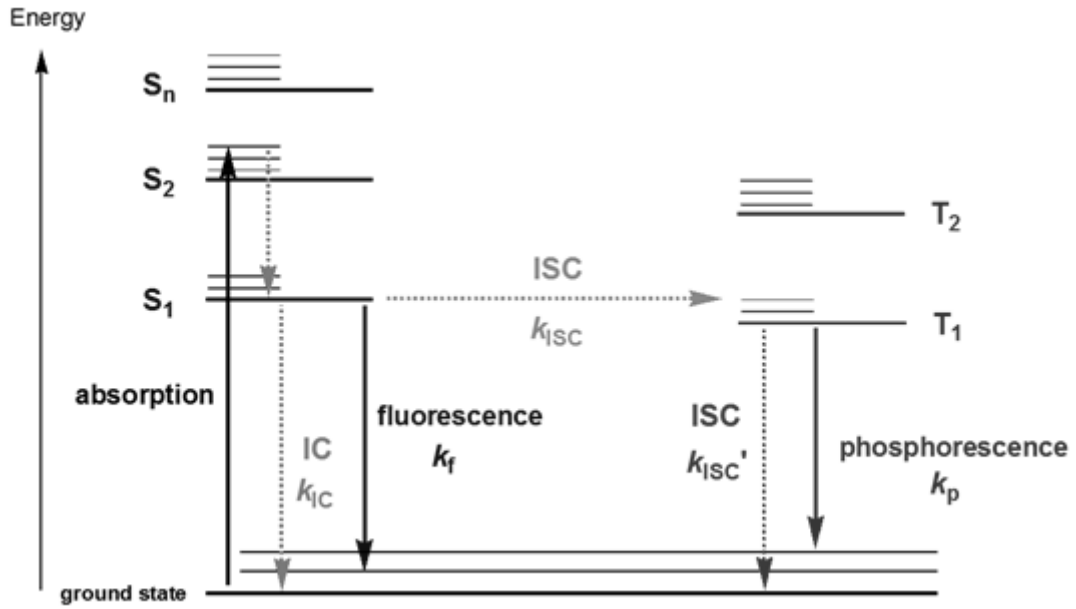

Fig. 1. A simplified Jabloski diagram representing the absorption and emission of energy in an organic molecule such as anthracene. Thick arrow represents absorption of light; dashed ones indicate vibrational relaxation and non-radiative decay. 'IC' represents *Internal Conversion* (an isoenergetic process) followed by vibrational relaxation; similarly 'ISC' represents *Inter System Crossing* followed by vibrational relaxation. The rate constant for key processes are defined in the text.

2. Electroluminescence and OLEDS

Luminescent materials can be found in a broad range of every-day applications such as cathode ray tubes (CRTs), projection televisions (PTVs), fluorescent tubes, and X-ray detectors, to name just few.[1] Besides classical areas of application, the demand for new materials for the vant guard field of light generation – *i.e.* displays and illumination - has generated significant activity in the last decade. Probably the most revolutionary technology for generating light is the direct excitation of organic semiconductors by electrical current in LEDs. The rapidly growing market for this technology is driving both academic and industrial research towards the development of new materials and advanced manufacturing technology. In particular, the demand for novel luminescent materials capable of both withstanding the manufacturing process and exhibiting the desired photophysical properties has generated significant activity in the last decade. Indeed *Organic Ligth-Emitting Diodes* (OLEDs) has been receiving a lot of attention over the world and are already replacing conventional display technologies.[2] In fact, OLEDs offers many appealing advantages such as, for example, selfluminescence which eliminates the requirement for backlighting and

allows thinner, lighter and more efficient displays than liquid crystal (LC). Besides in OLED light is emitted only from the required pixels rather than the entire panel, thus reducing the overall power consumption to 20 – 80% of that of LCDs.[3] Finally, OLED displays are aesthetically superior to LCDs providing truer colours, higher contrast and wider viewing angles.

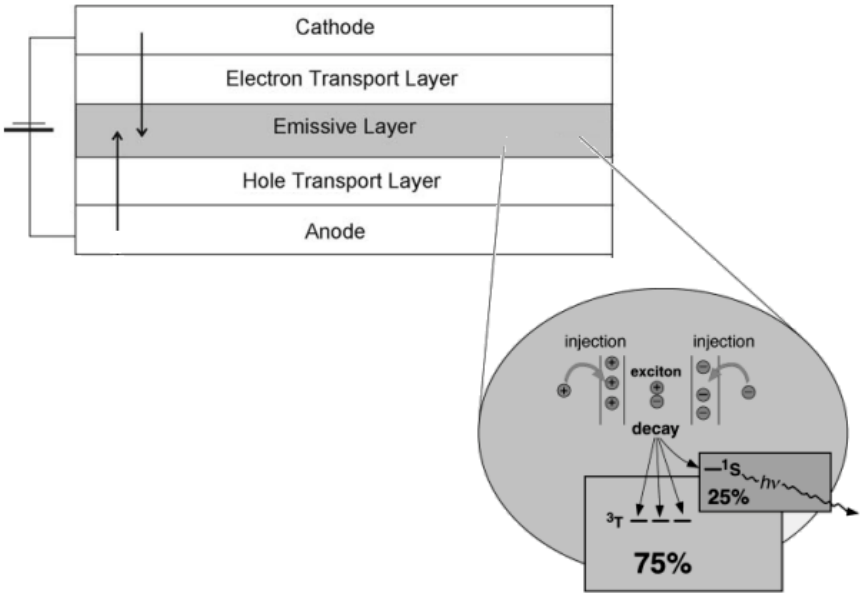

Figure 2. Schematic diagram of an electroluminescent device. Bottom: magnified illustration of the key process of light generation in the device.

Although electroluminescence for organic compound had already been observed by *Pope et al.* in 1963 the development of devices that can exploit this phenomenum was rather slow because of the high voltage required and the low efficiency.[4] In 1987 Tang and Van Slyke of Eastman Kodak Company presented what is considered the first organic light-emitting devices.[5] It was fabricated by vapour deposition of tris(8-hydroxyquinolate)aluminum, Alq_3, and a diamine (Fig. 3) in a double layer structure. Three years later Friend's group at Cambridge University develop a LED based on polymer (PLED) whose efficiency reached 0.05%.[6] A recent breakthrough using phosphorescent luminophores has demonstrated the possibility to make highly efficient organic electroluminescent devices.[7]

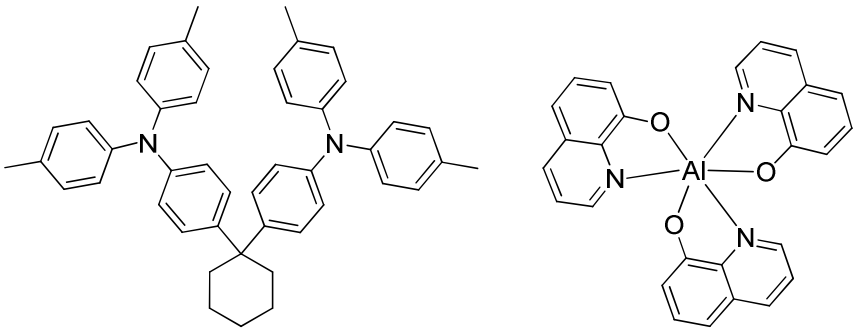

Figure 3. Schematic structure of tris(8-hydroxyquinolate)aluminum (Alq_3) e 1,1-bis(4-di-p-tolylaminophenyl) cyclohexane (Diamine)

Briefly OLEDs consist of a thin layer of emissive material incorporated between two electrodes. The anode is typically a transparent blend as indium tin oxide (ITO) while the metallic cathode is usually made of Mg–Ag or Li–Al. Fig. 2 illustrates a typical multilayered OLED. In these devices, holes and electrons are injected from the electrodes into opposite surfaces of a planar multilayer organic thin film. Under the influence of an electric field, holes and electrons migrate through the thin film, to a material interface, where they recombine to form neutral bound excited states, or excitons, whose relaxation to the ground state results in the emission of light.

The organic layers typically comprise a hole transport layer (HTL) that transport holes from the anode to the emitting layer; an electron transport layer (ETL) which is used to transport electrons from the methal catode to the emitting layer; and, in state-of-the-art devices, an exciton blocking layer, such as 2,9-dimethyl-4,7-diphenyl-1,10-phenanthroline (BCP), which confines excitons within the organic emitting layer improving the electroluminescence quantum efficiency.[8] The organic emitter is either deposited directly between the conducting layers or more commonly doped into the ETL, typically tris(8-hydroxyquinolate)aluminum (Alq_3) (Fig. 2). In devices where the organic emitter is doped in a host polymer layer, excitons formation occur in the polymer layer and excitation energy must be efficiently transferred to the excited states of the dopant molecules, which then relax radiatively to the ground state. The key point to operate OLEDs is to control the excitons so that holes and electrons meet in the emissive layer in equal quantities.

In contrast to photoluminescence, in electroluminescence both singlet and triplet excited states (*i.e.* excitons) are formed directly, and their proportion is governed primarily by the spin-statistics of charge carrier recombination, leading to a theorethical 1:3 (S:T) ratio.[9] This implies a limitation of 25% for the internal quantum efficiency for OLEDs based on a purely organic emitting-layer – where where excitons are restricted to singlet by spin conservation. The remaining furnished energy simply goes wasted into heatign up the device. As noted above, the introduction of a heavy metal ion onto conjugated organic molecule enhances

triplet formation. Thus, OLEDs can be fabricated that utilize all of the electrogenerated singlet and triplet excitons, thereby approching an internal efficiency of 100%.[10] Nevertheless device efficiency rarely reaches to this theoretical maximum. This is in part due to the long lifetime of the triplet excited state which results in severe triplet-triplet annihilation particularly at high currents and doping concentrations (Eq.1) where M represents the molecular dopant.[7a]

$$4(^3M^* + {}^3M^*) \rightarrow {}^1M^* + 3\ {}^3M^* + 4M \qquad \text{Eq.1}$$

In practice to obtain any advantage over fluorescence emitters phosphors emission quantum yield – *i.e.* ratio of emitted over absorbed photons - should be at least 25% at 298 K and lifetime in the region of 5-50 μs.[2a]

Emission wavelength is another crucial requisite. For full colour displays, efficient OLEDs emitting the three primary colours, blue (~ 450–470 nm), green (~ 500–550 nm) and red (~ 650–700 nm), are required. A critical parameter to define the colour quality of a display are the *Commission Internationale d'Eclairage* (CIE) chromaticity coordinates. From CIE coordinates in the diagram illustrated in Fig. 4 not only colour itself but also color saturation can be derived. The latter is highly important in display applications where the three primary colors have to be as saturated as possible – *i.e.* CIE have to be positioned close to the borders of the color triangle. Up to date red and green emitters for OLEDs have been readily identified, however blue emitters remain more challenging due to the large energy gap required between the excited triplet and ground states to obtain this emission wavelength.

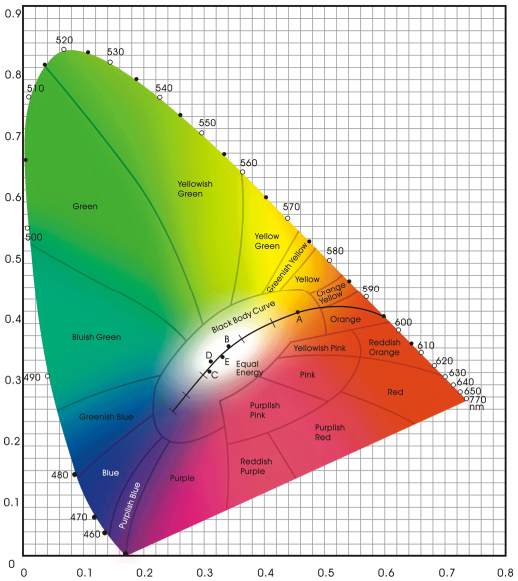

Figure 4. chromaticity diagram of colour coordinates (CIE).

3. Structural Classes Exhibiting Room-Temperature Phosphorescence: Transition Metal Complexes

The demand for novel luminescent materials capable of both withstanding the manufacturing process and exhibiting the desired photophysical properties has generated significant activity in the last decade. Concerning OLEDs, dopants containing organometallic systems offer a series of advantages with respect to purely organic emitting layers. For example the mixing of the singlet and triplet excited states, via spin-orbit coupling, removes the spin-forbidden nature of the radiative relaxation of the triplet state, leading to high phosphorescence efficiencies. Besides, organometallic molecules are more easily sublimable than high molecular weight polymer, being comparatively smaller, leading to a semplification in devices fabrication. Moreover the presence of a metal centre leads to the formation of new bands due to the mixing of the orbitals centered on the metal and those of the ligands. Thus, with judicious ligand selection it is possible to design a series of complexes where the identity of the emitting state is predetermined.[11] This is particularly important when designing new luminescent materials with a specific application in mind.
There are four types of electronic states or transitions expected for transition metal complexes (Fig. 5).

(i) dd states (metal-centred (MC) transition): Upon ligand coordination the metal d orbitals are split. Excited d-d states arise from promotion of an electron within d orbitals which are essentially confined to the metal centre.

(ii) dπ* states (metal-to-ligand-charge-transfer (MLCT)): These involve excitation of a metal centred electron to a π* anti-bonding orbital located on the ligand system.

(iii) π,π* or n,π* states (intraligand (IL) transition): Promotion of an electron from a π - bonding or non-bonding orbital to a higher energy anti-bonding orbital gives rise to these states.

(iv) πd states (ligand-to-metal-charge-transfer (LMCT)): These states arise from the transfer of electronic charge from the ligand π system to a metal centred orbital.

Furthermore metal complexes offers a set of coordination geometries and a range of binding strenght as well as the presence of distinct redox centers on metal and ligand.

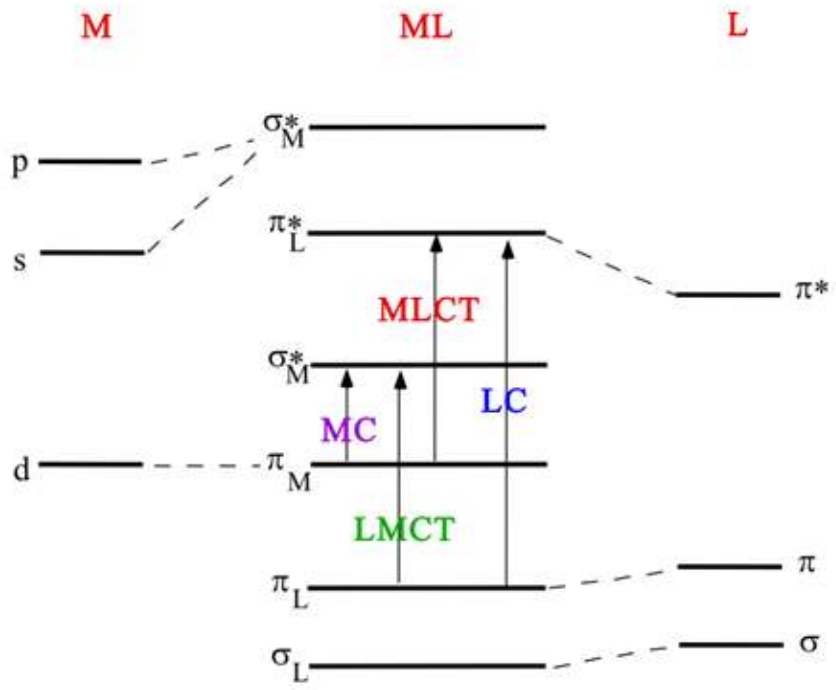

Figure 5. Schematic representation of electronic transitions expected for transition metal complexes (details in the text). M and L are, respectively, metal and ligand molecular orbital while ML are those of the complex.

4. Pt(II) Complexes as Triplet Emitter for OLEDs

In the search for novel phosphorescent materials organometallic complexes of Pt(II) has been widely invesigated[7a,12] due to the high spin–orbit coupling constant of the platinum nucleus (χ= 4481 cm^{-1}).[13] Thus emission could theorically emanate from states of exclusively triplet character so that unitary efficiency can be approached. However the validity of this assumption depends on the extent of the contribution of metal orbitals to the excited states. For excited states involving significant metal character, radiative rate constant of triplet emission is accelerated by factors up to 10^6. On the contrary, when the excited state is localised on a remote part of the ligand well removed from the metal centre, ligand-vased singlet fluorescence may be observed.[14] Equally important is the need to minimise the rate of non-radiative decay. The strong preference of Pt(II) complexes to be square planar, owing to ligand field stabilisation, results in the unoccupied $d_{x^2-y^2}$ orbital being strongly antibonding. Population of this orbital will be accompanied by elongation of Pt–L bonds and severe distortion, promoting non-radiative decay of metal-centred (d–d) excited states to the ground state at the isoenergetic crossing point of the potential energy surfaces. Even if

excited states of different character, such as MLCT (d–π*) or LC (π–π*) states, lie at lower energies than the d–d states, the latter can still exert a deleterious influence if they are thermally accessible (Fig. 6). This is the reason why until the late 1980s no square planar platinum complexes were reported to be emissive in room temperature solution.

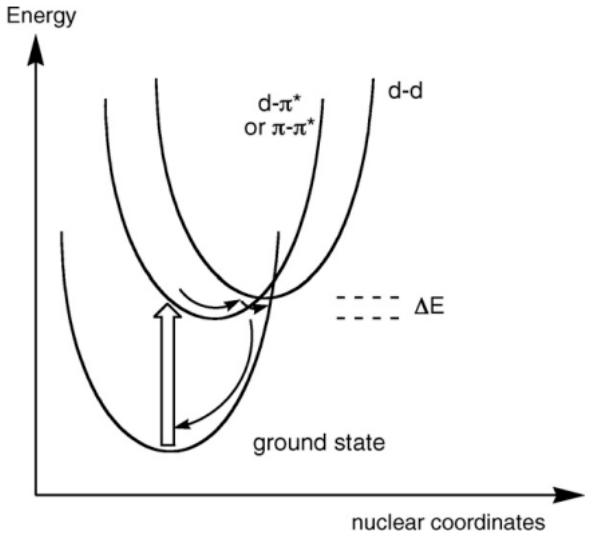

Figure 6. The potential energy surface of the d–d excited state in Pt(II) complexes is displaced relative to the ground state. d–π* or π–π* are other states at lower energy. Thick arrow represents absorption of light; thin ones indicate vibrational relaxation and non-radiative decay.

In order to overcome this problem it is necessary to utilize ligands - or co-ligands - with low-lying excited state or/and a large electron donor ability. The strong ligand field associated with such ligands raises the energies of d-d state making them thermally inaccessible. The substitution of weak-field halide ligands by strong-field cyanides provides an example of how an increase in the ligand field strength of the ancillary ligand promotes luminescence: several [Pt(N^N)$(CN)_2$] complexes emit in solution at room temperature, whereas the corresponding chloro complexes normally do not; *e.g.* for Pt(5,5'-Me2-bpy)$(CN)_2$, $\Phi_{lum} \sim 10^{-3}$,[15] and for $[Pt(tpy)CN]^+$, $\Phi_{lum} = 4 \times 10^{-4}$.[16] Acetylide co-ligands, R–C≡C–, proved to be more successful, and a large number of platinum(II) di- and tri-imine complexes containing two or one acetylides, respectively, have been discovered over the past decade that are luminescent at room temperature. In fact the R–C≡C– ligands are strongly donating, more, for example, than CN^-, which helps to ensure significant metal character in the HOMO, and hence larger radiative rate constants k_r^T. Overall, therefore, such complexes are often emissive in fluid solution at room temperature.[17] A further strategy is to make use of cyclometallating ligands – where a polydentate ligand binds the metal via a covalent bond – whose ligand-field strength is augmented, for example, with respect to bipyridine and

terpyridine even without the need for specific co-ligands. In fact, luminescnce under ambient conditions is observed from many cyclometalated ligand complexes, such as 2-phenylpyridine and its anolgue. In this case the ligating "carbon anion" acts as a very strong σ donor whilst the pyridyl group remains a good π-acceptor. The strong ligand field influence of the aromatic carbon atom, along with the added stabilization of σ donation from the metal into the aromatic ring, helps to make these types of chelates very stable, while concurrently increasing the energy gap of the MC excited states. The use of rigid systems allowed to further enhance luminescence over non-radiative decay pathways.[12f] For example terdentate ligands offer an advantage over bidentate ligands since their additional rigidity inhibits the D_{2d} distortion that bis-bidentate complexes can undergo - through twisting of the two planes relative to one another. Much work has been made on cyclometalated platinum (II) complexes with NˆNˆC-coordinating ligands.[18] The simplest example of such ligands is 6-Phenyl-2,2'-bipyridine (phbpyH), originally shown by Constable,[19] whose Pt(II) chloro complex exhibit an emission quantum yield of 2.5% under ambient conditions. The chloride ligand in [Pt(NˆNˆC)Cl] complexes can be readily displaced by other ligands, such as for example the afore mentioned R–CΞC– ones. Thus, Che and co-workers have carried out a comprehensive study of [Pt(NˆNˆC)(–CΞC–R)] complexes (Fig. 7), in which over 30 derivatives were prepared containing acetylides in the fourth coordination site.[20] Combining the benefits of terdentate cyclometallation with those associated with acetylide co-ligands and the rigidity of the terdentate ligand, an increased efficiency in luminescence was otained compared to the parent platinum chloro complex (quantum yields typically in the range 5%–10%). The origin of the luminescence has been assigned as derived from states of ^{3}MLCT [dπ→ π*] character, with some mixing of a [π(CΞC)→π*] ^{3}LLCT character. The thermal stability and sublimability of these complexes renders them appropriate for incorporation into the emissive layer of vapour-deposited OLEDs.[20]

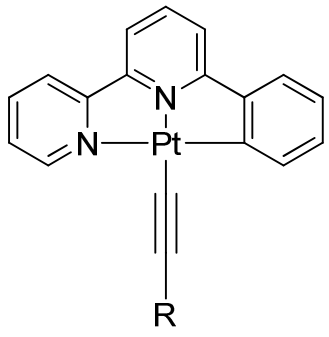

R = Ph, *p*-C_6H_5-Me, C_6F_5, ^{t}Bu

Figure 7. Schematic structure of [Pt(NˆNˆC)(–CΞC–R)] complexes.

4.1. Pt(N^C^N) Complexes

Recently Williams *et al.* reported an interesting series of Pt(II) complexes based on the 1,3-di(2-pyridyl)benzene (dpybH) structure, in which the cyclometallating phenyl ring occupies the central position, hence offering the metal an NˆCˆN environment (Fig. 8).[21] Structurally, this leads to shorter Pt–C bonds than in the isomeric NˆNˆC systems (about 0.14Å shorter); and indeed, exceptionally high phosphorescence quantum yields (Φ_{lum} = 0.58–0.68) were obtained, which are much higher than those previously reported for cyclometalated Pt(II) complexes. These complexes show intense green luminescence (λ_{em} = 480 – 580 nm) in solution, attributed to emission primarily from a $^3\pi$–π^*.

The excited state energy is influenced by substituents on the central phenyl and/or lateral pyridyl rings. Indeed DFT calculations revealed that the HOMO in this series of complexes is largely based on the metal and the cyclometallating ring, whereas the LUMO is essentially localized on the pyridyl rings.[22]

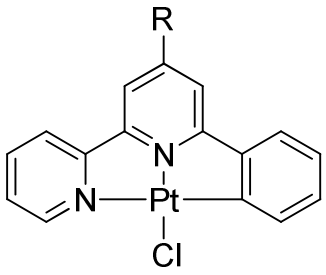

R = H, Me, CO_2Me

Figure 8. Schematic structure of [Pt(NˆNˆC)(–CΞC–R)] complexes.

Thus, the introduction of electron-releasing aryl groups at the 4-positin on the phenyl serves to increase the energy of th HOMO but not the LUMO shifting the emission increasingly to the red according to their electron-donating ability (Fig. 9).[21] Conversely, the electron-donating methoxy groups on the pyridyl rings have the effect of raising the LUMO energy so that emission wavelenght is shifted towards blue.[22]

Due to their remarkable luminescence properties thiss class of compelxes has been used in the fabrication of vapour-deposited OLED, whose external electroluminescence quantum efficiencies of 4–20% photons/electron and luminous efficiencies of 15 – 40 cd A^{-1} were achieved using this device structure, which were maintained over a 104 range in current density without suffering the high-current “roll-off” that is frequently observed.[22,23]

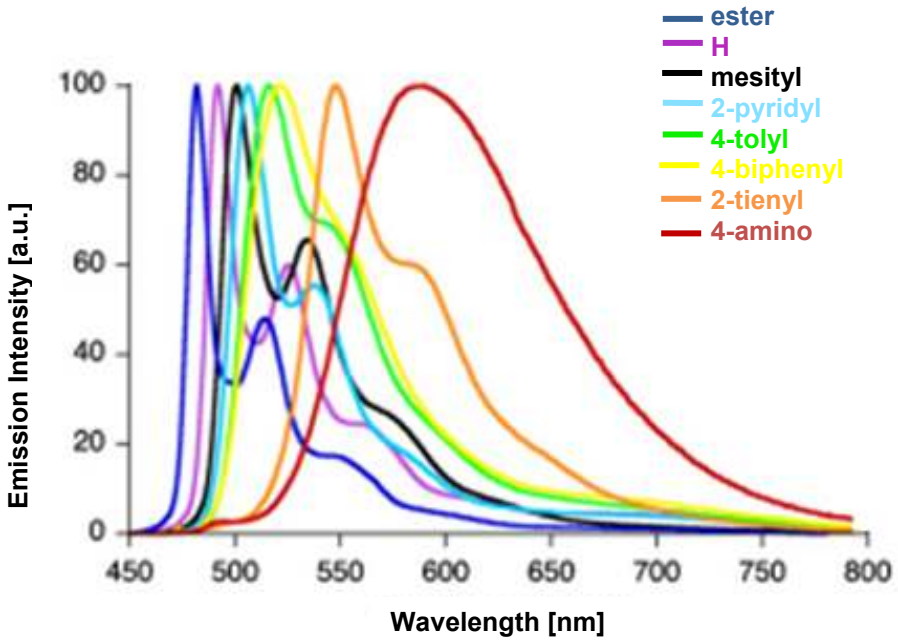

Figure 9. Emission spectra of 4-substituted NˆCˆN-coordinated complexes as in ref. 21 in dichloromethane at rt, excitation wavelength, λ_{ex} = 400 nm.

4.2. Excimer

Sterically unencumbered platinum(II) complexes are frequently susceptible to self-quenching at elevated concentrations or in film. This phenomenon has been well known since Che and co-workers reported concentration dependence of the emission intensity for the complex Pt(5,5'-dimethyl-2,2'-bipyridine)$(CN)_2$.[15] Other researchers have reported similar self-quenching for different platinum systems, along with the observation of weak excimer emission at elevated complexes concentrations.[15, 24] An excimer is a dimeric species that is formed from the weakly attractive interaction of a ground-state molecule with an identical molecule in its excited state. This results in a stabilisation of the excited state so that excimer emission is red-shifted compared to the isolated monomer. It is important to note that true excimers exist only in the excited state, since the potential energy surface is repulsive in the ground state, and no vibrational structure is observed. The mechanism used to explain the concentration dependent quenching process involves initial formation of the excited complex, M*, followed by its wavefunction ovelapping with a ground state complex to give an emissive excimer, [M,M]*.[25] This latter process is clearly dependent on the concentration of the metal complex. The model is identical to one used to describe the monomer/excimer fluorescence

kinetics of planar aromatic hydrocarbons like pyrene. Thus, the diffusion controlled self-quenching rate constants have been determined for a number of platinum complexes by monitoring the self-quenching reactions of the platinum complex as a function of concentration. Direct characterization of these platinum excimers, however, has been less documented due to limited solubility of the complexes, as well as weak emission and short lifetimes for the excimers.[24] Remarkably, in the case of N^C^N-coordinated complexes the excimers are intensely emissive, with quantum yields of excimer luminescence around 35% and emission wavelenght usually centred around 700 nm.[26] This feature is quite relevant in view of potential application in communications, biomedicine, and in optoelectronic devices operating in the near-infrared (NIR) spectral range.

Platinum (II) complexes are also well-known to undergo ground-state aggregation, often through overlap of the d_{z^2} orbitals that are orthogonal to the plane of the complex, an effect that was widely investigated in the 1970s and 80s for one-dimensional conductivity.[27] Such aggregates may themselves display red-shifted emission similar to that of the excimers in solution.[28, 29] The distinction between excimers and ground-state aggregates is sometimes clear-cut; for example, the latter may display low-energy absorption bands that are not present in the spectra of the isolated molecules in dilute solution.[30,31] Moreover, the emission of an aggregate tends to shift to lower energy with a decrease in temperature or increase in pressure, as the interaction between the molecules becomes stronger. [32] However, the nature of bi-molecular emissive states is still a challenging question concerning all planar organometallic platinum complexes.[22]

4.3. White OLED

Whilst high colour-purity dopants are required for full colour displays, the impetus for developing WOLEDs arises from the need for more economical alternatives to conventional incandescent bulbs and fluorescent tubes that currently dominate lighting. Among methods for producing white light, elctrophosphorescence stands out as the most effective mechanism for OLED emission due to its demonstrated potential for achieving 100% internal emission efficiency.[33] Several approaches have been used to generate white light in OLEDs.[34, 35] One involves the combination (either in mixed or separate layers) of three different dopants - red, green and blue - located within the emission zone of the device. By this approach a high *Color Rendering Index* (CRI) – i. e. the ability to display the colour of an irradiated object in a

natural way -is obtained necessary for lighting applications (for high-quality white-lighting source CRI above 80% is required). However, this strategy can be problematic due to different efficiencies of energy transfer to each dopant in the mix, leading to an imbalance in the white colour, or pronounced variations in colour with brightness. Segregation of the emitters into different layers can circumvent this problem, but at the expense of necessitating a more elaborate device architecture.[36] Furthermore, using multiple emissive dopant can lead to differential aging of the various chromophores. Hence, if one of the lumophore degrades at a different rate from the others, the colour coordinates of the device will shift over time.

One promising approach, proposed by Thompson and Forrest, to reducing the number of dyes and structural heterogenities inherent in the multiple layer architecture is to employ a lumophore that emitts simultaneously from monomer and excimer states. Hence by using only one, or at most two dopants, coverage of the entire visible spectrum is achieved with an electrophosphorescent excimer OLED. Square-planar Pt(II) complexes that emit from excimer or aggregate states are essentially ideal for this purpose.[37] Thus, with an emissive region doped with (4,6-dFppy)Pt(acac) (Fig. 10) otimized external power efficiency (η_{ext}) between 2 - 4% were reached.[37]

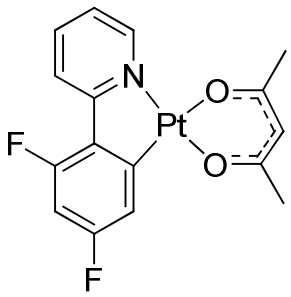

Figure 10. Schematic structures of (4,6-dFppy)Pt(acac).

To achieve efficient excimer emission from a doped layer, control of the dopant concentration is crucial. For example (4,6-dFppy)Pt(acac) showed bluish-green monomer emission in a 10^{-6} M solution of dichloromethane, and orange-red excimer emission in a concentrated 10^{-3} M solution. By adjusting the relative amount of blue and red emissive species, the colour of the light emission is tuned from bluish-green through green and white up to red. Beyond the inherent simplicity of this particular approach is the possibility for reduced differential colour aging in single dopant excimer devices. Given that only a single species is responsible for emission, it is anticipated that the colour coordinates will not shift with the device age.

This strategy was also applied by Cocchi *et al.* to N^C^N-coordinated Pt(II) systems which resulted in high purity white with remarkably high external quantum efficiency (EL QE

=12%).[22] Unfortunately the camel-shaped spectrum leads to a through of low emission intensity between the monomer and excimer regions, making the coverage across the visible less uniform than might be desiderable. Kalinowski et al. have found that this problem can be overcome by “filling in” this region with emission from an exciplex (Fig. 11).[38]

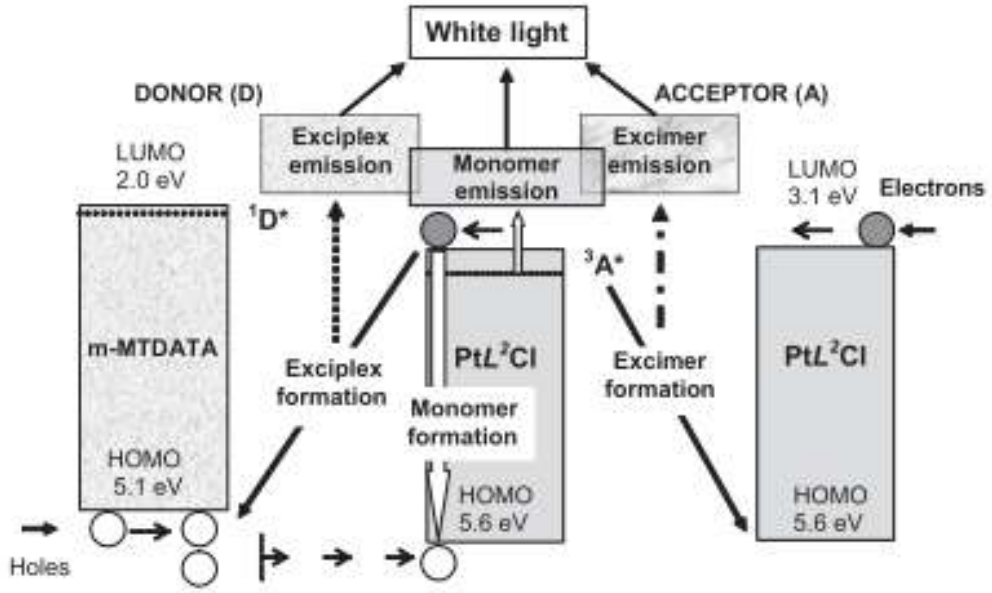

Figure 11. Proposed mechanisms for generation of white light in an organic LED based on a hole transporting material (m-MTDATA) acting as an electron donor (D) to an electron acceptor (A) molecule of the organic phosphor [methyl-3,5-di-(2-pyridyl) benzoate] chloride, (PtL^2Cl) mixed in an emissive layer, D:A (1:1). Details on the mechanism are given in the text.

In the emitting region, a starbust amine hole-transporting material acts as an electron donor (D) to an electron acceptor (A) molecule of an organic phosphor mixed in an emissive layer (D : A). The monomer phosphor triplets, ^{3}A*, their combination with the ground state phosphor acceptor molecules, *i.e.* excimers ^{3}(AA)*, and excited heterodimers, *i.e.* exciplexes ^{3} (DA)*, are generated throughout the emissive layer leading to white light with colour rendering indices up to 90.[38]

5. Film processing

Thin-film coating plays a prominent role in manufacture of optoelectronic devieces. The choice of deposition technique may, in many cases, be arbitrary depending mostly on what technology is available at the time of manufacturing. In the following paragraphs two of the

most-wide spread techniques for film deposition are briefly described, which had been actually used in the fabrication of the OLED presented in section: Electro-luminescence.

5.1. Spin-Coating

Spin-coating (or spin-casting), illustrated in the figure below, is relatively simple and economical solution process. The material to be deposited, usually polymer and/or small molecules, is dissolved in a solvent whose evaporation eventually leads to the formation of a thin film on the substrate. The substrate spins at high speed, typically around 3000 rpm, so that centripetal acceleration cause a spread of the solution allowing to obtain film thickness of 10μm independently on the initial amount of solution. Final thickness and other properties of the film depend on the nature of the solution itself (viscosity, drying rate, percent solids, surface tension, etc.) and the parameters chosen for the spin process. Spin-coating allows to achieve good film uniformity and reproducibility, on the other hand it inevitably entails a large wastage of organic materials.

.

Figure 12. The spin casting process

5.2. Vacuum Thermal Evaporation

When a material is non soluble processing associated with vacuum technologies are used. *Physical Vapor Deposition* (PVD) comprise a number of deposition technologies in which material is released from a source (atom-by-atom, molecule-by-molecule, or ion) and transferred to the substrate. One of them is *Vacuum Thermal Evaporation* (VTE) deposition

technique which consists in heating, under high vacuum, the material to be deposited until sublimation. The material vapor finally condenses to form a thin film on the cold substrate surface. Typically pressures about 10^{-7} or 10^{-5} Torr are used. At these low pressures, the mean free path of vapor atoms is the same order as the vacuum chamber dimensions, so that evaporated molecules travel in straight lines towards the substrate. The film morphological order is affected by substrate temperature and growth rate, this latter controlled by tuning the source boat temperature. This technique is often used in producing thin, 5 μm, coating but it also allows to obtain very thick, 1mm, layers of heat-resistant materials, such as MCrAlY which is a metal alloys - chromium, aluminum, and yttrium. Indeed vacuum techniques are largely employed for deposition of metals. Thickness of stacked layers can be closely monitored by means of a crystal microbalance.

This technology allows a good control of film deposition and is particularly appropriate for multilayer deposition and co-deposition of organic material. However, it requires complex and expensive equipment.

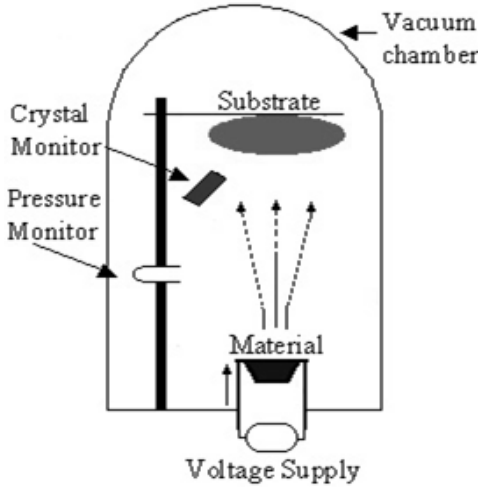

Figure 13. The vacuum thermal evaporation process.

References

[1] Jüstel, T.; Nikol, H.; Ronda, C. *Angew. Chem. Int. Ed*, **1998**, *37*, 3084.

[2] for example see: *(a)* Evans, R.C.; Douglas, P.; Winscom, C. J. *Coord. Chem. Rev*., **2006**, *250*, 2093. *(b)* Malliaras, G.; Friend, R. *Phys. Today*, **2005**, *14(5)*, 53. *(c)* Bergh, A.; Craford, G.; Duggal, A.; Haitz, R. *Phys. Today*, **2001**, 54(12), 42. *(d)* Holder, E.; Langeveld, B. M. W.; Schubert, U. S. *Adv. Mater.*, **2005**, *17*, 1109. *(e)* Sun, Y. R.; Giebink, N. C.; Kanno, H.; Ma, B. W.; Thompson M. E.; Forrest, S. R. *Nature*, **2006**, *440*, 908. *(f)* Slinker, J.; Bernards, D.; Houston, P. L.; Abruña, H. D.; Bernhard, S.; Malliaras, G. G. *Chem. Commun.*, **2003**, 2392.

[3] Borchardt, J.K. *Mater. Today,* **2004**, *7,* 42.

[4] Pope, M.; Kallmann, H.P.; Magnate, P. *J. Chem. Phys*. **1963**, *38*, 2042.

[5] Tang, C. W.; Van Slyke, S. A. *Appl. Phys. Lett.* **1987**, *51*, 913.

[6] Burroughes, J. H.; Bradley, D. D. C.; Brown, A. R.; Marks, R. N.; Mackay, K.; Friend, R. H.; Burn, P. L.; Holmes, A. B. *Nature* **1990**, *347*, 539.

[7] *(a)* Baldo, M. A.; O'Brien, D. F.; You, Y.; Shoustikov, A.; Sibley, S.;Thompson, M. E.; Forrest, S. R. *Nature* **1998**, *395*, 151. *(b)* Lamansky, S.; Djurovich, P.; Murphy, D.; Abdel-Razzaq, F.; Lee,H.-E.; Adachi, C.; Burrows, P. E.; Forrest, S. R.; Thompson, M. E. *J.Am. Chem. Soc*. **2001**, *123*, 4304.

[8] *(a)* Kwong, R.C.; Nugent, M.R.; Michalski, L.; Ngo, T.; Rajan, K.; Tung, Y.-J. ; Weaver, M.S.; Zhou, T.X.; Hack, M.; Thompson, M.E.; Forrest, S.R.; Brown, J.J. *Appl. Phys. Lett*. **2002**, *81*, 162; *(b)* Ikai, M.; Tokito, S.; Sakamoto, Y.; Suzuki, T.; Taga, Y. *Appl. Phys. Lett*. **2001**, *79,* 156 ; *(c)* Adachi, C.; Baldo, M.A.; Thompson M.E.; Forrest, S.R. *J. Appl. Phys*. **2001**, *90,* 5048 ; *(d)* Li, F.; Zhang, M.; Cheng, G.; Feng, J.; Zhao, Y.; Ma, Y.G.; Lui, S.Y.; Shen, J.C. *Appl. Phys. Lett.* **2004**, *84*, 148.

[9] Baldo, M. A.; O'Brien, D. F.; Thompson, M. E.; Forrest, S. R. *Phys. Rev. B* **1999**, *60*, 14422.

[10] *(a)* Baldo, M. A.; Lamansky, S.; Burrows, P. E.; Thompson, M. E.; Forrest, S. R. *Appl. Phys. Lett.* **1999**, *75*, 4 ; (b) Adachi, C.; Baldo, M. A., Forrest, S. R.; Thompson, M. E. *Appl. Phys. Lett.* **2000**, *77*, 904.

[11] Crosby, G.A. *Acc. Chem. Res.,* **1975**, *8*, 231.

[12] For reviews, see for example: (*a*) McMillin, D.R.; Moore, J. J. *Coord. Chem. Rev.*, **2002**, *229*, 113; (*b*) Lai, S.-W.; Che, C.-M. *Top. Curr. Chem.*, **2004**, *241*, 27; (*c*) Ma, B.; Djurovich, P.; Thompson, M. E. *Coord. Chem. Rev.*, **2005**, *249*, 1501; (*d*) Castellano, F. N.; Pomestchenko, I. E.; Shikhova, E.; Hua, F.; Muro, M. L.; Rajapakse, N. *Coord. Chem. Rev.*, **2006**, *250*, 1819; (*e*) Wong, K. M.-C.; Yam, V. W.-W. *Coord. Chem. Rev.*,

2007, *251*, 2477; (*f*) Williams, J. A. G.; Develay, S.; Rochester, D. L.; Murphy, L. *Coord. Chem. Rev.*, **2008**, *252*, 2596.

[13] Murphy, L.; Williams, J. A. G. in *Topics in organometallic chemistry 28*, *Molecular Organometallic Materials for Optics*, H. Le Bozec, and V. Guerchais (eds.), Springer Verlag Berlin Heidelberg **2010**, pp 75-111.

[14] Michalec, J.F.; Bejune, S.A.; McMillin, D.R. *Inorg. Chem*. **2000**, *39*, 2708.

[15] Che, C.-M.; Wan, K.-T.; He, L.-Y.; Poon, C.-K.; Yam, V.W.-W. *J. Chem. Soc. Chem.Commun.* **1989**, *943*.

[16] Wilson, M.H.; Ledwaba, L.P.; Field, J.S.; McMillin, D.R. *Dalton Trans.* **2005**, 2754.

[17] (*a*) Yam, V. W.-W.; Tang, R. P.-L.; Wong, K. M.-C.; Cheung, K.-K.; *Organometallics* **2001**, *20*, 4476; (*b*) Pomestchenko, *I.E.*; Luman, C.R.; Hissler, M.; Ziessel, R.; Castellano, F.N. *Inorg. Chem.* **2003**, *42,* 1394; (*c*) Hua, F.; Kinayyigit, S.; Cable, J.R.; Castellano, F.N. *Inorg. Chem.* **2006**, *45*, 4304.

[18] Whittle, V. L.; Williams, J. A. G. *Inorg. Chem.,* **2008**, *47*, 6596.

[19] King, K. A.; Watts, R. J. *J. Am. Chem. Soc.*, **1987**, *109*, 1589.

[20] Lu,W.; Mi, B.-X.; Chan, M. C. W.; Hui, Z.; Che, C.-M.; Zhu, N.; Lee, S.-T. *J. Am. Chem. Soc.,* **2004,** *126,* 4958.

[21] Farley, S. J.; Rochester, D. L.; Thompson, A. L.; Howard, J. A. K.; Williams, J. A. G. *Inorg. Chem.* **2005**, *44*, 9690.

[22] Cocchi, M.; Kalinowski, J.; Murphys, L.; Williams, J. A. G.; Fattori, V. *Organic Electronics*, **2010,** *11,* 388.

[23] Cocchi, M.; Virgili, D.; Fattori, V.; Rochester, D. L.; J Williams, J. A. G. *Adv. Funct. Mater.* **2007**, *17*, 285.

[24] (*a*) Kunkely, H.; Vogler, V. *J. Am. Chem. Soc.* **1990**, *112,* 5625; (*b)* Connick, W.B.; Gray, H.B. *J. Am. Chem. Soc.* **1997**, *119,* 11620; (*c*) Pettijohn, C.N.; Jochnowitz, E.B.; Chuong, B.; Nagle, J.K.; Vogler, A. *Coord. Chem. Rev.* **1998**, *171,* 85;(*d*) Connick, W.B.; Geiger, D.; Eisenberg, R. *Inorg. Chem.* **1999**, *38,* 3264; (*e*) Hissler, M.; McGarrah, J.E.; Connick, W.B.; Geiger, D.K.; Cummings, S.D.; Eisenberg, R. *Coord. Chem. Rev*. **2000**, *208*, 115; (*f*) Williams, J. A. G.; Beeby, A.; Davies, S.; Weinstein, J.A.; Wilson, C.; *Inorg.Chem*., **2003,** *42*, 8609.

[25] Ma, B.; Djurovich, P. I.; Thompson, M. E. *Coord. Chem. Rev*. **2005**, *249,* 1501.

[26] Rochester, D. L.; Develay, S.; Záliš, S.; Williams, J. A. G. Chem. Soc. Rev., 2009, 38, 1783.

[27] Chemistry and Physics of One-Dimensional Metals, ed. J. S. Miller, Plenum Press, New York, 1982.

[28] Houdling V. H.; Miskowski, V. M. *Coord. Chem. Rev*., **1991**, *111*, 145.

[29] Bailey, J. A.; Hill, M. G.; Marsh, R. E.; Miskowski, V. M.; Schaefer, W. P.; Gray, H. B. *Inorg. Chem.*, **1995**, *34*, 4591.

[30] Yam, V. W.-W.; Wong, K. M.-C.; Zhu, N. *J. Am. Chem. Soc.* **2002**, *124*, 6506;

[31] Yu, C.; Wong, K. M.-C.; Chan, K. H.-Y.; Yam, V. W.-W. *Angew. Chem*., Int. Ed., **2005**, *44*, 791.

[32] Connick, W. B.; Henling, L. M.; Marsh, R. E.; Gray, H. B. *Inorg. Chem.*, **1996**, *35*, 6261.

[33] Adachi, C.; Baldo, M. A.; Thompson, M. E.; Forrest, S. R. J. *Appl. Phys. Lett*. **2010,** *90,* 5048.

[34] D'andrade, B. W.; Thompson, M. E.; Forrest, S. R. *Adv. Mater.*. **2001,** *13,* 147.

[35] Feng, S.; Li, F.; Gao, W.; Liu, S.; Liu, Y.; Wang, Y.; . *Appl. Phys. Lett*. **2001,** *78,* 3947.

[36] D'Andrade, B.W.; Forrest, S.R. *Adv. Mater.,* **2004,** *16,* 1585.

[37] D'Andrade, B.W.; Brooks, J.; Adamovich, V.; Thompson, M. E.; Forrest, S. R. *Adv. Mater.* **2002**, *14*, 1032.

[38] Kalinowski, J.; Cocchi, M.; Virgili, D.; Fattori, V.; Williams J. A. G. *Adv. Mater*. **2007**, *19*, 4000.

RESULTS AND DISCUSSION

Owing to their remarkable luminescent properties, organometallic complexes of transition-metals have recently received considerable attention as phosphorescent emitters for *Organic Light Emitting Diodes* (OLEDs).[1, 2] In particular, various platinum(II) complexes with a cyclometallated 1,3-di(2-pyridyl)benzene ligand seem very promising in this respect as suggested by their impressively high luminescence quantum yields.[1] Furthermore in these systems the selection of substituents on both central and lateral rings offers a good versatile method for colour tuning.[3, 4]

These observations prompted us to develop new Pt(II) systems, [PtL^{n}Y], also based on substituted 1,3-di(2-pyridyl)benzene, L^n, with various Y ancillary ligands, [Y= chloride, acetilyde, thiocyanate, phenylthiazole thiol or tetrazole thiol], in order to explore their emission properties. Since it has never been investigated previously, we started studing the effect of a fluorine atom in 4 position on the central phenyl ring, **L^3** (Fig.1). Then, in analogy with cyclometallated phenylpyridine iridium complexes, we synthesised a new ligand which bears CF_3 moieties on the pyridyl rings, **L^4**, and its related Pt complex **[PtL^{4}Cl],** (Fig.1). In fact, it has been reported that the presence of CF_3 substituent in the case of Ir(III) complexes leads to a striking improvement in luminescence efficiency (from 14% for the unsubsituted phenylpyridines to 68% for the CF_3 substituted)[5] and therefore we wondered if CF_3 could have a similar effect on our platinum systems.

As far as ancillary ligands are concerned, we explored the effect of coordination to platinum through sulphur since, surprisingly, it had not been previously investigated. As parent complex was chosen platinum chloride complex of 1,3-di(2-pyridyl)toluene, **[PtL^{1}Cl]** (Fig.1), which was reported as the brightest amongst compounds of this class (Φ_{lum} =68%)[1] and to improve derivatives' solubility we also consider the 4-mesitylated ligand whose platinum(II) chloro complex, **[PtL^{2}Cl] (**Fig.1), was also reported as highly luminescent (Φ_{lum} =62%).[6] Finally since it is known that the strong ligand field associated with alkyne could promote luminescence (see "Introduction" section),[7-10] we also investigated substituted acetylides as other ancillary ligands. As expected, the complexes obtained are in most of the cases strongly emissive in fluid solution at room temperature (Φ_{lum} ranges from 20 - 77%).

In this chapter we first present synthesis and characterization of platinum (II) complexes focusing mainly on their remarkable luminescent properties, and then consider in more detail their application in luminescent devices.

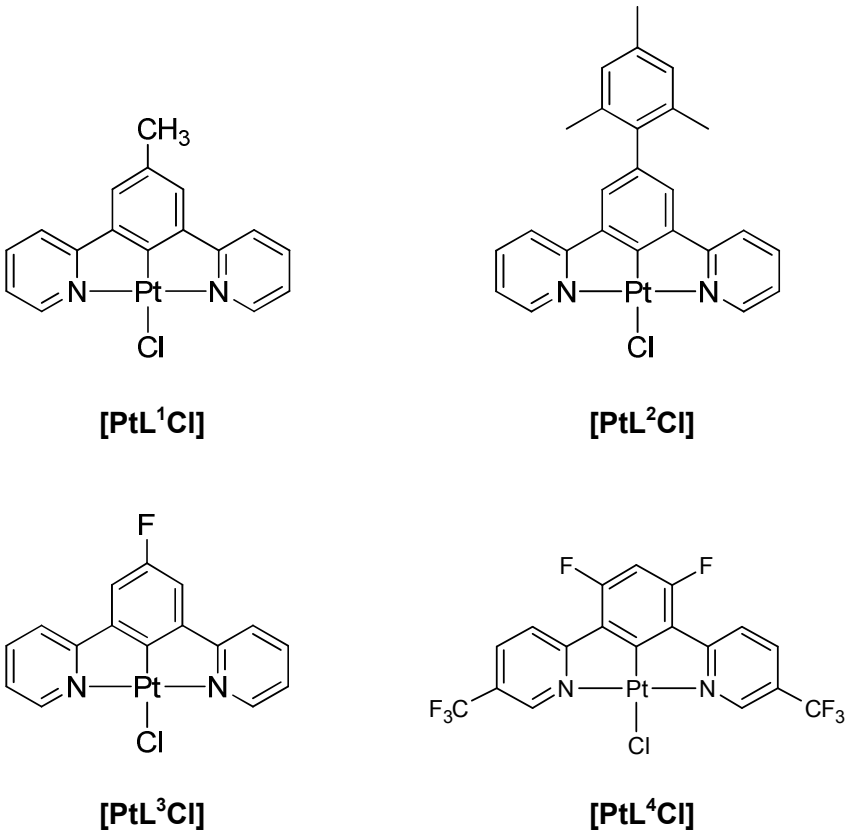

Figure 1: Schematic structure of cyclometallated Pt(II) chloro complexes based on substituted 1,3-di(2-pyridyl)benzene ligands: [**PtL^{1}Cl]**, **[PtL^{2}Cl]**, **[PtL^{3}Cl]** and **[PtL^{4}Cl]**.

6. Synthesis and Characterisation of Complexes.

Here we report comprehensive methods for the convenient preparation of new (N^C^N)-coordinated platinum(II) complexes - where N^C^N refers to a ligand that binds to the metal through two nitrogen atoms and a central metal-carbon bond - as well as of their precursors.

6.1. Synthesis of PtL^{n}Cl compounds

The platinum chloride complexes studied, [PtL^{n}Cl], are shown in Fig. 1, and strategies employed in the synthesis of the related ligands, L^n, are summarized in Scheme 1.

Scheme 1. Preparation of the terdentate ligands, L^n. a) Stille cross-coupling producing $\mathbf{L^1}$, $\mathbf{L^3}$ and the intermediate **dpyb-Br**; b) Suzuki cross coupling to obtain $\mathbf{L^2}$ from **dpyb-Br**; c) Synthetic routes for preparation of $\mathbf{L^4}$. The numbers in these structures designate each carbon atom.

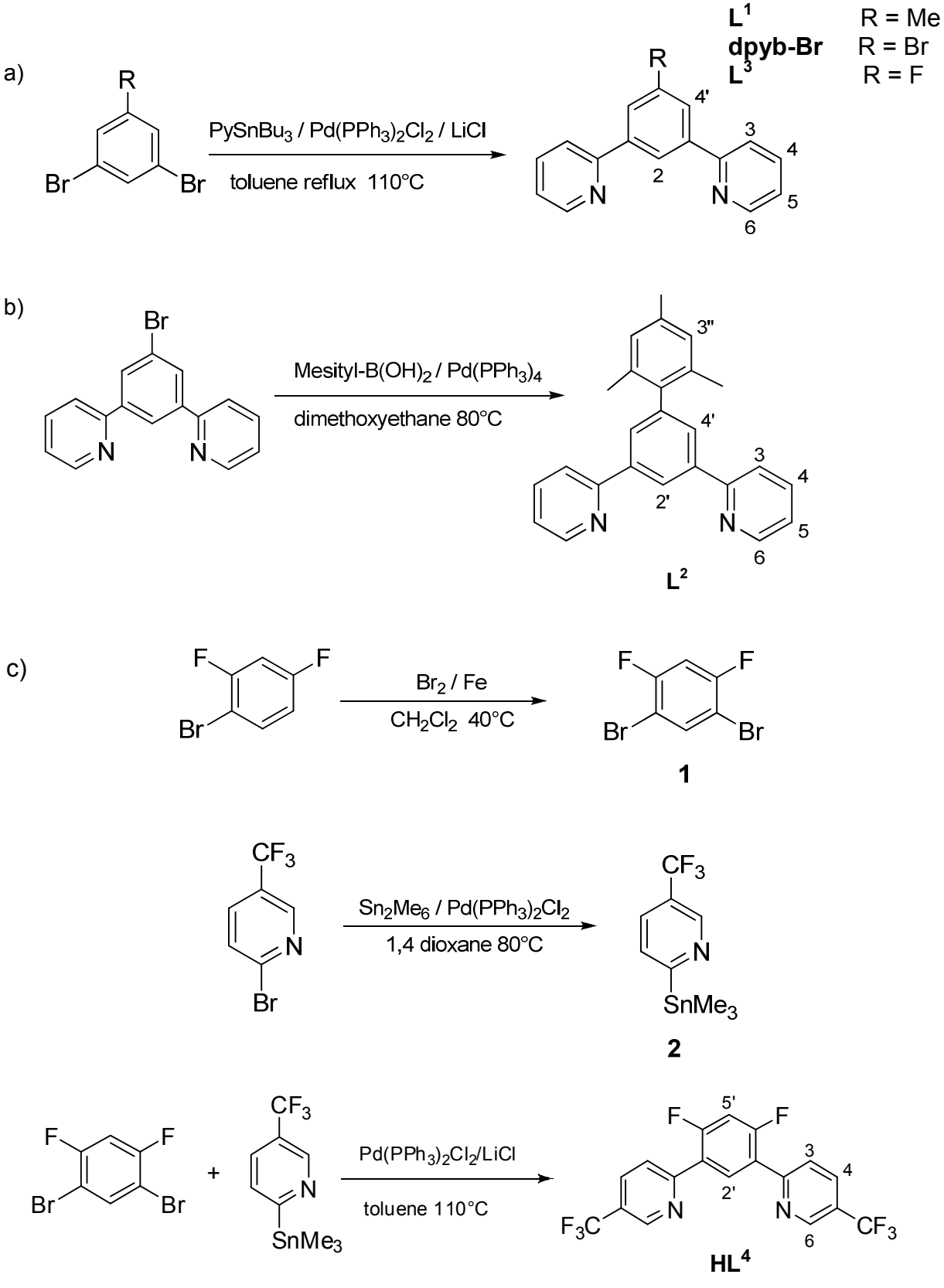

In this work substituents with different steric and electronic properties were introduced on the terdentate ligands. Since ligand **L^1** has been synthesized previously by a palladium-catalyzed Stille cross-coupling reaction,[11] this method was extended to the preparation of ligands **L^2**-**L^4** with minor modifications. Thus, 2-tri-*n*-butylstannyl-pyridine (2.2 equiv) was added to a requisite substituted 1,3-dibromobenzene in toluene in presence of $[Pd(PPh_3)_2Cl_2]$ and LiCl. Subsequently, in order to insert the mesityl substituent, the intermediate 1,3-di(2-pyridyl)-5-bromobenzene (**dpyb-Br**) reacted with mesitylboronic acid through a Suzuki cross-coupling to generate **L^2**, as previously described.[6] An alternative approach to prepare ligand **L^4** through copper-promoted coupling was also investigated, prior to reaction with the stannylpyridine, but only resulted in extensive homocoupling. Thus, the precursor 1,3-dibromo-4,6-difluorobenzene, **1**, was readily prepared as described by Manka *et al.*,[12a] while we found that reaction of hexamethylditin with 2-bromo-5-(trifluoromethyl)pyridine in 1,4-dioxane at reflux per 2 h provides a more convenient route to the synthesis of the starting CF_3-subsituted stannylpyridine, **2**, with respect to a procedure previously reported for the same compound (THF reflux per 15 h) – reaction yield improved from 60% to 80%.[12b]
All of the ligands were purified by chromatography to remove monosubstituted material and unreacted organostannane eccess.

The platinum(II) chloride complexes were prepared by reaction of the corresponding L^n ligands with K_2PtCl_4, using either acetic acid or a mixture of acetonitrile and water as solvent (Scheme 2). Previous synthesis of **[PtL^1Cl]** have proceeded in refluxing acetic acid for 3 days,[11] but it was noted during this present thesis that working in an alternative solvent system of acetonitrile/water under nitrogen led to an enhancement of reaction yields, passing from 40%[11] to 60%. This milder conditions, originally introducted by Càrdenas and co-workers for the synthesis of similar squar planar platinum complexes[13], allow us to avoid problems associated with protonation of pyridine rings of the ligands.

Scheme 2. The synthetic routes for preparation of platinum chloride complexes in different solvent systems: route A) acetic acid; route B) water/acetonitrile (1/1 vol).

route A

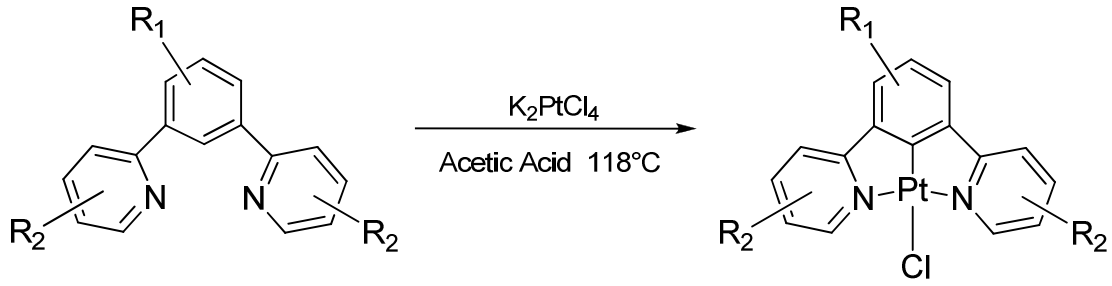

[PtL^n]Cl

route B

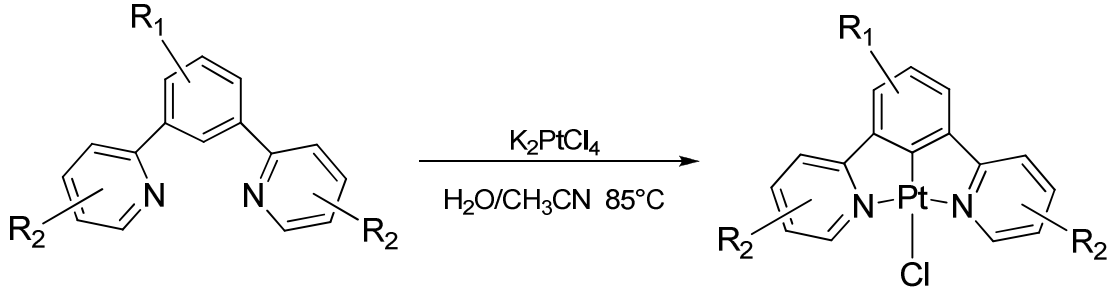

[PtL^n]Cl

The resultant complexes have relatively low solubility and precipitate from the reaction solutions as yellow solids (note that **[PtL^{4}Cl]** colour depends on the solvent system used). A simple washing sequence allows to isolate the pure compounds in yields typically of around 50 - 60%. The ^{1}H NMR of these compounds confirmed that cyclometalation had occurred (see Fig. 2). According to J. A. Williams,[6] apart from the obvious loss of the H$^{2'}$ resonance (see Scheme 1 for the numbering system), the main systematic changes in the ^{1}H NMR spectra of the ligands upon coordination to platinum(II) in an N^C^N manner were: (i) a shift to high frequency of the H^6 resonance ($\Delta\delta$ 0.5-0.6 ppm), accompanied by the appearance of welldefined ^{195}Pt satellites about this signal (^3J of ca. 40 Hz); (ii) a shift to low frequency of the H$^{4'}$, or H$^{5'}$, resonance of the central ring ($\Delta\delta$ 0.3-0.6 ppm), and (iii) with exception of **[PtL^{4}Cl]**, a reversal of the ordering or a strong shift of H^3 and H^4 signals in spectra of the complexes compared to those of their respective ligands. The chemical shifts of resonances in the pendent mesityl group were not substantially changed upon coordination.

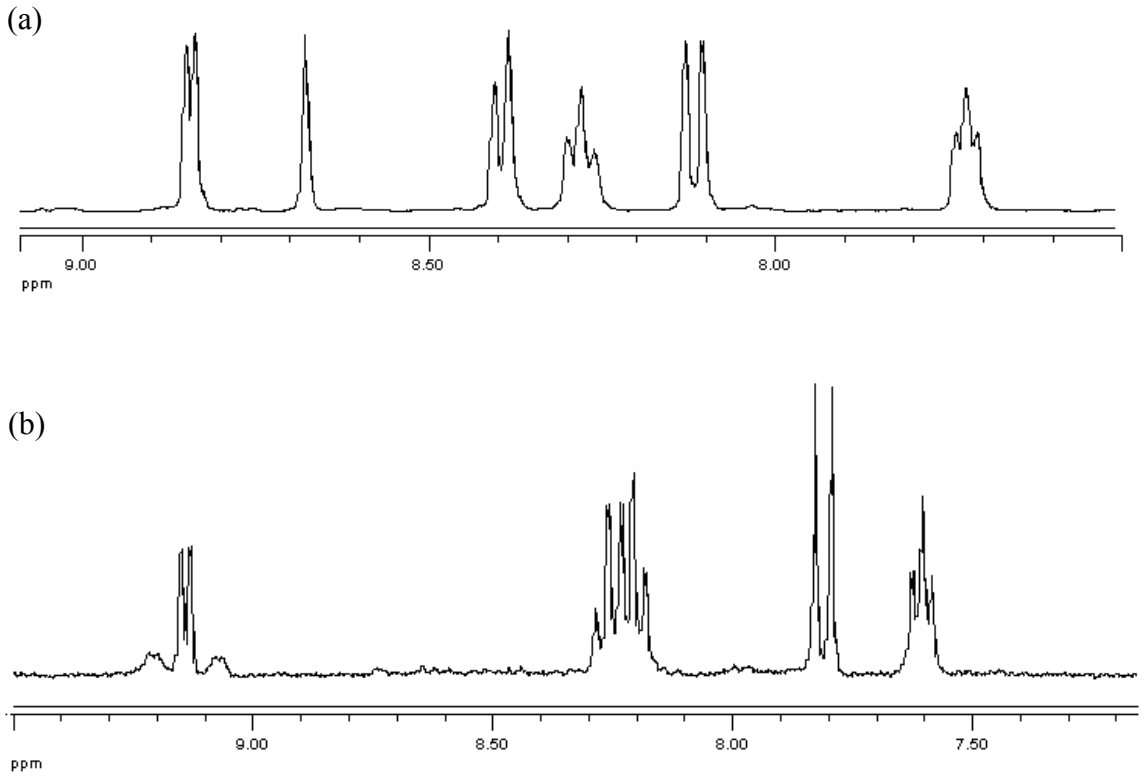

Figure 2. Aromatic region of ^{1}H NMR (400Mz) spectra in deuterated chloroform of: a) the ligand **L^{3}** and b) of his related Pt(II) chloride compex **[PtL^{3}Cl]**.

6.2. Synthesis of PtL^{n}SR compounds

Compexes [PtL^{n}S^{1}] were synthesized under inert atmosphere by adding sodium thiocyanate to a solution of the parent [PtL^{n}Cl] (Scheme 3) following procedure described for analogous compounds. Unfortunately, apart from **[PtL^{2}S^{1}],** the compounds obtained were relatively low soluble in most organic solvent, especially **[PtL^{3}S^{1}]** where the limited solubility prevents a full characterization.

Scheme 3: Preparation of platinum isothiocyanate complexes

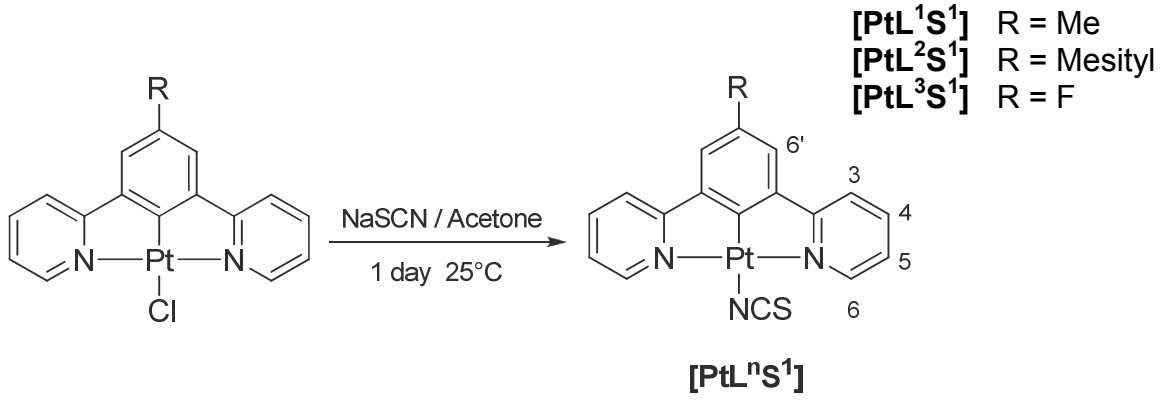

The ^{1}H NMR spectra revealed a consistent upfield shift of ^{6}H resonance, again accompanied by ^{195}Pt satellites (^{3}J of ca.40 Hz), with respect to the corresponding signal in the parent compounds spectra ($\Delta\delta$ 0.6 ppm) (see Scheme 3 for the numbering system). Resonances of the other protons remain virtually unchanged with the only exception of H^{5} and $H^{4'}$ signals in **[PtL^{1}S^{1}]** spectrum, whose order is reverted compared to **[PtL^{1}Cl]** spectrum (Fig. 3).

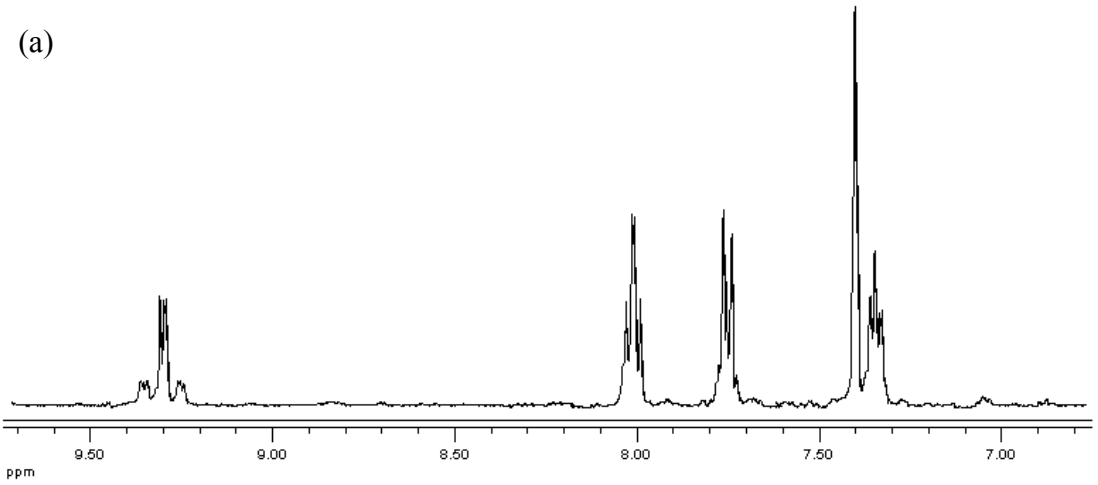

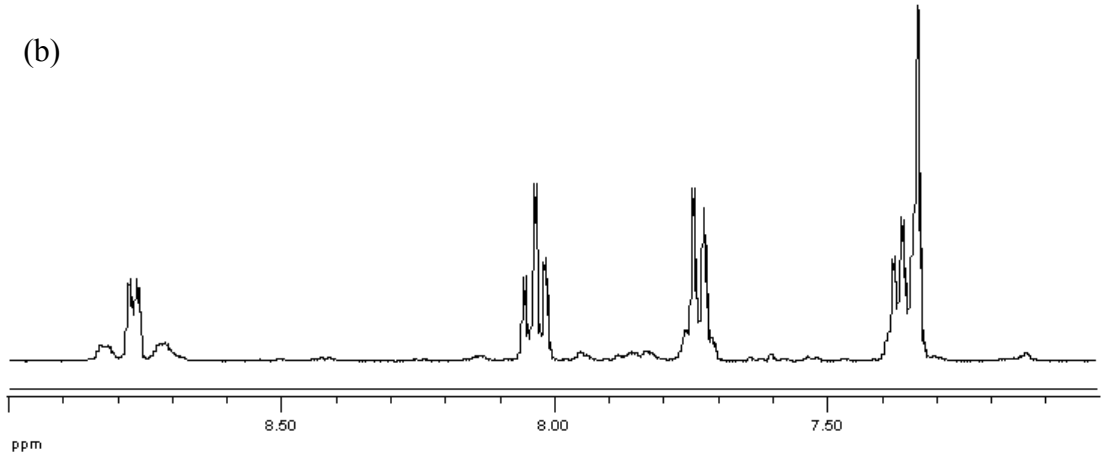

Figure 3. Aromatic region of ^{1}H NMR (400Mz) spectra in deuterated dichlorometane of: a) the parent platinum chloride **[PtL^{1}Cl]** and b) of his corresponding isothiocyanate derivative **[PtL^{1}S^{1}]**.

The infrared spectra of **[PtL^{1}S^{1}]** and **[PtL^{2}S^{1}]** recorded in chloroform solution showed a strong sharp peak at 2096 cm^{-1} assigned to the ν(SCΞN) stretching mode which would be in agreement with a SCN^{-} ion bound to the Pt atom through the N atom (*i.e.* as the isothiocyanate ligand).[14-16] This is apparently in contrast to the soft character (*i.e.* easily polarizable) of S in SCN^{-} which would suggest a coordination to soft acids (*e.g.* platinum). However, Burmeister[14] previously reported that for palladium(II) and platinum(II) complexes coordinated thiocyanate ion is either S- or N-bonded, depending upon the nature of the other ligands present. In particular the π-bonding ligands in [Pt(bipy)(SCN)$_2$] systems - where bipy is biyridiyl - tend to reduce the electron density on the metal and thereby change the soft metals to hard metals.[14] This is accompanied by a change in M-SCN bonding to M-NCS. Moreover steric factors can alter the nature of SCN bonding in these systems as well. In fact, M-SCN bonding on account of the angular structure of M-SCN has a larger steric requirement than does the linear structure of M-NCS.

Coordination through the N atom in our systems was confirmed by X-ray crystallography of **[PtL^{2}S^{1}]** (Fig. 4.) in collaboration with Prof. Demartin.

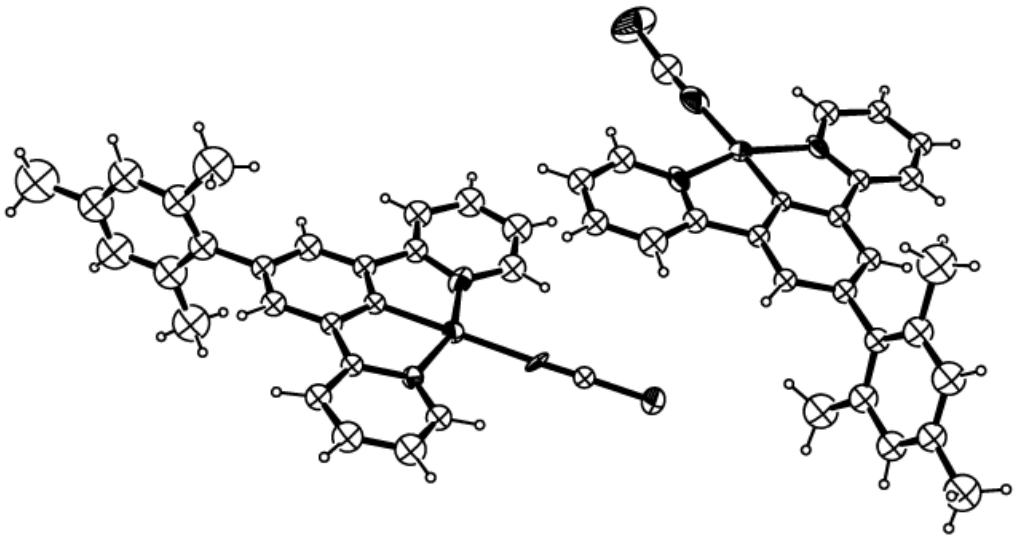

Figure 4. Molecular structure of **[PtL^{2}S^1]**

Attempts to prepare complexes where platinum (II) is coordinated to other sulphurous ancillary ligands led to mixtures of products, only one of which were we able to isolate cleanly (Scheme 4). The ^{1}H NMR of this compound confirmed that the reaction had occurred, but nevertheless further analysis were prevented by the rapid decompostition of the complex. Therefore we abandoned further studies with these complexes in favour of other ancillary ligands such as substituted aryl acetylides.

Scheme 4. Preparation of platinum thioazolate complex

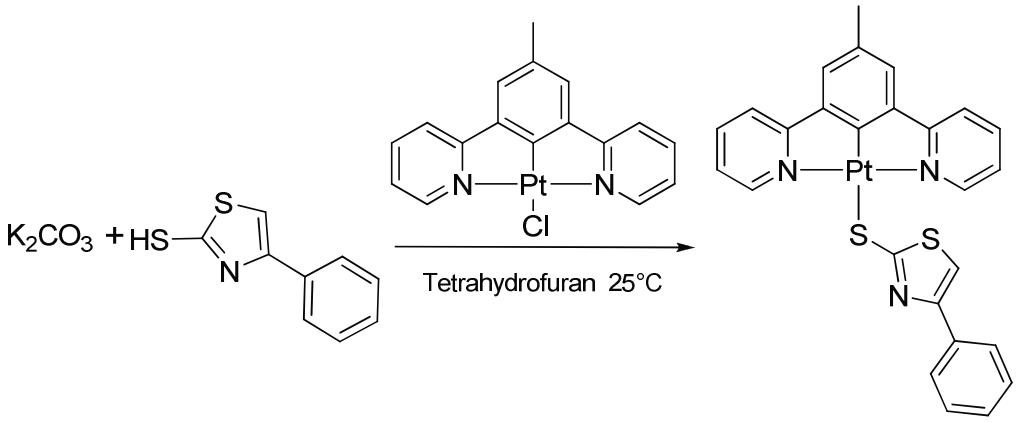

[PtL^{1}S^2]

6.3. Synthesis of $PtL^nAcetylide$ compounds

Lu et al.[10, 17, 18] have shown that (N^N^C) and (O^N^N) platinum (II) acetylide complexes can be prepared by employing Sonogashira's conditions (CuI/^{i}Pr$_2$NH/CH_2Cl_2). Our attempts to obtain the corresponding (N^C^N) derivatives following this synthetic route was unsuccessful despite the screening of different catalytic systems (for example CuI/^{i}Pr$_2$NH, CuI/Et_3N, CuOAc/^{i}Pr$_2$NH, CuOAc/Et_3N etc..). Indeed, in these condintions the non-coordinated (N^C^N) ligand was largely recovered. The reason for this behaviour is still under investigation. Platinum (II) phenyl acetylides complexes of 1,3-di(2-pyridyl)-5-bromotoluene, [PtL^1A^n], were more conveniently prepared by modification of other literature procedures using an excess of sodium methoxide.[19] This latter method also worked successfully when the platinum chloride of the mesitylated ligand, **[PtL^2Cl]**, was reacted with 1-ethynyl-3,5-difluorobenzene, A^1. Thus, **[PtL^2A^1]** was isolated as shown in Scheme 5.

Scheme 5. Preparation of platinum acetylide complexes from the corresponding platinum chloride **[PtL^1Cl]**

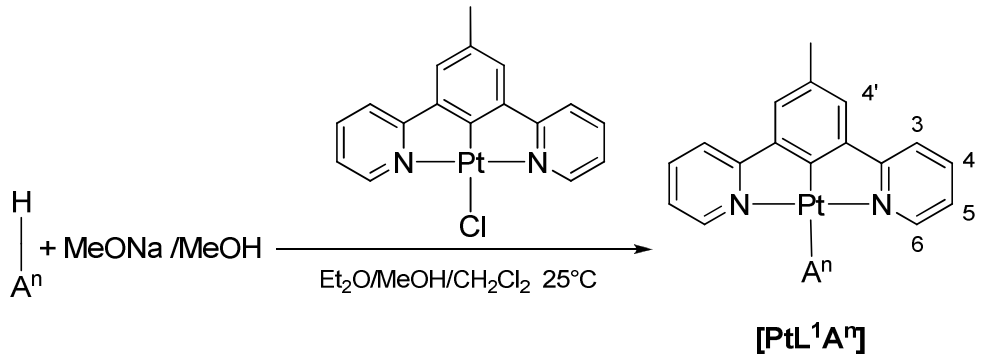

[PtL^1A^n]

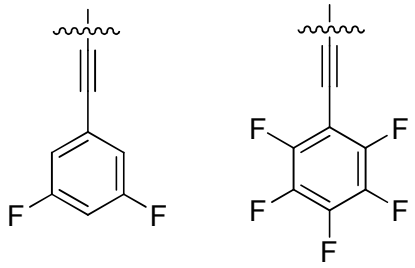

A^n = **A^1** **A^2**

Scheme 6. Preparation of (3,5-difluorophenyl)ethynyl derivative of **[PtL^{2}Cl]**

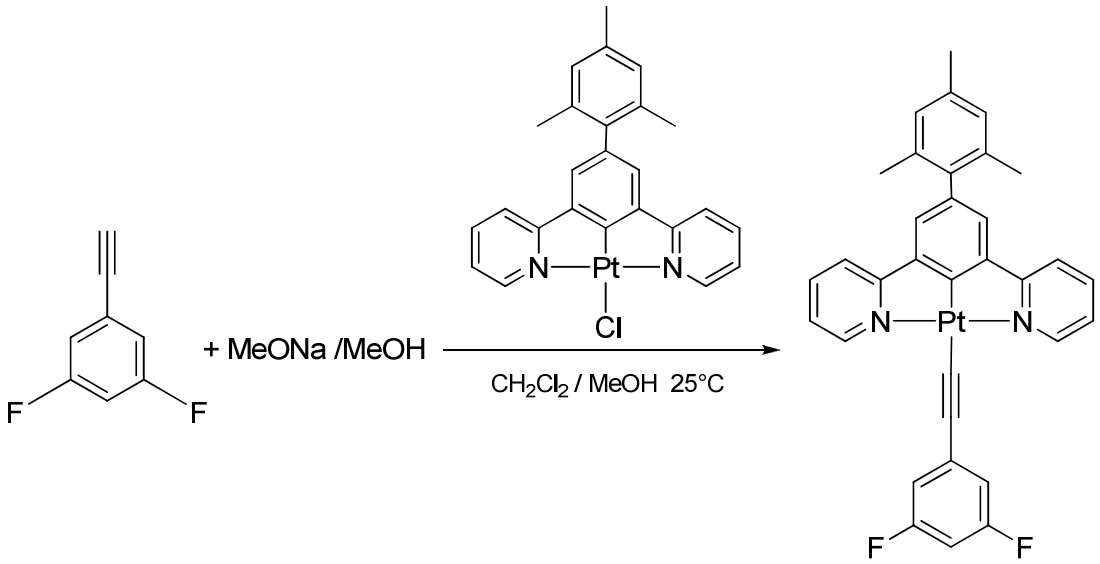

[PtL^{2}A^1]

Likewise, we have extended this procedure to the substrate that bears F and CF_3 on the terdentate ligand, *i.e.* **[PtL^{4}Cl]**. This time the reaction of **[PtL^{4}Cl]** with *N,N*-dimethyl-4-(prop-1-ynyl)aniline, A^4, in excess of sodium methoxide resulted in a mixture of products that were separated by precipitation. The ^{1}H NMR and MALDI-MS spectra of the main product suggested that the symmetry of the terdentate ligand had been lost because one fluorine atom on the benzene ring was displaced by the nucleophilic -OMe (see Fig.5). We speculated that this substitution could also occur on the free ligand, but that the process might be possibly promoted by coordination to the metal. These observations were confirmed by the different ratio of monometoxilated product, against difluoro, obtained from the ligand and the complex under the same reaction conditions. This ratio was derived indirectly by integration of the H$^{5'}$ signal in ^{1}H NMR of crude compounds since coupling whit fluorine splits its resounance in a doublet, H$^{5a'}$, or in a triplet, H$^{5b'}$, depending on the number of neighboring fluoro atoms (see Fig. 4 for numbering system); and its equal to 1:4 versus 1:1 for **[PtL^{4}Cl]** and **L^4**, respectively.

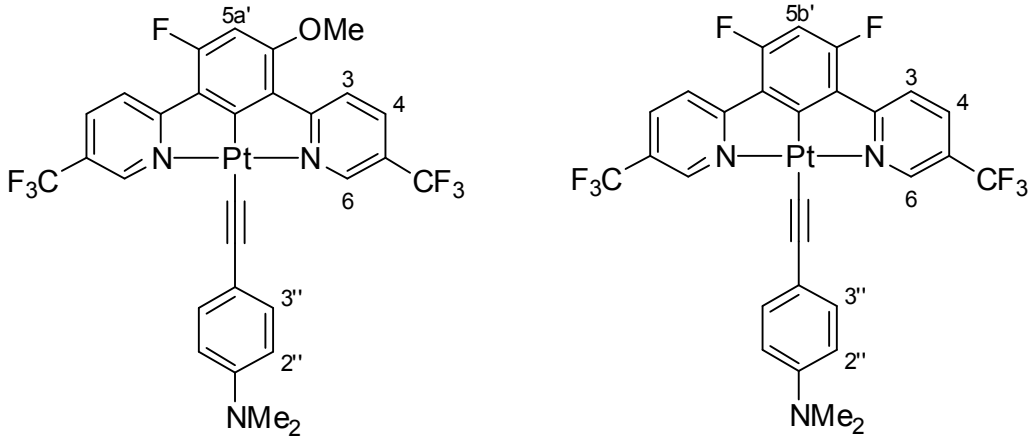

Figure 5. Schematic structure of metoxilated (**a**) and non-metoxilated (**b**) **[PtL^{4}A^4]**. The numbers in these structures designate each carbon atom.

We speculated that this substitution could also occur on the free ligand, but that the process might be possibly promoted by coordination to the metal. This observations were confirmed by the different ratio of monometoxilated product, against difluoro, obtained from the ligand and the complex under the same reaction conditions: respectively 1:4 versus 1:1. This ratio had been derived indirectly by integration of the $H^{5'}$ signal in ^{1}H NMR of crude compounds since coupling whit fluorine splits its rersounance in a doublet, $H^{5a'}$, or in a triplet, $H^{5b'}$, depending on the number of neighboring fluoro atoms (see Fig. 4 for numbering system).

Scheme 7. Preparation acetylide derivatives of **[PtL^{4}Cl]**

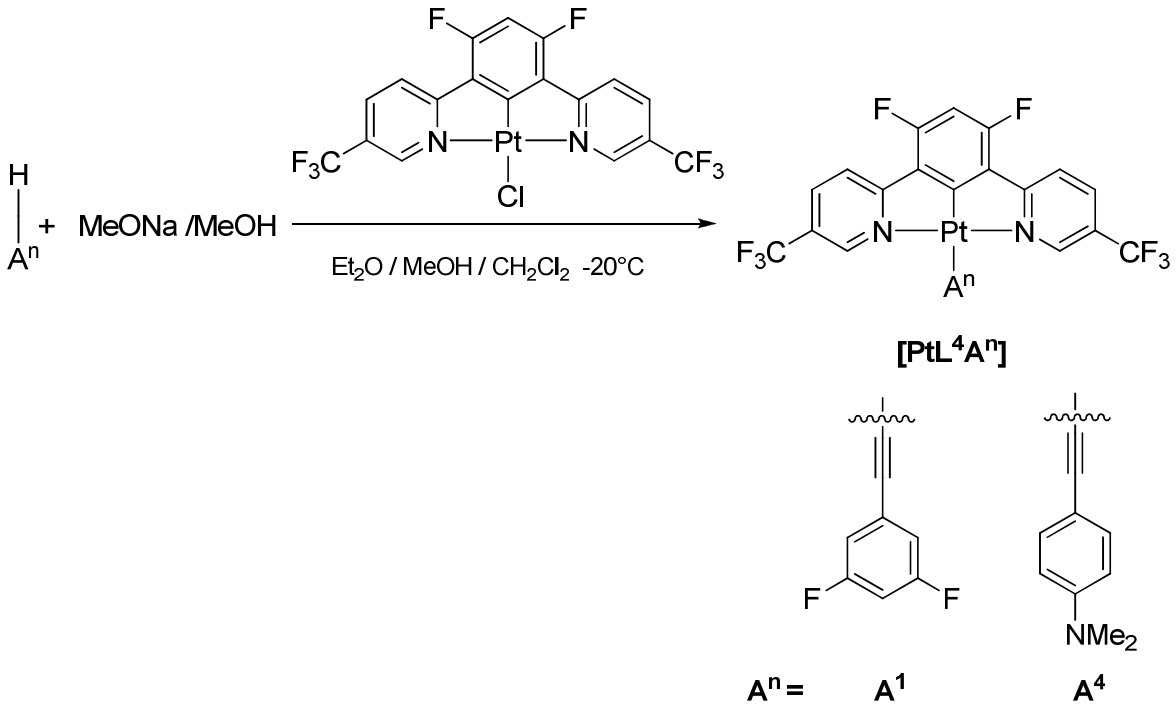

In order to inhibit this displacement we operate under kinetic control, *e.g.* -20C°, using a stoichiometric amount of base. Thus the desired products, **[PtL^{4}A^1]** and **[PtL^{4}A^4]**, were formed predominantly (Scheme 7). A simple purification by precipitation afforded to isolate the clean compounds with 40% yield (Fig. 6).

In general the coordination to alkyne lead to an upfield shift of the resonances of H^6 and, when present, of $H^{4'}$ in the ^{1}H NMR spectra of the platinum complexes with respect to the corresponding signals in parent platinum chlorides ($\Delta\delta$ 0.1 - 0.2 ppm) (see Fig. 4 for numbering system). Another obvious change in the ^{1}H - and ^{19}F in the case of fluorinated phenyl acetylides derivatives - NMR spectra that confirmed product formation, is the appearance of resonances of the protons, or the fluorines, present on the acetylide ligands.

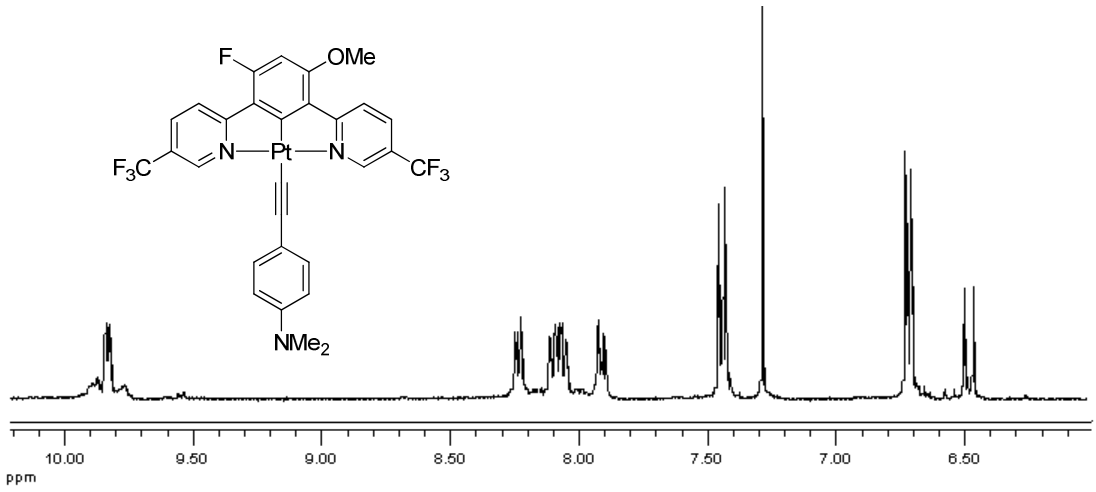

Figure 5. Aromatic region of ^{1}H NMR (400Mz, TDF) spectra of -OMe substituted derivative of **[PtL^{4}A^4]**.

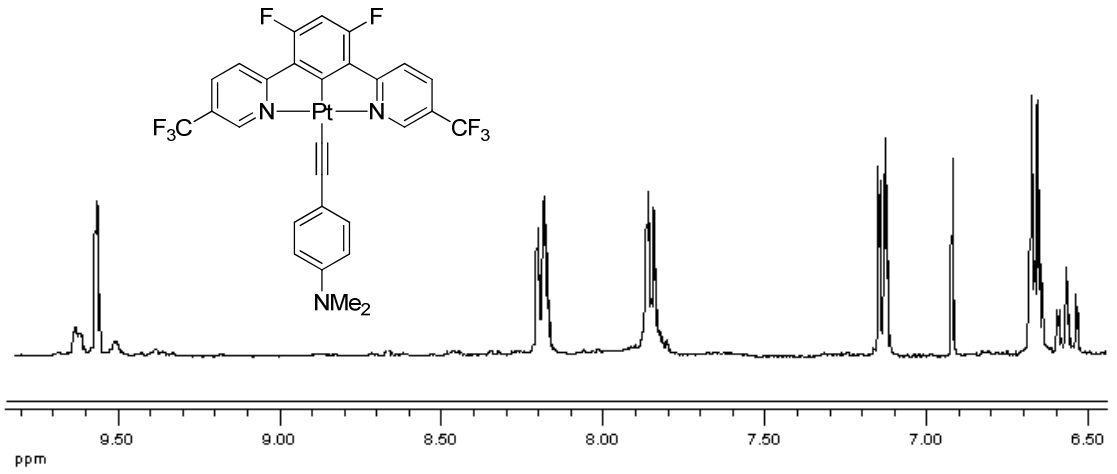

Figure 6. Aromatic region of ^{1}H NMR (400Mz, TDF) spectra of unsubstituted **[PtL^{4}A^4]**.

As far as terminal alkynes are concerned, they were all commercially available apart from 1-ethynyl-2,3,4,5,6-pentafluorobenzene, A^2, which was readily prepared by following a well established approach.[20, 21] The two steps synthetic procedure for the preparation of this starting acetylide is outlined in Scheme 8.

Scheme 8. Synthetic routes for preparation of 1-ethynyl-2,3,4,5,6-pentafluorobenzene, **A^2**, from reaction of ethynyltrimethylsilane with 1-bromo-2,3,4,5,6-pentafluorobenzene and subsequent basic cleavage of the protective silane:

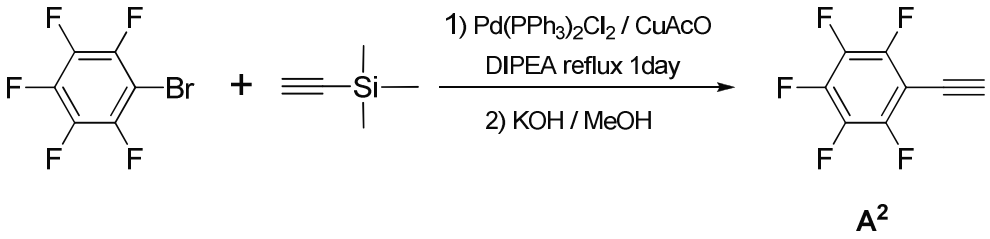

A^2

7. Electrochemistry

The electrochemistry of some complexes was examined using cyclovoltammetry during a stage in Prof. J. A. G. Williams laboratory (Durham University, UK). The results obtained are listed in Tab. 1 together with the corresponding values for previously studied compounds[6, 22] for comparison. Due to the different solubility of the complexes, measurements were performed in dichloromethane instead of the media reported in the literature (CH_3CN/CH_2Cl_2 [9:1 (v/v)][6] or DMF[22]). Furthermore, even in dichloromethane the potential values were not always easily determined owing to shifts of the peak maximum of anodic/cathodic curve with different scan rate being the processes electrochemically irreversible. Therefore any conclusion must be considered cautiously and any trend observed between the data only used as a guideline.

Within the range -2.3 to +1.3 V (vs (Fc/Fc^+)) all the complexes show one irreversible reduction process. In particular, cathodic potential of complexes **[PtL$^{1\text{-}3}$Cl]**, **Pt(dpb)Cl** and **Pt(dpdFb)Cl** (Fig. 7), $\mathbf{E_p^{RED}}$, is at a similar value of around -2.0 V in each case. The insensitivity of this potential towards 4-substituent is consistent with a description of *Lowest Unoccupied Molecular Orbital* (LUMO) states localized on pyridyl rings with little contribution from the formally anionic cyclometalating ring, as seen in previous works.[7] Nevertheless, it is difficult to assert that the presence of the CF_3 substituent on the pyridine strongly affects the LUMO by comparing the reduction potentials of **Pt(dpdFb)Cl** and of **[PtL^{4}Cl]** reported in Tab. 1 , since these values were obtained in different media.

Pt(dpdFb)Cl **Pt(dpb)Cl**

Figure 7. Schematic structure of platinum(II) chloride complexes of 1,3-Difluoro-4,6-di(2-pyridyl)benzene, Pt(dpdFb)Cl, as reported by Ghassan E. Jabbour et al[22] and of 1,3-di(2-pyridyl)benzene, Pt(dpb)Cl, as reported by Cardenas *et al.*[13]

The influence of the solvent system on cyclovoltammetry studies is evident in the case of complex Pt(dpb)Cl: its reduction potential, $\mathbf{E_p^{RED}}$, reported in the literature is -2.15 V in acetonitrile[11] and -2.03 V in a mixture of acetonitrile/dichloromethane (9/1),[6] which corresponds to a difference of 0.12 V between the measurements probably related to the

different ability of the solvent to stabilize, for example, the anionic product of the reduction process.

Table 1. Electrochemical properties of the platinum complexes

Complex	E_p^{OX} [V] [a]	E_p^{RED} [V] [a]	HOMO [eV] [b]	LUMO [eV] [b]
Pt(dpb)Cl	0,43[c]	-2,03[c,]	-5.23	-2.77
[PtL^{1}Cl]	0,37[c]	-2,02[c]	-5.17	-2.78
[PtL^{2}Cl]	0,58[c]	-1,99[c]	-5,38	-2,80
[PtL^{3}Cl]	0,22[d]	-2,07[d]	-5,02	-2,73
Pt(dpdFb)Cl	0,50[e]	-2,29[e]	-5,30	-2,51
[PtL^{4}Cl]	0,67[d]	-1,90[d]	-5,47	-2,90
[PtL^{1}S^1]	0,67[d]	-2,30[d]	-5,47	-2,50
[PtL^{1}A^1]	0,11 and 0,36[d]	-1,27[d]	-4,91	-3,53

[a] All process were electrochemically irreversible; $Ep^{ox\,/\,red}$ refers to peak potential of elettrochemically irreversible oxidation/reduction; values are reported relative to a ferricinium/ferrocene (Fc^+/Fc) redox couple used as an internal reference standard ($E_{1/2}$= +0.42V vs *saturated calomel electrode* SCE in dichloromethane);[b] HOMO and LUMO levels as calculated from the redox potentials:[c] Data from ref. [6] in CH_3CN/CH_2Cl_2 [9:1 (v/v)] at 298 K, in the presence of 0.1 M $[Bu_4N][BF_4]$ as supporting electrolyte, scan rate 300 mV s^{-1};[d] In CH_2Cl_2 at 298 K, in the presence of 0.1 M $[Bu_4N][PF_6]$ as supporting electrolyte, scan rate 300 mV s^{-1};
[e] Data from ref. [22] in anhydrous DMF at 298 K, in the presence of 0.1 M $[Bu_4N][PF_6]$ as supporting electrolyte, scan rate 300 mV s^{-1}.

With reference to previous studies on other platinum(II) complexes, a metal-centered oxidation from Pt(II) to Pt(III) is tentatively assigned.[9, 23a] Data for the anodic potentials, Ep^{ox}, of [PtL^{n}Cl] complexes show rather more variation with substitution than the cathodic ones, Ep^{RED}. As already noticed a quantitative comparison of the potentials is undermined by the use of a different solvent, nevertheless it seems that the introduction of electron-withdrawing subsituents on the phenyl ring gives an increase in the anodic potential Ep^{ox}. Thus, the observed order [PtL^{1}Cl] > Pt(dpb)Cl > [PtL^{2}Cl] > [PtL^{4}Cl] suggests that the *highest occupied molecular orbital* (HOMO) in these complexes is dominated by the central phenyl ring, as well as the metal, in accordance with previous DFT calculations.[24] The presence of mesityl in [PtL^{2}Cl] shifts the oxidation potential Ep^{ox} to a more positive value, compared to [**PtL^{1}Cl**], indicating that the aryl can be considered an electron-withdrawing substituent in terms of the σ-bonding as previously suggested.[25] As to the electron-accepting properties of the fluorine atom on complex **[PtL^{3}Cl]** we remind you to the 'Emission in Solution' section.
[PtL^{1}A^1] posses the lowest anodic potential, Ep^{ox} = 0.11 V, making it the most susceptible to oxidation among compounds studied, possibly on account of the presence of the acetylide ancillary ligand, although the lack of data prevents us from further observations.

Table 2. Emission energy maxima of the platinum complexes, λ_{max}, and energetic gap for the HOMO-LUMO transitions, Δ_{H-L}

Complex	λ_{max}[nm] [a]	λ_{max}[$cm^{-1}*10^3$] [a]	Δ_{H-L} [b]
Pt(dpdFb)Cl	470	21,276	2,79
[PtL^4Cl	484	20,661	2,57
Pt(dpb)Cl	491	20,367	2,46
[PtL^2Cl]	501	19,960	2,57
[PtL^1S^1]	501	19,960	2,97
[PtL^3Cl]	504	19,841	2,30
[PtL^1Cl]	505	19,802	2,39
[PtL^1A^1]	508	19,685	1,38

[a] Emission energy maxima of the platinum complexes recorded in dichloromethane solution at 298 K;

[b] Energetic gap for transition between HOMO and LUMO levels calculated from the redox potentials.

In table are reported emission maxima of the complexes and the energetic gap for the HOMO-LUMO transitions, Δ_{H-L}. This delta was obtained by subtraction of the LUMO energy level from the HOMO energy level which were calculated from the redox potentials by the equations E^{HOMO} = - (E_p^{OX} + 4,8) eV and E^{LUMO} = - (E_p^{RED} + 4.8) eV, using the internal ferrocene standard value of − 4.8 eV with respect to the vacuum as reported by Wong *et al.*[23b]

A general correlation can be observed between the data. This is consistent with a blue shift of emission maxima with the increasing energy gap for the HOMO-LUMO transitions. Strangely, **[PtL^1S^1]** exhibits the highest energy gap amongst these complexes which should correspond to the most shifted towards blue emission. This could be reasonably attributed to errors in the calculation of the reduction potential which was difficult to assign due to the weakness of the signal and overlapping of the band with the edge of the solvent window.

8. Photophysical Properties

Absorption and emission data for the complexes prepared are listed in Tab. 3, together with corresponding values for some previously studied compound for comparison.[6, 22] These N^C^N-coordinated platinum (II) derivatives are generally intensely luminescent in diluited solution at room temperature (quantum yield of luminescence, Φ_{lum}, around 50%) with relatively long emission lifetimes (order of microseconds). The highly structured spectra and the very small Stokes shift indicate that emission originates from a state of primarily $^3\pi$-π^* character[11] -although Sotoyama[24] recently suggested that a d-π^* character (*Metal to Ligand Charge Transfer*, MLCT) might affect the excited state T_1. Emission and absorption energy are influenced by substituition on both terdentate and ancillary ligands, offering a versatile method for colour tuning. Besides, these compounds are subjected to self-quenching via excimer formation, which is typical of square planar Pt(II) complexes.[7, 11] Interestingly the excimers of N^C^N-coordinater complexes are themselves intensely emissive (Φ_{exc}≈ 30%). Furthermore, the typically long-lived triplet excited state lifetime of platinum complexes enables efficient quenching of emission by dioxygen, with bimolecular rate constants for this process, Kq_{O2}, generally in the order of magnitude of 10^9 $M^{-1}s^{-1}$.[26] In this paragraph we shall discuss more in detail the photophysical results obtained during a stage in Durham University under the supervision of Prof. J. A. Gareth Williams.

Table 3: Photophysical data (to be continued in the next page):

COMPOUND	SUBSTITUENT ON terdentate(ancyllary) LIGAND	ABSORBANCE [a] λ_{max} [nm]	EMISSION [a] λ_{max} [nm]	Φ_{lum}% Degased(aereated)	T_0 [b] [μs]	K_{SQ} [c] [$10^9 M^{-1}s^{-1}$]	$K_{Q(O2)}$ [d] [$10^8 M^{-1}s^{-1}$]
Pt(dpb)Cl	H (Cl)	332 (6510), 380 (8690) 401(7010), 454(270), 485(240) [e]	491, 524, 562 [e]	60 (4) [e]	7.2 [e]	5.3 [e]	9.1 [e]
[PtL^{1}Cl]	Methyl (Cl)	335 (5710), 381(6900), 412 (6780), 460(190), 495 (130) [e]	505, 539, 578 [e]	68 (2) [e]	7.8 [e]	3.3 [e]	16 [e]
[PtL^{2}Cl]	Mesityl (Cl)	332 (5640), 363 (3850), 381 (5410), 410 (5210), 492sh (130) [e]	501, 534, 574(sh)	62 (5) [e]	7.9 [e]	1.0 [e]	7.4 [e]
[PtL^{3}Cl]	4-F (Cl)	322sh (6172), 377 (7744), 422 (8270), 486 (312)	504, 542	47 (3)	6.9	5.6	7.4
Pt(dpdFb)Cl	4,6-F(Cl)	336, 362, 376, 470 [f]	470, 500 [f]	46 [f]	3 [f]		
[PtL^{4}Cl]	4,6-F-Ph,CF_3-Py (Cl)	330 (7971), 342 (10410), 388 (11072), 479 (521)	484, 515	53 (16)	3.9	3.6	2.5

Table 3: Photophysical data:

COMPOUND	SUBSTITUENT ON terdentate(ancyllary) LIGAND	ABSORBANCE λ_{max} [nm]	EMISSION λ_{max} [nm]	Φ_{lum}% Degased(aereated)	T_0 [a] [μs]	K_{SQ} [c] [$10^9 M^{-1}s^{-1}$]	$K_{Q(O2)}$ [d] [$10^8 M^{-1}s^{-1}$]
[PtL^{1}S^1]	Me (isothiocyanate)	333(4759), 357(2798), 382 (3894), 406 (3819), 499(188)	501, 533	60 (5)	9.3	8.9	6.2
[PtL^{2}S^2]	Mesityl (Isothiocyanate)	331(3710),359sh(2590), 378(3689), 409 (3705),491(125)	496, 529	---	---	---	---
[PtL^{1}A^1]	Me (F_2phenylacetylene)	335sh (4928), 388 (5092), 406 (4529), 493 (111)	508, 538	77 (4)	7.8	2.9	15
[PtL^{1}A^2]	Me (F_5phenylacetylene)	330 (7971), 355 (4922), 380 (3782), 408br(4082)	502, 533	20 (2)	7.0	1.7	6.7
[PtL^{2}A^1]	Mesityl (F_2phenylacetylene)	333 (7395), 366 (7971), 387 (7174), 405 (5814), 489(290)	500, 529, 572	66 (4)	5.9	0.5	15
[PtL^{4}A^1]	4,6-F-Ph,CF_3-Py (F_2phenylacetylene)	327 (3871), 346 (3828), 392 (3824), 438br (394)	486, 514	27 (9)	5.2	2.4	3.1
[PtL^{4}A^4]	4,6-F-Ph,CF_3-Py (NMe_2phenylacetylene)	326sh (19362), 344sh (15838), 385 (6481), 493 (3050)	484, 513,558sh	23 (5)	2.2	9.6	2.2

[a] In dichloromethane at 295 K. [b]Lifetime at infinite dilution. [c] Self-quenching constant . [d] dioxygen quenching contstant. [e] data from ref. [11]; [f] data from letterature [22]. Sh stand for shoulder. Br stand for broad.

8.1. Absorption

The absorption properties of the complexes listed in Tab. 3 are typical of this class of compounds[11] and obey to Lambert-Beer law for concentration lower than 1.0 x 10^{-4} M in dichloromethane solution (*i.e.* absorption spectra of the diluted and concentrated samples are the same), suggesting the lack of any significant occurrence of complex aggregation. The similarity between the absorbance spectrum of uncomplexed ligand with that of the related complex, for example **L^4** and **[PtL^{4}Cl]** respectively, in the region below 300 nm (Fig. 8), suggests that these very intense bands (ε > 2,0 x 10^4 mol^{-1} cm^{-1}) are due to a ligand localised ^{1}π-π* transitions.[11] Notably these bands are apparently not affected by substitution on the pyridyl rings.

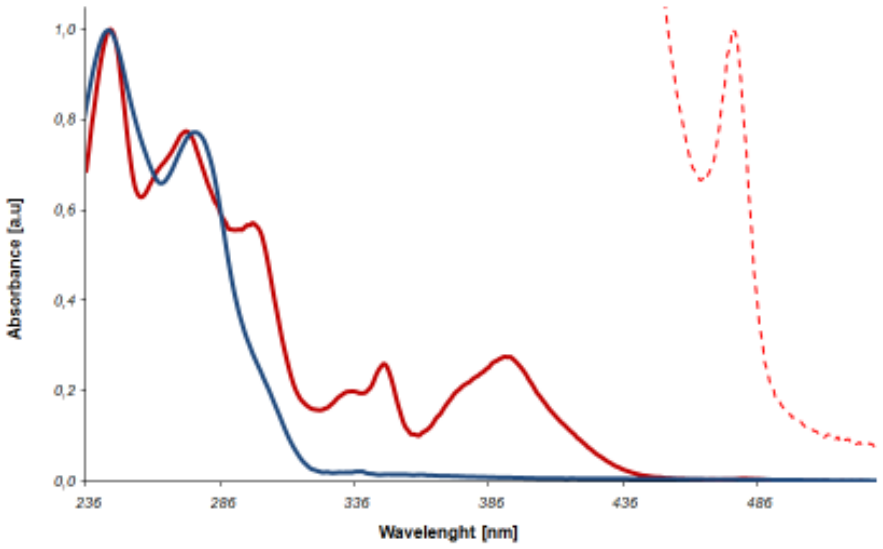

Figure 8. Absorption spectra of ligand **L^4** (solid blue) and of complex **[PtL^{4}Cl]** (solid red) in dichlorometane at 298K. The weak long wavelength band is shown on an expanded scale (dashed line); spectra have been normalised at 246 nm for clarity .

At 320 - 450 nm a series of lower intensity bands is exclusively observed in the complex spectrum (ε = 0.5 – 1 x 10^4 mol^{-1} cm^{-1}) and, consequently, is attribuited to the presence of the metal. In addition, the latter broader band energy exhibits a pronounced negative solvatochromic behaviour, typical of transitions with an appreciable degree of charge-transfer character, shifting from 386 nm in DMSO to 398 nm in CCl_4 (ΔE = 780 cm^{-1}, Fig. 9). According to Marcus,[27, 28] this blue shift of the peaks with increasing solvent polarity, suggests an excited state of lower dipole moment than the ground state. In the least polar solvent investigated, carbon tetrachloride, a weak band at lower energy can be observed

(around 420 nm). By increasing solvent polarity this band is probably blue-shifted and overlaps with the higher energy absorptions.

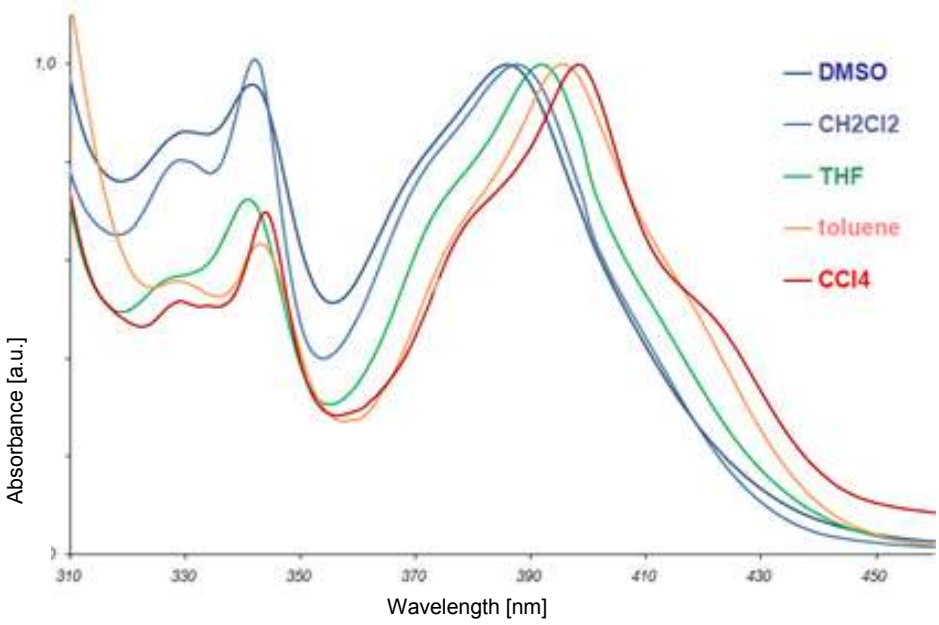

Figure 9. Absorption spectra of **[PtL^{4}Cl]** in various solvents

The band at higher wavelength displays a much weaker degree of solvatochromism shifting from 476 nm in DMSO to 482 nm in CCl_4. This band was attributed to direct population of $^3\pi$-π^* states promoted by the high spin-orbit coupling associated with the Pt(II) ion. The intensity of this band is extremely weak on account of the formally spin-forbidden transition ($\varepsilon < 500$ mol^{-1} cm^{-1}).

According to J.A.G. Williams, the component band at lowest energy is increasingly red-shifted as the 4-substituent become more electron donating.[2] Indeed, compared with the other [PtL^{n}Cl] (Fig. 10) the ^{1}MLCT and the triplet transition energies of **[PtL^{4}Cl]** – and of the corresponding complex unsubstituted on the pyridyl rings[22] - are higher suggesting a bigger singlet and triplet energy gaps for this latter. However, the extinction molar coefficient of triplet absorption of [PtL^{4}Cl] (ε = 521 M^{-1}cm^{-1}) is significantly larger than that of the others ($\varepsilon \approx 40$ M^{-1}cm^{-1}), while ^{1}MLCT transitions have similar intensities.[22] The sharpening of the band occurring around 330 nm, which is typical of all complexes derived from ligand **L^4**, does not depend on the CF_3 substituent on the pyridyl ring since the non-pyridyl-substituited difluorinated complex **Pt(dpdFb)Cl** has a similar shape.[22]

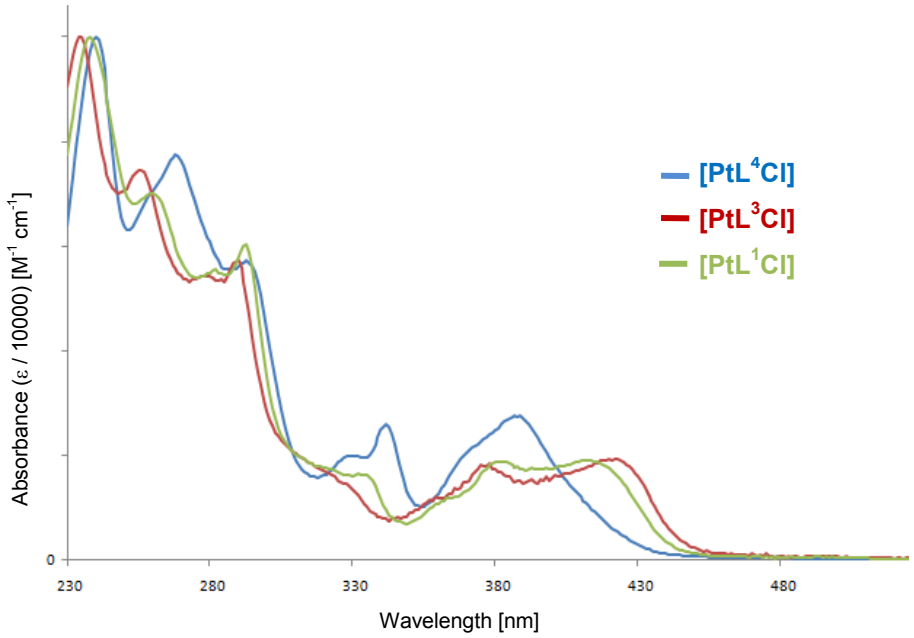

Figure 10. Absorption spectra of Pt chloro complexes: **[PtL^{1}Cl], [PtL^{3}Cl], [PtL^{4}Cl],** in various solvents

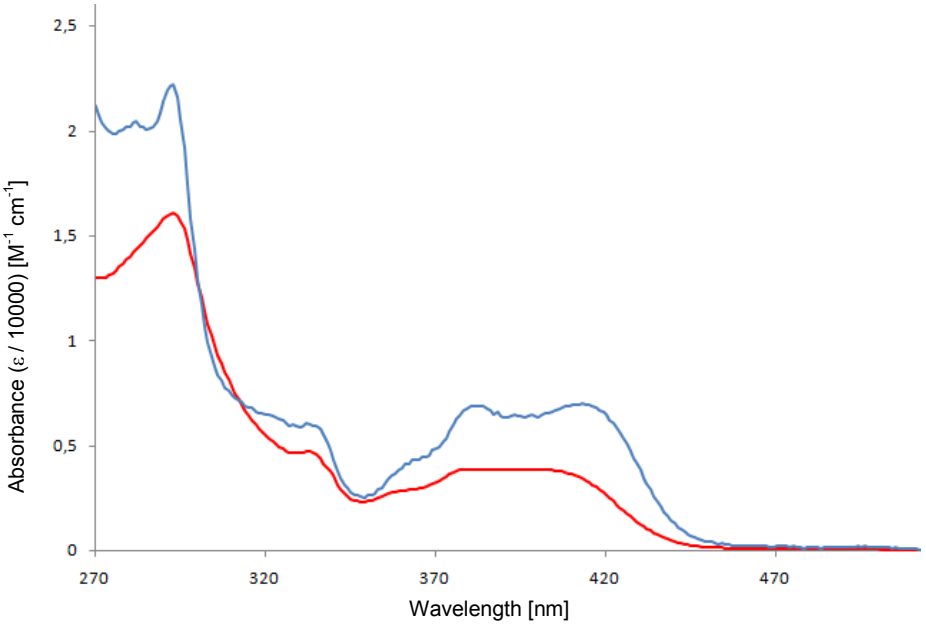

Figure 11. Absorption spectra of isothiocyanate complexes of 4-Methyl substituited ligand, **[PtL^{1}S^1]** (red line) and the related parent compound **[PtL^{1}Cl]** (blue line) in dichlorometane at 298K.

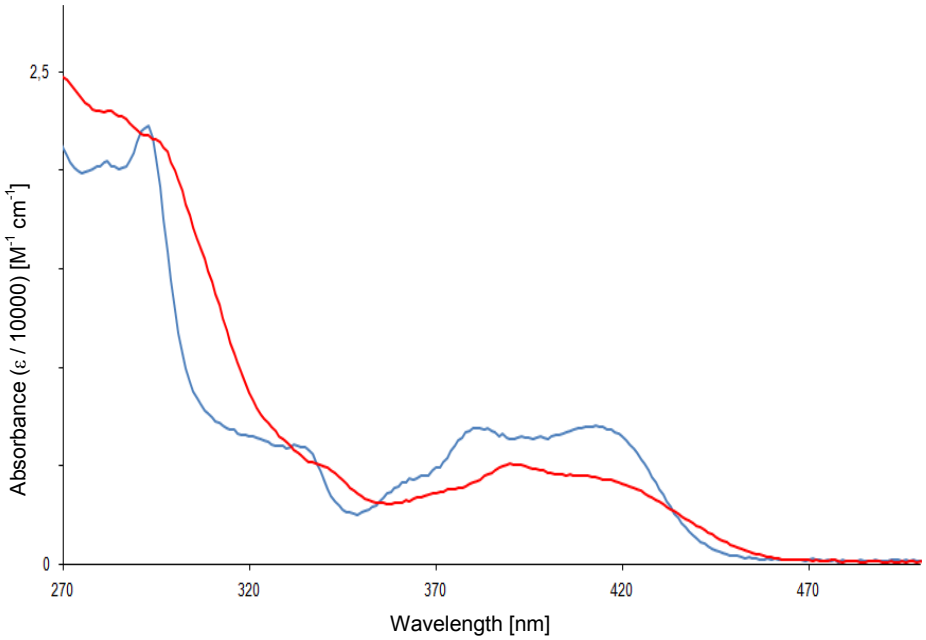

Figure 12. Absorption spectra of difluoro phenyl acetylide complex of 4-Methyl substituted ligand, **[PtL^{1}A^1]** (red line) and the related parent compound **[PtL^{1}Cl]** (blue line) in dichlorometane at 298K.

The absorption spectra of the parent platinum chloro complexes are slightly affected by coordination to isothiocyanate or acetylide. Upon coordination through sulphur (Fig. 11), the broader band at 350 – 450 nm seems slightly less structured, and less intense (see extinction molar coefficients, ε, in Tab. 3). A comparison between [PtL^{1}Cl] and the corresponding acetylide **[PtL^{1}A^1]** suggests that the π(CΞC)→π* *ligand to ligand charge transfer* (LLCT) *transition* - which according to Baik[19] is likely mixed with some MLCT - probably overlays with the broad band at 350-450 nm. A further evidence to this is the appearance of a peak at ca. 385 nm even though extinction molar coefficient, ε, value does not seem to increase (see Fig. 12).

8.2. Emission in solution

In the following, we focus mainly on the solution-state emission properties at both 298 K and 77 K.

In Fig. 13 are reported the absorption and emission spectra for complex **[PtL^{4}Cl],** but their shape is characteristic for all compounds of this class. The pronounced vibrational structure of the emission spectra obtained is typical of emission from a π-π* excited state. Besides, the very weak negative solvatochromism (ΔEnergy = 30 cm^{-1} between acetone and toluene solution, Fig. 14) and the very small Stokes shift (*i. e.* between the highest energy emission

band and the weakest energy absorption band, Fig. 13) are incompatible with a charge transfer excited state. These evidences, as well as the relatively long lifetimes (4 - 8 μs), indicate that emission originates from a state of primarily ^{3}π-π* character[11] although Sotoyama *et al.*[24] recently claimed that there is an admixture of π-π* (LC) / d-π* (MLCT) character. By this assumption the d-π* character could significantly affect the kinetics of deactivation processes - and in fact it could be an explanation of the relative short lifetimes observed - though the excited state T_1 character would always be primarily π-π*.[24] According to Sotoyama *et al.*[24] the considerable contribution from the metal character to the excited state would also be in agreement with the pronounced red shift (ΔE > 2000 cm^{-1}), observed in phosphorescence between the complexes and the corresponding free ligands (Fig. 15), which are much larger than those reported for complexes with ligand-centred emitting states such as $[Pt(bpy)^2]^{2+}$ (ΔE= 950 cm^{-1})[29] where bpy is 2,2′-bipyridine.

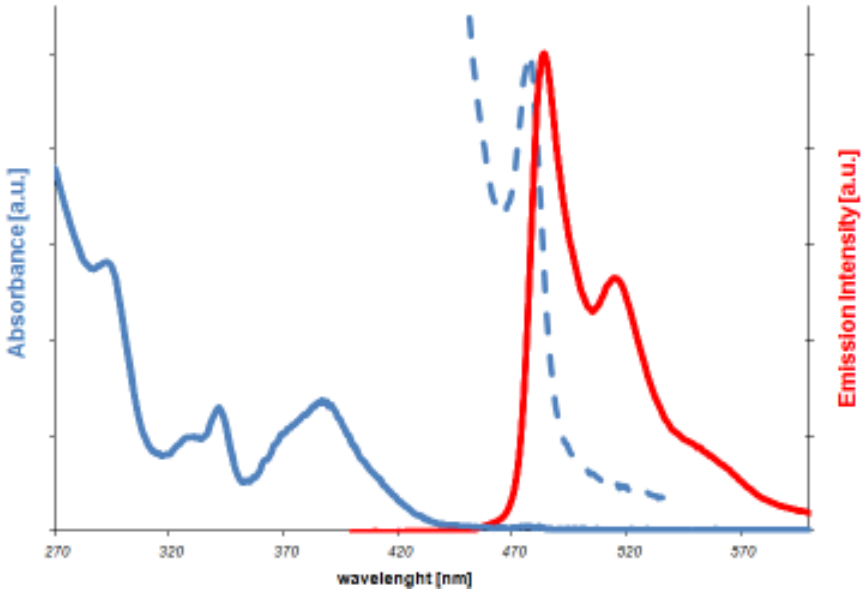

Figure 13. Absorption (solid blue line) and emission (red line) spectrum of complex [PtL^{4}Cl] in a 8,483x10^{-6}M dichlorometane solution at room temperature. The absorption maximum at 479nm (blue dashed line) is shown on an expanded scale for clarity.

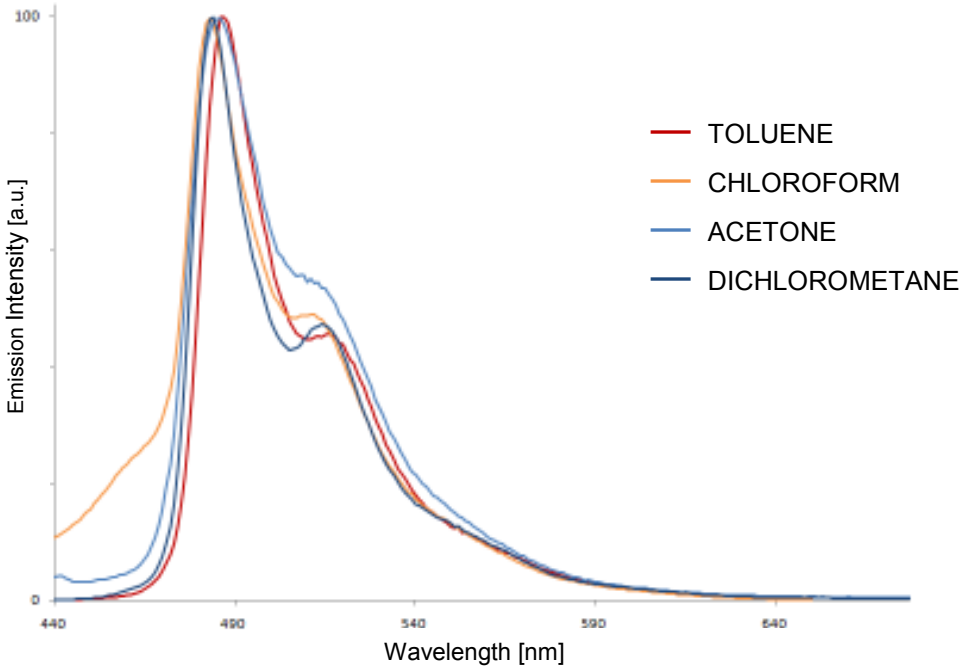

Figure 14. Normalised emission spectra of **[PtL^{4}Cl]** in various solvents

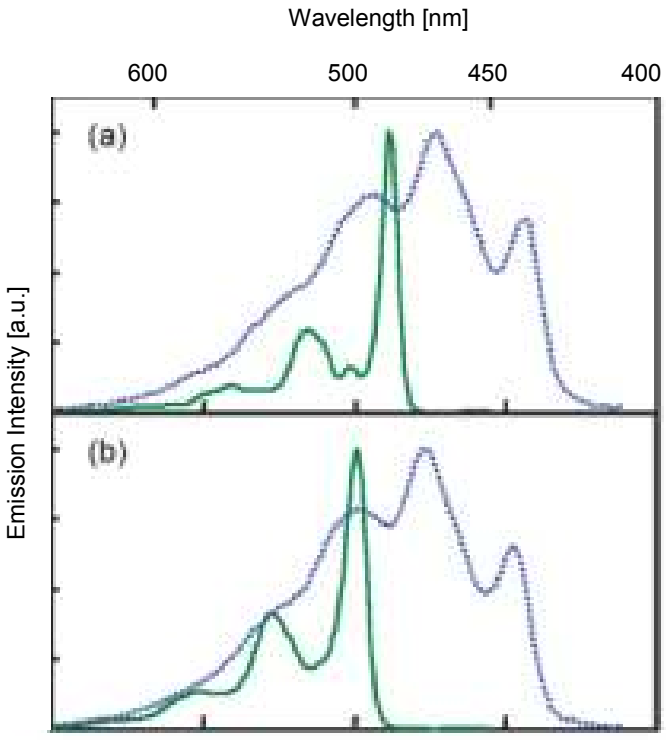

Figure 15. Emission spectra of the complexes (a) **Pt(dpb)Cl,** (b) **[PtL1Cl]** and the free ligands, respectively, in toluene at 77 K. Solid line (green), emission of the complexes; dotted line (blue), emission of the free ligands measured with a phosphoroscope as reported by ref. [24].

Previous spectroscopic work by Lu *et al.,*[10] showed that π-bonding conjugation between Pt(II) and an σ-alckynyl ligands significantly affects properties of the triplet excited state. On this basis the high-energy emission in the region of 480 – 550 nm of acetylide platinum (II) complexes has been assigned to triplet ^{3}MLCT excited states [(5d)Pt→π*(cyclometallated ligand)]. Nevertheless, more detailed theoretical investigations are required since the weak solvatochromic behaviour displayed by the complexses prepared, seems in contrast to a charge transfer character (**[PtL^{1}A^1]** λ_{em} = 508 nm in $CHCN_3$.; λ_{em} = 508 nm in CH_2Cl_2; broad band λ_{em} = 503 nm in CCl_4).

From Fig. 15 it emerges that there is a significant difference in the vibrational progressions of the complexes' spectra and those of their corresponding free ligand. The shape of emission spectra is determined by vibrational overlap factor, Frank-Condom factor, which is the quantum mechanical expression of Franck-Condon Principle (*there is no significant change in the position of the nuclei of a molecule during an elctronic transition, i.e. electronic transitions are vertical between the potential energy curves of the intial and final states*). When excited and ground state have similar potential energy surface in shape and equilibrium geometry (*i.e.* excited state is approximatively not distorted compared to the ground state) the most efficient transition - and therefore the most intense - is the one between the electronic vibrational states 0-0 (Fig. 16). This is the case of our complexes spectra where the component band of highest intensity is the one of highest energy (*i.e.* the 0-0 transition) indicating a minimal difference in geometry between the ground and excited electronic states. This results account for the rigidity of terdentate N^C^N systems – in contrast to that of the free ligand.[24] The less structured spectrum observed for compound **[PtL^{4}A^1]** might suggest that the molecules are subjected to significant electronic perturbations or to a change in geometry when excited.

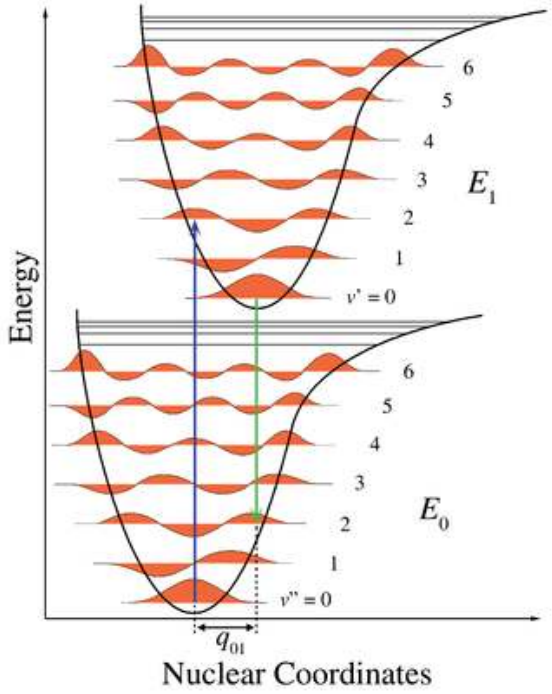

Figure 16. Potential energy curves (Morse curves) illustrating an electronic transition from the ground to the excited state.

As we have previously noted in section "Introduction", it is well acknowleged that the selection of substituents on both central and lateral rings in systems based on 1,3-di(2-pyridyl)benzene ligands, offers a good versatile method for colour tuning.[4, 7] Whilst the green and red regions are covered well by most of the complexes of this class, the blue component is more limited.[7] In particular It has been shown that substitution on the central phenyl ring with electron-withdrawing group, such as ester, leads to a blue shift in emission wavelength bringing the HOMO level to lower energy.[11] Indeed, this is also reflected in the emission energy trend observed for the compounds reported in Tab. 3, where complex bearing fluorine atoms in the 3´ and 5´ positions on the terdentate ligand, **Pt(dpdFb)Cl**,[12] is at the highest energy. Actually, the emission wavelengths for all the complexes based on **L^4** - which is difluorinated on the phenyl ring - are more shifted towards blue within the series (for example **[PtL^4A^1]** λ_{em} = 486, 514 nm versus **[PtL^1A^1]** λ_{em}= 508, 538 nm and **[PtL^2A^1]** λ_{em}= 500, 529, 574 nm), a trend that is also observed in the low energy absorbance maxima (0-0 transition). On the other hand, the lower emission energy observed for **[PtL^4Cl]** relative to **Pt(dpdFb)Cl**[12] confirms that substituents on the pyridyl rings significantly affect the LUMO level as previously observed by M. Cocchi *et al.*[4]

The apparently controversial effect on emission wavelength of a fluorine in 4-position on the central phenyl ring, **[PtL^3Cl],** can be rationalised in terms of electron-withdrawing or donating ability of this element. In fact, despite being strongly electronegative, and therefore

inductively electron-withdrawing, fluorine is also a mesomerically electron-releasing group due to overlap of p-orbitals (Fig. 16). This electron-donating resonance effect seems to be more significant when fluorine is in para position to the metal. By balancement of the two opposite electronic contributions results an increased electron density on the central phenyl ring and on platinum. These observations are consistent with the trend observed for the anodic potential, Ep^{ox} (see 'Electrochemistry' section), which suggests that the HOMO of **[PtL^{3}Cl]** is at higher energy compared to that of the unsubsituted complex **Pt(dpb)Cl**. The resulting emission is at wavelenght similar to that of a weak electron-donor such as methyl, **[PtL^{1}Cl]** (**[PtL^{3}Cl]** λ_{em} = 504, 542 nm Vs **[PtL^{1}Cl]** λ_{em} = 505, 539 nm).[11]

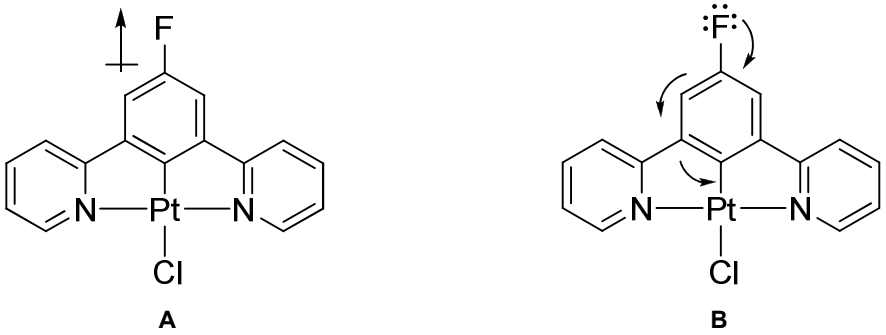

Figure 16. Schematic representation of inductive, A, and mesomeric, B, effect of the fluorine substituent in **[PtL^{3}Cl]**

For considerations concerning the influence of the mesityl substituent on the energy of the HOMO we remind you to the 'Electrochemisty' section.

Data seem to suggest that λ_{em} of the parent platinum chloro complexes are slightly affected by coordination to acetylide (Tab. 3). A similar behaviour had been previously observed by Kwok et *al.*[18] in the case of platinum complexes based on 6-(2-Hydroxyphenyl)-2,2'-bipyridine (**[(O^N^N)PtCl]** λ_{em} = 593nm versus **[(O^N^N)PtCl]** λ_{em} = 600 nm in DMF solution).[18] A comparison between emission wavelength of acetylides derived from the same parent complexes, *e.g.* **[PtL^{4}A^1]** and **[PtL^{4}A^4]**, appararently indicates that there is little influence of the electron donor/acceptor ability of the alcetylide substituents on emission energy, which is in contrast to the results reported for acetylides of N^N^C-coordinated and terpyridyl systems.[19, 9]

The substitution of chloro with isothiocyanate as ancillary ligand, apparently leads to a slight blue shift in emission wavelentgh with respect to the parent plainum chloro complexes (λ_{em} **[PtL^{1}S^1]** = 501, 533 nm versus **[PtL^{1}Cl]** = 505, 539 nm; λ_{em} **[PtL^{2}S^1]**= 496, 529 nm versus λ_{em} **[PtL^{2}Cl]** = 501, 534 nm Tab. 3).

8.2.1. Emission quantum yield. Radiative and non-radiative rate constants

The equation Eq.1 was used to calculate emission quantum yield values

$$\Phi_{lum} = \Phi_R \left\{ \frac{\eta_s^2 \, A_r \, I_s}{\eta_r^2 \, A_s \, I_r} \right\} \qquad \text{Eq.1}^{[30]}$$

where Φ_{lum} is the quantum yield of the sample, Φ_R is the quantum yield of the reference, η is the refractive index of the solvent, A_s and A_r are the absorbance of the sample and the reference at the wavelength of excitation, and I_s and I_r are the integrated areas of emission bands. Since the solvent used for the sample was the same as for the reference, *i.e.* dichlorometane, the terms η_s/η_r is equal to one. As the data in Tab. 3 show all the complexes are highly luminescent (Φ_{lum} ranges from 20-77%). In particular Φ_{lum} values are considerably superior to those of the analogous N^N^C complexes (*e.g.* **Pt(phbpy)Cl,** Fig. 17, Φ_{lum} = 3% andτ = 0.51μs).[31] As previously observed in section "Introduction" is likely that the stronger ligand field exerted by the N^C^N chelate, with its significantly shorter Pt-C bond compared to the N^N^C (about 0.14 Å shorter),[7] serves to further raise the energy of the d-d excited state. A further evidence of beneficial effects of N^C^N-coordination emerges upon comparison of radiative, k_{r} , and non-radiative, k_{nr}, rate constant with those of bidentate binded complexes, for example **(4,6-dFppy)Pt(acac)** (Fig. 17).[32] Indeed complex **(4,6-dFppy)Pt(acac)** has a k_{nr} value around an order of magnitude higher than that for the analogous terdentate compound **Pt(dpdFb)Cl,** (k_{r}= 3,0 x 10^6 s^{-1} [32] vs k_{r} ≈10^5 s^{-1} [22]) indicating that the greater rigidity of the terdentate system prevents the distortion that leads to non-radiative decay in the bidentate system. However, the introduction of a further pyridyl ring has also lead to a slight red shift in emission wavelength relative to the bidantate complexes,[30] maybe on account of the long distance between the pyridine which might limit conjugation.

In Tab. 4 are reported k_{r} and k_{nr} values for the compound sinthesized calculated using the following equations:

$$k_{\mathrm{r}} = \Phi_{\mathrm{lum}}/\tau_0 \qquad \text{Eq.2}^{[32]}$$

$$k_{\mathrm{nr}} = k_{\mathrm{r}}\left(\Phi_{\mathrm{lum}}^{-1} - 1\right) \qquad \text{Eq.3}^{[32]}$$

where τ_0 is the intrisic emission lifetime and Φ_{lum} is quantum efficiency for deareted solution. Although these equations strictly hold only if the emissive state is formed with unitary efficiency, this is likely to be a good approximation, especially given the close match between the excitation and absorption spectra. The greater is the k_{r} value obtained – the lower the k_{nr} value – the more efficient is the phosphor.

(4,6-dFppy)Pt(acac) **Pt(phbpy)Cl**

Figure 17. Schematic structure of platinum(II) (2-(4',6'-difluorophenyl)pyridinato-N,$C^{2'}$)(2,4-pentanedionato-*O,O*), (4,6-dFppy)Pt(acac), as reported by Thompson *et* al.,[32] and of Pt(II) chloro complex of 6-phenyl-2,2'-bipyridine, Pt(phbpy)Cl as reported by Lai *et al*.[31]

Tab. 4. Radiative, k_{r}, and non-radiative, k_{nr}, rate constant.

COMPOUND	K_r (K_{nr}) [$10^4 M^{-1}s^{-1}$]	COMPOUND	K_r (K_{nr}) [$10^4 M^{-1}s^{-1}$]
[PtL^{3}Cl]	7.4 (8.5)	**[PtL^{1}A^2]**	3.3 (13)
Pt(dpdFb)Cl	≈10[a]	**[PtL^{2}A^1]**	11 (5.7)
[PtL^{4}Cl]	14 (13)	**[PtL^{4}A^1]**	11 (29)
[PtL^{1}SCN]	7.0 (4.6)	**[PtL^{4}A^4]**	4.3 (14)
[PtL^{1}A^1]	13 (3.8)		

[a]Data from ref. [22]

The high k_{r} value obtained for **[PtL^{1}A^1]** and **[PtL^{2}A^1]** show that the strategy of introducing a strong ligand-field acetylide has proved to be successful in the case of the (3,5-difluorophenyl)ethynyl complex. In particular **[PtL^{1}A^1]** is exceptionally bright with Φ_{lum} = 77% at room temperature in deoxygenated dichloromethane. Also the more soluble mesityl derivative, **[PtL^{2}A^1]**, exhibit an enhanced emission efficiency with respect to the parent platinum chloride (Φ_{lum} = 66% vs Φ_{lum} = 62%[6] at room temperature in deoxygenated dichloromethane).

8.2.2. Concentration Dependence: Self-Quenching and Excimer Formation

An increase in concentration leads to a decrease in the observed lifetimes and the appearance of a new broad structureless emission band centered at ca. 700 nm in chloro and isothiocyanate complexes, Fig. 18 (whereas in acetylides derivatives it is at ca. 650 nm). This phenomenon had been attributted to self-quenching via excimer formation.[11] In fact the coordinative unsaturation of these square-planar platinum(II) complexes leads to weak attractive intermolecular interactions between a ground-state molecule and an identical molecule in its excited state.[32] Although self-quenching of cyclometalated complexes, such as those of N^N^C[31] or C^N^C[33] ligands, is usually not accompanied by detectable excimer emission, the majority of the N^C^N-coordinated complexes display very efficient excimers formation and the excimers themselves are remarkably emissive (Φ_{exc} = 30%).[11]

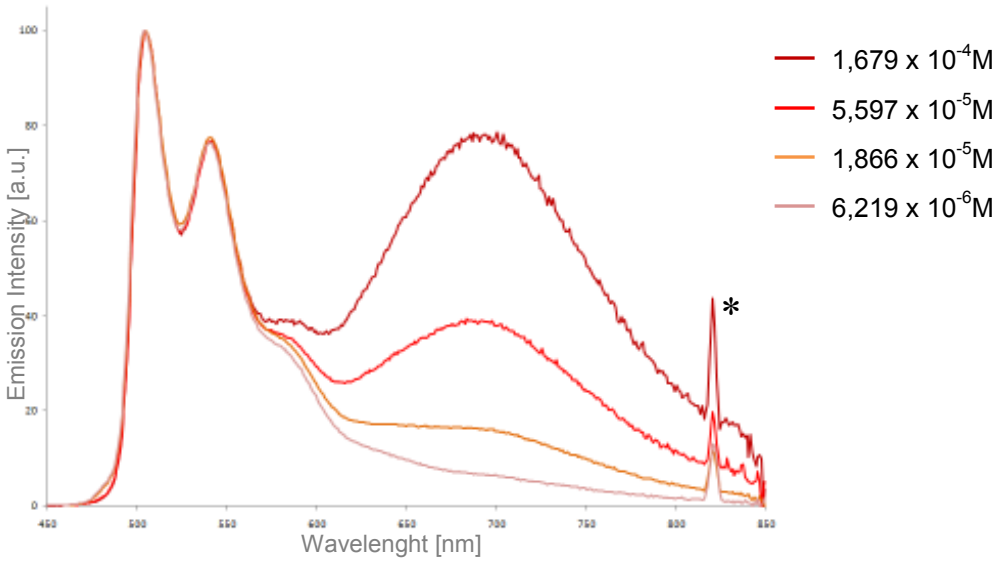

Figure 18. Normalised emission of complex **[PtL^{3}Cl]** in dichlorometane solution at different concentrations recorded at room temperature (λ_{exc} = 412 nm).

* The sharp peak at 824 nm is an instrumental artefact due to Bragg's law (*i.e.* nλ = 2*d* sinθ) that governs the grating-based monochromator function. When the excitation monochomator is set at 412 nm an emission at 824 nm (second order of λ_{exc} =2 x 412 nm) is detected. The use of a proper cut-off filter between the excitation monochromator and the sample should eliminates this peak.

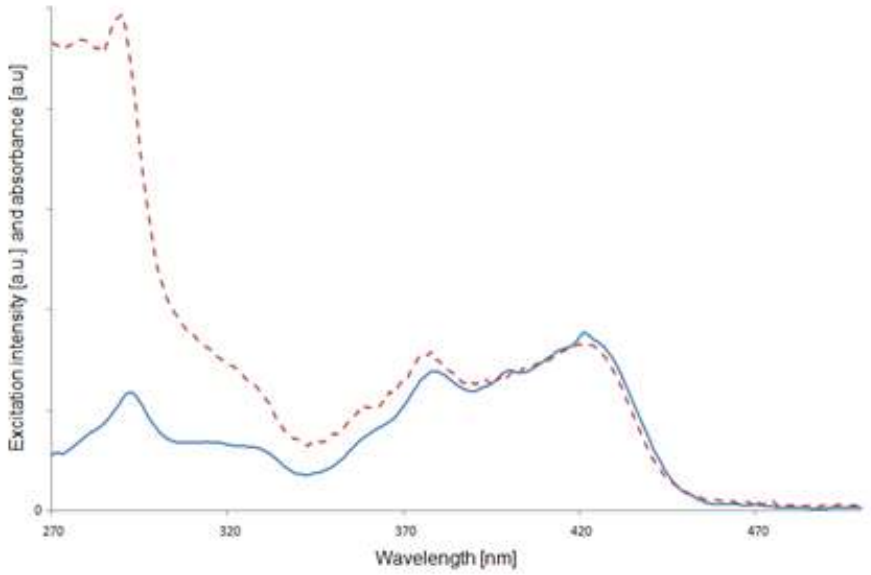

Figure 19. Normalised spectra of absorbance (red dashed line) and excitation (blue solid line) intensity of complex **[PtL^{3}Cl]** in dichlorometane solution at room temperature (λ_{em} = 540 nm).

However, the nature of the bimolecular emissive states responsible for the concentration dependent luminescent behaviour of square planar platinum (II) complexes – *i. e*. whether they are excited states of dimers that pre-exist in the ground state or excimer - is still in dispute.[3] Nevertheless, on the basis of the spectroscopic data obtained, the structured high energy emission band can be reasonably assigned to the monomer while the featureless low energy emission band can be assigned to an excimer (a bimolecular excited state which is dissociative - *i.e.* not bimolecular - in the ground state). One argument in support to this is, for example, that for low concentrations (10^{-4} to 10^{-6} M) in CH_2Cl_2, these complexes show no evidence of ground-state aggregation in absorbance spectra as noted in the previous section. Besides, the photoluminescence excitation spectra of the monomer and the excimer peaks are the same (Fig. 19), suggesting a common excitation pathways, which would not be the case for a different species (*e.g.* dimer).

Excimer emssion band - whose wavelenght seems to be unaffected by substitution on both terdentate and/or ancillary ligands - becomes progressively more intense at the expense of the shorter wavelength bands. Integration of these bands in the regions between 450 – 610 nm and 611 – 810 nm gives the relative instensity of the luminescence attribuited to monomer and dimer (excimer) excited state species, respectively. A plot of the ratio of these intensity as a function of concentration (Fig. 20), reveal, as expected, a linear relationship.

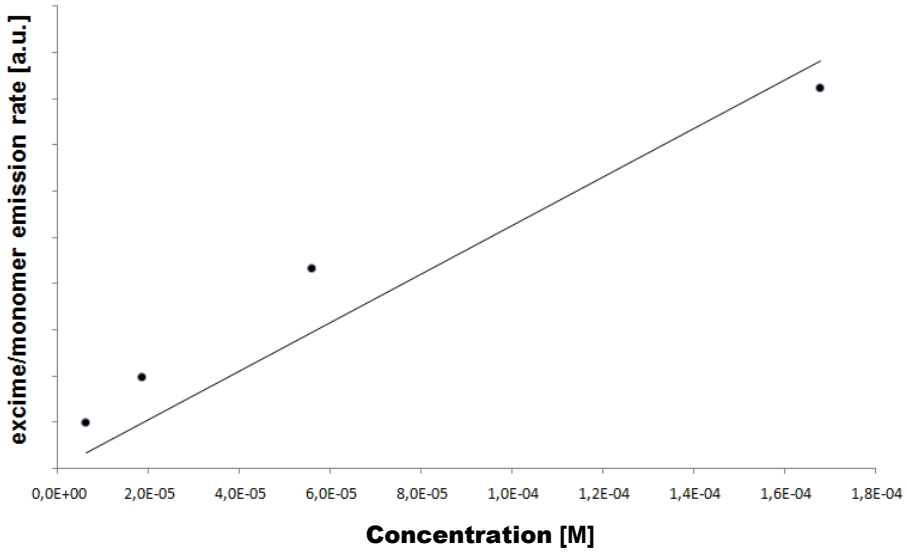

Figure 20. Ratio of excimer / monomer emission intensity as function of concentration (**[PtL^{3}Cl]**)

The self-quenching mechanism used to explain this concentration dependent quenching process involves initial formation of the excited complex, M*, followed by association with a ground state complex, M, to give an emissive excimer, [MM]*. The latter process is clearly dependent on the concentration of the metal complex (Fig. 21).

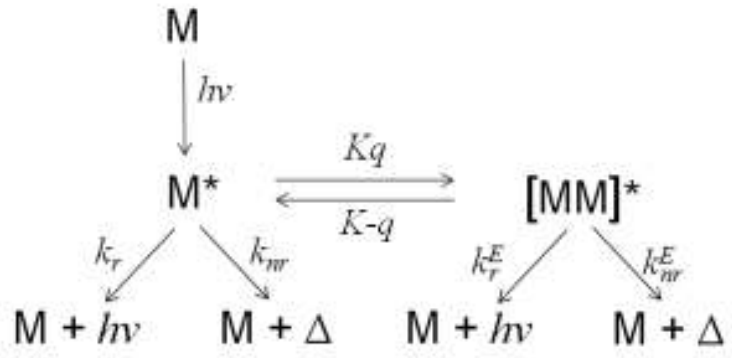

Figure 21. Mechanism of bimolecular self-quenching process via excimer formation. M stands for monomer molecule in its ground state; M* is the monomer molecule in its excited state; [MM*] is the excimer excited state; K_q represents the monomer self-quenching rate constant (also the rate constant for excimer formation), k_r represents the radiative decay rate for the monomer, and k_r^E is the radiative decay rate for the excimer.

Lifetimes were determined by monitoring temporal decay of the emission near emission maxima and they are all in the range typical of triplet character emission (μs). The emission decay registered in the monomer region (ca. 450 – 600 nm), where there is no significant

contribution from the excimer emission, is monoexponential (*i.e.* the signal shows emission decay starting immediately after the excitation pulse); while the excimer kinetic trace can be well fit with a bi-exponential function. In fact, excimer emission initially fast increases monoexponentially and then slowly decay, again monoexponentially, with the same rate constant as that of the monomer (Fig. 22). This behaviour is consistent with initial formation of the excimer followed by its relaxation back to the ground state.

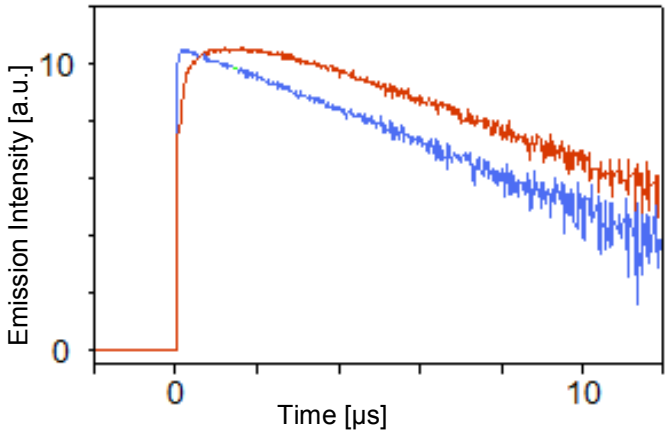

Figure 22. The emission kinetic traces for the solution of **[PtL^{3}Cl]** registered at 504 nm (monomer: blue line; and 720 nm (excimer; red line). The blue line is best fit with a monoexponential function (lifetime was estimated as $\tau_{monomer}$ = 0,9 μs); while the red line is better fitted by a double exponential ($\tau_{excimer}$ = 1,1 μs).

The rates of emission decay, k_{obs}, are well modelled by a modified Stern-Volmer expression (Eq. 4) where k_q is the diffusion controlled self-quenching rate constant (see Fig. 21), [Pt] is the concentration of the Pt complex and $1/\tau_0$ is the rate of excited-state decay at infinite dilution (*i.e.* in absence of self-quenching). In this model[32] excimer state is considered extremely stable towards dissociation back to M* and M. Thus, it can be assumed that the rate constant for the excimer dissociation, k_{-q}, is significantly small and can be neglected (this assumption is actually confirmed by the high value obtained for K_q). This explains why monomer emission exhibit monoexponential - instead of bi-exponential - decay over the whole range of concentrations studied, 10^{-4} – 10^{-6} M .

$$k_{obs} = 1/\tau_{obs} = 1/\tau_0 + k_q\,[Pt] \qquad \text{Eq.4}^{[34]}$$

By extrapolation of a plot of the observed emission decay rate constant, ($k_{obs}= 1/\tau_{obs}$), as a function of the concentration of the complex, [Pt], we determined the intrinsic emission

lifetime of the monomer (*i.e.* at infinite dilution), τ_0 and the apparent rate constant of self-quenching, k_q (Fig. 23).

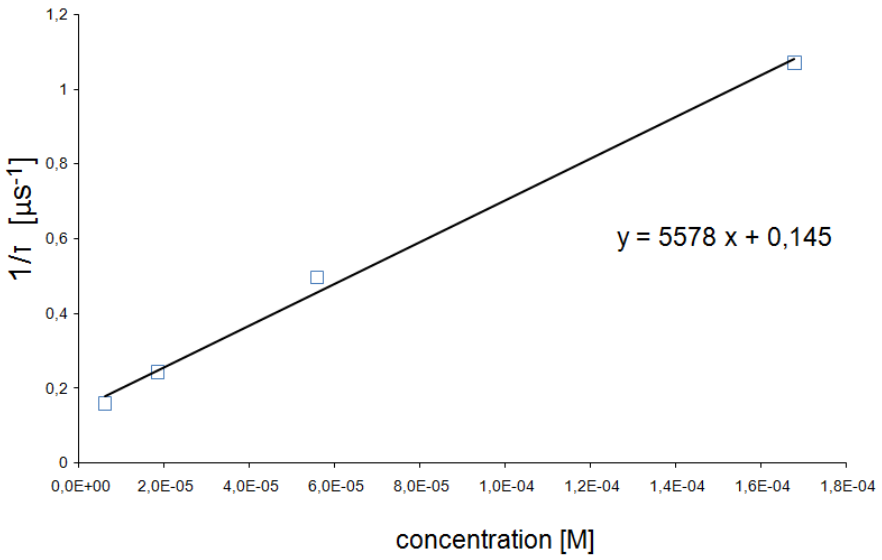

Figure 23. Plots of the measured luminescence decay constants (K = 1/τ) as function of concentration **[PtL^{3}Cl]**

The resulting high values of k_q (of the order of magnitude of 10^9, see Tab. 3) indicate efficient association of an excited monomer and a ground-state complex, and are comparable to values reported for other square platinum complexes.[6, 32, 35] Data also show how the presence of a steric hindred aryl substituent, such as mesityl, leads to a decrease in π-stacking fenomena and therefore reduces self-quenching of complexes as shown by the lower k_q value. In particular in case of compound **[PtL^{2}A^1]** there is no formation of excimer band even for concentrated solution (3×10^{-4} M).

Interestingly compound **[PtL^{4}A^1]**, whose emission at 500 nm is virtually structureless at room temperature, does not exhibit the formation of excimeric band upon increasing concentration (Fig. 24). Since steric effect are only part of the picture, in this case there might be an electronic influence of substituents which could play an important role in determining the affinity of the excited state molecule for a ground state molecule. This would be in agreement with our previous observation that **[PtL^{4}A^1]** molecules are subjected to significant electronic perturbations when excited.

Table 5: emission lifetimes of monomer and excimer, and self quenching rate constant

COMPOUND	SUBSTITUENT ON terdentate(ancyllary) LIGAND	LIFETIME [µs]			K_{SQ} $[10^9 M^{-1}s^{-1}]$
		τ_0	$\tau_{MONOMER}$	$\tau_{EXCIMER}$	
Pt(dpb)Cl	H (Cl)	7.2[a]	---	0.1[a]	5.3[a]
[PtL^{1}Cl]	Methyl (Cl)	7.8[a]	---	0.3[a]	3.3[a]
[PtL^{2}Cl]	Mesityl (Cl)	7.9[b]	---	---	1.0[a]
[PtL^{3}Cl]	4-F (Cl)	6.9	0.9	1.2	5.6
[PtL^{4}Cl]	4,6-F-Ph,CF_3-Py (Cl)	3.9	1.3	1.4	3.6
[PtL^{1}SCN]	Me (Thyocyanate)	9.3	---	0.2	8.9
[PtL^{1}A^1]	Me (F_2phenylacetylene)	7.8	1.4	1.8	2.9
[PtL^{4}A^4]	4,6-F-Ph,CF_3-Py (NMe_2phenylacetylene)	2.2	1.2	0.8	9.6

[a] data from ref. [11]; [b]data from ref. [6]

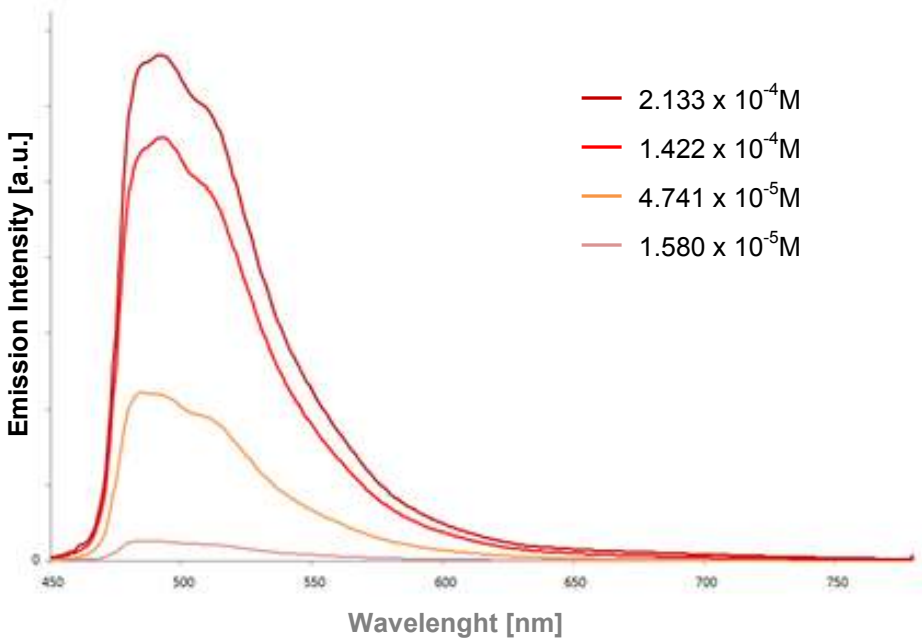

Figure 24. Concentration dependence of emission intensity of complex **[PtL^{4}A^1]** in dichloromethane solution at room temperature (λ_{exc} = 392 nm).

8.2.3. Temperature dependance and oxygen quenching

A further evidence supporting the assignement of a primarily ligand centred π-π* excited state is that the highly structured emission is scarsely shifted in position upon cooling to 77K

(Fig. 25, Tab. 6). Moreover, according to other previous studies,[6] the lifetimes in alcholic glass solution - where torsional rearrangement is inhibited - were similar to those determined at room temperature (Tab. 6).

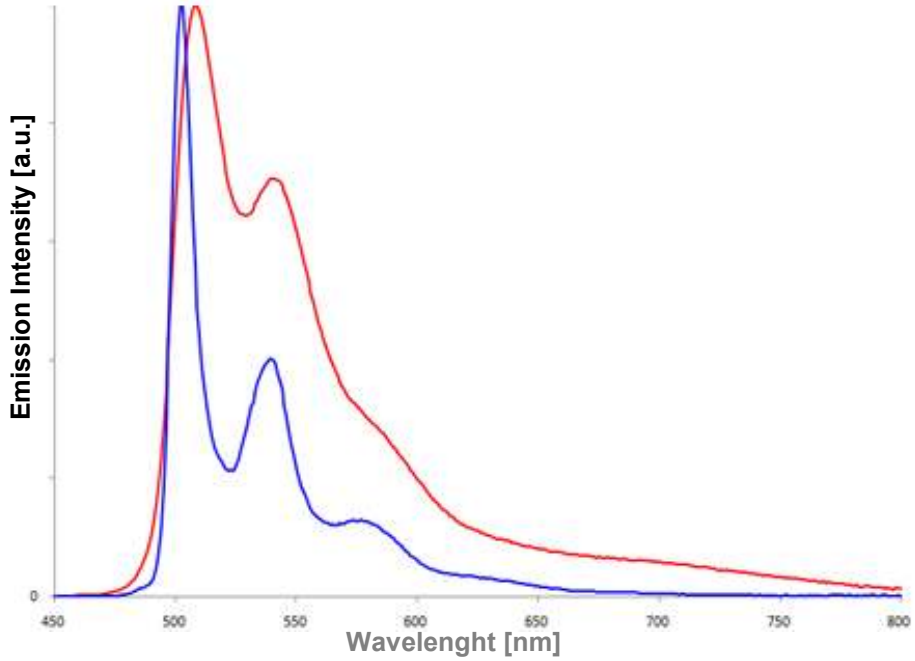

Figure 25. Normalised spectra of emission at 298 K (red line) and 77 K (blue line) of complex **[PtL^{1}A^1]** in dichlorometane and glass alchol solution, respectively (λ_{exc} = 407 nm).

This result puts in evidence that the rigidity of N^C^N-coordination is an efficient strategy in eliminating the pathways of potential thermally activated non-radiative decay (an exception be made for complex **[PtL^{4}A^4]** where the unusually long lifetime observed at low temperature, ca. 40 μs, as well as the strong red-shift, can be reasonably attribuited to aggregation fenomena). In fact Pt(II) complexes of bidentate ligands are usually instable with respect to distortion from D_{4h} to D_{2d} symmetry in the excited state and this is reflected in an enhancement in lifetime upon cooling. For example **Pt(ppy)(Hppy)Cl** (Fig.26), displays a luminescence lifetime of 641 ns at 298 K which increase to 11.2 μs at 77 K.[36]

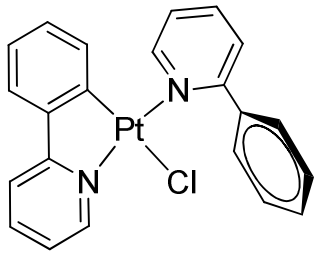

Pt(ppy)(Hppy)Cl

Figure 26. Schematic structure of the ortho-metalated Pt(II) complex **Pt(ppy)(Hppy)Cl** where ppy is the ortho-C-deprotonated form of 2-phenylpyridine and Hppy is 2-phenylpyridine**,** as reported by Ford *et al*.[36]

Table 6 lifetimes values, τ, at different temperatures

COMPOUND	SUBSTITUENT ON terdentate(ancyllary) LIGAND	EMISSION 298K (77K)[a] λ_{max} [nm]	LIFETIME [µs]		
			τ_0 [b]	τ_{298K} [c]	τ_{77K} [a]
[PtL^{3}Cl]	4-F (Cl)	504, 542 (502, 539, 576)	6.9	6.3	7.7
[PtL^{4}Cl]	4,6-F-Ph,CF_3-Py (Cl)	484, 515 (478, 510, 545, 706)	3.9	3.7	4.7
[PtL^{1}A^1]	Me (F_2phenylacetylene)	508, 538 (503, 539, 577)	7.8	5.9	6.8
[PtL^{1}A^2]	Me (F_5phenylacetylene)	502, 533 (497, 530, 564)	7.0	6.1	8.0
[PtL^{2}A^1]	Mesityl (F_2phenylacetylene)	500, 529, 572 (494, 526, 561, 601)	5.9	5.9	6.3
[PtL^{4}A^1]	4,6-F-Ph,CF_3-Py (F_2phenylacetylene)	486, 514 (475, 494, 522, 694)	5.2	2.5	6.5
[PtL^{4}A^4]	4,6-F-Ph,CF_3-Py (NMe_2phenylacetylene)	484, 513 (543, 568, 690)	2.2	5.3	40

[a]observed for the most diluited solution in in dichloromethane at 298K and in glass alchol at 77K. [b]Intrinsic lifetime estimated at infinite diluition. [c]observed for the most diluited deaereted solution in dichloromethane at 298K.

As far as excimers are concernes, since their formation includes a diffusion process in solution after photoexcitation, their lifetime depends on temperature as well as on samples concentration. In fact, generally in square planar Pt(II) complexes the excimer emission is weaken upon decreasing temperature untill it disappears at 77 K, even for high concentrated solution (10^{-3} M).[3, 32, 35] Complex **[PtL^{4}Cl]** represent a remarkable exception since even at low concentration the excimer band is clearly observed when working at low temperature (Fig.27), a behaviour never observed at least for this Pt(II) complexes family. As expected excimer emission is enhanced by increasing concentration (Fig.28).

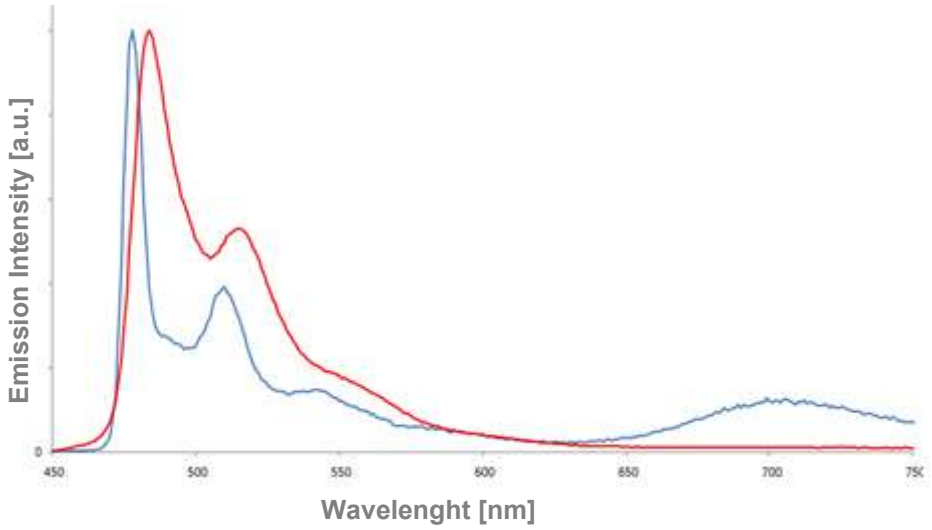

Figure 27. Normalised spectra of emission at 298K (red line) and 77K (blue line) for the most diluited solution (8.483 x 10^{-6}M) of complex **[PtL^{4}Cl]** in dichlorometane and glass water solution, respectively (λ_{exc}= 388 nm).

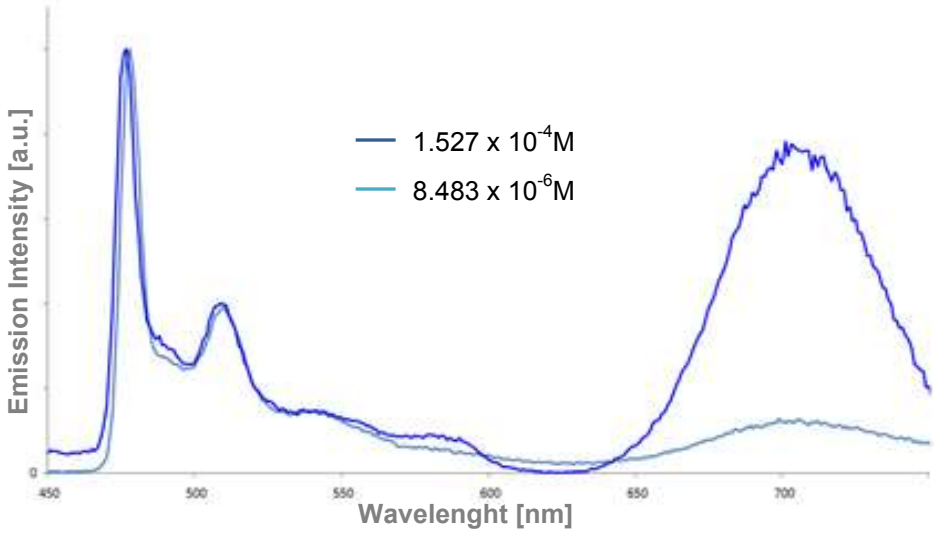

Figure 28. Concentration dependence of normalised emission spectra for complex **[PtL^{4}Cl]** in glass alchol solution at 77 K (λ_{exc} = 388 nm).

Interestingly dichloromethane solutions of this complex exhibit thermochromism – *i.e.* the ability of a substance to change color depending on temperature. In fact upon cooling to 77 K, the yellow solution turned into a deep green (Fig. 29). This phenomenum suggest that intermolecular interactions between molecules in their ground state, *i.e.* Pt---Pt distance, changes upon cooling although the emission energy is virtually the same. A similar behaviour had been observed for solid state emssion of thiocyanate terpyridyne salts.[37]

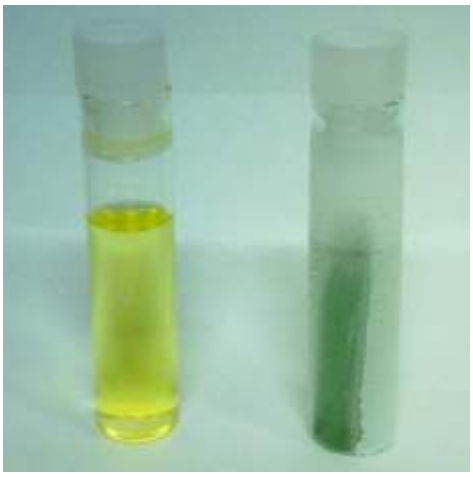

Figure 29. Termochromatic behaviour of **[PtL^{4}Cl]:** green solution is at 77 K while yellow is at 298 K.

It is known that the typically long-lived triplet excited state lifetime of platinum(II) complexes enables efficient quenching reactions by surrounding triplet molecules such as dioxygen (Fig. 30).[22, 38-40]

$$*Pt(T_1) + O_2(T_0) \rightarrow Pt(S_0) + *O_2(S_1)$$

Figure 30. Mechanism for bimolecular oxygen-quenching process via singlet oxygen formation. *Pt(T_1) stands for Pt(II) complex molecule in its excited state (triplet); $O_2(T_0)$ is the oxygen molecule in its ground state (triplet); Pt(S_0) is the complex in its ground state (singlet) and $O_2(S_1)$ is the oxygen molecule in its excited state (singlet).

The bimolecular rate constants for this process, $K_q^{O_2}$, can be calculated by a modified Stern-Volmer expression, Eq. 5, supposing oxigen concentration to be equal to 2,2 mmol dm^{-3} in a dichloromethane solution at room temperature and at 0.21 atm:[41]

$$K_q^{O_2} = \left\{\frac{1}{\tau_{aer}} + \frac{1}{\tau_{deaer}}\right\}/[O_2] \qquad \text{Eq. 5}$$

Where $\frac{1}{\tau_{aer}}$ and $\frac{1}{\tau_{deaer}}$ are the rate of emission decay for the aereted and the deareted solution respectively.

It turned out that **[PtL^{4}Cl]** and its derivatives are characterised by $K_q^{O_2}$ values of an order of magnitude lower than those reported for different cyclometalleted platinum systems (10^8 M^{-1} s^{-1} versus 10^9 M^{-1} s^{-1} Tab. 7).[6, 42] This implies that CF_3-pyridyl-substituited complexes are less sensible to dioxigen. In fact they are characterized by a relatively low ratio between quantum yield values for degassed, Φ_{deaer} and air saturated, Φ_{aer}, solution in contrast to the other complexes of the same family (Φ_{deaer} / Φ_{aer} ≈3 vs ≈10 or ≈20; see Φ value

reported in Tab. 7). This ratio is, of course, also reflected in the ratio between lifetimes at the same conditions (Tab. 7).

Table 7: photophysical results obtained in presence and absence of dioxygen

COMPOUND	SUBSTITUENT ON terdentate(ancyllary) LIGAND	Φ_{lum}% degased(aereted)	τ Degased (aereted) [μs]	$K_{Q(O2)}$ [$10^8 M^{-1}s^{-1}$]
Pt(dpb)Cl	H (Cl)	60 (4)[a]	7.2 (0.5)[a]	9.1[a]
[PtL^{1}Cl]	Methyl (Cl)	68 (2)[a]	7.8 (0.3)[a]	16[a]
[PtL^{2}Cl]	Mesityl (Cl)	62 (5)[a]	---	7.4[a]
[PtL^{3}Cl]	4-F (Cl)	47 (3)	6.3 (0.6)	7.4
[PtL^{4}Cl]	4,6-F-Ph,CF_3-Py (Cl)	53 (16)	3.7 (1,2)	2.5
[PtL^{1}S^1]	Me (Thyocyanate)	60 (5)	8.6 (0.7)	6.2
[PtL^{1}A^1]	Me (F_2phenylacetylene)	77 (4)	5.9 (0.3)	15
[PtL^{1}A^2]	Me (F_5phenylacetylene)	20 (2)	6.1 (0.6)	6,7
[PtL^{2}A^1]	Mesityl (F_2phenylacetylene)	66 (4)	5.9 (0.3)	15
[PtL^{4}A^1]	4,6-F-Ph,CF_3-Py (F_2phenylacetylene)	27 (9)	2.5 (1.0)	3,1
[PtL^{4}A^4]	4,6-F-Ph,CF_3-Py (NMe_2phenylacetylene)	23 (5)	5.3 (1.5)	2,2

[a] data from ref. [11];

In particular a comparison between the lifetimes observed for degassed, τ_{deaer}, and air saturated, τ_{aer}, dichlormetane solution of **[PtL^{4}Cl]** and of **Pt*L*^{33}Cl** (which is substituited with a methoxy group on the pyridine rings, Fig.31), puts in evidence the importance of the CF_3 moiety in stabilization towards oxygen quenching (**[PtL^{4}Cl]** τ_{deaer}/τ_{aer} ≈ 3 vs **Pt*L*^{26}Cl** τ_{deaer}/τ_{aer} = 7.8/0.58 ≈ 13).[43] This appealing characteristic could be an advantage in the preparation of devices.

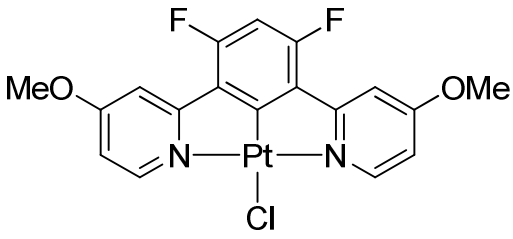

Pt*L*[26]Cl

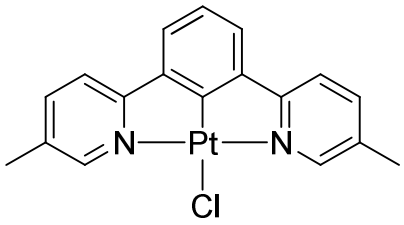

Pt(5dpb)Cl

Figure 31. Schematic structure of [1,3-di(4-methoxy-pyrid-2-yl)-4,6-difluorobenzene] chloride, **Pt*L*[26]Cl,** as reported by M. Cocchi *et a*l.;[43] and of [1,3-di(5-methyl-pyrid-2-yl)benzene] chloride, **Pt(5dpb)Cl**, as reported by Abe *et al.*[35]

8.3. Solid state emission

Preliminary results suggest that solid state emissions are significantly lower than those observed in solution (in some cases even too weak to determine lifetime). Therefore we have mainly focused our attention on the most promising **[PtL[4]Cl]**. The spectrum profile of the solid state emission for complex **[PtL[4]Cl]** is very different from that in dichlorometane soltution (Fig. 32). Indeed, it displays only an intense stuctureless band at ca. 700 nm which is a relevant finding since many applications (*e.g.* in communications or biomedicine), call for optoelectronic devices operating in the near-infrared (NIR) spectral range.[44]

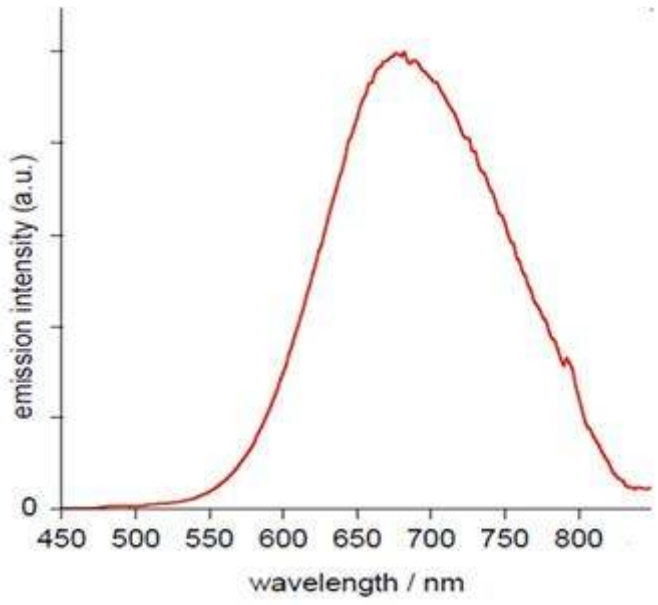

Figure 32. Solid state emission spectra of **[PtL[4]Cl]**

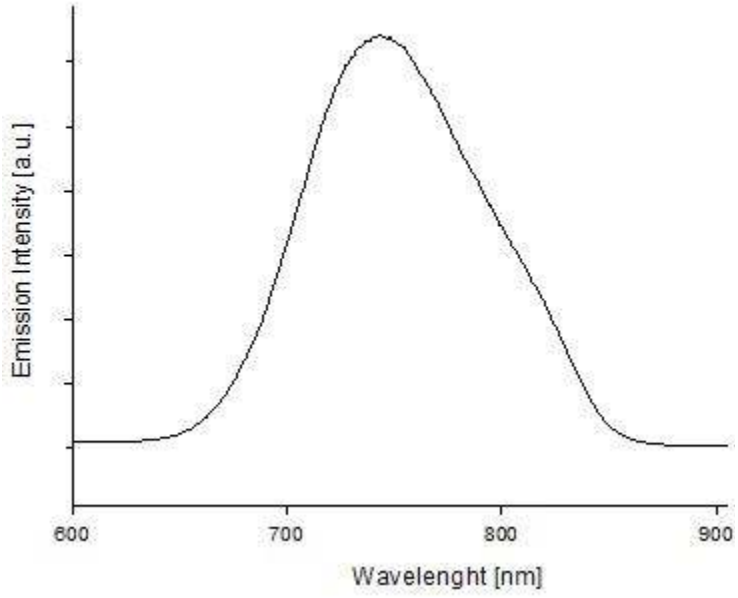

Figure 33. Solid state emission spectra of **[PtL^{4}Cl]** after grinding.

A similar behaviour has been also observed for the non-substituited complex **Pt(dpb)Cl** where the red luminescence of the powder had been attributed to emission of a dimer or an aggregate generated in an amorphous state.[44, 45] According to M. Cocchi *et al.*[44] the triplet character of this dimeric state - called excimer by similarity with the excited dimers formed in solution - is confirmed by the luminescent decay which show a measured lifetime about 1.3 μs. Actually solid state emission of **[PtL^{4}Cl]** is subtly dependent upon packing of molecules due to the d_z^2(Pt)-d_z^2(Pt) interactions. Thus, when crystals are crushed and ground with a spatula on a glass substrate, emission colour changes and move to lower energy reasonably owing to a shortening in Pt---Pt distances (and the consequent decrease in the HOMO-LUMO energy gap, Fig. 33). In this way the exciton and charge transfer interaction responsible for excimeric emission are more efficient.[44] This phenomenon is called mechanochromism and had been recently reported by Abe *et al.*[35] for methyl-pyrydyl-substituted Pt(II) complex (Fig. 31). In contrast to its behaviour in solution, the solid **[PtL^{4}Cl]** does not change colour upon cooling. These interesting features are still under investigation and in particular detailed cristallographic studies are required.

9. Electroluminescence

In the following section we shall report the fabrication of OLEDs based on some of our Pt(II) complexes as phosphor emitters. The excimer-like emission displayed by these complexes in the solid state is of particular interest concerning OLEDs that emitts white light, (WOLEDs). In fact, the employment of a lumophore that form broady emitting excimer allows to simplify the device architecture with respect to multiple-dopant-emissive layer devices (see section: Introduction).[46] In collaboration with dr. Cocchi's (CNR Bologna), and dr. Botta's (CNR Milano) groups we have explored two different approaches for the manifacturing of electrophosphorescent devices. In the first case film processing is based on a vacuum technology (see 'Introduction'), while in the second case the organic materials are coated onto substrate by spin-coating technique. The results for this studies shall be now presented.

9.1. Vacuum-deposited devices

The thermal stability and sublimability of our Pt (II) complexes renders them appropriate for incorporation into the emissive layer of vapour deposited OLEDs. Indeed, highly-efficiency devices have been previously fabricated by doping N^C^N-coordinated complexes into a 4,4',4''-tris(*N*-carbazolyl-triphenylamine), (TCTA), host in multilayer devices.[4] The same OLED structure has been used by M. Cocchi's group for the manifacturing of two prototype devices based on **[PtL^{4}Cl]** (Fig. 34).

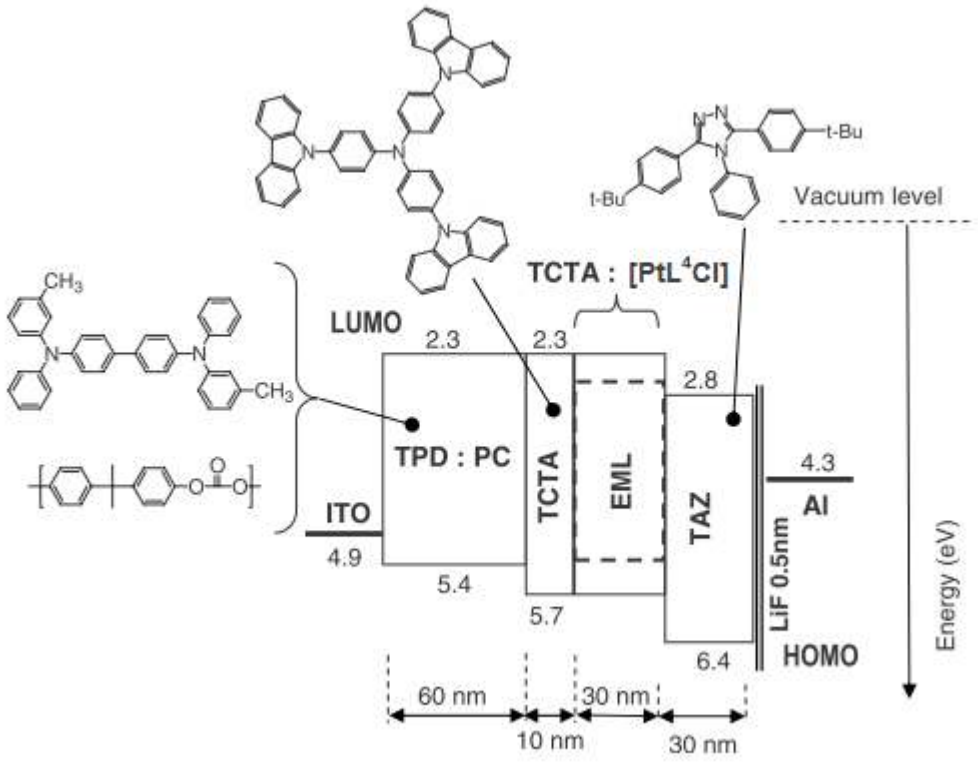

Figure 34. The architecture of the LEDs manufactured and molecular structures of the materials used: ITO/ TPD:PC [75%:25%] / TCTA / TCTA:[PtL^{4}Cl] [95%:5%] or [PtL^{4}Cl] 100% / TAZ / LiF / Al. These are completed with energy level diagram shown for understanding the exciton and electronic traffic within the devices. The HOMO obtained for each material corresponds to its ionization potential. The LUMO is equal to the molecular electronic affinity. The Fermi level positions for ITO and Al electrode contacts are added for completion. The positions of all the levels are indicated by the numbers in electron volts relative to the vacuum level at energy zero.

The architecture of the LEDs consist of an indium tin oxide, ITO, coated glass anode transparent to the light generated in the emissive layer. Holes are injected from the ITO anode and pass through a blend of N,N′-diphenyl-N,N′-bis(3-methyl)-1,1′-biphenyl-4,4′-diamine with a polycarbonate, TPD:PC, and TCTA hole-transporting layers and recombine in the emitting layer with electrons that were injected from an Al/LiF cathode and transported through the electron transporting layer of 3-phenyl-4-(1′-naphthyl)-5-phenyl-1,2,4-triazole, TAZ. The 10 nm-thick TCTA layer has been used to block triplet exciton transfer from the Pt complex to the nonradiative triplet of TPD. The 30 nm thick layer of TAZ plays a similar role inhibiting quenching of the Pt complex triplet excitons at the cathode while at the same time blocking holes. These features enable to confine the recombination process in a 30 nm thick emitting layer. Such a device architecture allows optimization of performance parameters.[4]

At a guest concentration of 5 wt % only the structured emission characteristic of monomeric excited states is observed with apparently no excimer-like emission, leading to bluish-green light (Fig. 35). On the contrary a vacuum evaporated layer of the neat complex exhibits exclusively excimer-like emission at ca. 700 nm, thus a near-infrared emitting electroluminescent device is obtained (Fig. 35). This, as we have remembered in the previous section, is a relevant finding since many current applications require optoelectronic devices operating in the near-infrared (NIR) spectral range. The emission colour for both devices was almost independent from the current density and the *Commission Internationale de l'Eclairage*, CIE, coordinates are reported in Fig. 35. By adjusting the relative amount of TCTA and **[PtL^{4}Cl]** it is possible to generate emission from both the monomer and the excimer, resulting in white electroluminescent.[38] Unfortunately efficient white light (*i.e.* x = 0.33; y = 0.33)[7] couldn't be obtained since the monomeric emission was significantly centred in the green spectral range and therefore the blue component was missing.

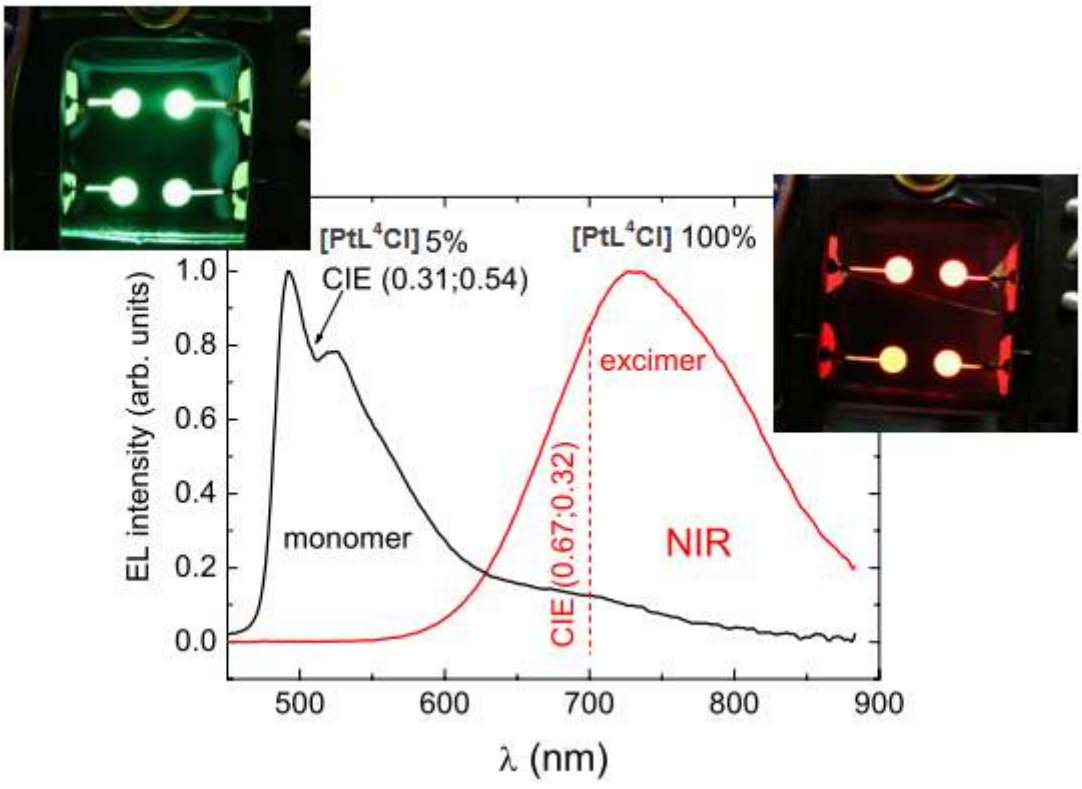

Figure 35. Electroluminescence spectra for devices based on a 5% and a 100% of **[PtL^{4}Cl]**, respectively, as emitting layer.

The highest external electroluminescence quantum yield, EL QE, achieved using complex **[PtL^{4}Cl]** at 5 % doping level within the TCTA host, is around 6% at 5 x 10^{-3} A cm^{-2} and therefore in the range of other devices previously fabricated (Fig. 36).[44] At the highest

doping ratio lower efficiency and inferior performance are observed a fact that had been generally attributed to aggregate-induced quenching.[7] Remarkably the electroluminescence efficiency decrease slowly on increasing voltage – the so called "roll-off" effect. This is attributed to the low exciton–exciton and exciton–charge quenching interactions taking place in the rather large recombination zone, where both charge and exciton concentrations are lower compared with a standard OLED structure where recombinations take place in a narrow zone at the emitting-layer interfaces.[47] Besides, the relatively short lifetimes of this complex help to reduce the roll-off resulting from electric-field-induced exciton quenching effects, exciton–exciton annihilation, and charge-carrier–exciton interactions on long lived excited states, as found for other electrophosphorescent devices.[48, 49]

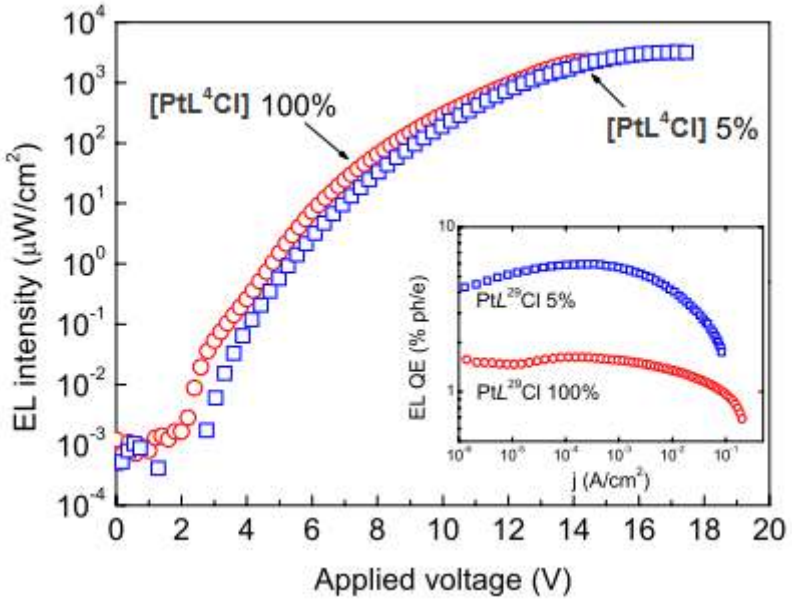

Figure 36. Electroluminescence performances of the two OLEDs having the configuration represented above: blue square refer to the TCTA: **[PtL^{4}Cl]** [95%:5%] blend and red circle to the **[PtL^{4}Cl]** 100% film pure as emitter layer. Electrollumunescence intensity vs applied voltage and external quantum efficiencies vs electric current (inset).

9.2. Spin-coated devices

For White OLEDs to gain acceptance in the general illumination market manifacturing costs must be below $3 per 1000 lm, and this target cost is difficult to realise with vaccum-deposited device architectures. Hence, consideration must be given to manifacturingelectrophosphorescent WOLEDs using solution processing, where costs are significantly lower to those associated with vacuum technologies. In collaboration with dr. C. Botta' group double layer electroluminescent devices were realised by simple spin-coating

the organic materials. This tecnique has the appealing advantage of being very economical and simple. The LEDs configuration is the following: ITO/100%(PVKc)/65%PVK:30%PBD:5%**[PtL^{x}Y]**/Ca, where PVK stands for poly(N-vinylcarbazole) and PVKc for high molecular weight PVK, while PBD is 2-(4-biphenylyl)-5-(4-*tert*-butylphenyl)-1,3,4-oxadiazole (see Experimental section). The bottom layer of PVKc (Fig. 38) plays a multiple role in the LEDs architecture inhibiting quenching of the Pt complex triplet excitons by PEDOT:PSS[50] while at the same time transporting holes. PVK is well known in OLED manifacturing by virtue of its good properties as hole transporting material.[50] Interestingly the use of an high molecular weight PVK, (*i. e.* PVKc, M_w=1000000 g mol^{-1}), have allowed us to partially prevent dilution of the bottom layer during spin-coating of the second film. Moreover, PVKc also prevents from direct contact of residual not dissolved material from the top layer with the anode, which is one of the reasons for short-circuits leading to a decrease in a device's performance. Top layer consist of the platinum complex (**[PtL^{1}Cl]**, **[PtL^{3}Cl]** and (**[PtL^{1}SCN]** respectively), dispersed in a PVK:PBD matrix. PBD is an electron transporting material, introduced in order to improve balance between charges.

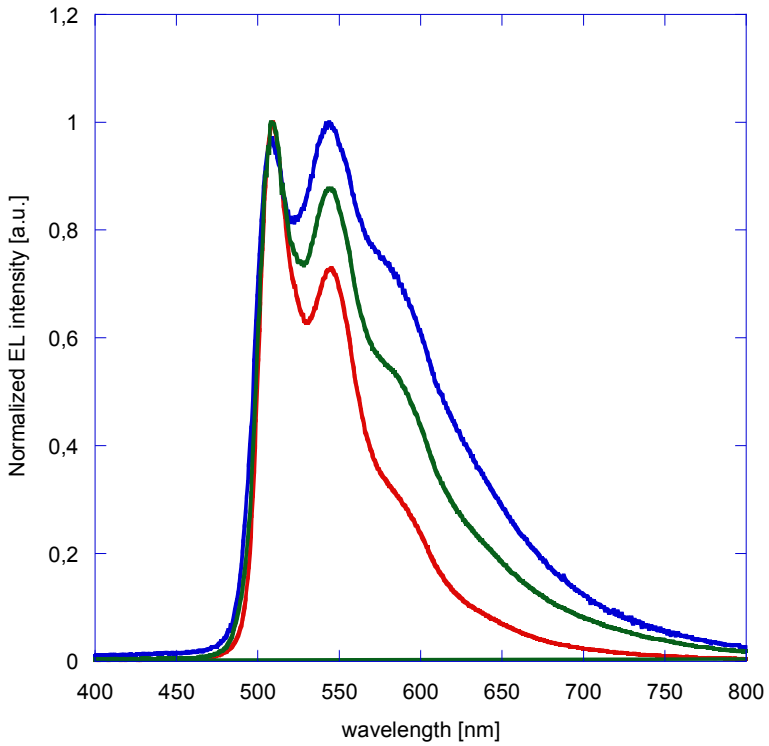

Figure 37. Molecular structures of PBD and PVKc/PVK. EL spectra of PVKc/65%PVK:30%PBD:5%Pt complex diodes. Red line for **[PtL^{3}Cl]**, green for **[PtL^{1}Cl]** and blue for **[PtL^{1}S^{1}]**.

In Fig. 37 the electroluminescence spectra of the OLEDs with 5 wt % of complexes as top layer is shown, while in Tab. 8, and Tab. 9, are reported the electrochemical and photophysical data of the complexes and devices performance information, respectively. Electroluminescence, EL, spectra have shapes similar to those of photoluminescence, PL, for diluted solutions with an increased intensity in the long wavelengths range in the order **[PtL3Cl]** < **[PtL^{1}Cl]** < **[PtL^{1}SCN]**. This behavior is more reasonably attributed to PVKc - or PVK - electromer/exciplex emission centered around 600 nm rather than to complex luminescence.[52]

Table 8: Electrochemical and photophysical data of **[PtL^{1}Cl]**, **[PtL^{3}Cl]** and (**[PtL^{1}SCN]**

Complex	PL QY (%)	HOMO [eV]	LUMO [eV]
[PtL^{3}Cl]	50	5.0	2.7
[PtL^{1}S^1]	60	5.5	2.5
[PtL^{1}Cl]	68[c]	5.2[b]	2.8[b]

[a] Quantum yield in degassed dichloromethane. [b]Based on data from ref. [48]. [c]Data from ref.. [11]

Table 9: Electrochemical and photophysical data of **[PtL^{3}Cl]**, **[PtL^{1}S^1]** and **[PtL1Cl]** with electroluminescence performance of devices with structure PVKc/65%PVK:30%PBD:5%Pt complex

	V_{on} [V]	EL QE (%)[a]	L [cd m^{-2}][b]	LE [cd A^{-1}][b]	PE [lm W^{-1}][b]	L_{max} [cd m^{-2}][b]	CIE (x,y)
[PtL^{3}Cl]	12	0.28	91	0.94	0.18	755	(0.32, 0.61)
[PtL^{1}SCN]	15	0.21	17	0.62	0.11	161	(0.39, 0.55)
[PtL^{1}Cl]	18	0.23	21	0.68	0.097	195	(0.37, 0.58)

[a] Maximum external quantum efficiency at forward direction. [b] At maximum external quantum efficiency.

PVKc - or PVK - blue emission can not be observed in the EL spectra since the absorption of the complexes overlaps with the emission from the polymer (see Fig. 37) being the PVKc bottom layer sufficiently thin to allow efficient energy transfer to the dye acceptors. On the other hand PVK electromer band is still visible because its energy level lays lower than emitting levels of ligands (see Tab. 8 and Fig. 37 for energy levels).

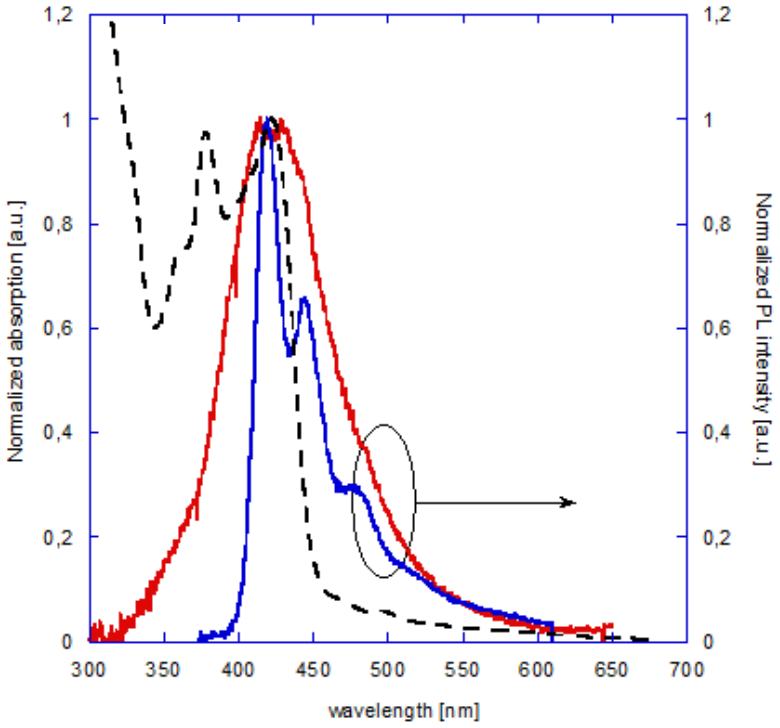

Figure 37. Absorption spectrum of **[PtL^{3}Cl]** (dashed line, 2.075 x 10^{-4} M) in dichloromethane and PL spectra of PFO (blue line, 325 nm) and of PBD:PVK (red line, 320 nm) films. Solution concentration and excitation wavelengths are given in the legend.

The observed ordered for the increasing intensity in electroplex spectral range can be explained in terms of trapping properties of the complexes. If a complex does not trap charge carriers efficiently, these can travel in a device more freely and therefore the probability that they will be trapped by PVK:PBD matrix increases. As a result, the worst trapping ability of a complex means the higher intensity of electromer band observed. Efficient trapping abilities is also connected with high external quantum efficiency, EL QE, of a device and should lead to a decrease in leakage current.[7] Indeed, in the present case **[PtL^{3}Cl]**, which has the highest EL QE value, has also the best trapping abilities, while **[PtL^{1}S^1]** the worst (see Tab. 9), even if photoluminescence quantum yields would suggest a higher efficiency for this latter (**[PtL^{1}S^1]** Φ_{lum} = 60%; versus **[PtL^{3}Cl]** Φ_{lum}= 47%).

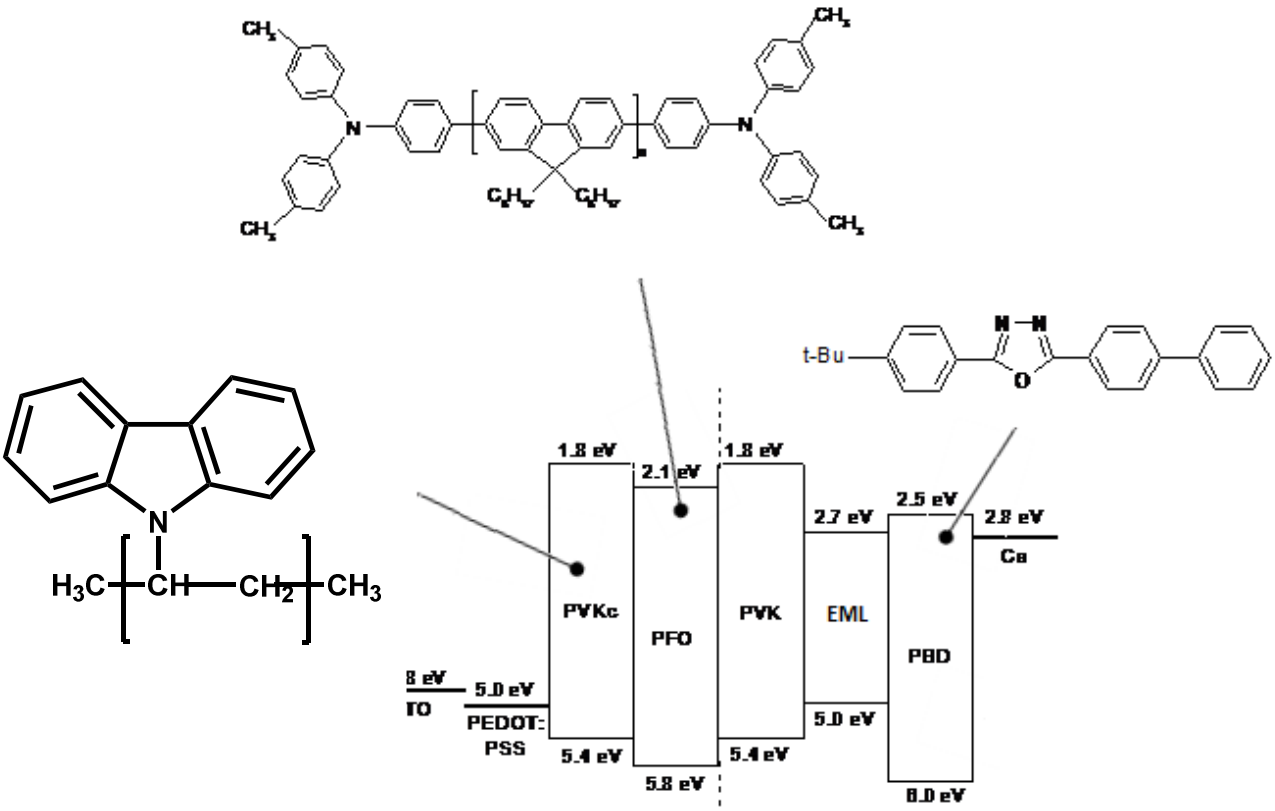

Figure 38. Energy levels of used materials.

By increasing concentration of the complex **[PtL^{3}Cl]** in the PVK:PBD matrix emission from single layer devices was tuned from green to red. The EL spectra are presented in Fig. 37). The band centered at 700 nm is assigned to excimer electroluminescence and should not be misinterpreted with PVK electromer emission. With OLED configuration: 40%PVK:20%PBD:40%FPtCl, a balanced green and red emission was observed. This preliminary result was exploited for the fabrication of double layer WOLED.

9.2.1. White OLED

In this section we present a WOLED employing multilayer emission mechanisms in simple solution processable double layer device with structure ITO/PEDOT:PSS/52%PVKc:48%PFO/40%PVK:20%PBD:40%FPtCl/Ca/Al; where PEDOT:PSS is a blend of poly(3,4-ethylenedioxythiophene) with poly(styrenesulfonate); while PFO is poly(9,9-dioctylfluorenyl-2,7-diyl) end capped with N,N-Bis(4-methyl-phenyl)-4-aniline. The bottom layer, which consists of mixture of PVKc with PFO, has

been used as blue emitting[53] and hole transporting layer. As in the case of PVK, PFO is also known for being a good hole transporter.[54] Moreover since the HOMO level of PVKc is lower compared to that of PEDOT:PSS injection of holes from the anode to PFO is facilitated. Besides, the HOMO levels of two polymers do not allow holes to be efficiently trapped in the bottom layer and, as a result, they may enter the top emitting layer. The top layer consists of platinum complex dispersed in a PVK:PBD matrix. Even though within such LED configuration holes can not be efficiently trapped in the hole transporting layer, **[PtL^{3}Cl]** is an effective hole trapping center and therefore collects holes that arrive from the bottom layer and prevents their migration towards the cathode, consequently decreasing leakage current.

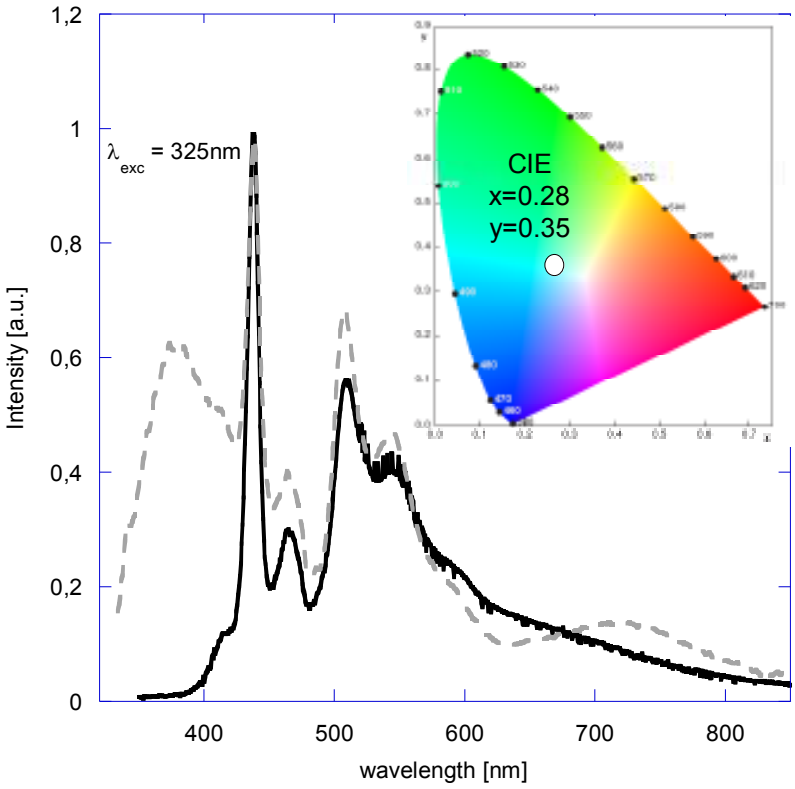

Figure 39. Comparison between EL (solid line, 7V) and PL (dashed line, λ_{exc}=325nm) spectra of ITO/PEDOT:PSS/52%PVKc:48%PFO/40%PVK:20%PBD:40%FPtCl/Ca/Al diode. In the inset CIE coordinates of EL spectrum are shown.

Fig. 39 shows the EL spectrum of the device, whose CIE coordinates are *x = 0.28*, *y = 0.35* and *Correlated Colour Temperature* (CCT) – *i.e.* the temperature of a black body radiator that has a colour that most closely matches the emission from a non-blackbody radiator - is 8145 K. These results are quite good considering that for high-quality illimination, sources with CIE coordinates similar to that of a blackbody radiator with a

CCT between 2500 K and 6500 K are required, *i.e.* x= 0.33 and Y= 0.33.[7] The shoulder observed at 400 - 420 nm is most likely a residual emission of PFO α phase,[55] which is strongly decreased on account of the thermal treatment performed on the bottom layer (see Experimental section). The sharp peaks at 438 nm and 465 nm represent vibrational structure of 0→0 and 0→1 transitions in β phase PFO. In this diode emitted blue light can go outside from the device immediately or after reflection from the cathode. In the last case partially absorbed light is used to excite platinum complex. Thus, by employing high concentration of **[PtL^{3}Cl]** in the top layer we could apply a single dopant as two color emitter. In fact the bands at 509 nm and 544 nm together with shoulder at 590 nm are attributed to phosphorescence from single **[PtL^{3}Cl]** molecules while the shoulder starting at 615 nm and decreasing towards low energy is assigned to excimeric emission. The much smaller intensity of the excimer band observed in WOLED, compared to that of the single layer device with the same concentration of the complex, is probably caused by dissolution of the bottom layer during preparation of the second film. In this process the complex may penetrate the bottom layer, decreasing balance between monomers and dimers, and, therefore, diminishing the red emission. A possible contribution to the red part of the spectrum may also be due to PVK electromer, which is centered around 600 nm. The light emitted from the top layer can not be absorbed by the polymers in the bottom layer and therefore leaves the device without obstacles. Thus, the combination of the electroluminescences from the two layers creates white light. In Fig. 39 the PL spectrum of the device is reported together with the EL spectrum. A comparison between the two spectra evidences a difference in the blue region, with stronger emission of PVKc and PVK:PBD in PL with respect to EL. Such discrepancy can be explained by considering the mechanisms responsible for two types of luminescence. In fact, in PL generation, and subsequent recombination, of excitons takes place directly on emitting sites in the whole bulk of the device, assisted by energy transfer process[56] from PVKc:PFO and PVK:PBD to **[PtL^{3}Cl]**. Long range dipole-dipole energy transfer is only possible if emission spectrum of a donor overlaps with absorption spectrum of an acceptor and the distance between donor and acceptor is sufficiently small. In the present case the first condition is fulfilled as shown by the spectra in Fig. 37. Dependence on donor-acceptor distance means that excitons created on donor sites in proximity of acceptors (bottom/top layer interface and top layer) may transfer their energy to **[PtL^{3}Cl]**, while excitons created in the bottom layer do not have such possibility. In the last case blue emission from PVKc and PFO is generated (Fig. 39): the intensity of both emitters spectra is comparable, though PFO has higher quantum yield than PVK.[57] Such behavior is due to the excitation wavelength chosen (325 nm), which happens to excite at

the proximity of the absorption maximum of PVK band, but at the minimum of PFO absorption. As a result balanced blue emission is observed. In electroluminescence transporting and trapping properties of the system have to be considered together with energy transfer process. It was pointed before that PVKc:PFO can not trap holes efficiently while the complex is a good trapping centre for this type of charge. As a consequence, during electrical operation, high concentration of holes is present in the bottom/top layer interface and in the top layer. In this region holes meet electrons, injected from the cathode, and create excitons localized on the complex which, during recombination, emits green and red light. The blue emission detected in EL suggests that electrons may enter into the bottom layer and bind there some holes on emitting centers localized on PFO. In contrast, in devices with bottom layer consisting of PVKc or PVKc:PBD blue EL was not detected. Such behavior was most likely caused by moderate quantum yields of those emitters and, more importantly, by good transporting properties of both materials which prevent efficient trapping of charge carriers on emitting centers. In contrast PFO is an efficient emitter and is also able to trap electrons in PFO:PVKc system in the bottom layer.

In conclusion, given the problem of charge balance the maxima power efficiencies of solution processed OLED remain, as expected, below that of OLED fabricated by vapor deposition (for comparison with a vacuum deposited OLED based on **[PtL^{1}Cl]** see ref. [44]). Nevertheless, they are higher than those reported for spin-coated OLEDs based on other N^C^N-Pt(II) complexes as emitting layers (EL QE ≈ 0.03 at 10 V).[58] From the data it also emerges that the device based on **[PtL^{3}Cl]** seems to display the best performances within the serie.

References

[1] *Evans*, *R.C. ;* Douglas, P.; Winscom, C. J. *Coord. Chem. Rev.,* **2006**, *250,* 2093.

[2] Jüstel, T.; Nikol, H.; Ronda, C. *Angew. Chem. Int. Ed*, **1998**, *37,* 3084.

[3] Rochester, D. L.; Develay, S.; Záliš, S.; Williams, J. A. G. *Chem. Soc. Rev.*, **2009**, *38*, 1783.

[4] Cocchi, M.; Kalinowski, J.; Fattori, V.; Williams, J. A. G.; Murphys, L. *Appl. Phys. Lett.* **2009**, *94*, 073309.

[5] Lowry, M. S.; Goldsmith, J. I.; Slinker, J. D.; Rohl, R.; Pascal, R. A.; Malliaras, G. G.; Bernhard, S. *Chem. Mater*., **2005**, *17*, 5712

[6] Farley, S. J.; Rochester, D. L.; Thompson, A. L.; Howard, J. A. K.; Williams, J. A. G. *Inorg. Chem,.* **2005**, *44*, 9690.

[7] Williams, J. A. G.; Develay, S.; Rochester, D. L.; Murphy, L. *Coord. Chem. Rev.*, **2008**, *252*, 2596.

[8] Crites, D.K.; Cunningham, C.t.; Mc Millin, D.R. *Inorganica Chimica Acta* **1998**, *273*, 346.

[9] Yam, V. W.-W.; Tang, R. P.-L.; Wong, K. M.-C.; Cheung, K.-K.; *Organometallics* **2001**, *20*, 4476.

[10] Lu,W.; Mi, B.-X.; Chan, M. C. W.; Hui, Z.; Che, C.-M.; Zhu, N.; Lee, S.-T. *J. Am. Chem. Soc*., **2004**, *126*, 4958.

[11] Williams, J. A. G.; Beeby, A.; Davies, S.; Weinstein, J.A.; Wilson, C. Inorg.Chem., **2003**, 42, 8609.

[12] (*a*) Manka, J. T.; Mckenzie ,V. C.; Kaszynski, P. *J. Org. Chem*., **2004**, *69,* 1967; (*b*) Dinnell, K.; Chicchi, G. G.; Dhar, M. J.; Elliott, J. M.; Hollingworth, G. J.; Kurtz, M. M.; Ridgill, M. P.; Rycroft, W.; Tsao, K.-L.; Williams, A. R.; Swain, C. J. *Bioorganic and medicinal Chemistry Letters,* **2001**, *11*, 1237.

[13] Càrdenas, D. J.; Echavarren, A. M.; Ramìrez de Arellano, M. C.; *Organometallics* **1999**, *18*, 3337.

[14] Burmeister, J. L.; Basolo, F. *Inorg. Chem.* **1964**, *3*, 1587

[15] Coyer,M. J.; Croft, M.; Chen, J.; Herber, R. H. *Inorg. Chem.* 1992, 31, 1752.

[16] Field, J. S.; Grimmer, C. D.; Munro, O. Q.; Waldron, B. P. *Dalton trans*., **2010**, *39*, 1558.

[17] Han, X.; Wu, L.; Zhang, L.; Tung, C. *Chinese Science Bulletin* **2006**, *51* 1005.

[18] Kwok, C.- C.; Ngai, H. M. Y.; Chan, S.-C.; Sham, I. H. T.; Che, C.-M.; Zhu, N. *Inorg. Chem.* **2005**, *44*, 4442.

[19] Baik, C.; Han, W.-S.; Kang, Y.; Kang, S. O.; Ko, J. *Journal of Organometallic Chemistry*, **2006**, *691*, 5900.

[20] Neenan, T.; Withesides, M. *J. Org. Chem*. **1988**, *53*, 2489.

[21] Maya, F.;Chanteau, S. H.; Cheng, L., Stewart, M. P.; Tour, J. M. *Chem. Mater.* **2005**, *17*, 1331.

[22] Yang, X.; Wang, Z.; Madakuni, S.; Li, J.; Jabbour, G. E. *Adv. Mater.* **2008**, *20*, 2405.

[23] (*a*)Blanton, C. B.; Murtaza, Z.; Shaver, R. J.; Rillema, D. P. *Inorg.Chem*., **1992**, *31*, 3230 ; (*b*) Wong, W. Y.; Wang, X.-Z.; He, Z.; Djuri, A. B.; Yip, X.-Z.; Cheung, K.-Y.; Wang, H.; Mak, C. S.K.; Wong, W.-k. C. Nature Materials. 2007, 6, 521.

[24] Sotoyama, W.; Satoh, T.; Sato, H.; Matsuura, A.; Sawatari, N. *J. Phys. Chem. A,* **2005**, *109*, 9760.

[25] Michalec, J. F.; Bejune, S. A.; Cuttell, D. G.; Summerton, G. C.; Gertenbach, J. A.; Field, J. S.;Haines, R. J.; McMillin, D. R. *Inorg. Chem*. **2001**, *40,* 2193.

[26] Djurovich, P. I.; Murphy, D.; Thompson, M.E.; Hernandez, B.; Gao, R.; Hunt, P.L.; Selke, M. *Dalton Trans*., **2007**, 3763.

[27] Marcus, R. A.; *J. Chem. Phys.* **1965**, *43*, 1261.

[28] Wilde, A. P.; Watts, R. J. *J. Phys. Chem.* **1991**, *95*, 622.

[29] Maestri, M.; Sandrini, D.; Balzani, V.; von Zelewsky, A.; Deuschel-Cornioley, C.; Jolliet, P. *Helv. Chim. Acta* **1988**, *71*, 1053.

[30] Brooks, J.; Babayan, Y.; Lamansky, S.; Djurovich, P. I.; Tsyba, I.; Bau, R.; Thompson, M.E. *Inorg. Chem*. **2002**, *41*, 3055.

[31] Lai, S.-W.; Chan, M. C.-W.; Cheung, T.-C.; Peng, S.-M.; Che, A.-M. *Inorg. Chem.* **1999**, *38*, 4046.

[32] Ma, B.; Djurovich, P. I.; Thompson, M. E. *Coord. Chem. Rev*. **2005**, *249,* 1501.

[33] Lu,W.; Chan, M. C. W.; Cheung, K.-K.; Che, C.-M. *Organometallics* **2001**, *20*, 2477

[34] Pettijohn, C.N.; Jochnowitz, E. B.; Chuong, B.; Nagle, J. K.; Vogler, A. *Coord. Chem. Rev.* **1998**, *171,* 85.

[35] Abe,T.; Itakura, T.; Ikeda, N.; Shinozaki, K. *Dalton Tras.* **2009**, 711.

[36] Mdeleleni, M. M.; Bridgewater, J. S.; Watts, R. J.; Ford, P. C *Inorg. Chem,.* **1995**, *34*, 2334.

[37] Rachford, A. A.; Castellano, F. N. *Inorg. Chem.*, **2009**, *48*, 10865.

[38] Murphy, L.; Williams, J. A. G. in *Topics in organometallic chemistry 28*, *Molecular Organometallic Materials for Optics*, H. Le Bozec, and V. Guerchais (eds.), Springer Verlag Berlin Heidelberg **2010**, pp 75-111.

[39] Djurovich, P. I.; Murphy, D.; Thompson, M.E.; Hernandez, B.; Gao, R.; Hunt, P.L.; Selke, M. *Dalton Trans*., **2007**, 3763.

[40] For reviews, see for example: (*a*) McMillin, D.R.; Moore, J. J. *Coord. Chem. Rev.*, **2002**, *229*, 113; (*b)* Ma, B.; Djurovich, P.; Thompson, M. E. *Coord. Chem. Rev.*, 2005, **249**, 1501; (*c*) Castellano, F. N.; Pomestchenko, I. E.; Shikhova, E.; Hua, F.; Muro, M. L.;

Rajapakse, N. *Coord. Chem. Rev.*, **2006**, *250*, 1819; (*d*) Wong, K. M.-C.; Yam, V. W. -W. *Coord. Chem. Rev.*, **2007**, *251*, 2477.

[41] Murov, S. L.; Carmichael, I.; Hug, G. L. Handbook of Photochemistry, 2nd ed.; Marcel Dekker: New York, 1993.

[42] Santoro, A.; Whitwood, A.C.; Williams, J. A. G.; Kozhevnikov, V. N.; Bruce, D. W. Chem Mater, **2009**, *21*, 3871.

[43] Cocchi, M.; Kalinowski, J.; Murphys, L.; Williams, J. A. G.; Fattori, V. *Organic Electronics*, **2010**, *11,* 388

[44] Cocchi, M.; Virgili, D.; Fattori, V.; Williams, J. A. G.; Kalinowski, J. *Appl. Phys. Lett.* **2007**, *90*, 023506.

[45] (*a*) Kalinowski, J.; Cocchi, M.; Virgili, D.; Fattori, V.; Williams J. A. G. *Adv. Mater*. **2007**, *19*, 4000; (*b*) Adamovich, V.; Brooks, J.; Tamayo, A.; Alexander, A. M.; Djurovich, P. I.; D'Andrade, B. W.; Adachi, C.; Forrest, S. R.; Thompson, M. E. *New J. Chem.,* **2002**, *26*, 1171; (*c*) Ma, B.; Djurovich, P. I.; Garon, S.; Alleyne, B; Thompson, M. E. *Adv. Funct. Mater.,* **2006**, *16*, 2438; Williams, E. L.; Haavisto, K. ; Li, J.; Jabbour, G. E *Adv. Mater.,* **2007**, *19*, 197.

[46] D'Andrade, B.W.; Forrest, S.R. *Adv. Mater.,* **2004**, *16,* 1585.

[47] Sotoyama, W.; Satoh, T.; Sato, H Sawatari, N.; Inoue, H. *Appl. Phys. Lett.* **2005**, 86, 153505.

[48] Cocchi, M.; Virgili, D.; Fattori, V.; Rochester, D. L.; J Williams, J. A. G. *Adv. Funct. Mater.* **2007**, *17*, 285.

[49] (*a*) Baldo, M. A.; Adachi, C.; Forrest, S. R. *Phys. Rev. B: Condens. Matter Mater. Phys.* **2000**, *62*, 10967; (*b*) Kalinowski, J.; Stampor, W.; Mezyk, J.; Cocchi, M.; Virgili, D.; Fattori, V.; Di Marco, P. *Phys. Rev. B: Condens. Matter Mater. Phys*. **2002**, *66*, 235321.

[50] Giovanella, U.; Betti, P.; Botta, C.; Destri, S.; Moreau, J.; Pasini, M.; Porzio, W.; Vercelli, B.; Bolognesi, A. *Chem. Mater.,* in press.

[51] Bos, F. C.; Burland, D. M. *Phys. Rev. Lett.,* **1987**, *58*, 152.

[52] Qian, L.; Bera, D.; Holloway, P. H.; *J. Chem. Phys.,* **2007**, *127*, 244707.

[53] Grice, A. W.; Bradley, D. D. C.; Bernis, M. T.; Inbasekaran, M.; Wu, W. W.; Woo, E. P. *Appl. Phys. Lett.,* **1998**, *73*, 629.

[54] Redecker, M.; Bradley, D. D. C.; Inbasekaran, M.; Woo, E. P. *Appl. Phys. Lett.,* **1998**, *73*, 1565.

[55] (*a*) A. J. Cadby, P. A. Lane, H. Mellor, S. J. Martin, M. Grell, C. Giebeler, D. D. C. Bradley, M. Wohlgenannt, C. An and Z. V. Vardeny, *Phys. Rev. B: Condens. Matter Mater. Phys.,* 2000, **62** 15604; (*b*) M. Grell, D. D. C. Bradley, X. Long, T. Chamberlain,

M. Inbasekaran, E. P. Woo and M. Soliman, *Acta Polym.,* 1998, **49**, 439; (*c*) M. Grell, D. D. C. Bradley, M. Inbasekaran and E. P. Woo, *Adv. Mater.,* 1997, **9**, 798.

[56] J. R. Lakowicz, in *Principles of Fluorescence Spectroscopy,* Kluwer Academic / Plenum Publishers, New York, 2nd edn., 1999, ch. 1, pp. 13-14.

[57] Mezyk, J.; Mróz, W.; Mech, A.; Giovanella, U.; Meinardi, F.; Botta, C.; Vercelli, B.; Tubino, R. *Phys. Chem. Chem. Phys.,* **2009**, *11*, 10152.

[58] Batema, G. D.; Lutz, M.; Spek, A. L.; van Walree, C. A.; de Mello Donegá, C.; Meijerink, A.; Havenith, R. W. A.; Pérez-Moreno, J.; Clays, K.; Büchel, M.; van Dijken, A.; Bryce, D. L.; van Klink, G. P.M.; van Koten, G. *Organometallics* **2008**, *27*, 1690.

ORGANOMETALLIC COMPOUND FOR NON LINEAR OPTICS

INTRODUCTION

8. Principles of Second-Order Non Linear Optics

Non-linear optics deals with optical phenomena, caused by the interaction of applied electromagnetic fields to molecules or materials with emission of new electromagnetic fields which differ in frequency, phase, or other physical properties from the incident ones.[1–3] This kind of optical phenomena are related to the polarizability of a molecule or of a bulk material. When a bulk material is subjected to an oscillating external electric field produced by an incident radiation, there is a polarization effect, expressed by

$$\vec{P} = \overrightarrow{P_0} + \overrightarrow{P_{ind}} = \overrightarrow{P_0} + x^{(1)}\vec{E} \qquad \text{(Eq.1)}$$

where $\overrightarrow{P_0}$ is the intrinsic polarity, $\overrightarrow{P_{ind}}$ the induced polarization, and $x^{(1)}$ the electrical susceptibility or linear polarizability tensor. If the electric field strength $\vec{E}$ of the incident radiation is very high, as is the case with laser pulses, the perturbation is not linear and the induced polarization is better expressed by a power seres according to

$$\vec{P} = \overrightarrow{P_0} + x^{(1)}\vec{E} + x^{(2)}\overrightarrow{E^2} + \cdots + x^{(n)}\overrightarrow{E^n} \qquad \text{(Eq.2)}$$

where $x^{(1)}$, $x^{(2)}$ and $x^{(n)}$ electrical susceptibilities, controlling the nonlinear response of the material. If, instead of a bulk material, the applied electromagnetic field is interacting with a molecule, the induced polarization is expressed by

$$\vec{P} = \overrightarrow{\mu_0} + \alpha\vec{E} + \beta\overrightarrow{E^2} + \gamma\overrightarrow{E^3} \qquad \text{(Eq.3)}$$

where $\overrightarrow{\mu_0}$ is the molecular ground state electric dipole moment, α the linear polarizability tensor, β and γ the non linear quadratic and cubic hyperpolarizability tensors, respectively, responsible for second- and third-order NLO effects.

The second-order NLO properties are of interest for a variety of NLO processes.[1] One of the most relevant is the SHG, originated by the mixing of three waves; two incident waves with frequency ω interact with the molecule or the bulk material with NLO properties, defined by a given value of the quadratic hyperpolarizability, β, or of the second-order electrical susceptibility, $x^{(2)}$, respectively, to produce a new electrical wave, named SH, of frequency 2ω (Fig.1).

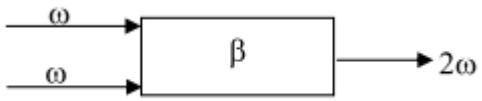

Figure 1. Second Harmonic Generation. ω is the frequency of the two incident waves and β is the quadratic hyperpolarizabilityof the material.

To obtain molecular or bulk materials displaying significant second-order NLO effects, high values of β or of $x^{(2)}$, respectively, are required. In the case of molecules, in 1977 Oudar gave a theoretical interpretation of the electronic factors controlling β. [2] The quadratic hyperpolarizability of a molecule is originated by the mobility of polarizable electrons under the effect of a strong electric field $\vec{E}$ associated with an incident radiation. It follows that it is dependent on electronic transitions which, being associated with a significant electronic mobility, are of high CT character. Oudar assumed that, when the second-order NLO response is dominated by one major CT process, β_{zzz} can be defined according to

$$\beta_{zzz} = \frac{3}{2h^2c^2}\frac{\nu_{eg}^2 r_{eg}^2 \Delta\mu_{eg}}{(\nu_{eg}^2-\nu_L^2)(\nu_{eg}^2-4\nu_L^2)} \qquad \text{(Eq.4)}$$

where z is the axis of the direction of the CT, ν_{eg} (cm^{-1}) the frequency of the CT transition, r_{eg} the transition dipole moment, $\Delta\mu_{eg}$ the difference between excited state μ_e and ground state μ_g molecular dipole moments, and μ_L the frequency of the incident radiation. Equation (4) is the so-called ‘‘two level’’ model, a way to estimate the frequency dependent quadratic hyperpolarizability for specific types of second-order NLO chromophores, characterized by a single dominant CT transition. The molecular quadratic hyperpolarizability b can be expressed both in the cgs (cm^4 statvolt $^{-1}$ = esu) or in the SI (C m^3 V^{-2}) unit systems (the conversion from the SI to the cgs system is given by the relation 10^{-50} C m^3 V^{-2} = 2.694 x 10^{-30} esu). From the ‘‘two level’’ model it is possible to extrapolate the dipolar electronic requirements that a molecule must fulfill in order to show a significant second-order NLO response. It must be noncentrosymmetric, with CT transitions with large $\Delta\mu_{eg}$ and r_{eg} and at relative low energy. This can be achieved, for instance, by separation of an electron-donor and an electron-acceptor group with a p-conjugated polarizable spacer, as occurs in classical 1D dipolar push–pull organic systems. Recently, multipolar systems, such as octupolar molecules, have been increasingly investigated, because it was shown that it is not only dipolar structures that may be the origin of significant SHG.[1, 3, 4]

The theoretical methods are a useful tool to derunderstanding hyperpolarizability–structure relationships, thus helping chemists to the design of new efficient molecular NLO. Various

quantum mechanical methods allow the calculation of the molecular quadratic hyperpolarizability, β. Among them, the ‘‘sum over states’’ (SOS) approach provides also information on the electronic origin of the NLO response. It describes the tensor β_{ijk} in terms of all the electronic states interacting with the perturbing electric field, as an infinite expansion over a complete set of unperturbed excited states. Obviously, a simplification of this approach is the two-state model (Eq. 4) described above. The most advanced theoretical methods are Density functional theory (DFT) and time-dependent DFT (TD-DFT) or time-dependent HF (TD-HF) calculations.[5]

9. Experimental techniques

Experimentally, mainly two techniques – the electric field induced second harmonic generation (EFISH) and hyper-Rayleigh scattering (HRS, also termed harmonic light scattering method) – are used in order to determine in solution the experimental value of the quadratic hyperpolarizability of molecular NLO chromophores.

The EFISH technique[6], suitable for dipolar neutral molecules, provides information on the molecular NLO properties through

$$\gamma_{EFISH} = (\mu\beta_{\lambda}/5kT) + \gamma(-2\omega; \omega, \omega, 0) \qquad \text{(Eq. 5)}$$

where $\mu\beta_{\lambda}/5kT$ represents the dipolar orientational contribution, and $\gamma(-2\omega; \omega, \omega, 0)$ a β_{λ} third-order term at frequency ω of the incident wavelength, is the electronic contribution which is negligible for many molecules with a limited electronic polarizability. β_{λ} is the projection along the dipole moment axis of β_{VEC} , the vectorial component of the β_{ijk} tensor of the quadratic hyperpolarizability, working with an incident wavelength λ of a pulsed laser. To obtain the value of β_{λ}, it is thus necessary to know the value of the ground state dipole moment μ of the molecule. Moreover, in order to avoid overestimation of the quadratic hyperpolarizabilty due to resonance enhancements, it is necessary to choose an incident wavelength whose second harmonic is far from any electronic absorption of the molecule.

The HRS technique [7] involves the detection of the incoherently scattered second harmonic generated by themolecule in solution under irradiationwith a laser of wavelength λ, leading to the mean value of the β x β tensor product. By analysis of the polarization dependence of the second harmonic signal, which can be evaluated selecting the polarization of the incident and scattered radiation, it is possible to obtain information about the single components of

the quadratic hyperpolarizability tensor β. Unlike EFISH, HRS can also be used for ionic molecular species and for nondipolar molecules such as octupolar molecules. In this thesis, the quadratic hyperpolarizability measured with an incident wavelength λ by the EFISH and HRS techniques will be indicated as $\beta_{EFISH,\lambda}$ and $\beta_{HLS,\lambda}$, respectively.

10. Organic Molecular Materials

As stated in the previous paragraph, the noncentrosymmetry is generally a prerequisite for second-order NLO activity of a molecule. Besides, in order to obtain efficient second-order molecular responses, intense, low-energy electronic transitions having CT character are required. Two main families of organic molecular NLO chromophores can be identified: dipolar and octupolar species. The former, which are not centrosymmetric, follow a general "push-pull" scheme involving a polarizable molecular structure (*e.g.*, a π-conjugated pathway) having an asymmetrical charge distribution (*e.g.*, with donor and/or acceptor group substituents) to form a donor–π–conjugated bridge-acceptor (D–π–A) network (Fig. 2).

Figure 2. Schematic representation of a "push-pull" system. A is the electron-withdrawing group, while D is the electron-donor.

The prototypical example of a dipolar molecule is represented by *p*-nitroaniline. The second-order optical nonlinearity originates from the existence of D→A electronic CT transitions mediated by the π -conjugated-bridge, which in many cases are referred to the lowest-energy transition, so that the ''two level'' model applies quite well. To this category of molecular materials belong most conjugated organic species. Octupolar molecules, instead, may be centrosymmetric but they imply the existence of twofold (D_2) or threefold (D_3) rotational axes. They are characterized by multidirectional CT excitations.

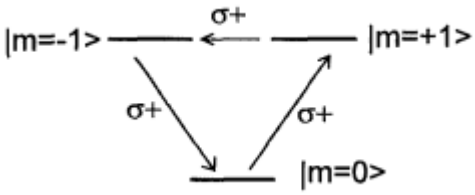

Figure 3. Three-level model used to account for the second-order nonlinearities of an octupolar molecule. In the D_{3h} symmetry group of the octupolar molecule, the electronic states may labelled according to the component of orbital angular momentum along the C_3 or z-axis, m. The m = O states are singly degenerate states, while the m = ± 1 states correspond to the doubly degenerate states. While the degenerate m = 1 and -1 states do not possess a permanent dipole moment, there is a dipole moment matrix element between them. These doubly degenerate states in the octupolar molecule are thus the analogues of the charge transfer states in dipolar molecules. The arrows represent the three transitions, σ +, contributing to $\beta_{\sigma\sigma\sigma}$.[3]

The theoretical description of nonlinearity of such systems implies, even in the simplest case, a three-level approach. One way of viewing the octupolar molecule, is as a superposition of three dipolar molecules, rotated by 0°, 120°, and 240°, respectively. Such a summation cancels the dipole moment but leaves a finite β. [3]

The prototypical example of an octupolar molecule is represented by 1,3,5-triamino- 2,4,6-trinitrobenzene (Fig.4).

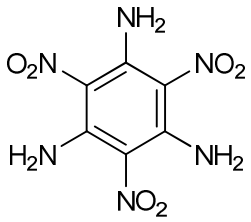

Figure 4. Schematic structure of a typical octupolar molecule 1,3,5-triamino- 2,4,6-trinitrobenzene.

11. Effect of coordination to a methal centre on NLO properties

The vast majority of the molecules studied for NLO are purely organic “push–pull” systems. Comparatively, the utilization of metal complexes in this area has been less explored.[8] Ferrocene[9] or ruthenium complexes[10] are typical examples of metal complexes employed as an electron donor (D), whereas chromium carbonyl arene was instead used as an electron acceptor (A). Metal complexes are appealing building blocks for the design of new and efficient NLO chromophores because of their rich photochemical properties. The

complexes can indeed exhibit several types of charge transfer transitions including metal to ligand (MLCT), intraligand (ILCT), ligand to ligand (LL'CT) and ligand to metal (LMCT) transitions that play a crucial role in the NLO properties of a chromophore (see next paragraph). Besides the presence of d and/or f electrons and can increase the polarizability of the organic system, improving conjugation and the number of excited states with low energy. A second attractive feature of metal complexes systems from their usually rich redox activity that makes it possible to alter their NLO response by oxidizing or reducing the metal and thereby opening an access to redox switching materials.[10a] Finally, the structural versatility of the metal complexes, offers the additional advantage that different compounds can easily be prepared by changing only a few components such as the metal or one of the ligands.

8.1. Pyridines and Stilbazoles

The effect of coordination to a metal center on the second-order NLO response of pyridine and stilbazole ligands has been deeply studied.[4,11] The quadratic hyperpolarizability β, measured in solution by the EFISH technique, of *para*-substituted pyridines and stilbazoles, such as 4-R-C_5H_4N and 4,4'-*trans* or *trans,trans*-R-$C_6H_4(CH{=}CH)_n{-}C_5H_4N$ (R= donor or acceptor substituent; n = 1, 2), increases upon coordination to various metal centers, the enhancement factor (EF)[4] being modulated by the nature of the metal which , as mentioned afore, can act as an electron-acceptor or an electron-donor. This ambivalent donor or acceptor role of a zerovalent metal has suggested two different mechanisms controlling the second-order NLO response of this kind of NLO organometallic chromophores (Schemes below).[11] When the R substituent is a strong electron-donating group, the increase of the value of the quadratic hyperpolarizability β is dominated by an ILCT transition, with the metal center, which behaves as an electron-acceptor, producing a red-shift of this transition and therefore an increase of the value of β according to the ''two level'' model.[2]

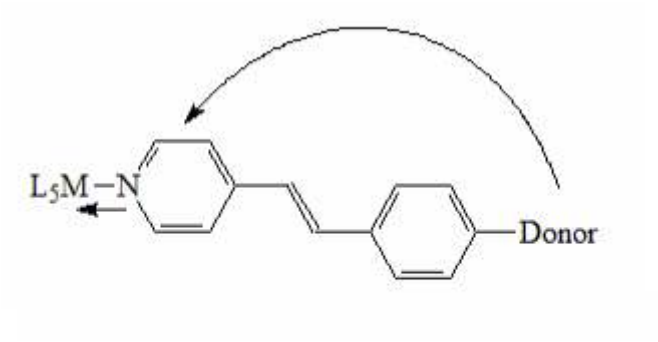

Mechanism A

significant LLCT: $\Delta\mu > 0$ ($\Delta\mu = \mu_{excited} - \mu_{ground}$)

In contrast, when R is a strong electron-accepting group, the quadratic hyperpolarizability β is dominated mainly by an MLCT transition. In this latter case the negative sign of β is due to a reduction of the dipole moment in the excited state of the MLCT transition ($\Delta\mu_{eg}$ <0), according to the ‘‘two level’’ model.[2]

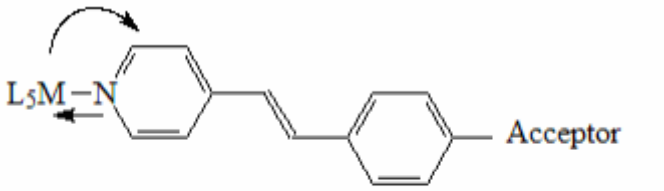

Mechanism B

significant MLCT: $\Delta\mu < 0$ ($\Delta\mu = \mu_{excited} - \mu_{ground}$)

An extended EFISH investigation of the second-order NLO response of cis-[M $(CO)_2Cl(4\text{-}R\text{-}C_5H_4N)$] (M = Rh, Ir) and fac-[$Os(CO)_3Cl_2(4\text{-}R\text{-}C_5H_4N)$] (R = electron-donor or -acceptor substituent) has confirmed such interpretation of the ambivalent role of the metal center.[12]

8.2. Compounds with Macrocyclic Ligands

The macrocyclic structure of porphyrins, consisting of an extended π system formed by four pyrrolic rings connected by methine bridges, is a typical example of a very polarizable architecture with a variety of low lying excited states. Therefore the presence of various substituents in the meso or pyrrolic position of the porphyrin ring could produce significant perturbations. These structural features, together with the high chemical and thermal stability, can explain the widespread interest in these chromophores during the last few

decades in the area of new optical materials. In the last two decades a significant amount of work has also been devoted to the investigation of the second-order NLO properties of porphyrin architectures of increasing complexity.[13] In particular, Pizzotti et al. reported[14] an EFISH investigation, working in $CHCl_3$ solution with a nonresonant incident wavelength of 1.907 μm, on the second-order NLO response of various push–pull tetraphenylporphyrins and their Zn(II) complexes substituted at the β pyrrolic position by a π-delocalized organic substituent carrying either an electron-withdrawing or electron-donating group (Fig.5).

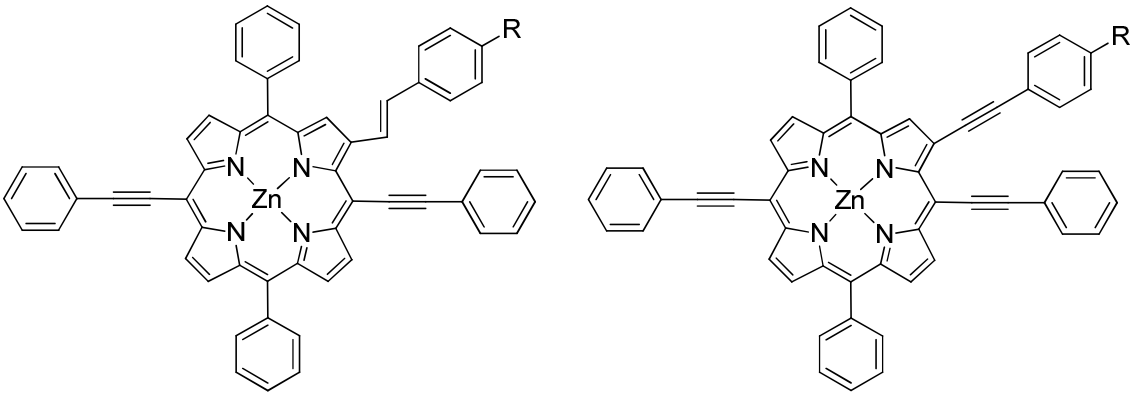

Figure 5. Schematic structure of metalloporphyrine as reported in ref.14

The value of $\beta_{EFISH,1.907}$ decreases only slightly on going from the free porphyrin to its Zn(II) complex, in agreement with the assumption that the second-order NLO response is controlled by a CT process, favored by π conjugation, from the occupied π levels of the pyrrolic ring, acting as a push system, to the π* antibonding orbitals of the linker. This latter process should be scarcely affected by coordination of the porphyrin ring to Zn (II).

Another class of metallocyclic compound with interesting NLO properties are phthalocyanines. These are macrocycles characterized by an extensive 2D planar and centrosymmetric 18 π-electron system. For this reason they have been widely investigated as third-order NLO materials. Only in the last decade have the second-order NLO properties been investigated and some reported significant results.[13,15] The high value found for centrosymmetric phthalocyanine clearly shows that, for this kind of second-order NLO chromophores, the electronic contribution $\gamma(-2\omega;\omega,\omega,0)$ to the EFISH measurement is significant and cannot be neglected.

References:

[1] J. Zyss in Molecular nonlinear optics: materials, physics and devices. Academic, Boston, **1994**.

[2] (*a*) Oudar, J.L.; Chemla, D.S. *J. Chem. Phys.,* **1977**, *66*, 2664; (*b*) Oudar, J.L. *J. Chem. Phys.* **1977**, *67,* 446.

[3] Joffre, M.; Yaron, D.; Silbey, R. J.; Zyss, J. *J. Chem. Phys.* **1992**, *97*, 5607.

[4] Cariati, E.; Pizzotti, M.; Roberto, D.; Tessore, F.; Ugo, R. *Coord. Chem. Rev.* **2006**, *250*, 1210.

[5] Kanis, D. R.; Ratner, M. A.; Marks, T. J. *Chem. Rev.* **1994**, *94*, 195.

[6] Ledoux, I.; Zyss, J. *Chem. Phys.,* **1982**, *73*, 203.

[7] Maker P.D. *Phys Rev A* **1970**, *1*, 923

[8] S.R. Marder in Inorganic Materials, Eds. D.W. Bruce, D.O'Hare, Wiley, Chichester, **1992**, 136.

[9] (*a*)Liao, Y.; Eichinger, B. E.; Firestone, K. A.; Haller, M.; Luo, J.; Kaminsky, W. Benedict, J. B.; Reid, P. J.; Jen, A. K. Y.; Dalton, L. R.; Robinson, B. H. *J. Am. Chem. Soc.*, **2005**, *127*, 2758; (*b*) Cariati, E.; Pizzotti, M.; Roberto, D.; Tessore, F.; Ugo, R. *Coord. Chem. Rev.*, **2006**, *250*, 1210.

[10] (*a*) Coe, B. J.; Houbrechts, S.; Asselberghs, I.; Persoons, A. *Angew. Chem*. Int. Ed., **1999**, *38*, 366; (*b*) Yuan, P.; Yin, J.; Yu, G.-A.; Hu, Q.; Liu, S. H. O*rganometallics*, **2007**, *26*, 196.

[11] Kanis, D. R.; Lacroix, P. G.; Ratner, M. A.; Marks, T. J. *J. Am. Chem. Soc.* **1994**, *116,* 10089.

[12] Roberto, D.; Ugo, R.; Bruni, S.; Cariati, E.; Cariati, F.; Fantucci, P.C.; Invernizzi, I.; Quici, S.; Ledoux, I.; Zyss, J. *Organometallics,* **2000**, *19*, 1775.

[13] Senge, M. O.; Fazekas, M.; Notaras, E. G. A.; Blau, W. J.; Zawadzka, M.; Locos, O. B.; Mhuircheartaigh, E. M. N. *Adv. Mater.* **2007**, *19*, 2737.

[14] Annoni, E.; Pizzotti, M.; Ugo, R.; Quici, S.; Morotti, T.; Bruschi, M.; Mussini, P. *Eur. J. Inorg. Chem.* **2005**, 3857.

[15] De la Torre, G.; Vàsquez, P.; Agullò-Lòpez, F.; Torres, T. *Chem. Rev.* **2004**, *104*, 3723.

RESULT AND DISCUSSION

5. Anellated Hemicyanine and their Ir complexes

In the last few years, organometallic and coordination complexes have emerged as interesting molecular chromophores for second-order nonlinear optical (NLO) applications, because they may offer a great diversity of tunable electronic properties by virtue of the metal centre.[1] For example, coordination of various organic push-pull NLO-phores acting as ligands such as stilbazoles bearing a NR_2 donor group produces a significant increase of their quadratic hyperpolarizability due to a red-shift of the intraligand charge- transfer transition, major origin of their second order NLO response. [1] In particular, the product $\mu\beta$ (μ = dipole moment, β = quadratic hyperpolarizability) of *cis*-[$Ir(CO)_2Cl$(4,4'-*trans*-$NC_5H_4CH{=}CHC_6H_4NMe_2$)], measured in solution by the Electric-Field Induced Second Harmonic (EFISH) generation technique, is 3 times higher than that of the free stilbazole ligand and comparable to that of an important NLO-phore such as Disperse Red One.[2] In this thesis we studied the second order NLO properties of highly delocalized pyridine systems containing a substituent amino group: 7-*N*,*N*-dibutylamino-2-azaphenanthrene, **L^3**, and 8-*N*,*N*-dibutylamino-2-azachrysene, **L^4** (Fig. 1). We then investigated systems containing an electron-withdrawing substituent (-CN), **L^5** (Fig.1). For comparison the NLO response of *N,N*-dimetyl-4-(pyridin-4-yl)aniline, **L^1**, and *N*-methyl-*N*-hexadecylaminostilbazole, **L^2** (Fig. 1),[3] the corresponding non-anellated chromophores of **L^3** and **L^4** respectively, were also investigated. Finally we synthesized *cis*-[$Ir(CO)_2ClL^3$], **[IrL^3]**, and *cis*-[$Ir(CO)_2ClL^4$], **[IrL^4]** complexes and methylated salts to evaluate the modification of the chromophores electronic properties and their effect on the NLO activity.

Here we report comprehensive methods for the convenient preparation of the iridium complexes, as well as of their precursors, and the NLO results measured by the *Electric Field Induced Second Harmonic* generation (EFISH) technique.[4]

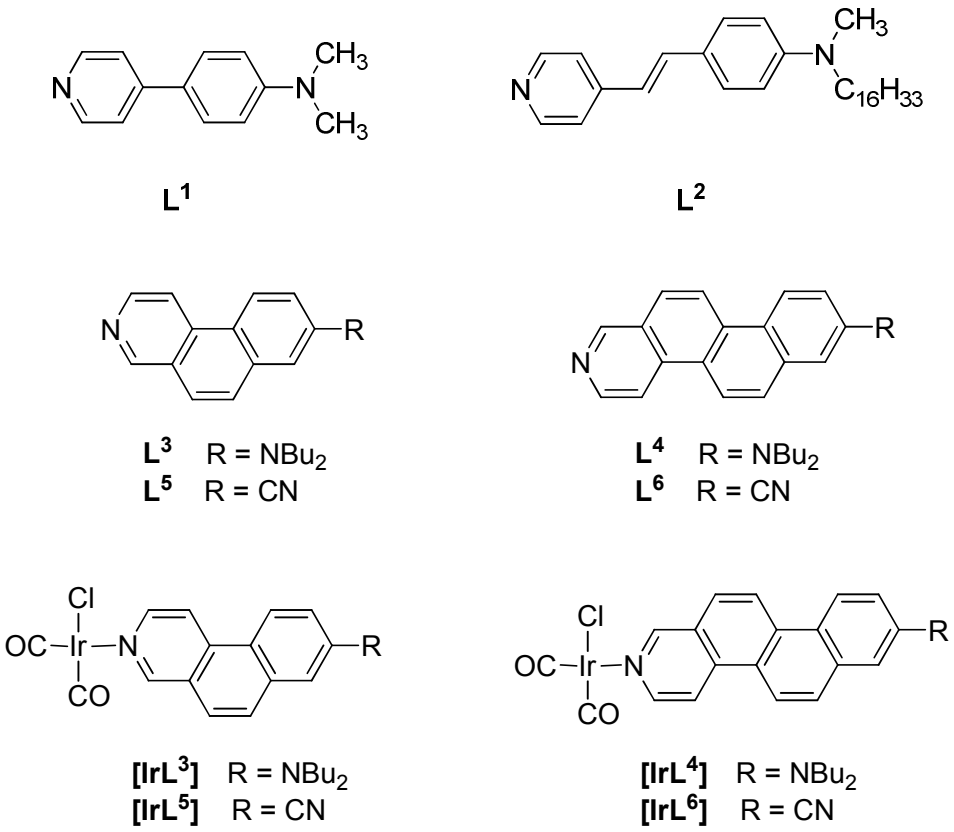

Figura 1. Schematic structure of anellated hemicyanine ligand and thei related iridium complexes.

5.1. Synthesis and Characterization

The highly π-delocalised pyridine ligands **L**^{3} and **L**^{4} have been previously reported as intermediates for the preparation of anellated emicyanine dyes.[5] However the synthetic procedures described are quite complicated and in many cases the characterization of products is unsatisfactory. Therefore the compounds used i this ph.D. work have been prepared, in colloboration with dr. Quici's group, by careful modification and optimization of the known procedure for **L**^{3}, and using a different synthetic approach for **L**^{4}.[7] The methyl pyridinium iodide salt of **L**^{4}, (**L**^{4}**MeI**) was prepared by reaction with MeI following a standard procedure.[7, 8] Details on the synthesis and characterization of these compounds are given in Experimental Section.

Scheme 1. Preparation of the ligand **L**^{1}. *Reagents and conditions*: (h) acqueous Na_2CO_3 tetrakis(triphenylphosphine)palladium(0), THF, 80 °C, 18 h, 79%.

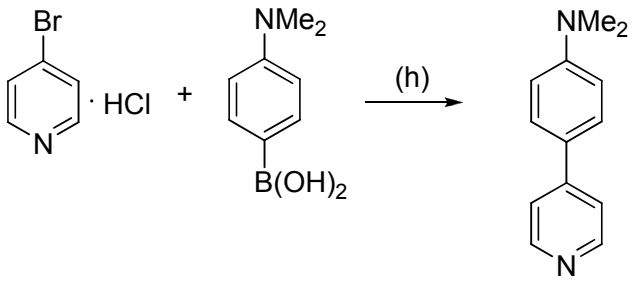

L²

Scheme 2. Preparation of the ligands **L³** and **L⁴**. *Reagents and conditions*: (a) PPh_3, CCl_4, THF, 48 h, 95%; (b) PPh_3, heptane, reflux, 24 h, 82%; (c) 3-pyridinecarboxaldehyde, ^{t}BuOK, dry MeOH, N_2, reflux, overnight, 82%; (d) 2-Me-THF, hν, 1.5 h, -15 °C, 46%; (e) isoquinoline-5-carbaldehyde, ^{t}BuOK, dry MeOH, N_2, reflux, overnight, 82%; (f) THF, hν, 8 h, 17 °C, 33.5%; (g) THF, MeI, RT, overnight, 85%

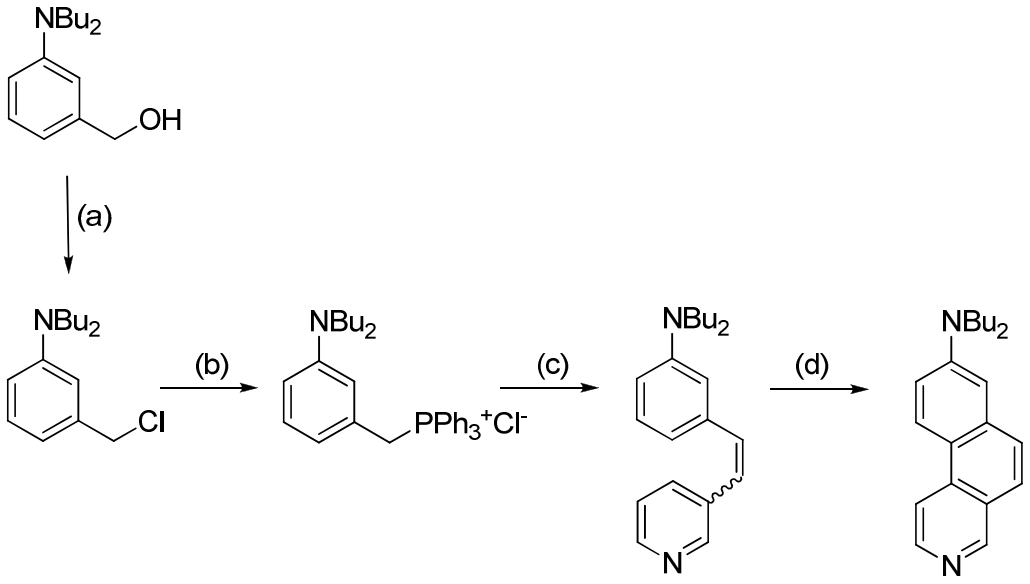

1 **2** **3** **L³**

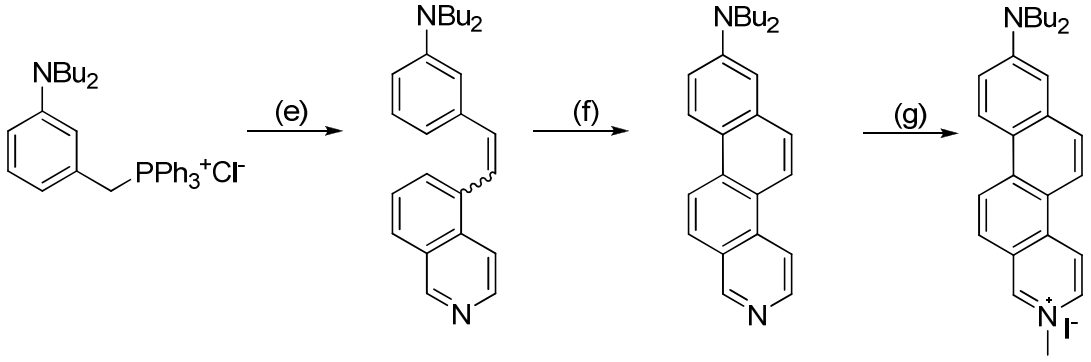

2 **4** **L^4** **L^{4}MeI**

Scheme 3. Preparation of the ligands **L^5** and **L^6** *Reagents and conditions*: (a) PPh_3, heptane, reflux, 24 h, 93%; (b) 3-pyridinecarboxaldehyde, NaOH, CH_2Cl_2, N_2, reflux, overnight, 72%; (c), hν, 2h, -17°C, 36%; (d) isoquinoline-5-carbaldehyde, NaOH, CH_2Cl_2, N_2, overnight, 93%; (e) CH_2Cl_2,, hν, 6 h, 15 °C, 15%;

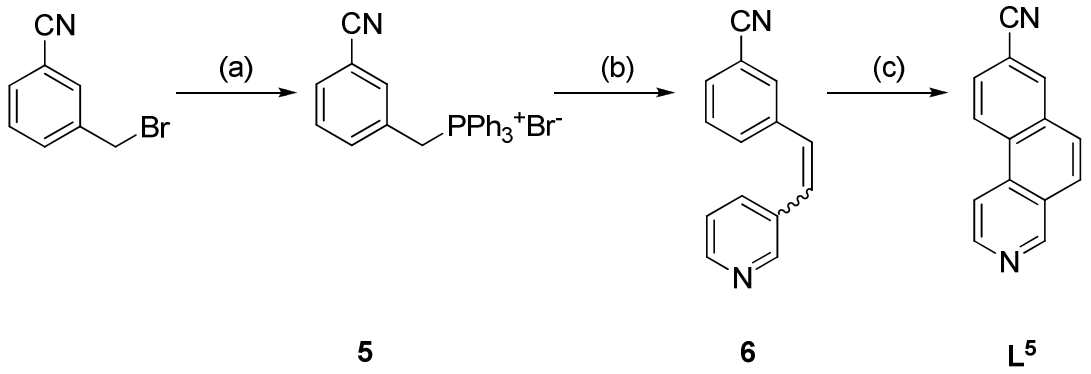

5 **6** **L^5**

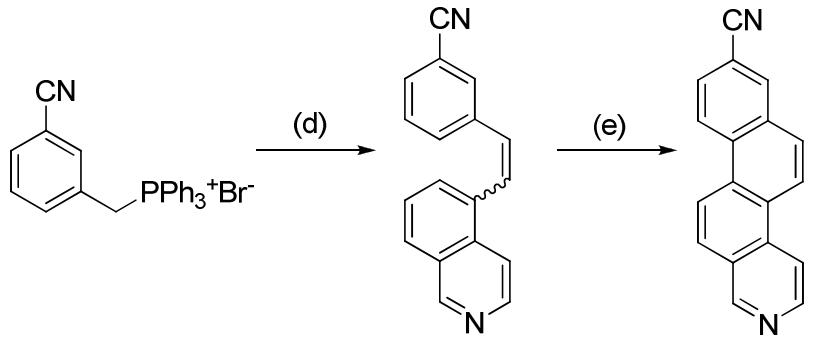

5 **7** **L^6**

The scheme for the synthesis of **[IrL^3]** and **[IrL^4]** is represented in Scheme 4. The precursor $[Ir(COT)_2Cl]_2$, (COT = cyclooctene) was prepared by reaction of $IrCl_3.nH_2O$ with cyclooctene according to literature procedure.[9] $[Ir(COT)_2Cl]_2$ does not dissolve in acetonitrile, but as soon as CO is bubbled the initial complex disappeared due to the formation of the $[Ir(CO)_2Cl]_2$ solvated species. The infrared spectrum confirmed that the reaction was completed after 10min ($[Ir(CO)_2Cl]_2$ $\upsilon_{(CO\ stretching)}$ = 2085 and 2008 cm^{-1}). Concentration of the starting solution is a key factor. In fact, in high concentrated solution a dark powder precipitates, due to the formation of polymeric $[Ir(CO)_2Cl]_n$.[10] The Ir(I) complexes, **[IrL^3]** and **[IrL^4]** were readily prepared by room temperature reaction of **L^3** and **L^4** ligand with the dimeric organometallic complex $[Ir(CO)_2Cl]_2$ as previously described for similar compounds.[2, 7] The reaction was followed by IR spectroscopy monitoring the decrease of carbonyl stretching frequencies ($\Delta\upsilon$ ca. 10 cm^{-1}). As expected an increase of the electron-withdrawing strength of the ligand substituent (*i.e.* –CN), lead to a lower decrease in frequencies (*e.g.* **[IrL^3]** υ = 2073, 1994 cm^{-1} vs **[IrL^5]** υ 2077, 1998 cm^{-1}).

Scheme 4. Preaparation of Iridium complexes of anellated hemicyanine ligands, **L^n**

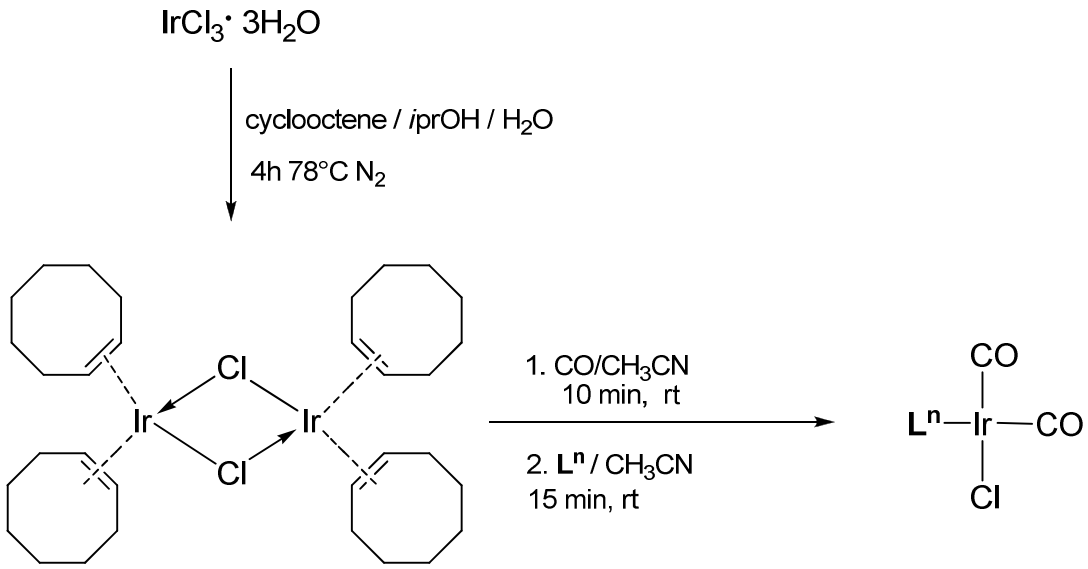

The main systematic change in the ^1H NMR spectra of the ligands upon coordination is that the signals of hydrogens in α position to the ligand pyridyl nitrogen atoms are shifted to lower fields with respect to those of the free NBu_2-substituted ligands (*e.g.* $\Delta\delta$ in $CDCl_3$ 0.13 ppm for **[IrL^4]**, Fig. 2). This shift is related to the electron transfer from the nitrogen donor atoms to the metal center, which appears to be, in agreement with the Lewis acidity of the metal centre. The presence of the electron withdrawing -CN substituent. effect leads to an opposite effect.On the contrary, the chemical shift due to the NBu_2 protons are similar in the free

ligand and in their iridum carbonyl complexes, suggesting a limited perturbation of the donor properties of the NBu_2 group when these π-delocalized systems interact with Ir(I) metal centre.

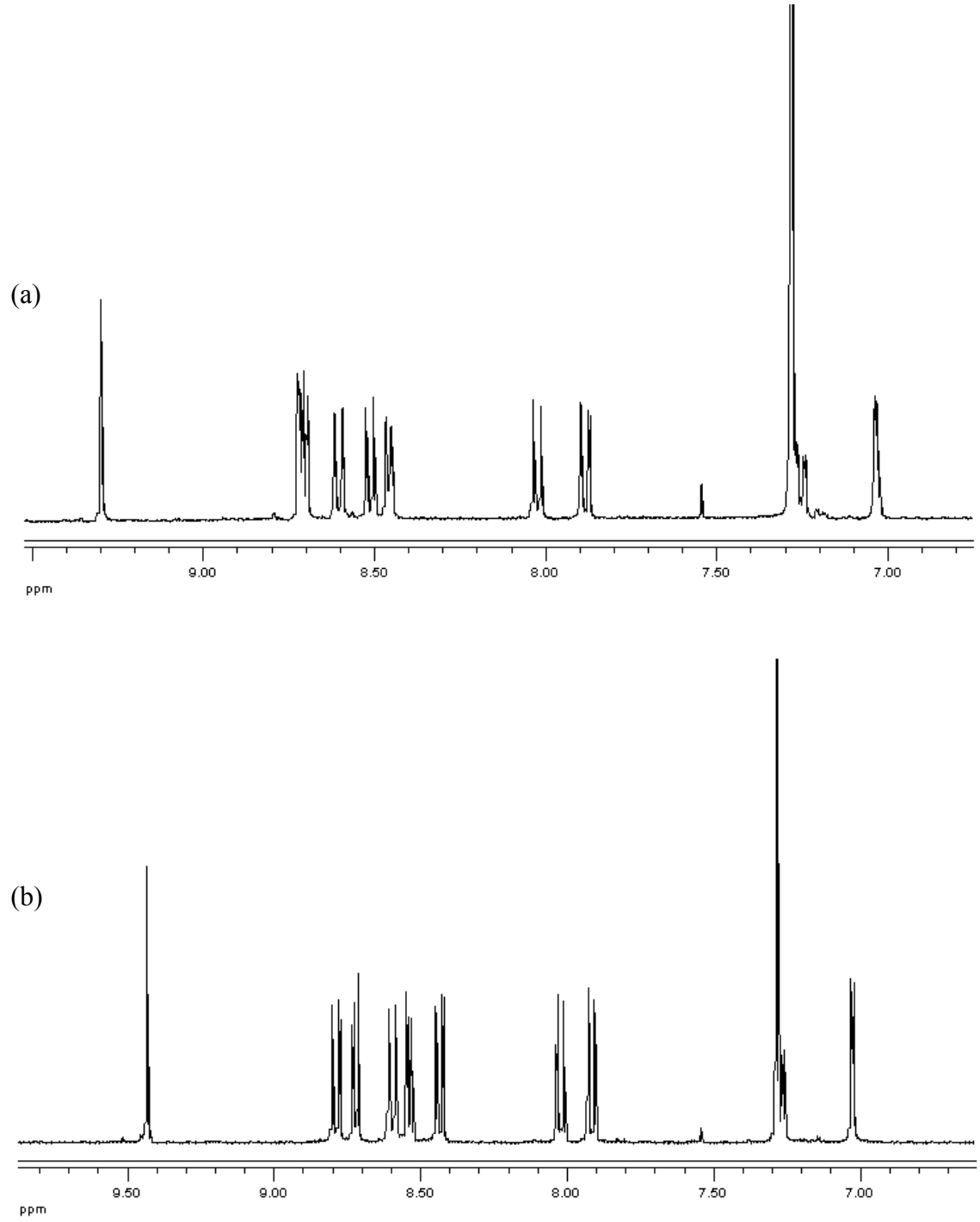

Figura 2. Aromatic region of 1H NMR spectra in deuterated chloroform of (a) 8-N,N-dibutylamino-2-azachrysene, L4, and of (b) [$Ir(CO)_2Cl$(8-N,N-dibutylamino-2-azachrysene)], [IrL4].

5.2. Study of Second-Order NLO properties by *Electric-Field Induced Second-Harmonic* (EFISH) generation technique and Theoretical investigation

The experimental electronic spectra are reported in Tab. 1, along with their $\mu\beta_{1.907}$ values measured with the EFISH technique.[4] As previously mentioned the β_{EFISH} is the projection of the hyperpolarizability tensor β along the dipole moment components, defined as:

$$\beta_{\mathrm{EFISH}} = \sum \mu\beta_i / (\sum \mu_i^2)^{\frac{1}{2}} \qquad \text{(Eq. 1)}$$

where i = x, y, z, μ_i are the dipole moment components and

$$\beta_{\mathrm{i}} = \beta_{\mathrm{iii}} + \frac{1}{3}\sum_{i\neq j}\left(\beta_{ijj} + \beta_{jij} + \beta_{jji}\right) \qquad \text{(Eq. 2)}$$

The theoretical dipole moment values, μ, of all compounds are also given together with the experimental values of **L²**, **L³** and **L⁴**.[10]

Table 1. Experimental electronic spectra, EFISH $\mu\beta_{1.907}$ and μ values of ligands **L³** and **L⁴** and related iridium complexes.

COMPOUND	λ_{MAX} [a] [nm] (ε [M^{-1} cm^{-1}])	$\mu\beta_{1.907}$ [a,b] [10^{-48}esu]	μ [c] (μ_{theor}) [D]	$\beta_{1.907}$ [10^{-30}esu]
L¹	417 (46500), 506 (9160)	48	2.4	20[d]
L²	381[e]	223[e]	3.7[e]	60[e]
L³	278 (28626), 347 (14397)	430	3.5 (7.6)	123[d] (56)[e]
[IrL³]	279 (35420), 390 (25670)	620	(16.2)	(38)[e]
L⁴	305 (41462), 361 (17179)	1800	4.2 (8.0)	429[d](224)[e]
[IrL⁴]	272(34541), 421 (12737)	-2310	(16.9)	(-137)[e]
L⁴MeI	272 (39886), 285 (37869), 315 (19045),364 (14386), 473 (26523)	1820	(18.9)	(96)[f]

[a]In $CHCl_3$ at 10^{-4} M with an incident radiation of 1.907 μm. [b]The error on EFISH measurements is ± 10%. [c]Experimental μ obtained by the Guggenheim method[11] in $CHCl_3$; the error is ± 1x10^{-18} esu. [d]By using experimental μ. [e]Data from ref. [3] [f]By using theoretical μ. [g]There is a band tail a ca 400 nm.

As expected **L[1]** is characterized by a low value of $\mu\beta_{1.907}$ in $CHCl_3$ due to the absence of a complete π-conjugation between the two aromatic rings. However this value increases drastically by a factor of 8.9, if the single bond is included into the polyaromatic scaffold of **L[3]**. Remarkably, an increase of the π-conjugation of the free ligand leads to a huge positive effect on the second order NLO response, with an enhancement factor of 4.4 on going from **L[3]** to **L[4]**, reaching a $\mu\beta_{1.907}$ value much higher than that of the related stilbazole **L[2]**.

Surprisingly, contrarily to what was observed in the case of stilbazolium salts,[8, 12] methylation of the pyridine ring of **L[4]** does not affect strongly the second order NLO response although there is a relevant red shift ($\Delta\lambda_{max}$ = 112 nm) of the ILCT transition. This effect might be related to a different orientation of the dipole moment in the two salts, which determines the overall EFISH response.

Unexpectedly coordination of L^3 to the "$Ir(CO)_2Cl$" moiety leads to a decrease in β value which even becomes negative when L^4 is coordinated (Tab. 1), indicating that the μ of the excited state is lower than μ of the ground state. This fact can be possibly attributed to the sum of two opposite contribution:ILCT transition ($\beta > 0$) and MLCT transition ($\beta < 0$).

This behaviour is in contrast with that observed upon coordination of **L[2]** to the same Ir(I) moiety where $\mu\beta_{1.907}$ is enhanced but remains positive, being dominated by an ILCT transition.[3] The increasing NLO response when an annine substituted with a withdrawing group, CN L^5, is coordinated to the iridium fragment would be in agreement with the importance of the MLCT transition(Tab. 2).

It is worth noting that the very high $\mu\beta_{1.907}$ values of **L[3]** and **L[4]** are due to large $\beta_{1.907}$ values since their dipole moments are quite similar to that previously reported [3] for **L[2]**.

Table. **2**. NLO response of CN substituted ligands, **L[5]** and **L[6]** and related iridium complexes.

Ligands	$\mu\beta_{1.907}$ [10^{-48} esu] [a]	Complexes	$\mu\beta_{1.907}$ [10^{-48} esu] [a]
L[3]	587	**[IrL[3]]**	819
L[5]	-1030	**[IrL[5]]**	-2350
L[6]	-1830	**[IrL[6]]**	-1990

[a]In DMF at 10^{-4} M with an incident radiation of 1.907 μm. The error on EFISH measurements is ± 10%

It is worth noting that the very high $\mu\beta_{1.907}$ values of **L**^{3} and **L**^{4} are due to large $\beta_{1.907}$ values since their dipole moments are quite similar to that previously reported [3] for **L**^{2}. Furthermore of particular interest is the unexpectedly very high thermal stability of **L**^{4} measured by Differential Scanning Calorimetry (DSC) (Fig. 3). The sample was subjected to three reversible cycles of melting and crystallization with a heating rate of 5 °C/min under nitrogen atmosphere. As it is evident from the DSC spectrum, the melting and the crystallization peaks show similar intensities within the three cycles thus indicating that there is neither sublimation nor partial decomposition of the product. The decomposition temperature of 434 °C was determined by further heating of the sample over its melting temperature. The very high thermal stability, combined with its high NLO activity, makes **L**^{4} particularly appealing from an applicative point of view. As we have afore noted NLO chromophores should be highly resistant to thermal degradation for a practical use in electrooptic systems, where temperatures higher than 300 °C are required to process and assemble NLO-active materials into devices.[13]

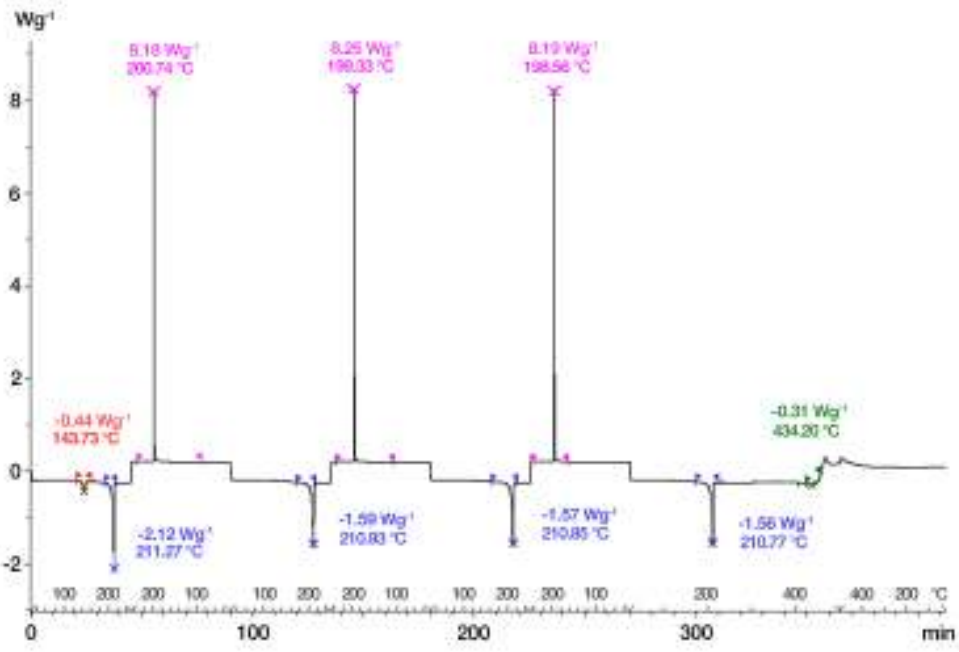

Figura 3. Differential Scanning Calorimetry (DSC) spectrum of **L**^{4}.

In order to get insight on the peculiar second order NLO properties of the, newly synthesized systems, in collaboration with Simona Fantacci we carried out DFT (Density Functional Theory) and Time Dependent DFT (TDDFT) computational studies by means of Gaussian 03 (G03) program package.[14] The geometry optimization of **L**^{3} and **L**^{4} provides very similar molecular structures characterized by planarity of the azaphenanthrene and azachrysene

and similar CC and CN bond distances (Fig. 4). The $N(Butyl)_2$ moiety goes out of the plane of the anellated rings by ca. 6° for both species, with the two butyl groups oriented in opposite directions. We computed similar dipole moments both in vacuo, 5.2 and 5.6 D, and in $CHCl_3$ solution, 7.6 and 8.0 D, for **L^3** and **L^4**, respectively. The optimized **[IrL^3]** and **[IrL^4]** are square planar complexes with the **L^3** and **L^4** twisted with respect to the square planar coordination plane, by 54° and 65°, respectively (Fig. 4).

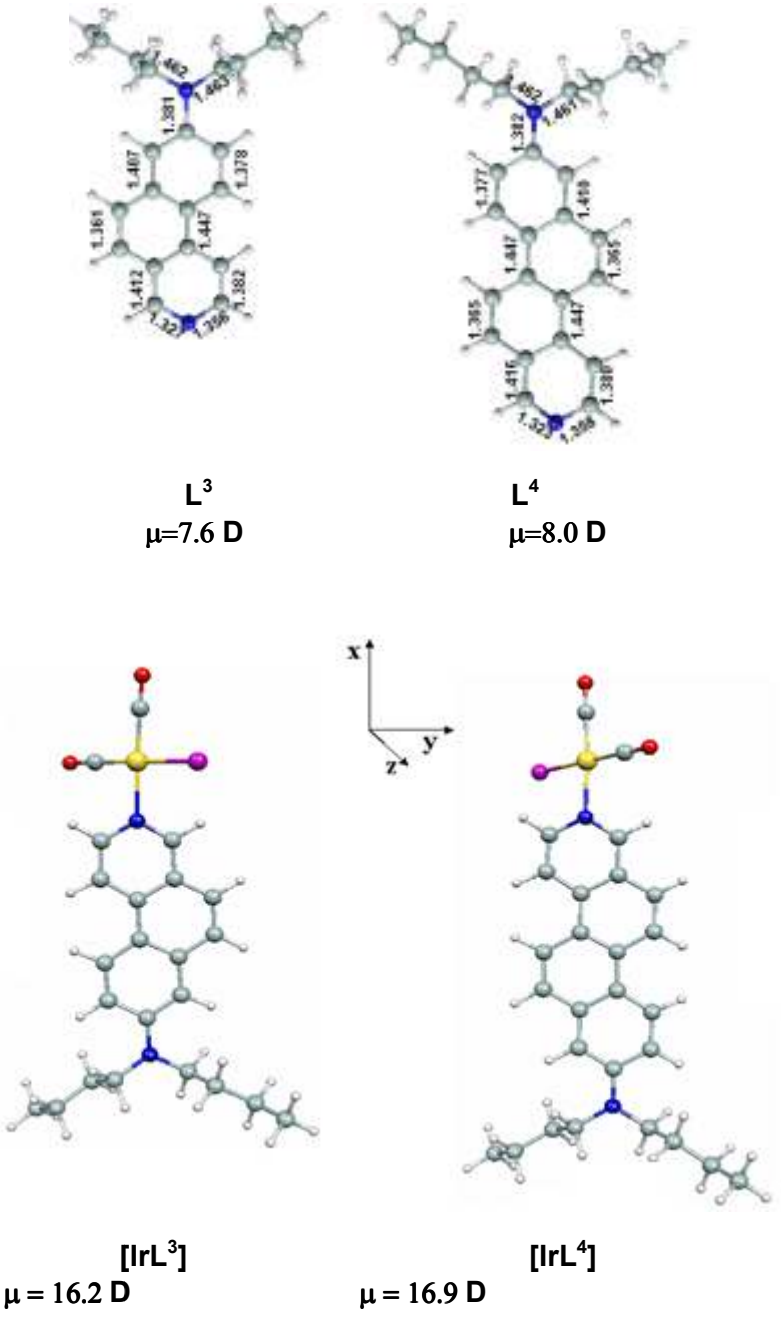

Figure 4. Optimized molecular structures of annine ligands and their relative iridium complexes togheter with their ground state dipole moments.

From the analysis of the electronic structure of **L**^{3} and **L**^{4} it emerges that the highest occupied orbitals (HOMOs) are of π character and show similar energies and similar charge distribution apart from an increased delocalization due to the presence of four rings in **L**^{4}. The **L**^{4} lowest unoccupied orbitals (LUMOs) of π^* character are, on the other hand, the result of different carbon and nitrogen p orbitals combinations with respect to **L**^{3} (Fig. 5), which is reflected by their different energies. The **L**^{4} LUMO is at lower energy with respect to that of **L**^{3} as a consequence of the increased π-conjugation, leading to a 0.38 eV decrease of the **L**^{4} HOMO-LUMO gap.

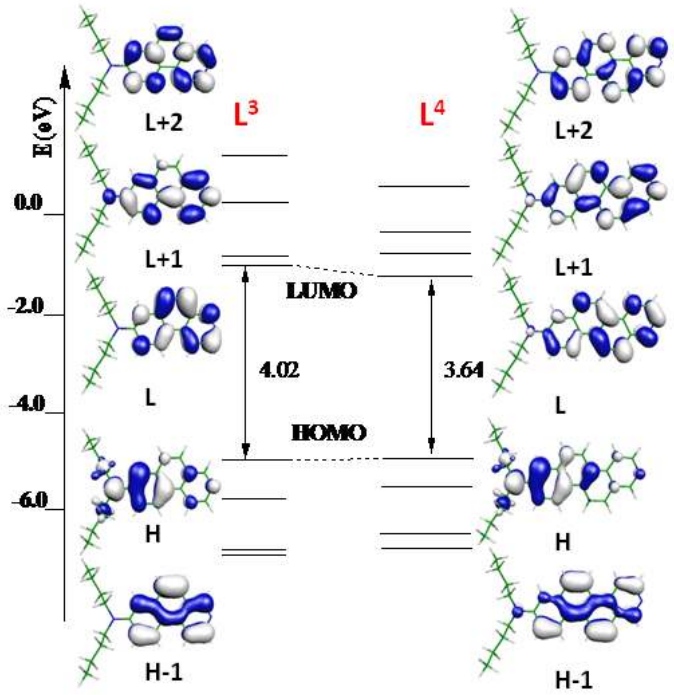

Figure 5. Schematic representation of frontier molecular orbitals of **L**^{3} and **L**^{4}.

We then simulated the absorption spectra of both systems by computing the lowest 20 singlet-singlet excitations, the comparison between the experimental and computed spectra of **L**^{3} and **L**^{4} are reported in Fig. 6. The agreement between theory and experiment is good, in the **L**^{3} case we are able to reproduce all the features of the experimental absorption spectrum, and only the lowest absorption band is computed slightly red-shifted by 0.16 eV. For **L**^{4}, the calculated intensity distribution does only qualitatively compares with the experimental absorption bands, even though also in this case the computed transitions nicely fit with the main experimental features, see Fig. 6.

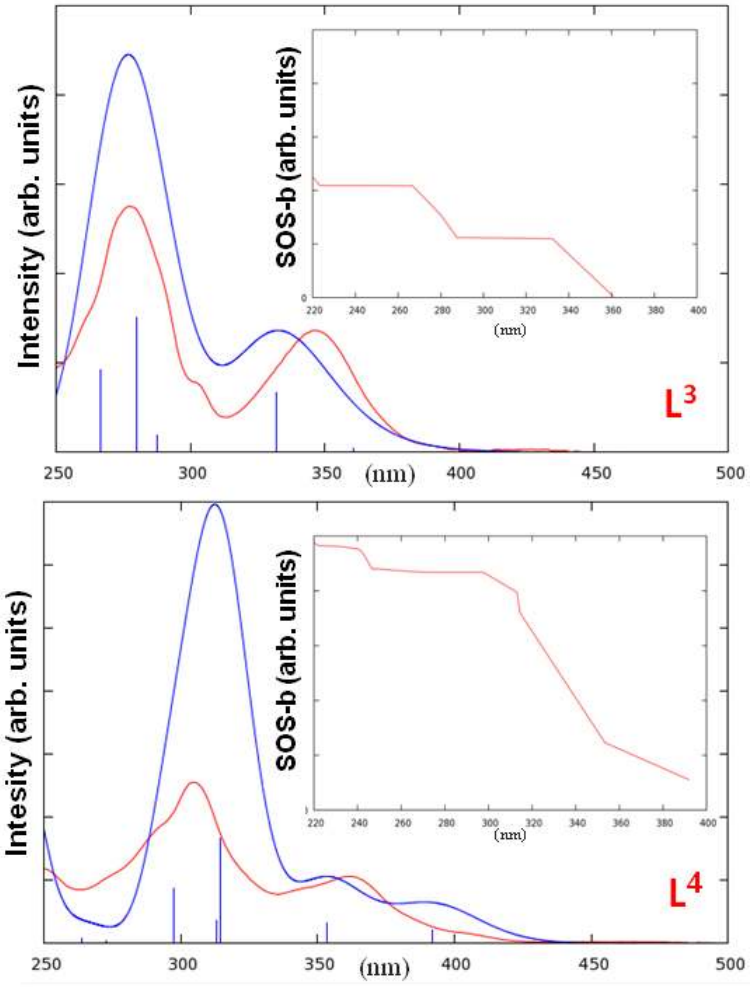

Figure 6. Comparison between theoretical (blue line) and experimental (red line) spectra of **L**^{3} and **L**^{4} with related computed hyperpolarizabilities through a SOS approach in the insets.

The absorption spectrum of **L**^{3} is characterized by a low-energy band computed at 332 nm and one more intense at 277 nm, to be compared with the experimental absorption bands at 347 and 287 nm. The lowest transition is calculated as being a rather weak HOMO-LUMO excitation at 361 nm, of π-π* character. The transition giving rise to the band at 332 nm is essentially from the HOMO to the LUMO+1 and has charge-transfer character, going from the donor dibutylamino part of the ligand to the acceptor pyridine ring. The absorption band computed at 277 nm is constituted by two main transitions of global π-π* character. The experimental absorption spectrum of **L**^{4} has a quite similar shape with respect to that of **L**^{3}, even though it is red-shifted and it shows the appearance of a band tail at ca. 400 nm. We computed a band at 353 nm and a more intense one at 312 nm to be compared to the experimental absorption bands at 361 nm and 305 nm. The band at 353 nm is a charge-transfer transition essentially of HOMO-LUMO+1 character. We computed a weak lower energy transition at 392 nm of charge transfer character, corresponding to the HOMO-LUMO

transition, related to the low energy experimental feature and more intense than that of the **L**^{3} ligand, consistently with the experimental spectra.

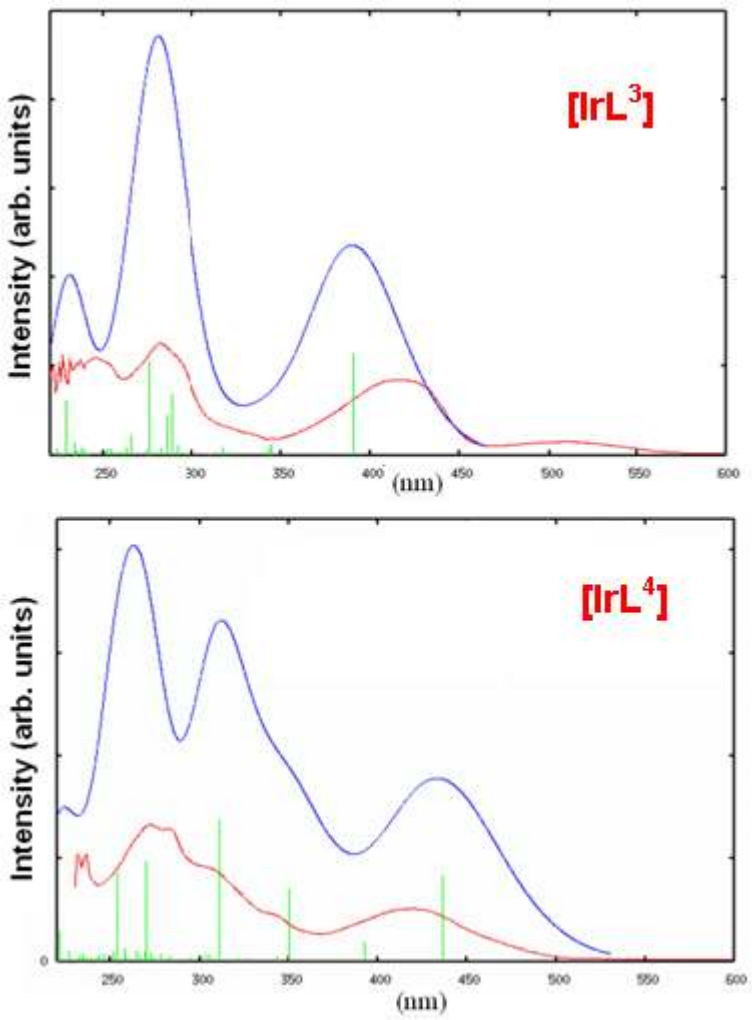

Figure 7. Comparison between theoretical (blue line) and experimental (red line) spectra of **[IrL^{3}]** and **[IrL^{4}]**. The computed transitions are reported in green.

Then we simulated the absorption spectra of Ir complexes **[IrL^{3}]** and **[IrL^{4}]** computing the lowest 50 singlet-singlet excitations. As shown by Fig. 7 there is a good agreement between the experimental and computed spectra in $CHCl_3$. Unexpectedly, it turned out that the first absorption band of the spectra of complexes **[IrL^{3}]** and **[IrL^{4}]** has a different character. In fact in complex **[IrL^{3}]** this band is originated by a ligand to ligand-metal charge transfer transition while in complex **[IrL^{4}]** it has essentially an intraligand charge transfer character. The different character of the two bands could explain the different hyperpolarizability of complexes **[IrL^{3}]** and **[IrL^{4}]**.

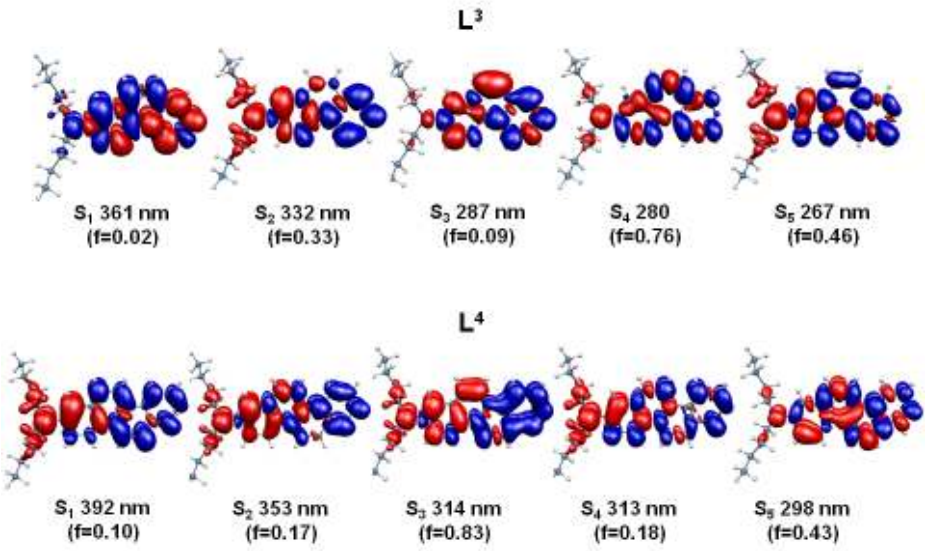

Figure 8. Isodensity plots of the electron density difference between S_1-S_5 excited states and the ground state of **L**^{3} and **L**^{4} ligands involved in the control of the EFISH $\beta_{1.907}$ value. A red (blue) color indicates a decrease (increase) of the electron density upon excitation. The excitation wavelengths, oscillator strengths are also reported.

To gain insight into the electronic transitions responsible of the observed quadratic hyperpolarizability β of **L**^{3} and **L**^{4}, in collaboration with dott.ssa Simona Fantacci we performed a Sum Over States (SOS) analysis.[16] The results, reported as insets of Fig.6, show in both cases a converged positive value in agreement with the experimental evidence. The ratio of the computed β values of **L**^{3} and **L**^{4} is 2.2, which is in line with the experimental increase of the EFISH β value observed passing from **L**^{3} to **L**^{4}. This increase is mainly due to the red-shifted absorption spectrum of **L**^{4}, related to the HOMO-LUMO gap decrease. Indeed, according to the two-level model, β increases quadratically with decreasing the energy of the electronic transitions. From an in depth analysis of calculated SOS β values, we noticed that the largest contributions to β are provided for both **L**^{3} and **L**^{4} by ILCT transitions. Visualization of the charge transfer processes originating the NLO response is reported in Fig. 8. We found that for **L**^{4} the lowest energy transition considerably contributes to the calculated β, for **L**^{3} such excited state has almost vanishing contribution to β, due to its higher energy and considerably lower transition dipole moment. Moreover, at higher energy the 314 nm transition is that mainly responsible for the converged higher β value of **L**^{4} compared to **L**^{3}, indeed the same state in **L**^{3} is characterized by a lower transition dipole moment. In conclusion the polyaromatic push-pull chromophores **L**^{3} and **L**^{4} used in the present study are particularly appealing because of their notable values of EFISH $\mu\beta_{1.097}$ that are likely due to the absence of photorotamerism and photoisomerism processes operating

in the corresponding compounds **L[1]** and **L[2]** respectively. These properties together with the absence of isolated double bonds ensure the astonishingly high thermal stability of **L[4]** that makes it a good candidate for the preparation of materials characterized byhigh second harmonic generation properties. We believe that, because of their relevant technological interest, the results here reported can constitute a springboard for the design of other NLO chromophores of the same family such as 11-*N,N*-dibutylamino-3-azapicene and 12-*N,N*-dibutylaminobenzo[m]-3-azapicene with 5 and 6 rings respectively.

6. (N^C^N)-Pt complexes

Metal complexes are appealing building blocks for the design of new and efficient NLO chromophores thanks to their rich photochemistry.[17] In particular square-planar d^8 platinum(II) compounds possess several favorable structural and physical properties[18] amenable to NLO study[19, 20] including (i) rigid planar structures, (ii) high thermal stability, (iii) polarizable metal, (iv) solvatochromic transitions, (v) significant metal-ligand orbital overlap, and (vi) charge-transfer transitions. Besides, according to Zhou *et al.*[20] the NLO response can be greatly enhanced by π-delocalization on the polypyridyl and phenylacetylide fragments.This prompted us to investigate the second-order NLO properties of our highly luminescent cyclometallated 1,3-di(2-pyridyl)benzene)platinum(II) complexes. The preliminary results for this study determined by both EFISH and HLS techniques are presented in the following paragraphs.

6.1. Inestigation of Second-Order NLO properties by both *Electric-Field Induced Second-Harmonic* (EFISH) generation and *Harmonic Light Scattering* (HLS) techniques

In Tab. 3 are reported the NLO results measure by EFISH tecnique[4] for **[PtL[1]Cl]** in two different solvents. The decrease in NLO response upon increasing concentration suggests that some aggregation fenomena occurs in concentrated $CHCl_3$ solution (10^{-3} M). For this reason all the other measurements reported in Tab. 3 had been performed in DMF solution where such inconvenient does not present as shown by the strong similarity of the value $\mu\beta_{EFISH,1.907}$ obtained for concentrated DMF solution (10^{-3} M) with that of the most diluted

$CHCl_3$ solution ($3x10^{-4}$M). The absence of aggregates is also confirmed by absorbance spectra in this solvent at the highest concentration (i.e. 10^{-3} M).

As afore mentioned EFISH measurements provides the dipolar contribution expressed as the product μ x $\beta_{1.907}$ where μ is the ground state dipole moment, and $\beta_{1.907}$ is the projection along the dipole moment axis of the vectorial component of the tensor of the quadratic hyperpolarizability working with an incident wavelength 1.907 μm of a pulsed laser. By using a theoretical μ = 7.07 D,[21] a $\beta_{EFISH,1.907}$ of 74 x 10^{-30} esu was calculated. Substitution of the methyl group with a fluorine (*i.e.* **[PtL^{3}Cl]**) leads to an inversion of the sign of $\beta_{EFISH,1.907}$ (Tab. 4) - implying that μ of the excited state is lower than μ of the ground state - and a remarkable increase of the absolute value of $\mu\beta_{EFISH,1.907}$ which is larger than that reported for other Pt systems (≈ 55 x 10^{-30} esu).[22]

Table 3. NLO response of **[PtL^{1}Cl]** compex in chloroform and dimethylformamide solutions

CONCENTRATION [M]	$\mu\beta_{EFISH}$[x10^{-48} esu]	
	DMF	$CHCl_3$
$3x10^{-4}$		505
$6x10^{-4}$		233
10^{-3}	525	71

[a] measured with an incident radiation of 1.907 μm. The error on EFISH measurements is ± 10%

As shown by data in Tab.3 the presence of the PtCl moiety in the cyclometallated dipyridyl complexes enhances the NLO properties compared to other organic and organometallic compounds,[22] reasonably on account of the rigidity of the systems.[20] Some of the complexes are, for example, characterized by a $\mu\beta_{1.907}$ value higher than that of Disperse Red One, an NLO chromophore currently used in electro-optics polymers.[23]

Table 4. NLO response of Pt (II) compexes

COMPOUND	ABSORBANCE[a] λ_{max} [nm]	$\mu\beta_{EFISH}$[b] [x 10^{-48} esu]	β_{HLS}[b] [x 10^{-30} esu]
[PtL^{1}Cl]	335 (5710), 381(6900), 412 (6780), 460(190), 495 (130)	525	285
[PtL^{3}Cl]	322sh (6172), 377 (7744), 422 (8270), 486 (312)	-950	432
[PtL^{4}Cl]	330 (7971), 342 (10410), 388 (11072), 479 (521)	-270	---
[PtL^{1}SCN]	333(4759), 357(2798), 382 (3894), 406 (3819), 499(188)	-3350	409
[PtL^{1}A^2]	330 (7971), 355 (4922), 380 (3782), 408br(4082)	-1890	345
[PtL^{4}A^4]	326sh (19362), 344sh (15838), 385 (6481), 493 (3050)	-700	278

[a] In dichloromethane at 298 K . [b] In DMF at 298 K measured with an incident radiation of 1.907 μm.

In Tab. 4 are also reported the NLO results measured by the HLS tecnique[24] which provides the average value of the possible orientations of all the components of the tensor *β*. Similarly to stilbenoid-N^C^N-pincer platinum complexes[25] at first sight no clear relationship is present between the electronic properties of substituents and the obtained values which could be related to the irrelevant red shift of the lower-energy CT transition. However the complexes show a good hyperpolarizability, reflected by the $\beta_{HLS,1.907}$ absolute values ranging from 278 to 432 x 10^{-30} esu which are of the same order of magnitude of the afore mentioned substituted stilbenoid-N^C^N-pincer platinum(II) (164 to 1324 x10^{-30}esu).[25] The *β* values, especially that of **[PtL^{3}Cl]**, are also in line with, and sometimes higher than, other organometallic molecules.[26, 27]

By using a combination of the EFISH and HLS techniques, it is possible to evaluate the dipolar (J = 1) and octupolar (J = 3) contributions to the total quadratic hyperpolarizability $\left\|\overline{\beta}\right\|$ (Eq. 3) of **[PtL^{1}Cl]**. In fact, for a molecule with a symmetry such as $C_{2\ or\ \infty,v}$, the dipolar contribution $\left\|\overline{\beta}^{J=1}\right\|$ can be calculated from β_{EFISH} by Eq. 4; if the value of $<\beta_{HLS}>$ is also known, the octupolar contribution $\left\|\overline{\beta}^{J=3}\right\|$ can then be calculated by Eq.5[28]

$$\left\|\overline{\beta}\right\|^2 = \left\|\overline{\beta}^{J=1}\right\|^2 + \left\|\overline{\beta}^{J=3}\right\|^2 \qquad \text{(Eq. 3)}$$

$$\left\|\beta^{J=1}\right\| = \sqrt{\frac{3}{5}}\beta_{EFISH} \qquad \text{(Eq. 4)}$$

$$\left\langle \beta_{HLS}^2 \right\rangle = \left\langle \left|\beta_{XXX}\right|^2 \right\rangle + \left\langle \left|\beta_{ZXX}\right|^2 \right\rangle = \frac{2}{9}\left\|\overline{\beta}^{J=1}\right\|^2 + \frac{2}{21}\left\|\overline{\beta}^{J=3}\right\|^2 \qquad \text{(Eq. 5)}$$

For **[PtL^{1}Cl]**, $\left\|\overline{\beta}^{J=1}\right\|$, calculated from Eq. 4, is 57 x 10^{-30} esu. The relatively high value of $\langle\beta_{HLS}\rangle$, 285 x 10^{-30} esu, is due to a high octupolar $\left\|\overline{\beta}^{J=3}\right\|$ component (919 x 10^{-30} esu, calculated from Eq. 5) since the dipolar component $\left\|\overline{\beta}^{J=1}\right\|$ is less than 7% of the octupolar one. Therefore the total quadratic hyperpolarizability $\left\|\overline{\beta}\right\|$ (calculated from Eq. 4, 920 x 10^{-30} esu) is almost equal to $\left\|\overline{\beta}^{J=3}\right\|$, although the difference between the quadratic hyperpolarizability $\left\|\overline{\beta}\right\|$ and $\langle\beta_{HLS}\rangle$ is quite large because $\langle\beta_{HLS}\rangle$ contains isotropic mean factors that decrease this parameter as evidenced by the coefficients in Eq. 5.

In conclusion, our work confirms what previously reported in the case of β-diketonate complexes of various lanthanide ions[28e] and represents a new step in the understanding of the major role of the octupolar components on the NLO properties of metal complexes with π-delocalized ligands.

7. Octupolar compound with organometallic fragment

Although the majority of NLO chromophores features relatively simple dipolar electronic structures, octupolar compounds form an increasingly important class of materials for potential second-order NLO applications.[29] Indeed, despite having zero net ground-state dipole moments, octupolar molecules can display large values of the first hyperpolarizability *β* which governs quadratic NLO effects at molecular level. As we mention afore organometallic complexes are an interesting subclass of molecular NLO compounds offering extensive scope for the creation of multifunctional optical materials.[30] These reasons prompted us to study the second order NLO properties of an octupolar tripodic ligand, **O^1**, terminating with pyridyl groups that can be easily coordinated to an organometallic fragment (Fig. 9). Indeed in collaboration with dott.ssa Francesca Tessore, Zn complexes of a commercial porphyrin, **Zn^1**, or phtalocyanine, **Zn^2** (Fig. 10), were linked to our octupolar core. Besides, for comparison, we also investigated the quadratic hyperpolarizability *β* of a monopodal ligand, **O^2** (Fig. 9), and of its complexes with the same organometallic fragments. In the following paragraphs the results by th Harmonic Light Scattering technique shall be presented.

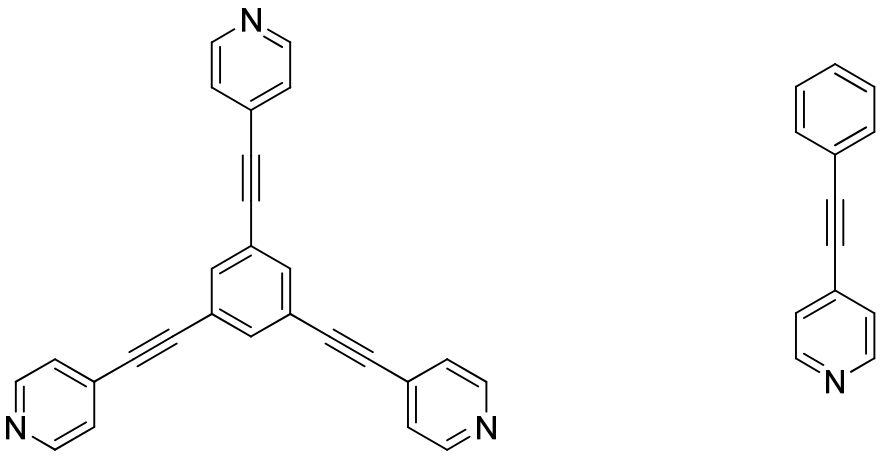

O^1 **O^2**

Figure 9: Schematic representation of the ligands tripodic, **O^1** , and mono-branched, **O^2**

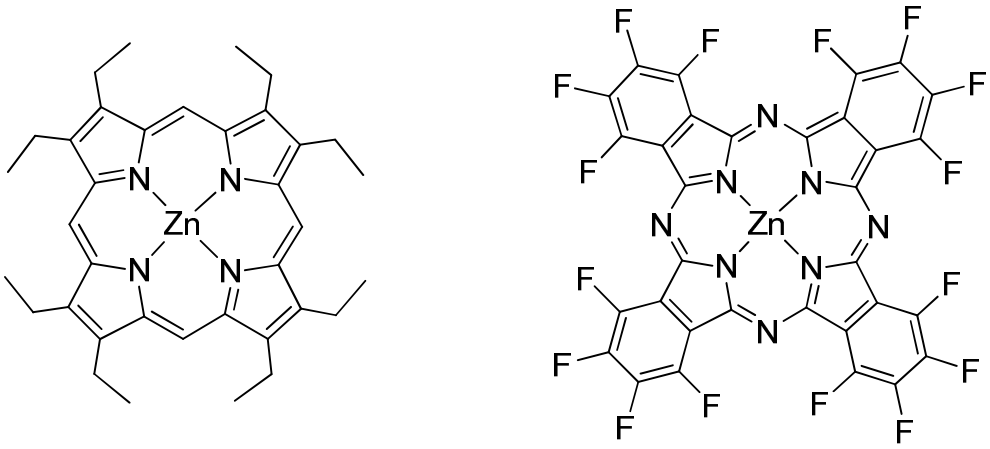

Zn[1] **Zn[2]**

Figure 10: Schematic representation of Zn complexes of the commercial porphyrine, **Zn[1]**, and phtalocyanine, **Zn[2]**.

7.1. Synthesis of the compounds

The strategy employed in the synthesis of the octupolar tripode, **O[1]**, is summarized in Scheme 5. For the synthesis of 1,3,5-triethynylbenzene, **1**, 1,3,5-tribromobenzene in diethylamine was treated under mild condition with trimethylsilylacetylene in the presence of the Pd-Cu catalytic system according to litterature procedures,[31] followed by basic cleavage of the protective silane. Subsequently, another Sonogashira coupling was performed between **1** and 4-bromopyridine hydrochloride as previously described for similar compound.[32] ^{1}H NMR and UV-spectra, as well as elementar analysis confirmed the presence of the product. The overall reaction yield for the preparation of the octupolar compound **O[1]** is 35%. The same synthetic route was followed in order to obtain the relative monopodal ligand, **O[2]**. As mentioned above, in collaboration with F. Tessore the coordination of two organometallic fragment, **Zn[1]** and **Zn[2]**, to the ligands **O[1]** and **O[2]** were performed as described in Schemes 6-7. Details on the synthesis and characterization of these compounds are given in Experimental Section.

Scheme 5: Preparation of the tripodic ligand, **O[1]**, through Sonogashira couplings; the same strategy has been applied for the synthesis of monopodic ligand **O[2]**:

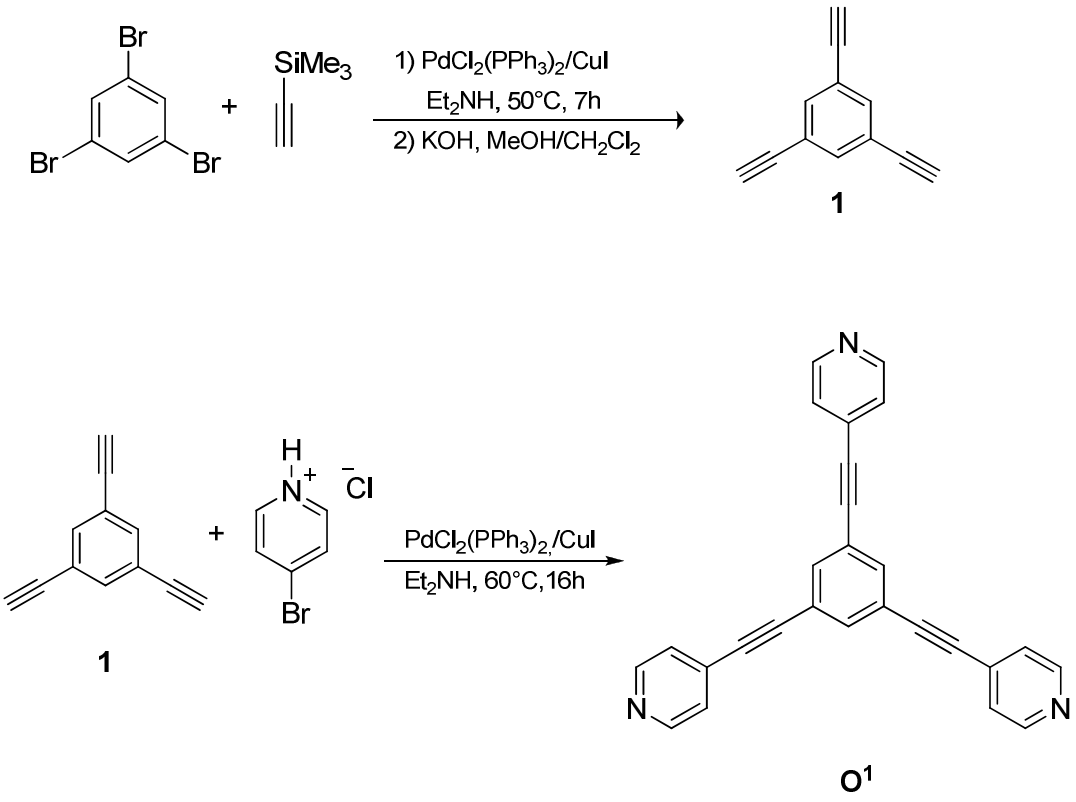

Scheme 6: Preparation of the coordination complex , **O[2]Zn[1]** by reaction of ligand **O[2]** with Zn-porphyrin **Zn[1]**; the same strategy has been applied for the synthesis of the coordination complexes of ligand **O[1]** with Zn-porphyrin, **O[1]Zn[1]**:

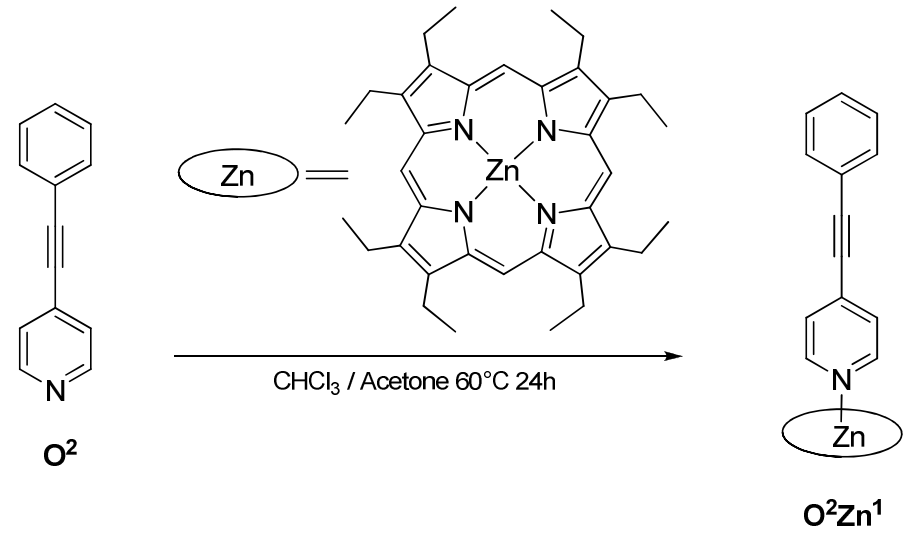

Scheme 7: Preparation of the coordination complex $\mathbf{O^2Zn^1}$ by reaction of ligand $\mathbf{O^2}$ with Zn-phtalocyanine $\mathbf{Zn^2}$; the same strategy has been applied for the synthesis of the coordination complexes of ligand $\mathbf{O^1}$ with Zn-phtalocyanine, $\mathbf{O^1Zn^2}$:

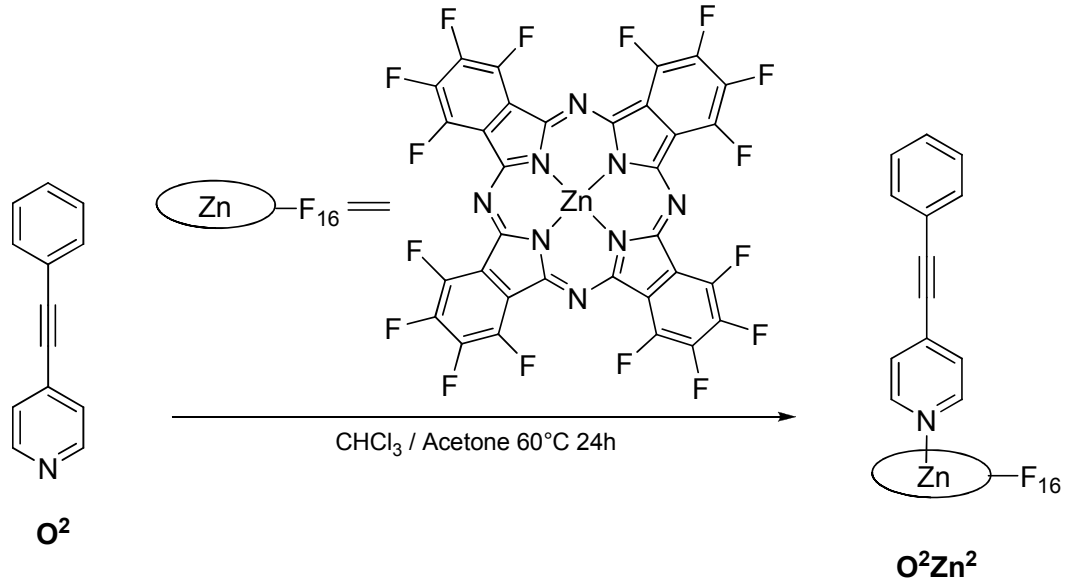

$\mathbf{O^2}$ $\mathbf{O^2Zn^2}$

7.2. Inestigation of Second-Order NLO Properties by *Harmonic Light Scattering* (HLS) technique

In Tab. 5 are reported the experimental $\beta_{HLS,1.907}$ values measured with the HLS technique.[24] In fact, in contrast ot the EFISH tecnique,[4] Harmonic Light Scattering is also appropriate for the study of the NLO properties of non-dipolar molecules – *e.g.* octupolar ones - providing the average value of the possible orientations of all the components of the tensor β (see section: Introduction). As expected there in an increase in NLO response by passing from monopodal to tripodal ligand (Enhancement Factor ≈2). From data emerges that, unfortunately, the coordination of the organometallic fragments to our octupolar core, $\mathbf{O^1Zn^1}$ and $\mathbf{O^1Zn^2}$ did not lead to a substantial change in $\beta_{HLS,1.907}$ value, which is indeed very similar to that of the free Zn-porphyrine, $\mathbf{Zn^1}$, or Zn-phtalocyanine, $\mathbf{Zn^2}$ (Tab. 5).

Table 5: NLO results measured by HLS tecnique

COMPOUND	CONCENTRATION [M]	$\beta_{HLS,\ 1.907}$ [a] [x 10^{-30} esu]
Zn[1]	$1.0x10^{-4}$	1003
Zn[2]	$1.9x10^{-4}$	670
O[1]	$3.8x10^{-3}$	313
O[1]Zn[1]	$1.3x10^{-4}$	1000
O[1]Zn[2]	$1.3x10^{-4}$	776
O[2]	$3.0x10^{-3}$	168
O[2]Zn[1]	$2x10^{-4}$	231
O[2]Zn[2]	$2.2x10^{-4}$	700

[a] In DMF solution with an incident radiation of 1.907 μm.

However this study allows to put in evidence the remarkably high $\beta_{HLS,1.907}$ value displayed by the Zn-porphyrine itself which, interestingly, is significantly higher than that of other more structurelly sofisticated Zn-porphyrines, **Zn[3]**, **Zn[4]** and **Zn[5]** (Fig. 11 **Zn[3]** $\beta_{HLS,1.064}$ = $12x10^{-30}$esu;[33] **Zn[4]** $\beta_{HLS,1.064}$ = $92x10^{-30}$esu;[33] **Zn[5]** $\beta_{HLS,1.907}$ = $540x10^{-30}$esu[34]) especially considering that β_{HLS} values working with a laser incident wavelength of 1.064μm - *i.e.* $\beta_{HLS,1.064}$ - are higher than $\beta_{HLS,1.907}$ ones. Besides, it is worth noting that **Zn[1]** NLO response is not too much lower than that of Zn-porphyrine **Zn[6]** (Fig. 11), (**Zn[6]** $\beta_{HLS,1.300}$ = $2200x10^{-30}$esu)[35] which has been reported as one with the highest $\beta_{HLS,1.907}$ value although compared with **Zn[1]** has a very complicated push-pull structure, whereas ours is very simple and commercially availiable.

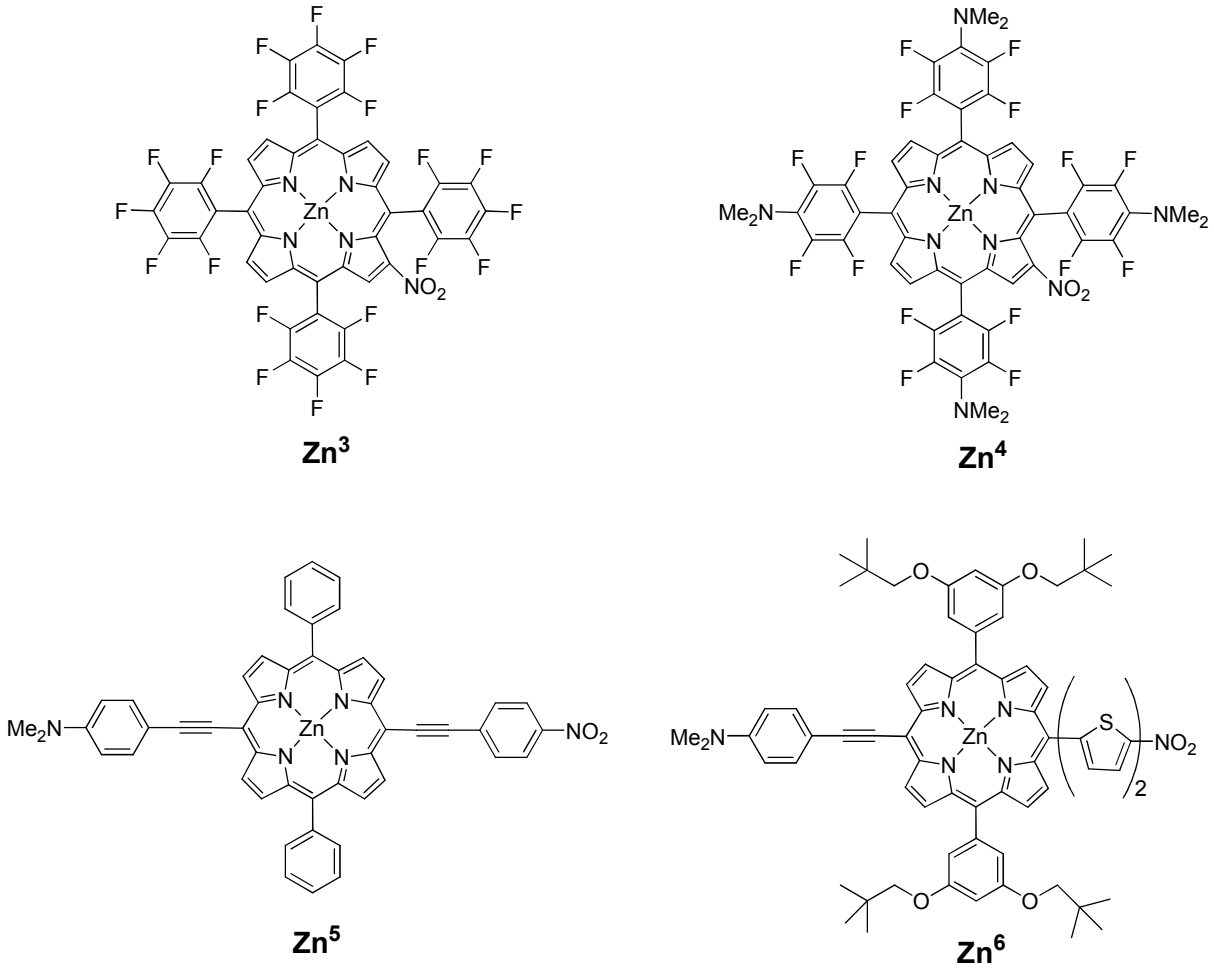

Figure 11: Schematic structure of Zn-porphyrines

References:

[1] for example see (a) Cariati, E.; Pizzotti, M.; Roberto, D.; Tessore, F.; Ugo, R. *Coord. Chem. Rev.* **2006**, *250*, 1210; (b) Coe, B. J. *Acc. Chem. Res.,* **2006**, *39*, 383.

[2] Roberto, D.; Ugo, R.; Bruni, S.; Cariati, E.; Cariati, F.; Fantucci, P.C.; Invernizzi, I.; Quici, S.; Ledoux, I.; Zyss, J. *Organometallics,* **2000**, *19*, 1775.

[3] Locatelli, D.; Quici, S.; Righetto, S.; Roberto, D.; Tessore, F.; Ashwell, G. J.; Amiri, M. *Prog. in Solid State Chem.,* **2005**, *33*, 223.

[4] Ledoux, I.; Zyss, J. *Chem. Phys.,* **1982**, *73*, 203.

[5] G. Hubener, A. Lambacher, P. Fromherz *J. Phys. Chem. B,* **2003**, *107*, 7896.

[6] Z. Sekkat, W. Knoll, in *Photoreactive Organic Thin Films*, ed. Accademic Press: San Diego, California.

[7] Valentina Calabrese Ph.D. Thesis, University of Milan, Italy, 2008.

[8] Tessore, F.; Cariati, E.; Cariati, F.; Roberto, D.; Ugo, R.; Mussini, P.; Zuccaccia, C:; Macchioni, A. *Chem. Phys. Chem.*, **2010**, *11*, **495**.

[9] Herde, J. L.; Lambert, J. C.; Senoff, C. V. Inorg. *Synth.* **1974**, *15*, 18.

[10] Roberto, D.; Cariati, E.; Psaro, R.; Ugo, R. *Organometallics,* **1994**, *13*, 4227.

[11] (a) E. A. Guggenheim, *Trans. Faraday Soc.,* 1949, 45, 714. (b) H. B. Thompson, *J. Chem. Educ*., 1966, *43*, 66.

[12] V. Alain, M. Blanchard-Desce, I. Ledoux-Rak, J. Zyss, *Chem. Comm*., **2000**, 353.

[13] D. M. Burland, R. D. Miller, C. A. Walsh, *Chem. Rev.* **1994**, *94*, 31.

[14] M. J. Frisch et al., *Gaussian 03*, Revision C.02; see Experimental section.

[15] This approach requires in principle the calculation of dipole matrix elements between all possible couples of excited states (three level terms), in addition to ground to excited states transition dipole moments (two level terms).[16] However two- and three-level terms show approximately the same scaling with the number of excited states as two-level terms, so that the latter can be used for a semi-quantitative assessment of the contributions to the quadratic hyperpolarizability.

[16] Kanis, D. R.; Lacroix, P.G.; Ratner, M. A.; Marks, T. J. *J. Am. Chem. Soc.,* **1994**, *116*, 10089.

[17] (*a*) Cariati, E.; Pizzotti, M.; Roberto, D.; Tessore, F.; Ugo, R. *Coord. Chem. Rev.* **2006**, *250*, 1210.; (*b*) Humphrey, M.G.; Samoc, M. *Advances in Organometallic Chemistry* **2008**, *55*, 61. 3; (*c*) Farley S.J.; Rochester D. L.; Thompson A.L., Howard J.A.K., Williams, J.A.G, *Inorg. Chem.* **2005**, *44,* 9690.

[18] (*a*)Cummings, S. D.; Eisenberg, R. *J. Am. Chem. Soc*. **1996**, *118*, 1949; (*b*) Connick, W. B.; Gray, H. B. *J. Am. Chem. Soc.* **1997**, *119*, 11620.

[19] Cummings, S. D.; Cheng, L.-T.; Eisenberg, R. *Chem. Mater.* **1997**, *9,* 440.

[20] Zhou, X.; Pan, Q. - J.; Xia, B. H.; Li, M. X.; Zhang,H. X.; Tung, A. U. *J. Phys. Chem. A* **2007**, *111*, 5465.

[21] Sotoyama, W.; Satoh, T.; Sato, H.; Matsuura, A.; Sawatari, N. *J. Phys. Chem. A,* **2005**, *109*, 9760.

[22] Buey, J.; Coco, S.; Dìez, L.; Espinet, P.; Martìn-Alvarez, J. M.; Miguel, J. A.; Garcìa-Granda, S.; Tesouro, A.; Ledoux, I.; Zyss, J. *Organometallics* **1998**, *17*, 1750.

[23] Singer, K. D.; Sohn, E.; King, L.A.; Gordon, H. M.; Katz H. E. and Dirk, P. W. *J. Opt. Soc. Am. B* **1989**, *6*,1339.

[24] Maker P.D. *Phys Rev A* **1970**, *1*, 923.

[25] Batema, G. D.; Lutz, M.; Spek, A. L.; van Walree, C. A.; de Mello Donegá, C.; Meijerink, A.; Havenith, R. W. A.; Pérez-Moreno, J.; Clays, K.; Büchel, M.; van Dijken, A.; Bryce, D. L.; van Klink, G. P.M.; van Koten, G. *Organometallics* **2008**, *27*, 1690.

[26] Verbiest, T.; Houbrechts, S.; Kauranen, M.; Clays, K.; Persoons, A. J. Mater. Chem. 1997, 7, 2175.

[27] Romaniello, P.; Lelj, F. *Chemical Physics Letters* , **2003**, *372*, 51.

[28] (*a*) Brasselet, S.; Zyss, J. *Journal of the Optical Society of Ameica B: Optical Physics* **1998**, *15*, 257; (*b*) Zyss, J. *Journal of Chemical Physics*, **1993**, *98*, 6583; (*c*) Brasselet, S. Ph.D. Thesis, Université de Paris XI Orsay, France 1997. (*d*) Thi, K. H. Ph.D. Thesis, Ecole Normale Supérieure de Cachan, France, 2008. (*e*) Valore, A. ; Cariati, E. ; Righetto, S. ; Roberto, D. ; Tessore, F. ; Fragalà, I. L. ; Fragalà, M. E. ; Malandrino, G. ; De Angelis, F. ; Belpassi, L. ; Ledoux-Rak, I. ; Thi, K.H. ; Zyss, J. *Journal of American Chemical Society*, **2010**, 132, 4966.

[29] (a) Ledoux, I.; Zyss, J.; Siegel, J. S.; Brienne J.; Lehn, J.-M. *Chem. Phys. Lett*. **1990**, *172*, 440. (b) Joffre, M.; Yaron, D.; Silbey, R. J.; Zyss, J. *J. Chem. Phys.* **1992**, *97*, 560. (c) Naiwa , H. S.; Watanabe, T. ; Miyata, S. *Optical Materials*, **1993**, *2*, 73 (d)Verbiest, T.; Clays, K.; Samyn, C.; Wolff, J.; Reinhoudt, D.; Persoons, A. *J. Am. Chem. Soc*. **1994**, *116*, 9320. (e) Wolff, J. J.; Siegler, F.; Matschiner, R.; Wortmann, R. *Angew. Chem., Int. Ed.* **2000**, *39*, 1436-1439. (f) Cui, Y. Z.; Fang, Q.; Lei, H.; Xue, G.; Yu, W. T. *Chem. Phys. Lett.* **2003**, *377*, 507-511. (g) Ray, P. C.; Leszczynski, J. *Chem. Phys. Lett.* **2004**, *399*, 162-166. (h) Coe, B. J.; Harris, J. A.; Brunschwig, B. S.; Asselberghs, I.; Clays, K.; Garìn, J.; Orduna, J. *J. AM. CHEM. SOC*. **2005**, *127*, 13399.

[30] (a) Kanis, D. R.; Ratner, M. A.; Marks, T. J. *Chem. Rev*. **1994**, *94*, 195. (b) Long, N. J. *Angew. Chem., Int. Ed. Engl*. **1995**, *34*, 21. (c) Whittall, I. R.; McDonagh, A. M.; Humphrey, M. G.; Samoc, M. *Adv. Organomet. Chem*. **1998**, *43*, 349. (d) Heck, J.; Dabek, S.; Meyer-Friedrichsen, T.; Wong, H. *Coord. Chem. Rev*. **1999**, *190-192*,1217-1254. (e) Le Bozec, H.; Renouard, T. *Eur. J. Inorg. Chem.* **2000**, 229. (f) Barlow, S.;

Marder, S. R. *Chem.Commun*. **2000**, 1555. (g) Lacroix, P. G. *Eur. J. Inorg. Chem*. **2001**, 339. (h) Di Bella, S. *Chem. Soc. Rev.* **2001**, *30*, 355.

[31] Weber, E.; Hecker, M.; Koepp, E.; Orilia, W.; Czugler, M.; Csöregh, I. *Chem. Soc. Perkin Trans*, **1988**, *2*, 1251.

[32] Lewis, J. D.; Moore, J. *Dalton trans.*, **2004**, 1376.

[33] Sen, A.; Ray, P. C.; Das, P. K.; Krishnan, V. *J. Phys. Chem*. **1996**, *100*, 19611.

[34] Kim, K.S.; Vance, F.W.; Hupp, J.T.; Le Cours, S.M.; Therien, M. J. *J. Am. Chem. Soc.* **1998**, *120,* 2606.

[35] Zhang, T.-G.; Zhao, Y.; Asselberghs,I.; Persoons, A.; Clays,K.; Therien, M. J. *J. Am. Chem. Soc*. **2005**, *127*, 9710.

EXPERIMENTAL

1. Methods

General comments

All reagents and solvents were purchased from Sigma-Aldrich and Fluka, while $IrCl_3$ hydrate was purchased from Engelhard. All reactions were carried out under nitrogen atmosphere. ^1H NMR spectra were obtained on a Bruker Advance DRC 300 and Bruker AMX 400 MHz instrument. Elemental analyses were carried out with Perkin-Elmer 2400 CHN. Some products were also characterized by infrared (Jasco FT-IR 420 Spectrometer) spectroscopy.

Electrochemistry

Cyclic voltammetry was carried out using a μAutolab Type III potentiostat with computer control and data storage *via* GPES 110 Manager software. Solutions of concentration 1 mM in CH_2Cl_2 were used and tetrabutylammonium hexafluorophosphate (0.1 M) was used as a supporting electrolyte. Solutions were purged for 5 minutes with solvent-saturated nitrogen prior to measurements being taken without stirring. A three-electrode assembly was employed, consisting of a platinum working electrode, platinum wire counter electrode and platinum flag reference. The voltammograms were referenced to a ferrocene-ferrocenium couple as the standard ($E^{1/2}$ = 0.18 V under same conditions).

Instrumentation for photophysical measurements

In Università degli Studi di Milano absorption spectra were recorded using a JASCO V530 spectrometer at room temperature in a 1cm pathlength quartz cuvette, while in Durham Unifersity a Biotek Instruments XL spectrometer was used.

The steady-state emission spectra were measured with a Jobin Yvon FluoroMax-2 instrument, equipped with a Hamamatsu R928 photomultiplier tube. Emission spectra shown are corrected for the wavelength dependence of the photomultipler tube, and stated emission maxima refer to values obtained from the corrected spectra.

Solutions for fluorescence measurements were contained in 1 cm quartz cuvettes. Degassing was achieved *via* a minimum of three freeze-pump-thaw cycles whilst connected to the vacuum manifold; final vapour pressure at 77 K was < 5 x 10^{-2} mbar, as monitored using a Pirani gauge. Emission spectra at low temperature were recorded for alcholic glass solution (*i.e.* $C_4H_{10}O/C_2H_5OH/C_2H_5OH$ =2/2/1). Luminescence quantum yields were determined using [PtL^3Cl] (HL^3 is 4-methyl 1,3-di(2-pyridyl)benzene)[1] in dichloromethane as standard. The luminescence lifetimes of the complexes were measured by time-correlated single-photon counting, following excitation at 374.0 nm with an EPL-375 pulsed-diode laser. The emitted light was detected at 90◦ using a Peltier-cooled R928 PMT after 30 passage

through a monochromator. The estimated uncertainty in the quoted lifetimes is ± 10% or better.

Vacuum-deposited OLED fabrication

LEDs were fabricated by growing a sequence of thin layers on clean glass substrates precoated with a 100 nm thick layer of ITO with a sheet resistance of 20 /sq. A 60 nm thick TPD:PCblend hole-transporting layer was deposited on top of ITO by spin coating from a 10 mg/ml dichloromethane solution at room temperature. All remaining organic layers were deposited in succession by thermal evaporation under vacuum of 10 − 6 hPa, followed by high vacuum 10−6 hPathermal evaporation of the cathode layer consisting of a 0.5 nm thick LiF and by a 100 nm thick Al cap. The EML was deposited by coevaporation of the phosphor and TCTA to form a 30 nm thick blend film. All measurements were carried out at room temperature under argon atmosphere and were reproduced for many runs, excluding any irreversible chemical and morphological changes in the devices.

Solution-processed OLED fabrication and performance measurements

Glass substrates patterned with indium tin oxide (ITO) were cleaned ultrasonically in distilled water, acetone and 2-propanol. Subsequently 50nm layers of filtered (nylon 0.45μm) poly(3,4-ethylenedioxythiophene) / poly(styrenesulfonate) (PEDOT:PSS) (H.C.Starck Clevios P VP.AI 4083) were spincoated and annealed at 100^{o}C for 10 minutes under nitrogen atmosphere. In the case of green emitting OLEDs (5% dopant in the emissive layer) on such prepared substrates a film of poly(N-vinylcarbazole), with average M_w=1000000 g/mol (PVKc) was spincoated from dichloromethane solution (12mg/ml). Then samples were annealed at 150^{o}C for 30 minutes and left to cool down. After that emitting layer, consisting of poly(N-vinylcarbazole) (PVK, M_w=42000g/mol) and 2-(4-biphenylyl)-5-(4-*tert*-butylphenyl)-1,3,4-oxadiazole (PBD) (both from Aldrich), and lumophores were spincoated from deaerated dichloromethane solution (8mg/ml) with mass ratio 65%PVK:30%PBD:5%Pt complex. Finally 5 nm of barium and 60 nm of aluminium were deposited by thermal vacuum evaporation at 10^{-6} mbar. In the case of WOLED on substrates with PEDOT:PSS a film of PVKc, mixed with poly(9,9-dioctylfluorenyl-2,7-diyl) end capped with N,N-Bis(4-methyl-phenyl)-4-aniline (PFO, American Dye Source) with ratio 52%PVKc:48%PFO (w/w) was spincoated from toluene solution (15 mg/ml). After that samples were annealed at 100^{o}C for 30 minutes. Then the second layer, with mass ratio 40%PVK:20%PBD:40%FPtCl, was spincoated from dichloromethane solution (2 mg/ml).

Finally 10 nm of calcium and 60 nm of aluminium were deposited by thermal vacuum evaporation at 10^{-6} mbar.

EL and photoluminescence (PL) spectra were recorded by liquid nitrogen cooled charge-coupled device (Spex) combined with monochromator (Spex 270M). Steady state PL was excited by monochromated xenon lamp. The spectra were corrected for the instruments response. Current-voltage (I-V) devices characterization was performed with Keithley 2602 source meter combined with calibrated photodiode. External quantum efficiency (EL QE) was calculated by measuring light emitted in the forward direction with Lambertian source assumption. Devices preparation and characterization was performed in nitrogen atmosphere. CCT was evaluated according to ref. [2]. Luminance (L), luminance efficiency (LE) and power efficiency (PE) were calculated using formulas from ref. [3].

Theorical calculation

The molecular structures of **L^3**, **L^4**, **[IrL^3]** and **[IrL^4]** have been optimized in $CHCl_3$ using B3LYP exchange-correlation functional, a 6-31G* basis set for C, H and N and Lanl2DZ basis set with related pseudo-potentials for Ir and Cl. The solvation effects have been included by means of a Polarizable Continuum Model (PCM) as implemented in G03.[4, 5]

EFISH Measurement

EFISH measurements were carried out working in CH_2Cl_2 (usually 10^{-3} M) at a non resonant incident wavelength of 1.907 μm, using a Q-switched, mode-locked Nd 3+ :YAG laser manufactured by Atalaser equipped with a Raman shifter.

2. Synthetic Details and Analytical Data

2.1. Synthetis of Pt(II) complexes

2.1.1. Synthesis of substituted 1,3-di(2-pyridyl)benzene ligands, HL^n

All HL^n ligands (L^n= 4-substituted-1,3-di(2-pyridyl)benzene) were prepared with the same procedure - or minor modifications - described previously by Williams[1, 6] , and reported here below in the case of HL^1. Synthesis of the precursors are repoted before that of the ligands.

2,2'-(5-methyl-1,3-phenylene)dipyridine, L^1

A mixture of 3,5 dibromo toluene(1.38 g, 5.52 mmol), 2-(tri-*n*-butylstannyl)pyridine (5.38 g, 14.61 mmol), lithium chloride (2.58 g, 55.10 mmol), and bis(triphenylphosphine)palladium(II) chloride (0.31 g, 0.44 mmol), in toluene (24 ml), was degassed via five freeze−pump−thaw cycles and then heated at reflux under an atmosphere of dinitrogen for 48 h at reflux under nitrogen. A saturated aqueous solution of potassium fluoride (10 mL) was added to the solution, after cooling to ambient temperature, and stirred for 30 min. The insoluble residue formed was removed by filtration and washed with toluene. The toluene was removed from the combined filtrate and washed under reduced pressure, giving a crude product, which was taken up into dichloromethane (3 x 50 mL) and washed with aqueous $NaHCO_3$ s.s. (2 × 50 mL). The organic phase was dried over anhydrous Na_2SO_4 and evaporated to dryness. The brown residue was purified by chromatography on silica gel, gradient elution from 100% hexane to 80% diethyl ether, giving the product as a yellow oil (1.09 g, 80%). ^{1}H NMR (400 MHz, $CDCl_3$): δ 8.73 (d, 2H^6), 8.39 (s, 1 H$^{2'}$), 7.92(s, 2 H$^{6'}$), 7.85 (d, 2H^3), 7.77 (td, 2H^4), 7.26 (td, 2H^5), 2.54 (s, 3H, –CH_3).

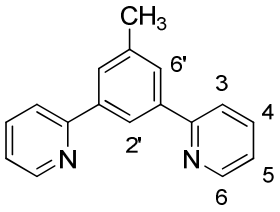

Bromo-Substituted Intermediate, dpyb-Br.

The method employed by was similar to that described above for HL^1, starting from tribromobenzene (0.75 g, 2.53 mmol), in place of 3,5-dibromotoluene, but in this case, only 2.2 equiv of the pyridylstannane was used. After refluxing for 20 h under nitrogen, the mixture was worked up as above. The crude compound was chromatographed on silica, gradient elution from hexane to 50% hexane/50% diethyl ether, leading to the product as a

colorless solid (0.42 g, 53%). ^{1}H NMR (400 MHz, $CDCl_3$): δ 8.75 (d, 2H), 8.59 (s, 1H), 8.25 (d, 2H), 7.85 (m, 4H), 7.32 (ddd, 2H).

2,2'-(2',4',6'-trimethylbiphenyl-3,5-diyl)dipyridine, L^2.

Dimethoxy-ethane (25 mL) was added to a mixture of dpyb-Br (0.530 g, 1.71 mmol), (2,4,6-trimethylphenyl)boronic acid (0.310 g, 1.88 mmol), and $Ba(OH)_2$ **.**$8H_2O$ (0.632 g, 2.00 mmol) in an oven-dried Schlenk tube. The mixture was degassed via three freeze-pump-thaw cycles and placed under nitrogen. Tetrakis(triphenylphosphine)-palladium(0) (0.023 g, 0.02 mmol) was added under a flow of nitrogen and the mixture heated at reflux (85 °C) under a nitrogen atmosphere for 24 h. The solvent was then removed under reduced pressure and the crude residue taken up into dichloromethane (50 mL) and $NaHCO_3$ (5% by mass, 150 mL). The organic layer was separated, washed with $NaHCO_3$ (2 x 150 mL), and dried over anhydrous K_2CO_3. The solvent was removed under reduced pressure, and the pale-brown residue was recrystallized from ethanol to give off white crystals of the desired product (0.072 g, 12%). ^{1}H NMR (400 MHz, $CDCl_3$): δ 8.75 (d, 2H^6), 8.72 (t, 1H$^{4'}$), 7.89 (d, 2H^3), 7.86 ((s, 2H$^{2'}$), 7.79 (td, 2H^4), 7.28 (ddd, 2H^5), 7.00 (d, 2H$^{5''}$), 2.37 (s, 3H *p*-CH_3), 2.12 (s, 6H *o*-CH_3).

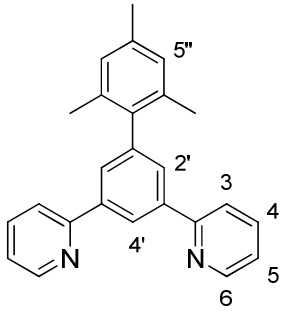

2,2'-(5-fluoro-1,3-phenylene)dipyridine, L^3

This compound was prepared by a procedure similar to that described above for HL [1], but againg a different amount of pyridylstannane (2.5 eq) and of catalists (0.26eq) were used. Thus a mixture of 1,3 dibromo-5-fluoro benzene (0.279 g, 1.103 mmol), 2-(tri-*n*-butylstannyl)pyridine (1.001 g, 2.716 mmol), lithium chloride (0.074 g, 1.655 mmol) and bis(triphenylphosphine)palladium(II) chloride (0.203 g, 0.287 mmol) in toluene (7 ml) was degassed via five freeze−pump−thaw cycles and then heated at reflux under an atmosphere of dinitrogen for 72 h at reflux under nitrogen. Workup as above led to a brown residue, which was purified by chromatography on silica gel, gradient elution from 90% hexane/ 10% diethyl ether to 50% hexane/ 50% diethyl ether, giving the product as a white solid (0.146 g, 53%). ^{1}H NMR (400 MHz, DMSO): δ 8.83 (d, 2H^6), 8.68 (s, 1H$^{2'}$), 8.39 (dd, 2H^3),

8.27 (ddd, 2H[4]), 8.11 (d, (J (^{19}F) 9.8, 2H[6']), 7.72 (ddd, 2H[5]). Anal. Calcd for $C_{16}H_1FN_2$: C, 76.79; H, 4.43; N, 11.19; Found: C, 76.15; H, 4.69; N, 11.16.

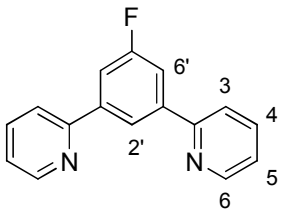

1,3-dibromo-4,6-difluoro benzene, 1

1,3-dibromo-4,6-difluoro benzene was prepeared as previously described by Manka[7] Thus, a mixture of 1-bromo-2,4-difluorobenzene (7.00 g, 36.3 mmol), electrolytic grade iron powder (0.407 g, 7.26 mmol) and CH_2Cl_2 (9 ml) was heated at reflux for 30 min. A solution of bromine (6.38 g, 39.9 mmol) was added dropwise; the resulting mixture was stirred for 3 h under reflux and then poured into a 10 % water solution of $Na_2S_2O_5$ (50 mL) until the colour went from red to colourless. After filtration, the organic product was extracted with CH_2Cl_2 (2 x 20 mL). The extracts were dried (Na_2SO_4) and the solvent evaporated to dryness under reduced pressure. The resulting crude product was short path distilled (bp 35°C/2Torr) to give the product as a low melting white solid (80 % yield). ^{1}H NMR (400 MHz, $CDCl_3$): δ 7.76 (t, 1H), 7.01 (t, 1H).

2-trimethyl tin-5(trifluoromethyl) pyridine, 2

Bis(triphenylphospine)palladium dichloride (24.9 mg, 0.0354 mmol) and hexamethylditin (580 mg, 1.77 mmol) were added to a solution of 2-bromo-5-(trifluoromethyl)pyridine (199 mg, 0.885 mmol) in anhydrous dioxane (10 mL). The mixture was degassed *via* four freeze-pump-thaw cycles, and then heated at reflux under a nitrogen atmosphere for 3 h. After cooling to room temperature, the resulting black suspension was filtered through a Celite pad to give an oil. This was taken up in ether (10 mL) and the solution was washed several times (3 x 5 mL) with water and then dried (Na_2SO_4). The ether was evaporated to dryness under reduced pressure affording **1** as a pale yellow oil (82 % yield). ^{1}H NMR (400 MHz, $CDCl_3$): δ 9.01 (s, 1H), 7.76 (t, 1H), 7.63 (d, 1H).

6,6'-(4,6-difluoro-1,3-phenylene)bis(3-(trifluoromethyl)pyridine), L^4

To a mixture of 1,3-dibromo- 4,6-difluoro benzene (158.1 mg, 0.580 mmol), lithium chloride (243 mg, 5.80 mmol) and bis(triphenylphosphine)palladium(II) dichloride (83.0 mg, 0.116 mmol) in toluene (25 mL) was added dropwise 2-trimethyl tin-5(trifluoromethyl) pyridine (538.9 mg, 1.74 mmol) dissolved in 10 mL of toluene. Then the mixture was degassed *via* five freeze−pump−thaw cycles and heated at reflux

temperature under a nitrogen atmosphere for 4 h. After cooling to room temperature, a saturated aqueous solution of potassium fluoride (10 mL) was added to the dark solution and stirred for 30 min. The insoluble residue formed was removed by filtration and washed with toluene. The solvent was removed from the combined "filtrate and washings" under reduced pressure, giving a crude product. This was taken up into dichloromethane and washed with a saturated solution of aqueous $NaHCO_3$ (2 × 20 mL). The organic phase was dried over anhydrous Na_2SO_4 and evaporated to dryness under reduced pressure. The brown residue was purified by chromatography on silica gel (eluent: hexane) giving HL^4 as a white solid (40 % yield). ^1H NMR (400 MHz, $CDCl_3$): δ 9.02 (s, $2H^2$), 8.87 (t, $1H^{2'}$), 8.05 (d, $2H^4$), 7.97 (d, $2H^5$), 7.13 (t, $1H^{5'}$).

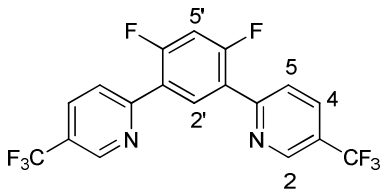

2.1.2. Platinum(II) Complexes

(a) Synthesis of substituted 1,3-di(2-pyridyl)benzene Pt(II) chloro complexes, $[PtL^n]$

All **Pt(II) chloro complexes** were prepared following the general procedure described previously by Williams [1,6], and reported here below in the case of **$[PtL^1]$**. When possible (see section Synthesis in Chapter 1) a method similar to that described by Cárdenas was adopted.[8] Below are reported both strategy used for the synthesis of **$[PtL^4]$**.

Synthesis of $[PtL^4Cl]$ (strategy 1)

To a solution of K_2PtCl_4 (32.1 mg, 0.0742 mmol) in acetic acid (23 mL) was added 6,6'-(4,6-difluoro-1,3-phenylene)bis(3-(trifluoromethyl)pyridine (30.0 mg, 0.0742 mmol) and the resulting solution was degassed by four freeze-pump-thaw cycles. The mixture was then heated at reflux temperature under nitrogen for 3 days. Upon cooling to room temperature, a yellow precipitate was separated, washed with methanol and diethylether (4 x 5 mL), and then dried under reduced pressure (24.9 mg, 50 % yield). ^1H NMR (400 MHz, $CDCl_3$): δ 9.64 (s, $J(^{195}Pt)$ 22 Hz, $2H^6$), 8.25 (d, $2H^4$), 8.07 (d, $2H^3$), 6.83 (t, $J(^{19}F)$ 11 Hz, $1H^{4'}$). ^1H NMR (400 MHz, THF): δ 9.63 (s, $J(^{195}Pt)$ 22 Hz, $2H^6$), 8.52 (d, $2H^4$), 8.13 (d, $2H^3$), 6.84 (t, $J(^{19}F)$ 11 Hz, $1H^{4'}$). Anal. Calcd for $C_{18}H_7F_8N_2Pt$: C, 34.11; H, 1.11; N, 4.42; Found: C, 34.11; H, 1.70; N, 4.03.

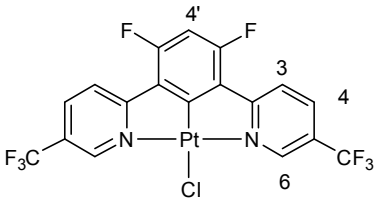

Synthesis of [PtL^{2}Cl]

Yield: 15.8 mg (20%, starting from 49.9 mg, 0.136 mmol of HL^2).

^{1}H NMR (400 MHz, $CDCl_3$): δ 9.42 (d, J(^{195}Pt) 25 Hz, 2H^6), 7.98 (td, 1H^4), 7.66 (d, 2H^3), 7.34 (t, 2H^5), 7.27 (s, 2H$^{6'}$), 7.01 (s, 2H$^{5''}$), 2.39 (s, 3H *p*-C*H*$_3$), 2.11 (s, 6H *o*-C*H*$_3$).

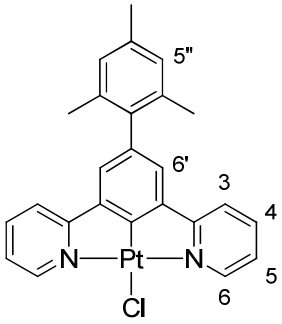

Synthesis of [PtL^{4}Cl] (stategy 2)

A solution of $KPtCl_4$ (30.3 mg, 0.30 mmol) in water (3 mL) was treated with a solution of 6,6'-(4,6-difluoro-1,3-phenylene)bis(3-(trifluoromethyl)pyridine (31.0 mg, 0.0766 mmol) in acetonitrile (2 mL) and the mixture heated at reflux for 72 h. After cooling to ambient temperature, the insoluble orange residue formed was collected by filtration and washed with 12 mL of water-ethanol (5:1 v/v) and then dried under reduced pressure, giving the product as a green solid (29.1 mg, 60% yield). NMR data are consistent with values reported above for this compound.

Synthesis of [PtL^{1}Cl]

Yield: 258.8 mg (67%, starting from 210.6 mg, 0.856 mmol of HL^1).

^{1}H NMR (400 MHz, $CDCl_3$): δ 9.34 (d, J(^{195}Pt) 19 Hz, 2H^6), 7.93 (td, 2H^4), 7.66 (d, J(^{195}Pt) 6 Hz, 2H^3), 7.29 (s, 2H$^{6'}$), 7.28 (not fully resolved due to overlap with former signal and solvent, m, 2H^5), 2.36 (s, 3H -CH_3). ^{1}H NMR (400 MHz, CD_2Cl_2): δ 9.29 (d, J(^{195}Pt) 19 Hz, 2H^6), 8.00 (td, 2H^4), 7.74 (d, J(^{195}Pt) 6 Hz, 2H^3), 7.39 (s, 2H$^{6'}$), 7.35 (ddd, 2H^5), 2.42 (s, 3H -C*H*$_3$). Anal. Calcd for $C_{17}H_{13}ClN_2Pt$: C, 42.91; H, 2.75; N, 5.89; Found: C, 43.10; H, 2.86; N, 5.52.

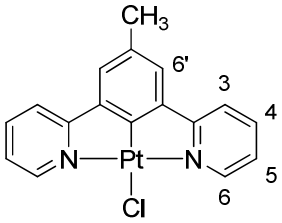

Synthesis of [Pt L^3Cl]

Yield: 49.8 mg (60%, starting from 43.4 mg, 0.173 mmol of HL^3).

^{1}H NMR (400 MHz, DMSO): δ 9.10 (d, J(^{195}Pt) 15 Hz, 2H^6), 8.24 (td, 2H^4), 8.17 (d, 2H^3), 7.78 (s, J(^{19}F) 10 Hz, 2H$^{6'}$), 7.60 (ddd, 2H^5). Anal. Calcd for $C_{16}H_{10}ClFN_2Pt$: C, 40.05; H, 2.10; N, 5.83; Found: C, 40.72; H, 2.10; N, 5.76.

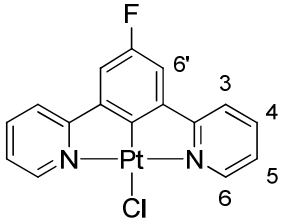

(b) Synthesis N^C^N-coordinated Pt(II) complexes with sulphor-donor ligands [PtL^nS^n]

Pt(II) isothiocyanate complexes were prepared by the corresponding Pt(II) chloro complex following the general procedure below reported for compound **[PtL^1S^1]**. **[PtL^1S^2]** was obtained by a similar procedure as indicated below.

Synthesis of [PtL^1S^1].

To a suspension of [PtL^1Cl] (50.3 mg, 0.105 mmol) in methanol/acetone (5/20 v/v) was added sodium thiocyanate (18.1 mg, 0.210 mmol). The reaction mixture was stirred at room temperature for 1 day. The product was obtained as red solid by two crystllizations from pentane dry (25.9 mg, 50% yield).

^{1}H NMR (400 MHz, CD_2Cl_2): δ 8.77 (d, J(^{195}Pt) 20 Hz, 2H^6), 8.04 (td, 2H^4), 7.73 (d, J(^{195}Pt) 6 Hz, 2H^3), 7.36 (ddd, 2H^5), 7.33 (s, 2H$^{6'}$), 2.42 (s, 3H -CH_3). IR ν/cm^{-1} 2096 (SCΞN). Anal. Calcd for $C_{18}H_{13}N_3PtS$: C, 43.37; H, 2.63; N, 8.43; Found: C, 43.87; H, 3.10; N, 8.92.

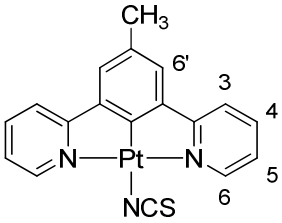

Synthesis of [PtL^{2}S^1].

Yield: 32.5 mg (45%, starting from 70.2 mg, 0.120 mmol of **[PtL^{2}Cl]**).

^{1}H NMR (400 MHz, $CDCl_3$): δ 8.81 (d, J(^{195}Pt) 19 Hz, 2H^6), 7.98 (td, 1H^4), 7.64 (d, 2H^3), 7.33 (td, 2H^5), 7.27 (s, 2H$^{6'}$), 7.02 (s, 2H$^{5''}$), 2.39 (s, 3H *p*-C*H*$_3$), 2.11 (s, 6H *o*-C*H*$_3$). IR ν/cm^{-1} 2097 (SCΞN). Anal. Calcd for $C_{26}H_{21}N_3PtS$: C, 51.82; H, 3.51; N, 6.97; Found: C, 52.07; H, 3.32; N, 6.72.

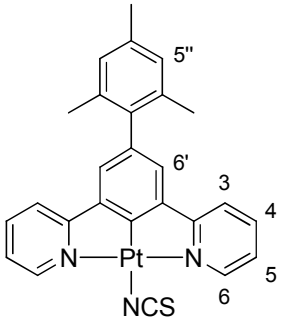

Synthesis of [PtL^{1}S^2].

To a solution of 4-phenylthiazole-2-thiol (12.2 mg, 0.063 mmol) and K_2CO_3 dry in THF dry was added [PtL^{1}Cl] (15.0 mg, 0.032 mmol). The reaction mixture was stirred at reflux overnigth. After cooling to ambient temperature, the solvent was removed under reduced pressure, giving a yellowish crude compound. The product was obtained as yellow solid by three crystllizations from pentane dry under nitrogen atmosohere (12.0 mg, 30% yield). ^{1}H NMR (300 MHz, CD_2Cl_2): δ 9.43 (d, J(^{195}Pt) 21 Hz, 2H^6), 7.98 (td, 2H^4), 7.88 (d, 2H$^{2''}$), 7.77 (d, J(^{195}Pt) 6, Hz 2H^3), 7.53 (t, 1H$^{4''}$), 7.46 (s, 2H$^{6'}$), 7.39 (t, 2H^5), 7.27 (ddd, 2H$^{3''}$ and 1H$^{4''}$), 6.98 (s, 1H$^{1''}$), 2.45 (3H -C*H*$_3$). Anal. Calcd for $C_{26}H_{19}N_3PtS_2$: C, 49.36; H, 3.03; N, 6.64; Found: C, 49.77; H, 3.09; N, 6.68.

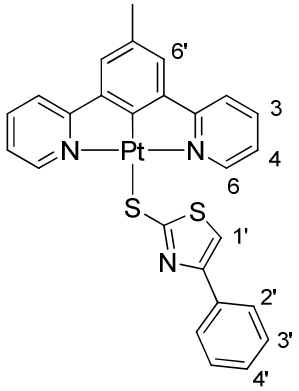

(c) Synthesis of N^C^N-coordinated Pt(II) σ-phenylacetylide complexes, [PtL^{n}A^n];

Pt(II) σ-acetylide complexes derived from [PtL^{n}Cl], where L^n=L^1, L^2, were prepared following the general procedure below reported for [PtL^{1}A^1] which with minor modification has been previously described by Baik.[9] Alkynyl derivatives of [PtL^{4}Cl] were only obtained in the conditions reported below for [PtL^4 A^1].

Synthesis of [PtL^{1}A^1] (A^1 =1-ethynyl-3,5-difluorobenzene)

A mixture of 1-ethynyl-3,5-difluorobenzene (22.1 mg, 0.161 mmol) and 0.5 M sodium methoxide (2.8 mL, 0.181 mmol) in methanol (1 mL) was stirred for 30 min at room temperature. Then [PtL^{1}Cl] (76.2 mg, 0.161 mmol) dissolved in MeOH/CH_2Cl_2 (4/1 v/v) was added and the mixture was left for one day at room temperature. The solution changed colour passing from yellow to red. Then the solvents were removed and the crude product was washed with water, methanol and *n*-hexane. A further purification by precipitation with pentane gave the desired product as a red solid in almost quantitative yield (89 mg). ^{1}H NMR (400 MHz, $CDCl_3$): δ 9.39 (d, J(^{195}Pt) 25 Hz, 2H^6), 7.93 (td, 2H^4), 7.66 (d, J(^{195}Pt) 5 Hz, 2H^3), 7.36 (s, 2H$^{6'}$), 7.21 (td, 2H^5), 7.07 (dd, J(^{19}F) 8 Hz, 2H$^{2''}$), 6.64 (tt, J(^{19}F) 10 Hz, 1H$^{4''}$), 2.38 (3H -C*H*$_3$). IR ν/cm^{-1} 2083(CΞC). Anal. Calcd for $C_{25}H_{16}F_2N_2Pt$: C, 52.00; H, 2.79; N, 4.85; Found: C, 52.01; H, 2.83; N, 4.27.

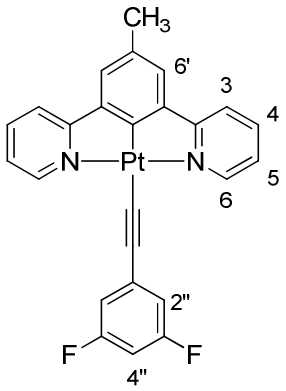

Synthesis of Trimethylpentafluorophenylethynylsilane, 3

Following the Sonogashira protocol reported in ref. [10] to a mixture of 1-bromo-2,3,4,5,6-pentafluorobenzene (1.02 g, 4.049 mmol), bis(triphenylphosphine)palladium(II) chloride (0.143 g, 0.202 mmol) and copper acetate (0.05 g, 0.202 mmol) in freshly distilled diisopropylamine (5 mL) was added dropwise trimethylsilylacetylene (1.25 mL, 8.908 mmol) over a period of 10 min at room temperature. Then the solution was heated at reflux for 6 h. The solution was allowed to cool to room temperature and was filtered to remove the precipitated diethylamine hydrobromide salt. The solvent was removed under reduced pressure and the residue was taken up into dichloromehane. Extraction with a 5% HCl (10 mL) solution followed by extraction with water (2 x 10 mL), drying the

organic layer, and removal of the solvent yielded the crude compound as a dark oil. This was purified by chromatography on silica gel (eluent: hexane) giving the product as clear liquid (0.750 mg, 70% yield). ^{1}H NMR (400 MHz, $CDCl_3$): δ 0.22 (s).

Synthesis of 1-ethynyl-2,3,4,5,6-pentafluorobenzene, 4

Basic hydrolisis (50% KOH) of trimethylpentafluorophenylethynylsilane (39.7 mg, 1.500 mmol) in MeOH yielded the product as clear liquid (25.4 mg, 87% yield). ^{1}H NMR (400 MHz, $CDCl_3$): δ 3.61 (s). IR $\nu/\chi m^{-1}$ 2130 (CΞC).

Synthesis of [PtL^{1}A^2] (A^2 = 1-ethynyl-2,3,4,5,6-pentafluorobenzene)

Almost quantitative yield (128 mg, starting from 101.0 mg, 0.210 mmol of [PtL^{1}Cl]).
^{1}H NMR (300 MHz, $CDCl_3$): δ 9.46 (d, J(^{195}Pt) 24 Hz, 2H^6), 7.93 (t, 2H^4), 7.67 (d, 2H^5), 7.35 (s, 2H$^{6'}$), 7.23 (t, 2H^5), 2.40 (3H -C*H*$_3$). ^{19}F NMR (300 MHz, $CDCl_3$): δ -136.7 (d, 2F), -157.7 (t, 1F), -159.9 (t, 2F), IR ν/cm^{-1} 2081 (CΞC). Anal. Calcd for $C_{25}H_{13}F_5N_2Pt$: C, 47.55; H, 2.08; N, 4.44; Found: C, 47.67; H, 2.10; N, 4.02.

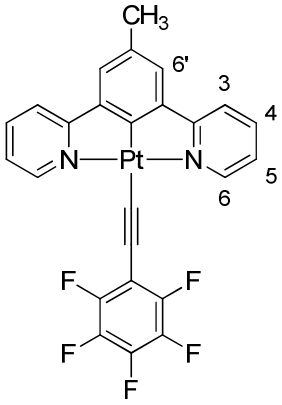

Synthesis of [PtL^{2}A^1] (A^1 =1-ethynyl-3,5-difluorobenzene)

Almost quantitative yield (102.6 mg , starting from 90.2 mg, 0.156 mmol of [PtL^{2}Cl]). ^{1}H NMR (400 MHz, CD_2Cl_2): δ 9.41 (d, J(^{195}Pt) 20 Hz, 2H^6), 8.01 (td, 2H^4), 7.70 (d, J(^{195}Pt) 7 Hz, 2H^3), 7.37 (s, 2H$^{6'}$), 7.31 (td, 2H^5), 7.07 (dd, J(^{19}F) 9 Hz, 2H$^{2''}$), 7.00 (s, 2H$^{5''}$),6.71 (tt, J(^{19}F) 11 Hz, 1H$^{4''}$), 2.37 (3H *p*-C*H*$_3$), 2.12 (6H *o*-C*H*$_3$). IR ν/cm^{-1} 2083(CΞC). Anal. Calcd for $C_{33}H_{24}F_2N_2Pt$:: C, 58.15; H, 3.55; N, 4.11; Found: C, 58.22; H, 3.70; N, 3.92.

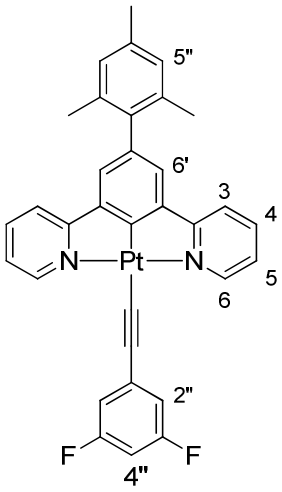

Synthesis of [PtL^4 A^1] (A^1 = 1-ethynyl-3,5-difluorobenzene)

The method employed for the synthesis of **[PtL^4 A^1]** is similar to that described above for **[PtL^{1}A^1]**, starting from **[PtL^{4}Cl]**, instead of **[PtL^{1}Cl]**, but in this case only a stoichiometric amount of base was used and the reaction was conducted at low temperature. Thus a solution of 1-ethynyl-3,5-difluorobenzene (19.5 mg, 0.143 mmol) and 0.5 M sodium methoxide (3.5 mL, 0.143 mmol) in methanol (1 mL) was stirred for 30 min at room temperature. Then the mixture was added to a solution of **[PtL^{4}Cl]** (90.86 mg, 0.143 mmol) in MeOH/CH_2Cl_2 (5/1) which had been previously cooled to -20°C. The mixture was left stirring at -20°C for 4h and then to room temperature overnight, changing colour from yellow to dark red. The solvents were removed and the crude product was washed with water, methanol and *n*-hexane. A further purification by precipitation with pentane dry gave the desired product as a red solid (41.7 mg, 40% yield). ^{1}H NMR (400 MHz, THF): δ 9.76 (d, J(^{195}Pt) 24 Hz, 2H^6), 8.51 (d, 2H^4), 8.17 (d, 2H^3), 6.98 (m, 1H$^{4'}$ and 2H$^{2''}$), 6.83 (td, J(^{19}F) 10 Hz, 2H$^{4''}$). IR ν/cm^{-1} 2084(CΞC). Anal. Calcd for $C_{26}H_{10}F_{10}N_2Pt$: C, 42.46; H, 1.37; N, 3.81; Found: C, 42.57; H, 3.96; N, 3.62.

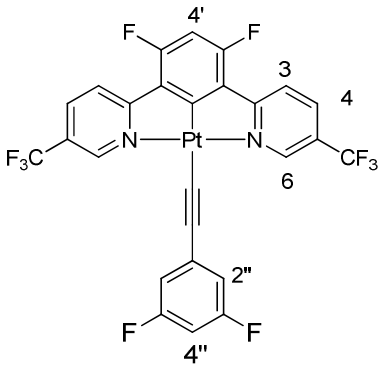

Synthesis of [PtL^{4}A^4] (A^4 =4-ethynyl-N,N-dimethylaniline)

Yield: 63.2 mg (40% starting from 134.7 mg, 0.212 mmol of [PtL^{4}Cl]). ^{1}H NMR (400 MHz, THF): δ 9.58 (d, J(^{195}Pt) 24 Hz, 2H^6), 8.21 (d, 2H^4), 7.86 (d, 2H^3), 7.15 (d, 2H$^{3''}$), 6.68 (d, 2H$^{2''}$), 6.58 (d, J(^{19}F) 11 Hz, 2H$^{4''}$), 2.37 (6H -(CH_3)$_2$). IR ν/cm^{-1} 2085(C≡C). Anal. Calcd for $C_{28}H_{17}F_8N_3Pt$: C, 45.29; H, 2.31; N, 5.66; Found: C, 44.87; H, 2.72; N, 5.22.

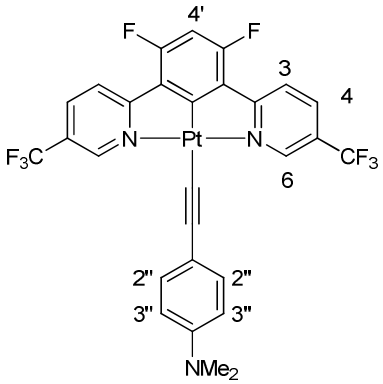

2.2. Synthetis of Ir(I) complexes.

Below are reported the synthesis of the anellated hemicyanine ligand, **L^4**, **L^3** and **L$^?$** their related iridium complexes. Synthesis of the precursors are repoted before that of the compounds.

***N,N*-dibutyl-3-(chloromethyl)aniline, 1**

To a solution of 3-(dibutylamino)benzyl alcohol (3.8 g, 16.15 mmol) in dry THF (30 mL) under nitrogen atmosphere was added PPh_3 (6.3 g, 24 mmol) and CCl_4 (1.9 mL, 20 mmol) and the mixture was refluxed for 48 h. After cooling at room temperature the white precipitate was filtered off and the organic phase concentrated *in vacuo*. The crude product was purified by silica gel column chromatography using pure CH_2Cl_2 as eluent affording compound **1** as a colourless oil (4.04 g, 95%). ^{1}H NMR (300 MHz, $CDCl_3$): δ 7.17 (t, *J* 8 Hz, 1H^5), 6.64 (m, 1H^2 and 1H^6), 6.59 (dd, *J* 8, 2.4 Hz, 1H^4), 4.54 (s, 2H, N-CH_2), 3.27 (t, *J* 7.6 Hz, 4H, NCH_2 -(CH$_2$)$_2$ -CH$_3$), 1.55 (m, 4H, CH$_2$CH_2CH$_2$CH$_3$), 1.37 (sexstet, *J* 7.6 Hz, 4H, N(CH$_2$)$_2$CH_2CH$_3$), 0.96 (t, *J* 7.6 Hz, 6H, N(CH$_2$)$_3$CH_3,); ^{13}C NMR (300 MHz, $CDCl_3$): δ 148.48, 138.33, 129.52, 115.16, 111.72, 111.61, 50.75, 47.27, 29.38, 20.36, 14.01; *m/z* (ESI) 254.2 [M + H$^+$], calcd. 253.16.

(3-*N,N*-dibutylamino)benzyltriphenylphosphonium chloride, 2

To a solution of *N,N*-dibutyl-3-chloromethylaniline (2.95 g, 11.6 mmol) in heptane (5 mL) was added PPh_3 (3.6 g, 13.7 mmol) and the mixture was refluxed for 24 h. After cooling at room temperature the white precipitate was filtered and washed with heptane and Et_2O, then concentrated *in vacuo* affording pure **2** (4.9 g, 82%). ^{1}H NMR (400 MHz, $CDCl_3$): δ 7.76 (m, 15H, P*Ph*$_3$), 6.90 (t, *J* 8 Hz, 1H^5), 6.46 (dt, *J* 8 Hz, 1H^6), 6.28 (d, *J* 2 Hz, 1H^2), 6.16 (d, *J* 8 Hz, 1H^4), 5.15 (d, 2H, *J* 14 Hz, C*H*$_2$P), 3.02 (t, *J* 7 Hz, 4H, NC*H*$_2$(CH$_2$)$_2$CH$_3$), 1.25 (m, 8H, NCH$_2$(C*H*$_2$)$_2$CH$_3$), 0.87 (t, 6H, *J* 7 Hz, N(CH$_2$)$_3$C*H*$_3$); ^{1}C NMR (100 MHz, $CDCl_3$): δ 148.47, 134.82, 134.38 (d, $J_{C\text{-}P}$ 10 Hz), 130.08 (d, $J_{C\text{-}P}$ 12 Hz), 129.55 (d, $J_{C\text{-}P}$ 3 Hz), 127.69 (d, $J_{C\text{-}P}$ 8 Hz), 118.30 (d, $J_{C\text{-}P}$ 85 Hz), 117.74 (d, $J_{C\text{-}P}$ 5 Hz), 114.52 (d, $J_{C\text{-}P}$ 5 Hz), 111.68 (d, $J_{C\text{-}P}$ 3 Hz), 50.46, 31.41 (d, $J_{C\text{-}P}$ 43 Hz), 29.20, 20.24, 14.02; *m/z* (ESI) 480.4 [M$^+$], calcd. 480.28.

(E,Z)-3-(3-*N,N*-dibutylaminostiryl)pyridine, 3

(3-*N,N*-dibutylamino)benzyltriphenylphosphonium chloride (1.09 g, 2.12 mmol) was dissolved in dry MeOH (30 mL) under nitrogen atmosphere, ^{t}BuOK (236 mg, 1.93 mmol) was added and the solution was heated to reflux. After 4 h 3-pyridinecarboxaldehyde (206 mg, 1.93 mmol) was added and the solution was refluxed overnight. The solvent was concentrated *in vacuo*, the residue was dissolved in CH_2Cl_2 and washed twice with water. The organic phase was dried over Na_2SO_4 and evaporated *in vacuo*, then 10 mL of hexane/AcOEt (1:1 v/v) solution was added to the crude product to allow the precipitation of triphenylphosphine oxide which was filtered off. The organic phase was evaporated *in vacuo* and the crude product was purified by silica gel column chromatography (hexane/AcOEt 8:2) affording **3** (488 mg, 82% yield) as E/Z isomers mixture. This product was generally used as isomeric mixture. The two isomers were once isolated as pure compounds only for characterization. Z isomer- ^{1}H NMR (400 MHz, $CDCl_3$): δ 8.52 (d, *J* 2.4 Hz, 1H^2 –p*y*), 8.40 (dd, *J* 4.8, 2 Hz, 1H^6 -py), 7.59 (dt, *J* 7.6, 1.6 Hz, 1H^4 –*py*), 7.11 (m, 1H^5 –*Ar* and 1H^5 -*py*), 6.72 (d, *J* 12 Hz, 1H, ArCH=C*H*), 6.50 (m, 1H, ArC*H*=CH, and H^2, H^4 and H^6 -*Ar*), 3.11 (t, *J* 7.6 Hz, 4H, NC*H*$_2$(CH$_2$)$_2$CH$_3$,), 1.42 (quint., *J* 7.6 Hz, 4H, NCH$_2$C*H*$_2$CH$_2$CH$_3$,), 1.25 (sextet, *J* 7.2 Hz, 4H, N(CH$_2$)$_2$C*H*$_2$CH$_3$), 0.90 (t, *J* 7.2 Hz, 6H, N(CH$_2$)$_3$C*H*$_3$); ^{1}C NMR (100 MHz, $CDCl_3$) : δ 150.34, 148.23, 147.84, 137.25, 135.92, 133.95, 133.43, 129.35, 125.59, 122.87, 115.75, 111.73, 111.18, 50.79, 25.34, 20.27, 13.95; *m/z* (ESI) 309.3 [M + H$^+$], calcd: 308.23. E isomer ^{1}H NMR (400 MHz, $CDCl_3$): δ 8.72 (d, *J* 2 Hz, 1H^2 -p*y*), 8.48 (dd, *J* 4.8, 1.6 Hz, 1H^6 -*py*), 7.84 (dt, *J* 7.6, 1H -p*y*H$_4$, , 1.6 Hz), 7.25 (m, 2H p*y*H$_5$, -*Ar*H$_5$), 7.14 (d, *J* 16 Hz, 1H -ArCH=C*H*), 7.02 (d, *J* 16 Hz, 1H ArC*H*=CH), 6.85 (d, *J* 7.6 Hz, 1H -*Ar*H$_4$), 6.75 (broad s, 1H, *Ar*H$_2$), 6.61 (dd, *J* 8, 2.8 Hz, 1H *Ar*H$_6$,), 3.31 (t, *J* 7.6 Hz, 4H -NC*H*$_2$(CH$_2$)$_2$CH$_3$,), 1.59 (q, *J* 8 Hz, 4H -NCH$_2$C*H*$_2$CH$_2$CH$_3$), 1.40 (sextet, *J* 8 Hz, 4H -N(CH$_2$)$_2$C*H*$_2$CH$_3$), 0.98 (t, *J* 7.2 Hz, 6H -N(CH$_2$)$_3$C*H*$_3$,); ^{1}C NMR (100

MHz, $CDCl_3$): δ 148.56, 148.34, 137.49, 133.31, 132.61, 132.1, 129.56, 124.19, 123.48, 113.53, 112.00, 110.36, 50.82, 29.47, 20.41, 14.07; *m/z* (ESI) 309.3 [M + H^+], calcd. 308.23.

8-(*N,N*-dibutylamino)benzo[*f*]isoquinoline, L^3

A magnetically stirred solution of E/Z-3-(3-*N,N*-dibutylaminostiryl)pyridine (468 mg, 1.52 mmol) in 2-Me-THF (500 mL) was irradiated by a Hg high pressure lamp in a quartz reactor for 1.5 h at -15 °C. The solvent was evaporated *in vacuo* and the brown oil residue was purified by silica gel column chromatography (hexane/AcOEt 1:1) affording pure **L^3** (216 mg, 46%). ^{1}H NMR (400 MHz, CD_3OD): δ 8.79 (d, *J* 0.7 Hz, 1H^4), 8.53 (d, *J* 9.2 Hz, 1H^{10}), 8.45 (d, *J* 6 Hz, 1H^1), 8.37 (d, *J* 6 Hz, 1H^2), 7.70 (m, *J* 8.8 Hz, 1H^5 and H^6), 7.22 (dd, *J* 9.2, 2.4 Hz, 1H^9), 7.00 (d, *J* 2.4 Hz, 1H^7), 3.47 (t, *J* 7.6 Hz, 4H -NC*H*$_2$(CH$_2$)$_2$CH$_3$), 1.69 (m, 4H -NCH$_2$C*H*$_2$CH$_2$CH$_3$), 1.46 (sextet, *J* 7.6 Hz, 4H -N(CH$_2$)$_2$C*H*$_2$CH$_3$,), 1.03 (t, *J* 7.6 Hz, 6H -N(CH$_2$)$_3$C*H*$_3$); ^{1}C NMR (100 MHz, $CDCl_3$): δ 149.22, 148.94, 142.05, 136.57, 136.19, 128.85, 125.26, 124.98, 124.93, 117.84, 115.65, 114.43, 107.13, 50.86, 29.41, 20.37, 14.02; m/z (ESI) 307.21658 [M + H^+], calcd. 306.21688.

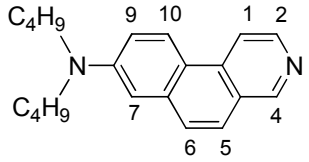

Syntesis di $Ir(COT)_2Cl]_2$ (COT = cyclooctene)

To $IrCl_3$•$3H_2O$ (5.673 mmol, 352.55 mmol) in 2-propanol (22mL) and H_20 (8mL) is added cyclooctene (4mL) under nitrogen atmosphere. The solution was stirred at room temperature for 2 min and then at reflux for 3h. The product was obtained as red solid by two crystllizations from pentane dry was refluxed or 6 h. The solution changed colour passing from dark red to orange. Upon cooling to room temperature, a orange-yellow precipitate was separated under nitrogen atmosphere and washed with ice-cold methanol (3 x 20 mL). Then the solvent were removed at room temperature under vacuum. exane. The product $Ir(COT)_2Cl]_2$ is obtained as a yellow powder (1.5 g, 59% yield). Anal. Calcd for $C_{32}H_{56}Cl_2Ir_2$: C, 42.89; H, 6.30; Found: C, 42.87; H, 6.64.

[$Ir(CO)_2Cl$(8-(*N,N*-dibutylamino)benzo[*f*]isoquinoline)], [IrL^3]

A sample of $[Ir(COT)_2Cl]_2$ (119.4 mg, 0.13 mmol) was suspended in dry CH_3CN (50 mL) under nitrogen atmosphere. After 2 min, the nitrogen was replaced by carbon monoxide and the suspension turned yellow for the formation of $[Ir(CO)_2Cl]_2$ complex. 8-(*N,N*-dibutylamino)benzo[*f*]isoquinoline (76.4 mg, 0.25 mmol) was added and after 1 h the solution

was evaporated to dryness *in vacuo* affording pure **[IrL^3]** (159.0 mg, quantitative yield). ^{1}H NMR (400 MHz, $CDCl_3$): δ 9.18 (s, 1 H^4), 8.61 (d, *J* 6.5 Hz, 1H^2), 8.42 (d, *J* 9.2 Hz, 1H^{10}), 8.28 (d, *J* 6.5 Hz, 1H^1), 7.74 (d, *J* 9.2 Hz, 1H^5), 7.65 (d, *J* 9.2 Hz, 1H^6), 7.18 (dd, *J* 9.2, 2.8 Hz, 1H^9), 6.93 (d, *J* 2.8 Hz, 1H^7), 3.47 (t, *J* 6.5 Hz, 4H -NC*H*$_2$(CH$_2$)$_2$CH$_3$), 1.69 (m, 4H -NCH$_2$C*H*$_2$CH$_2$CH$_3$), 1.47 (m, 4H -N(CH$_2$)$_2$C*H*$_2$CH$_3$), 1.03 (t, *J* 7.6 Hz, 6 H -N(CH$_2$)$_3$C*H*$_3$,); ν/cm^{-1} 2073 (CO), 1994 (CO); Anal. Calcd for $C_{23}H_{26}N_2O_2IrC$: C, 46.81; H, 4.44; N, 4.75; Found: C, 46.83; H, 4.42; N, 4.74.

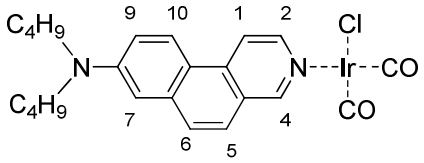

(E,Z)-5-(3-*N,N*-dibutylaminostiryl)isoquinoline, 4

A solution of **2** (2.20 g, 4.2 mmol) in dry MeOH (50 mL) and ^{t}BuOK (513 mg; 4.2 mmol) was refluxed for 4 h, then isoquinoline-5-carbaldehyde (609 mg, 3.8 mmol) dissolved in dry MeOH (5 mL) was added and the solution was refluxed overnight. The solvent was evaporated *in vacuo* and the residue was dissolved in CH_2Cl_2 (50 mL) and washed with water. The organic phase was dried over $MgSO_4$ and evaporated *in vacuo* to give a brown residue. Then 10 mL of a 4:1 v/v hexane/AcOEt solution was added to the crude product to allow the precipitation of triphenylphosphine oxide which was filtered off. The organic phase was evaporated *in vacuo* and the residue was purified by column chromatography on silica gel (hexane/AcOEt 1:1) to afford **4** as mixture of E/Z isomers as yellow oil (1.12 g, 82%). This product was generally used as isomeric mixture. The two isomers were once isolated as pure compounds only for characterization. Z isomer ^{1}H NMR (400 MHz, $CDCl_3$): δ 9.26 (s, 1H^1, *Isoquin*), 8.50 (d, *J* 6 Hz, 1H^3 *Isoquin*,), 7.86 (m, 2H, *Isoquin*H$_4$, *Isoquin*H$_6$), 7.65 (d, *J* 7.2 Hz, 1H *Isoquin*H$_8$,), 7.51 (t, *J* 7.2 Hz, 1H *Isoquin*H$_7$), 7.02 (t, *J* 7.8 Hz, 1H *Ar*H$_5$,), 6.90 (d, *J* 12 Hz, 1 H, ArCH=C*H*), 6.86 (d, *J* 12 Hz, 1H, ArC*H*=CH), 6.45 (br. s, 2 H, *Ar*H$_4$, *Ar*H$_6$), 6.26 (br. s, 1 H, *Ar*H$_2$,), 2.87 (t, *J* 7.2 Hz, 4H NC*H*$_2$(CH$_2$)$_2$CH$_3$), 1.20 (m, 4 H, NCH$_2$C*H*$_2$CH$_2$CH$_3$), 1.06 (sexstet, *J* 7.2 Hz, 4H N(CH$_2$)$_2$C*H*$_2$CH$_3$), 0.79 (t, *J* 7.2 Hz, 6H N(CH$_2$)$_3$C*H*$_3$,); ^{13}C NMR (100 MHz, $CDCD_3$): δ 152.60, 142.80, 136.95, 135.09, 134.41, 134.26, 130.92, 129.10, 128.80, 127.17, 126.81, 118.13, 116.86, 115.28, 50.90, 29.03, 20.25, 13.87. E isomer ^{1}H NMR (400 MHz, $CDCD_3$): δ 9.29 (s, 1 H, *Isoquin*H$_1$), 8.60 (d, *J* 6 Hz, 1H *Isoquin*H$_3$,), 8.00 (m, 2H *Isoquin*H$_4$, *Isoquin*H$_6$), 7.93 (d, *J* 8 Hz, 1H *Isoquin*H$_8$,), 7.75 (d, *J* 16 Hz, 1H ArCH=C*H*,), 7.64 (t, *J* 7.6 Hz, 1H *Isoquin*H$_7$), 7.28 (t, *J* 8 Hz, 1H *Ar*H$_5$,), 7.19 (d, *J* 16 Hz, 1H ArC*H*=CH,), 6.97 (d, *J* 8 Hz, 1H *Ar*H$_4$,), 6.85 (s, 1 H, *Ar*H$_2$), 6.67 (dd, *J* 8, 2.4 Hz, 1H *Ar*H$_6$,), 3.36 (t, *J* 7.6 Hz, 4H -NC*H*$_2$(CH$_2$)$_2$CH$_3$,), 1.65 (m, 4H -NCH$_2$C*H*$_2$CH$_2$CH$_3$), 1.42 (sexstet, *J* 7.2 Hz, 4H -

$N(CH_2)_2CH_2CH_3$,), 1.20 (t, *J* 7.2 Hz, 6H -$N(CH_2)_3CH_3$,); ^{13}C NMR (400 MHz, $CDCl_3$): δ 153.15, 148.60, 143.22, 137.97, 134.41, 134.13, 133.99, 129.60, 127.20, 127.10, 123.17, 116.73, 113.54, 111.95, 110.55, 50.84, 29.46, 20.41, 14.06.

8-*N*,*N*-dibutylaminonafto[2,1-*f*]isoquinoline, L^4

A magnetically stirred solution of E/Z-5-(3-*N,N*-dibutylaminostiryl)isoquinoline (600 mg, 1.67 mmol) in THF (500 mL) was irradiated by a Hg high pressure lamp in a quartz reactor for 8 h at 17 °C. After the evaporation of the solvent the residue was purified by column chromatography on silica gel (hexane/AcOEt 1:1) then by crystallization from hexane to afford a pale yellow solid (200 mg, 33.5%). mp 211 °C. ^{1}H NMR (400 MHz, $CDCl_3$): δ 9.28 (s, 1H^1), 8.70 (d, *J* 6 Hz, 1H^3), 8.64 (d, *J* 9 Hz, 1H^{11}), 8.56 (d, *J* 9 Hz, 1H^{10}), 8.46 (d, *J* 8.8 Hz, 1H^6), 8.39 (d, *J* 6 Hz, 1H^4), 7.96 (d, *J* 8.8 Hz, 1H^{12}), 7.85 (d, *J* 8.8 Hz, 1H^5), 7.23 (dd, *J* 8.8, 2.8 Hz, 1H^9), 7.01 (d, *J* 2.8 Hz, 1H^7), 3.47 (t, *J* 7.6 Hz, 4H -$NCH_2(CH_2)_2CH_3$), 1.70 (m, 4H -$NCH_2CH_2CH_2CH_3$), 1.47 (sextet, *J* 7.6 Hz 4H -$N(CH_2)_2CH_2CH_3$), 1.04 (t, *J* 7.6 Hz, 6H -$N(CH_2)_3CH_3$); ^{13}C NMR (100 MHz, $CDCl_3$): δ 151.50, 147.43, 143.29, 135.27, 135.00, 131.29, 127.39, 126.32, 125.26, 124.67, 123.47, 122.55, 120.95, 120.94, 116.77, 115.12, 106.61, 50.85, 29.53, 20.43, 13.97; *m/z* (ESI) 357.23204 [M + H$^+$], calcd, 356.2325.

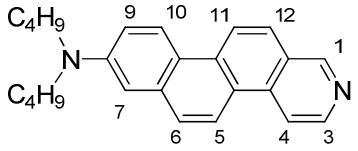

[Ir(CO)$_2$Cl(8-*N*,*N*-dibutylaminonafto[2,1-*f*]isoquinoline)], [IrL^4]

A sample of $[Ir(COT)_2Cl]_2$ (53.3 mg, 0.42 mmol) was suspended in dry CH_3CN (50 mL) under nitrogen atmosphere. After 2 min, the nitrogen was replaced by carbon monoxide and the suspension turned yellow for the formation of $[Ir\text{-}(CO)_2Cl]_2$ complex. Then 8-*N*,*N*-dibutylaminonafto[2,1-*f*]isoquinoline (30.3 mg, 0.08 mmol) was added and after 1 h the solution was evaporated to dryness *in vacuo* affording pure **[IrL^4]** (52.5 mg, quantitative). ^{1}H NMR (400 MHz, $CDCl_3$): δ 9.41 (s, 1H^1), 8.76 (d, *J* 9.2 Hz, 1H^5), 8.70 (d, *J* 6.5 Hz, 1H^3), 8.58 (d, *J* 9.2 Hz, 1H^{10}), 8.51 (d, *J* 6.5 Hz, 1H^4), 8.41 (d, *J* 9.0 Hz, 1H^{12}), 8.00 (d, *J* 9.0 Hz, 1H^{11}), 7.89 (d, *J* 9.1 Hz, 1H^6), 7.25 (dd, *J* 9.6, 2.8 Hz, 1H^9), 7.00 (d, *J* 2.8 Hz, 1H^7), 3.47 (t, *J* 7.6 Hz, 4 H -$NCH_2(CH_2)_2CH_3$), 1.69 (m, 4 H, $NCH_2CH_2CH_2CH_3$), 1.46 (m, 4H, $N(CH_2)_2CH_2CH_3$), 1.02 (t, 6 H, $N(CH_2)_3CH_3$); ν/cm^{-1} 2074 (CO), 1995 (CO). Anal. Calcd for $C_{27}H_{28}N_2O_2IrCl$: C, 50.65; H, 4.41; N, 4.38; Found: C, 50,60; H, 4.40; N, 4.38.

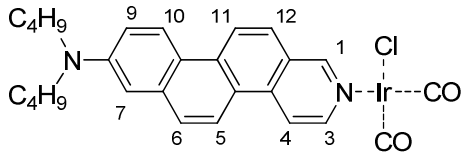

8-(*N*,*N*-dibutylamino)-2-methylnaphto[2,1-*f*]isoquinolinium iodide, L^4MeI

8-*N*,*N*-dibutylaminonafto[2,1-*f*]isoquinoline (120 mg, 0.33 mmol) was dissolved in THF (10 mL) and MeI was added (149 μl, 2.31 mmol) and the solution was reacted at room temperature overnight. The resulting red precipitate was filtered, washed with few millilitres of THF and dried under vacuum, affording the pure product **L^4MeI** (140 mg, 85%). mp 259-260.7 °C. ^{1}H NMR (400 MHz, CD_3OD): δ 9.55 (s, 1H^1), 9.03 (m, 1H^3 and 1H^{11}), 8.69 (d, *J* 9.2 Hz, 1H^{10}), 8.57 (m, 1H^4 and 1H^6), 8.19 (d, *J* 9.2 Hz, 1H^{12}), 7.98 (d, *J* 9.2 Hz, 1H^5), 7.35 (dd, *J* 9.2, 2.4 Hz, 1H^9), 7.09 (d, *J* 2.4 Hz, 1H^7), 4.46 (s, 3H -NC*H*$_3$), 3.53 (t, *J* 7.6 Hz, 4H -NC*H*$_2$(CH$_2$)$_2$CH$_3$), 1.68 (quintet, *J* 7.6 Hz, 4H -NCH$_2$C*H*$_2$CH$_2$CH$_{34}$), 1.47 (sextet, *J* 7.2 Hz, 4H -N(CH$_2$)$_2$C*H*$_2$CH$_3$), 1.03 (t, *J* 7.2 Hz, 6H -N(CH$_2$)$_3$C*H*$_3$); ^{13}C NMR (100 MHz, CD_3OD): δ149.01, 147.36, 137.48, 136.84, 136.18, 134.76, 129.17, 126.66, 125.84, 125.44, 125.02, 122.09, 120.69, 120.54, 119.92, 115.58, 106.19, 50.33, 46.53, 29.21, 19.90, 12.96 ; *m/z* (ESI) 371.24789 [M$^+$], calcd. 371.24818.

***N,N*-dimetyl-4-(pyridin-4-yl)aniline, L^2**

In a Schlenk tube a stirred mixture of 4-bromopyridine hydrochloride (593 mg, 3.05 mmol), 4-(dimethylamino)phenylboronic acid (1.00 g, 6.10 mmol), aqueous Na_2CO_3 (15 mL, 15.3 mmol) and tetrakis(triphenylphosphine)palladium(0) (176 mg, 0.153 mmol) in dry tetrahydrofuran (60 mL) was heated at 80°C under nitrogen for 18 h. After cooling at room temperature, organic solvent was removed *in vacuo* and the aqueous phase was extracted with CH_2Cl_2. The collected organic phases were dried over Na_2SO_4 and the solvent removed *in vacuo*. The crude product was purified by column chromatography on silica gel using pure chloroform as eluent to afford the product **L^2** (480 mg, 79%) as pale white solid. mp 231-233 °C. ^{1}H NMR (400 MHz, $CDCl_3$): 8.57 (d, *J* 6.2 Hz, 2H), 7.60 (d, *J* 8.9 Hz, 2H), 7.48 (d, *J* 6.2 Hz, 2H), 6.79 (d, *J* 8.9 Hz, 2H); ^{13}C NMR (400 MHz, $CDCl_3$): 151.17, 149.77, 147.50, 127.68, 124.96, 120.33, 112.46, 40.31.

(3-cyanobenzyl)triphenylphosphonium bromide, 5

To a solution of 3-(bromomethyl)benzonitrile (3 g, 15.3 mmol) in heptane (45 mL) was added PPh_3 (4.8 g, 18.3 mmol) and the mixture was refluxed for 24 h. After cooling at room temperature the white precipitate was filtered and washed with heptane and Et_2O, then concentrated *in vacuo* affording pure **5** (6.5 g, 93%). ^{1}H NMR (400 MHz, $CDCl_3$): δ 7.80 (m,

1H –NC-C-$(CH)_2$-C*H*- and 9H -P*Ph*$_3$); 7.63 (m, 6H -P*Ph*$_3$); 7.44 (d, *J*: 8 Hz, 1H CN-C-C*H*-); 7.25 (t, *J*: 8 Hz, 1H –NC-C-CH-C*H*-); 7.11 (s., 1H –NC-C-C*H*-C); 5.86 (d, *J*: 16 Hz. 2H CNPh-C*H*$_2$). ^{1}C NMR (100 MHz, $CDCl_3$): δ 136.91; 135.20; 134.47; 134.18; 131.78; 130.27; 129.79; 129.69; 117.89; 117.39; 112.39; 52.67. *m/z* (ESI) 378.2 [M^+], calcd. 378.1. mp: 287.3 – 291.8 °C.

(E,Z)-3-(2-pyridin-3-yl) vinyl benzonitrile, 6

To NaOH (1.18 g, 29.5 mmol) sospended in CH_2Cl_2, under nitrogen atmosphere was added (3-cyanobenzyl)triphenylphosphonium bromide (3 g, 6.54 mmol) . Then a solution of pyridinecarboxaldehyde (637 mg, 5.9 mmol) in CH_2Cl_2 (5 mL) was added and the solution was stirred overnight. The reaction mixture was washed twice with water. The organic phase was dried over $MgSO_4$ and evaporated *in vacuo*, then 10 mL of hexane/AcOEt (1:1 v/v) solution was added to the crude product to allow the precipitation of triphenylphosphine oxide which was filtered off. The organic phase was evaporated *in vacuo* and the crude product was purified by silica gel column chromatography (AcOEt/hexane 6:4) affording **6** (870 mg, 72% yield) as E/Z isomers mixture. E/Z isomers mixture: ^{1}H NMR (400 MHz, $CDCl_3$): δ 8.76 (d, *J*: 2.4 Hz, 1H^E); 8.55 (dd, *J*: 4.8, 1.6 Hz, 1H^E); 8.49 (dd, *J*: 4.8, 1.6 Hz, 1H^Z); 8.45 (d, *J*: 2.4 Hz, 1H^Z); 7.87 (m, 1H^E); 7.80 (t, *J*: 1.6 Hz, 1H^E); 7.75 (dt, *J*: 7.6, 1.6 Hz, 1H^E); 7.58 (d., *J*: 7.6 Hz 1H^E); 7.52-7.33 (3H^E, 5H^Z); 7.18 (m, 1H^Z); 7.14 (s, 2H^E); 6.71 (d, *J*: 12 Hz, 1H^Z); 6.8 (d, *J*: 12 Hz, 1H^Z).

Benzo[*f*]isoquinoline-8-carbonitrile, L^5

A magnetically stirred solution of (E,Z)-3-(2-pyridin-3-yl) vinyl benzonitrile, (375 mg, 1.82 mmol) in CH_2Cl_2 (500 mL) was irradiated by a Hg high pressure lamp in a quartz reactor for 2 h at -17 °C. The solvent was evaporated *in vacuo* and the brown oil residue was purified by silica gel column chromatography (hexane/AcOEt 1:1) affording pure **L^5** (136 mg, 36%). ^{1}H NMR (400 MHz, DMSO): δ 7.98 ((s, H^1), 8.34 (d, *J* 6 Hz, 1H^3), 8.77 (d, *J* 8 Hz, 1H^5), 8.43 (d, *J* 6 Hz, 1H^4), 8.30 (d, *J* 6 Hz, 1H^8), 7.96 (d, *J* 8 Hz, 1H^9),7.92 (dd, *J* 8, 1.6 Hz, 1H^6), 7.88 (d, *J* 8 Hz, 1H^{10}). ^{1}C NMR (100 MHz, $CDCl_3$): δ 152.06; 145.98; 133.96 ; 133.74; 133.04; 131.00; 128.61; 127.57; 126.83; 124.50; 118.53; 116.30; 112.31; m/z (ESI). 205.07567 [M + H^+], calcd. 205.07602. λ_{max}(DMF): 269; 332, 348, 365 nm melting point : 149.8 – 159.5 °C.

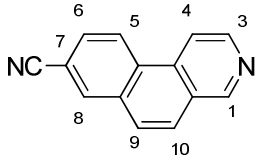

***cis*-[Ir-$(CO)_2$Cl(benzo[f]isoquinoline-8-carbonitrile)], [IrL^5]**

In a three-necked flask [Ir-$(COT)_2Cl]_2$ (109.6 mg; 0.122 mmol) was added to dehydrated CH_3CN (50 mL) under nitrogen. The suspension was stirred for 2 min at room temperature, and then nitrogen was replaced by CO. A yellow solution was obtained immediately, due to the conversion of $[Ir(COT)_2Cl]_2$ in $[Ir(CO)_2Cl]_2$. After 5 min under CO, the desired substituted 5-CN-Annine (50.4mg, 0.244 mmol) was added. After ca. 10 min, all $[Ir(CO)_2Cl]_2$ had been converted in**[IrL^5]**, as shown by infrared spectroscopy. After 1 h, the browned solution was evaporated to dryness. The resulting violet solid was dried under vacuum, affording pure in quantitative yield, which was stored in the dark under nitrogen. ^{1}H NMR (DMSO) δ 9.67 (s, 1H^1), 9.18 (d, *J* 8.7, 1H^3), 9.05 (d, *J* 5.32, 1H^5), 8.94 (d, *J* 6.2, 1H^9), 8.77 (s, 1H^7), 8.24 (m, 1H^4, 1H^6 and H^8); λ_{max}(DMF): 292, 347, 363, 374 nm; ν/cm^{-1} 2077 (CO), 1998 (CO). Anal. Calcd for $C_{27}H_{28}N_2O_2IrCl$: C, 39.39; H, 1.65; N, 5.74; Found: C, 39,70; H, 2.00; N, 5.38.

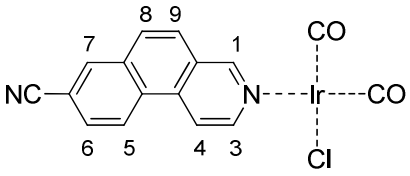

(E,Z)-3-(2-(isoquinolin-5-yl)vinyl)benzonitrile, 7

To NaOH (780 mg, 19.5 mmol) sospended in CH_2Cl_2 (30 mL), under nitrogen atmosphere was added (3-cyanobenzyl)triphenylphosphonium bromide **5** (2 g, 4.3 mmol). Then isoquinoline-5-carbaldehyde (614 mg, 3.9 mmol) dissolved in dry MeOH (5 mL) was added and the solution was stirred overnight. The reaction mixture was washed twice with water. The organic phase was dried over $MgSO_4$ and evaporated *in vacuo*, then 20 mL of hexane/AcOEt (4:1 v/v) solution was added to the crude product to allow the precipitation of triphenylphosphine oxide which was filtered off. The organic phase was evaporated *in vacuo* and the residue was purified by column chromatography on silica gel (AcOEt/hexane 7:3) to afford **7** as mixture of E/Z isomers as yellow oil (934 mg, 93%). This product was generally used as isomeric mixture. Z isomer ^{1}H NMR (400 MHz, $CDCl_3$): δ 9.28 (s, 1H); 8.53 (d, *J*: 6 Hz, 1H); 7.93 (m, 1H); 7.77 (d, *J*: 6 Hz, 1H); 7.50 (m, 2H); 7.40 (dt, 1H); 7.36 (s all., 1H); 7.20 (m, 2H); 7.12 (d, *J*: 12 Hz, 1H); 6.87 (d, *J*: 12 Hz, 1H).

Nafto[2,1-*f*] isochinoline-8-carbonitrile, L^6

A magnetically stirred solution of (E,Z)-3-(2-(isoquinolin-5-yl)vinyl)benzonitrile **7** (700 mg, 2.73 mmol) in CH_2Cl_2. (500 mL) was irradiated by a Hg high pressure lamp in a quartz reactor for 6 h at 15 °C. After the evaporation of the solvent the residue was washed with CH_2Cl_2. then purified by by crystallization from MeOH to afford a brown solid **L^6** (105 mg, 15%). mp 211 °C. ^{1}H NMR (400 MHz, DMSO): δ 9.59 (s, 1H^1), 9.21 (d, *J* 8.8 Hz, 1H^{10}), 9.16 (d, *J* 9.2 Hz, 1H^{11}), 9.10 (d, *J* 9.2 Hz, 1H^5), 8.95 (d, *J* 6 Hz, 1H^4), 8.85 (d, *J* 6 Hz, 1H^8), 8.80 (d, *J* 1.6 Hz, 1H^7), 8.40 (d, *J* 9.2 Hz, 1H^{12}), 8.31 (d, *J* 9.2 Hz, 1H^6), 8.14 (dd, *J* 8.8, 1.6 Hz, 1H^9); ^{13}C NMR (100 MHz, $CDCl_3$): δ 152.06; 144.55; 134.77; 134.41; 132.53; 132.23; 130.28; 128.73; 128.33; 127.48; 127.18; 126.08; 124.00; 123.79; 119.34; 117.77; 110.50; *m/z* (ESI) 255.09154 [M + H$^+$], calcd, 255.09167 λ_{max}(DMF): 284; 296, 306, 320, 343, 360, 379 nm: mp. 286 °C

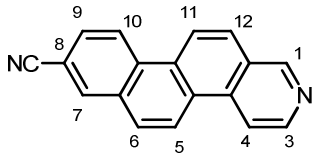

***cis*-[Ir-$(CO)_2$Cl(naphtho[2,1-f]isoquinoline-8-carbonitrile)], [IrL^6]**

In a three-necked flask [Ir-$(COT)_2Cl]_2$ (61.6 mg; 0.0689 mmol) was added to dehydrated CH_3CN (25 mL) under nitrogen. The suspension was stirred for 2 min at room temperature, and then nitrogen was replaced by CO. A yellow solution was obtained immediately, due to the conversion of $[Ir(COT)_2Cl]_2$ in $[Ir(CO)_2Cl]_2$. After 2 min under CO, a solution of naphtho[2,1-f]isoquinoline-8-carbonitrile (35.0mg, 0.138 mmol) in DMF (6mL) was added. After ca. 10 min, all $[Ir(CO)_2Cl]_2$ had been converted in *cis*-[Ir-$(CO)_2$Cl-(naphtho[2,1-f]isoquinoline-8-carbonitril)], as shown by infrared spectroscopy. After 1 h, the browned solution was evaporated to dryness. The resulting violet solid was dried under vacuum, affording pure **[IrL^6]** in quantitative yield, which was stored in the dark under nitrogen. ^{1}H NMR (DMSO): δ 9.51 (s, 1H^2), 9.21 (d, *J* 8.8, 1H^5), 9.12 (d, *J* 9.0, 1H^4), 9.09 (d, *J* 9.1, 1H^{12}), 8.85 (d, *J* 5.9, 1H^9), 8.83 (d, *J* 5.9, 1H^{10}), 8.80 (d, *J*= 1.5, 1H^8), 8.37 (d, *J* 9.0, 1H^3), 8.12 (dd, $J_{6,5}$ 8.8 $J_{6,8}$ 1.5, 1H^6); λ_{max}(DMF): 296, 307, 320, 343, 380; 359 nm; ν/cm^{-1} 2076 (CO), 1996 (CO).

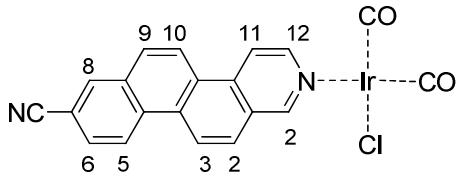

2.3. Synthesis of octupolar chromphore

Ligands **O^1** and **O^2** were prepared with the same procedure - or minor modifications - described previously by Moore,[11] and reported here below for **O^1** along with the syntesis of the porphyrin and phtalocyanine coordination complexes. Synthesis of the precursors are repoted before that of the ligands.

Synthesis of 1,3,5-triethynylbenzene, 1

Following the procedure reported in ref. [12] 1,3,5-tribromobenzene (951 mg, 3.019 mmol), was dissolved in freshly distilled diethylamine (25 mL). Copper iodide (5.0 mg, 0.020 mmol) and bis(triphenylphosphine)palladium(II) chloride (42.1 mg, 0.060 mmol) were added to the stirred solution. Trimethylsilylacetylene was dropped (901.3 mg, 10.798 mmol) over a period of 30 min at room temperature. Then the solution was heated at reflux for 7 h. After cooling to room temperature the precipitated diethylamine hydrobromide salt was filtered. The solvent was removed under reduced pressure. The crude compound was purified by chromatography on alumina gel (eluent: hexane) to give 1,3,5-tris(trimthylsilylethynyl)benzene as an intermediate. Basic hydrolysis of this compound (KOH 50%) in MeOH followed by a standard work-up procedure involving evaporation of the organic solvent, extraction of the residue with ether, drying and removal of the solvent under reduced pressure, yielded the pure **1** as colourless powder (406 mg, 85% yield). ^{1}H NMR (400 MHz, DMSO): δ 7.59 (s, 3H -*Ar*), 3.13 (s, 3H -CΞC*H*).

Synthesis of 1,3,5-tris(pyridin-4-ylethynyl)benzene, O^1

Following the Sonogashira protocol reported in ref. [11] to a suspansion of 4-bromopyridine hydrochloride (419.9mg, 2110 mmol) in (3mL) freshly distilled diethyl amine were added copper iodide (6.4 mg, 0.033 mmol) and bis(triphenylphosphine)palladium(II) chloride (23.0 mg, 0.033 mmol) stirring for 30 min at room temperature in the dark. Then 1,3,5-triethynylbenzene was added and the reaction mixture was left at reflux for 16 h. After cooling to room temperature the solvent was removed under reduced pressure. The residue was was taken up into ethylacetate and washed with water (3 × 30 mL). The organic phase was dried over anhydrous Na_2SO_4 and evaporated to dryness under reduced pressure. The red residue was purified by chromatography on silica gel (eluent: 5% methanol/dichloromethane) giving **O^1** as a yellow solid (79 mg, 30 % yield). ^{1}H NMR (400 MHz, $CDCl_3$): δ 8.66 (d, *J* 6 Hz, 6H^7), 7.76 (s, 3H^1), 7.41 (d, *J* 6 Hz, 6H^6); $\lambda(CHCl_3)$/nm 283.

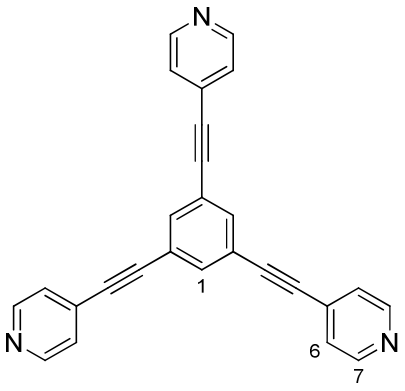

Synthesis of 4-(phenylethynyl)pyridine, O^2

This was prepared in an identical manner to **O^1**, according to the procedure reported in ref. [11], except that ethynylbenzene (504.2 mg, 4.941mmol) was used as starting material instead of 1,3,5-triethynylbenzene. The product was obtained as white crystals (442.2 mg, 50% yield). ^{1}H NMR (400 MHz, THF): δ 8.59 (d, 2H^2), 7.56 (m, 2H$^{2'}$), 7.41(m, 2H^3 and 2H$^{3'}$ and 1H$^{4'}$)

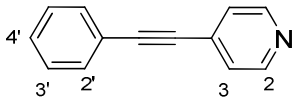

Synthesis of O^1Zn^1

After heating a reflux Zn-porphyrin **Zn^1** (200 mg, 0.334 mmol) in $CHCl_3$ (100 mL), 1,3,5-tris(pyridin-4-ylethynyl)benzene (42.5 mg, 0.111 mmol) dissolved in $CHCl_3$ (5 mL) was added. The solution was refluxed overnight. After cooling at room temperature the precipitate was filtered and washed with heptane affording pure **O^1Zn^1** (213.3 g, 21%). ^{1}H NMR (400 MHz, $CDCl_3$): δ 7.32 (d, 6H), 6.63 (d, 3H),6.44 (d, 6H), 4.14 (m, 16H), 1.94 (t, 24H); $\lambda(CHCl_3)$/nm 283 ; Anal. Calcd for $C_{63}H_{59}N_7Zn$: C, 74.52; H, 6.81; N, 9.66; Found: C, 72.97; H, 6.64; N, 9.05 (ESI) 378.2 [M^+], calcd. 378.1. mp: 287.3 – 291.8 °C.

Synthesis of O^2Zn^1

Yield: .22.3 mg (30%, starting from 17.5 mg, 0.0979 mmol of **O^2**).

^{1}H NMR (400 MHz, $CDCl_3$): δ 8.81). ^{1}H NMR (400 MHz, $CDCl_3$): δ 7.54 (m, 5H$'$), 7.40 (m, 2H), 7.26 (not fully resolved due to overlap with former signal and solvent, m, 2H) 4.11 (q, 16H), 3.74 (t, 24H).

Synthesis of O^1Zn^2

After heating at reflux a solution of Zn-ptalocyanine **Zn^2** (310 mg, 0.359 mmol) in acetone (100 mL), 1,3,5-tris(pyridin-4-ylethynyl)benzene (41.5 mg, 0.109 mmol) dissolved in $CHCl_3$

(10 mL) was added. The solution was refluxed overnight. After cooling to room temperature the precipitate was filtered and washed with heptane affording pure **O^1Zn^2** (129 mg, 40%). ^{1}H NMR (400 MHz, THF): δ 8.64 (d, 6H), 7.85 (s, 3H), 7.45 (d, 6H),

Synthesis of O^2Zn^2

Yield: .54.8 mg (39%, starting from 23.7 mg, 0.132 mmol of **O^2**).

^{1}H NMR (400 MHz, $CDCl_3$): δ 8.81). ^{1}H NMR (400 MHz, $CDCl_3$): δ 7.54 (m, 5H$^{'}$), 7.40 (m, 2H), 7.26 (not fully resolved due to overlap with former signal and solvent, m, 2H) 4.11 (q, 16H), 3.74 (t, 24H).): δ 8.59 (d, 2H^2), 7.57 (m, 2H$^{2'}$), 7.41(m, 2H^3 and 2H$^{3'}$ and 1H$^{4'}$)

References:

[1] Williams, J. A. G.; Beeby, A.; Davies, S.; Weinstein, J.A.; Wilson, C.; *Inorg.Chem*., **2003,** *42*, 8609.

[2] (*a*) McCamy, C. S.; *Color Res. Appl.,* **1992**, *17*, 142; (*b*) Hernandez-Andres, J.; Lee, R. L. Jr.; Romero, J. *Appl. Opt.,* **1999**, *38*, 5703.

[3] Li, H.; Zhang, C.; Li, D., Duan, Y. *J. Lumin*. **2007**, *122-123*, 626.

[4] M. Cossi and V. Barone, *J. Chem. Phys.*, 2001, **115**, 4708

[5] Gaussian 03, Revision C.02, M. J. Frisch G. W. Trucks, H. B. Schlegel, G. E. Scuseria, M. A. Robb, J. R. Cheeseman, J. A. Montgomery, Jr., T. Vreven, K. N. Kudin, J. C. Burant, J. M. Millam, S. S. Iyengar, J. Tomasi, V. Barone, B. Mennucci, M. Cossi, G. Scalmani, N. Rega, G. A. Petersson, H. Nakatsuji, M. Hada, M. Ehara, K. Toyota, R. Fukuda, J. Hasegawa, M. Ishida, T. Nakajima, Y. Honda, O. Kitao, H. Nakai, M. Klene, X. Li, J. E. Knox, H. P. Hratchian, J. B. Cross, V. Bakken, C. Adamo, J. Jaramillo, R. Gomperts, R. E. Stratmann, O. Yazyev, A. J. Austin, R. Cammi, C. Pomelli, J. W. Ochterski, P. Y. Ayala, K. Morokuma, G. A. Voth, P. Salvador, J. J. Dannenberg, V. G. Zakrzewski, S. Dapprich, A. D. Daniels, M. C. Strain, O. Farkas, D. K. Malick, A. D. Rabuck, K. Raghavachari, J. B. Foresman, J. V. Ortiz, Q. Cui, A. G. Baboul, S. Clifford, J. Cioslowski, B. B. Stefanov, G. Liu, A. Liashenko, P. Piskorz, I. Komaromi, R. L. Martin, D. J. Fox, T. Keith, M. A. Al-Laham, C. Y. Peng, A. Nanayakkara, M. Challacombe, P. M. W. Gill, B. Johnson, W. Chen, M. W. Wong, C. Gonzalez, and J. A. Pople, Gaussian, Inc., Wallingford, CT, 2004.

[6] Farley, S. J.; Rochester, D. L.; Thompson, A. L.; Howard, J. A. K.; Williams, J. A. G. *Inorg. Chem.* **2005**, *44*, 9690.

[7] Manka, J. T.; Mckenzie ,V. C.; Kaszynski, P. *J. Org. Chem*., **2004 ,** *69* , 1967.

[8] Baldo, M. A.; O'Brien, D. F.; You, Y.; Shoustikov, A.; Sibley, S.; Thompson, M. E.; Forrest, S. R. Nature, 1998, 395, 151.

[9] Baik, C.; Han, W.-S.; Kang, Y.; Kang, S. O.; Ko, J. *Journal of Organometallic Chemistry*, **2006**, *691*, 5900.

[10] Neenan, T.; Withesides, M. *J. Org. Chem*. **1988**, *53*, 2489.

[11] Lewis, J. D.; Moore, J. *Dalton trans.*, **2004,** 1376.

[12] Weber, E.; Hecker, M.; Koepp, E.; Orilia, W.; Czugler, M.; Csöregh, I. *Chem. Soc. Perkin Trans*, **1988**, *2*, 1251.

CONCLUSIONS

We successfully synthesized new square planar platinum(II) complexes containing (N^C^N)-cyclometallated ligands whose photophysical and electrochemical properties have been investigated. Some of these complexes have very high luminescence quantum efficiencies, being among the brightest Pt(II) emitters known. Furthermore the emission energy can be fine-tuned via substituents on both terdentate and ancillary ligand. These complexes are generally easily prepared, neutral, stable in air, and sublimable, making them good candidates for use in optoelectronic devices. Actually, some of these Pt complexes have been recently incorporated into solution-processed monochrome OLEDs as well as in a device which emitts white light. The manifacturing of electrophosphorescent devices using solution processes significantly reduce costs although efficiency remains below those of vacuum-deposited OLEDs.
Remarkably, some of our novel complexes are characterized by a relatively low sensibility to oxygen, an appealing characteristic that could be an advantage in the devices fabrication. In addition, these complexes easily forms excimers, both in solution and in the solid state. This interesting feature has been exploited in a preliminary study of phosphorescent excimer diodes. By changing the complex concentration in the emitting layer, we obtained green to red electrophosphorescence achieving reasonable efficiency.
Excimer emission at ca. 700 nm (solid state) is quite a relevant finding suggesting a potential applications in communications, biomedicine, and in optoelectronic devices operating in the near-infrared (NIR) spectral range.

With respect to the influence of coordination to a metal centre on the non-linear optical properties of new chromophore, the EFISH measurments showed that anellated hemicyanine ligands and their Ir(I) coordination compounds are a new type of highly efficient NLO-active systems. The very high thermal stability, combined with its high NLO activity, makes them particularly appealing from an applicative point of view.

Concerning the NLO response of N^C^N-coordinated platinum(II) complexes, as expected, the presence of the PtCl moiety enhances the NLO properties compared to other organic and organometallic compounds. Some of the complexes are, for example, characterized by a $\mu\beta_{1.907}$ value higher than that of Disperse Red One [trans-4,4'-$O_2NC_6H_4$-N=$NC_6H_4NEt(CH_2CH_2OH)$], an NLO chromophore currently used in electro-optics polymers and therefore are of particular interest for technological applications. Besides, our work confirms what previously reported in the case of β-diketonate complexes of various lanthanide ions – *i.e.* the major contribution to the total quadratic hyperpolarizability is controlled mainly by the octupolar part - and represents a new step in the understanding of

the major role of the octupolar components on the NLO properties of metal complexes with π-delocalized ligands.

Finally an octupolar tripodal ligand had been prepared which terminates with pyridyl groups that were easily linked to organometallic fragments. Although coordination of our octupolar core to Zn complexes of a commercial porphyrine, or phtalocyanine, did not lead to a substantial change in $\beta_{HLS,1.907}$ value, this study puts in evidence the remarkably large second order NLO response of the free Zn-porphyrine itself especially considering its very simple structure and commercially availiability.

Ringraziamenti

Ringrazio sentitamente il Prof. Renato Ugo per avermi dato la possibilità di svolgere questo lavoro di tesi e per i suoi illuminanti consigli professionali.

Un particolare ringraziamento va alla Prof.ssa Dominique Marie Roberto che mi ha istruito e sostenuto in ogni fase di questo lavoro, dimostrando in ogni momento una grandissima disponibilità umana.

Ringrazio anche la Dott.ssa Claudia Dragonetti per la sua dolcezza e il suo sostegno e in particolare per la pazienza con cui ha corretto questa tesi.

Ringrazio sentitamente il Prof. J. A. Gareth Williams per la sua grande ospitalità e disponibilità sia professionale che umana.

Ringrazio di cuore anche il Dott. Luigi Falciola per i suoi preziosi consigli professionali.

Un grazie particolare va a Pasquale Illiano che con pazienza mi ha insegnato a usare lo spettrometro NMR e che si è sempre mostrato disponibile per consigli e aiuti.

Un grazie anche ai miei cari colleghi di laboratorio (in ordine alfabetico): la Sig.ra Adriana, il nostro Mac Giver (ma si scrive così?) Alessia, la mia amica Annalisa, la anche-se-da-poco-tra-noi carissima Cinzia, il Giuseppe che è unico, l'indipendente Elisa, la geniale Marcella, l'insostituibile Marco Ronchi, la donna giusta Stefania Righetto, il mio personal trainer Willi Deer che mi hanno "sopportato" e consigliato con pazienza, e che hanno sempre saputo regalarmi giornate di allegria e serenità contribuendo a creare un clima favorevole alla stesura di questa tesi. Ringrazio anche Alessio, Tommaso, Daniele, Gabriele e Michele per la compagnia.

Un grazie di cuore va alla dott.ssa Francesca Tessore che è per me un esempio dal momento che riesce a conciliare una elevata professionalità a una vita familiare alquanto movimentata, il tutto condito da un grande altruismo.

Non posso inoltre dimenticare i «giovani» che sono stati «ospiti graditi» del laboratorio in cui ho lavorato e che di tanto in tanto passano ancora a salutare: il Batta, Chiara, Cristina, Edoardo, Enrico, Ivan, Marta, Michele, Paolo, Riccardo, Saretta, Silvio, Stefania.

Inoltre vorrei ringraziare la dott.ssa Clara Baldoli, mia ex correlatrice di tesi, per essere stata presente al «passaggio di consegne» ovvero la mia prima presentazione di dottorato, e per essere sempre stata disponibile professionalmente e umanamente.

Ringrazio con tanto affetto tutti i miei colleghi di corso e in particolare il mio fedele "amico di chimica fisica" Stefano, la sua carissima morosa Daria, il Maurino delle Torte, il Robi Sondrio e la sua Claudia, il Fra, Robi Vercelli per la loro amicizia sincera, per il sostegno e l'allegria che hanno saputo regalarmi. Ringrazio inoltre Fabietto, il Pino, la Sonia, la Silvia e tutti coloro che passando per il bunker hanno allietato i «giorni pizza»

Ringrazio di cuore la mia famiglia (in particolare lo Puccio e la Pijulina sui quali è gravata la maggior parte del mio nervosismo) e tutti i miei cari amici che mi sono sempre stati vicini. Non cercherò di esprimere con parole limitate quanto vi voglio bene: ognuno di voi sa quanto è importante per me!

E in ultimo vorrei ringraziare il mio Patrick che ha dovuto, forse più di tutti, portare pazienza durante la stesura di questa tesi: grazie!!

Ester